# Dissertation

Submitted to the

Combined Faculty of Natural Sciences and Mathematics
of the Ruperto Carola University Heidelberg, Germany

for the degree of
Doctor of Natural Sciences

Presented by
Paula Sophie Werner, M.Sc.
Born in: Offenbach am Main, Germany
Oral examination: 02.10.2020

# Development, Maintenance, and Role of Stem Cell Based Interferon Signaling Heterogeneity in the Hematopoietic System

Referees:

Prof. Dr. Andreas Trumpp

Prof. Dr. Nina Papavasiliou

*I dedicate this work to my mother* ***Jutta Werner***
*for teaching me to never give up*

*Nothing in life is to be feared, it is only to be understood.*
*Now is the time to understand more, so that we may fear less.*
**Marie Curie**

# Table of contents

## Abstract

Inflammation or infections have a great impact on an organism. In order to protect the hematopoietic system from exhaustion during pathogenic insult, heterogeneity in metabolic activity, gene expression patterns, differentiation capacity, and responsiveness to cytokines such as interferons (IFN) have been revealed. However, how this diversity in the system is generated and maintained remains poorly understood. In this thesis, I explored three aspects of IFN signaling heterogeneity in the hematopoietic system. First, I investigated the origin of IFN signaling heterogeneity during hematopoietic development (**1.**). Here, I was able to show that differences in baseline IFN signaling are already present at the onset of definitive hematopoiesis at embryonal day (E) 10.5 of development. In addition, I identified the placenta as an embryonic niche that provides definitive hematopoietic stem cells (HSCs) with stable high basal IFN signaling. Second, I investigated the function of IFN signaling heterogeneity both during embryonic development and in different cell populations of the adult system (**2.**). I uncovered a potential role for higher baseline IFN signaling in mediating protection against infections and pathogen invasion in hematopoietic cells during development. Furthermore, in the adult my data indicate that T cells with different levels of baseline IFN signaling display different activation efficiencies and expression of immune checkpoint molecules following *in vitro* stimulation. Thirdly, I investigated the mechanisms of IFN signaling heterogeneity (**3.**). Analysis of DNA methylation patterns of cells with different levels of basal IFN signaling revealed possible epigenetic differences both during development as well as in the adult hematopoietic system. Understanding the origin, function, and mechanism of IFN signaling heterogeneity during hematopoietic development and in the adult hematopoietic system will allow targeting of specific aspects of the pathway to improve response to infections, inhibit development of infectious diseases and possible hematological malignancies, improve existing treatments or develop new treatment approaches.

In addition to the investigation of IFN signaling heterogeneity in the hematopoietic system, a fourth aim of my PhD thesis concentrated on the role of the extracellular matrix (ECM) in the stress-induced activation of HSCs (**4.**). Previous studies from our group (Uckelmann *et al.*, 2016) could show that the ECM component Matrilin-4 (Matn4) plays an indispensable direct role in the activation of HSCs upon inflammatory stress. I investigated several other ECM components, but only found minor differences in the hematopoietic compartment of mice lacking these components during homeostasis and under inflammatory stress. However, the ECM is a complex and dynamic network of constantly interacting components and novel approaches will be necessary to understand the two-way communication between HSCs and the ECM under inflammatory stress.

## Zusammenfassung

Entzündungen und Infektionen haben einen großen Einfluss auf einen Organismus. Um das hämatopoetische System vor Erschöpfung während eines Angriffs von Pathogenen zu schützen, konnte Heterogenität in metabolischer Aktivität, Genexpressionsmustern, Differenzierungskapazität und Reaktivität auf Zytokine wie Interferon (IFN) gezeigt werden. Wie diese Diversität im System gebildet wird, bleibt jedoch schlecht verstanden. In dieser These habe ich drei Aspekte der IFN Signalheterogenität im hämatopoetischen System untersucht. Zuerst habe ich den Ursprung der IFN Signalheterogenität während der hämatopoetischen Entwicklung erforscht (**1.**). Dabei konnte ich zeigen, dass Unterschiede in der basalen IFN Signalisierung bereits zum Start der definitiven Hämatopoese am embryonalen Entwicklungstag (E) 10.5 vorhanden sind. Außerdem konnte ich die Plazenta als embryonale Nische identifizieren, die den hämatopoetischen Stammzellen (HSZ) stabil eine hohe IFN Signalisierung übermittelt. An zweiter Stelle habe ich die Funktion der IFN Signalheterogenität sowohl währen der embryonalen Entwicklung als auch in verschiedenen Zellpopulationen des erwachsenen Systems untersucht (**2.**). Hier konnte ich eine potentielle Rolle der IFN Signalheterogenität beim Schutz vor Infektionen und vom Eindringen von Pathogenen in hämatopoetische Zellen während der Entwicklung aufdecken. Zusätzlich zeigen meine Daten, dass T Zellen mit unterschiedlichen Leveln an basaler IFN Signalisierung nach *in vitro* Stimulierung verschieden effizient aktiviert werden und Immuncheckpoint Moleküle exprimieren. An dritter Stelle habe ich die Mechanismen der IFN Signalheterogenität untersucht (**3.**). Die Analyse von DNA Methylierungsmustern in Zellen mit verschiedenen Leveln an IFN Signalisierung zeigte mögliche epigenetische Unterschiede sowohl während der Entwicklung als auch im erwachsenen hämatopoetischen System. Das Verständnis des Ursprungs, der Funktion und der Mechanismen von IFN Signalheterogenität während der hämatopoetischen Entwicklung und im erwachsenen hämatopoetischen System wird es erlauben, spezifische Aspekte dieses Signalweges gezielt zu manipulieren, um die Antwort auf Infektionen zu verbessern, die Entwicklung von Infektionskrankheiten und möglicher hämatologischer Krankheiten zu hemmen, bestehende Behandlungen zu verbessern und neue Behandlungsansätze zu entwickeln.

Zusätzlich zu der Untersuchung der IFN Signalheterogenität im hämatopoetischen System, habe ich mich als viertes Ziel meiner Dissertation auf die Rolle der extrazellulären Matrix (EZM) während der stressinduzierten Aktivierung von HSZ konzentriert (**4.**). Frühere Studien unserer Gruppe (Uckelmann *et al.*, 2016) konnten zeigen, dass die EZM Komponente Matrilin-4 (Matn4) eine unverzichtbare und direkte Rolle in der Aktivierung von HSZ nach Entzündungsstress spielt. Ich habe in meiner These mehrere andere EZM Komponenten untersucht, habe jedoch nur minimale Unterschiede im hämatopoetischen System von Mäusen, denen diese EZM Komponenten fehlen, während Homöostase und

Entzündungsstress gefunden. Die EZM ist ein komplexes und dynamisches Netzwerk aus andauernd miteinander interagierenden Komponenten und neue Ansätze sind notwendig, um die duale Kommunikation zwischen HSZ und EZM unter Entzündungsstress zu verstehen.

# 1. INTRODUCTION

## 1.1. Hematopoiesis and stem cells

Today, hematopoietic stem cells (HSCs) are one of the most studied tissue-specific stem cells. Already in 1951, Jacobson *et al.* where able to show the recovery of irradiated mice by shielding the spleen from irradiation. Back then, they suspected non-cellular substances to be responsible for the rescue and thought a migrating cell from the spleen to the periphery to be highly unlikely (Jacobson *et al.*, 1951). The concept of specific cells being able to reconstitute the blood system after irradiation injury was first introduced in 1956 in two independent bone marrow (BM) transplantation studies (Ford *et al.*, 1956; Nowell *et al.*, 1956), opening the field of hematopoietic stem cell research. In 1961, Till and McCulloch were the first to claim the existence of the hematopoietic stem cell (Till and McCulloch, 1961). However, the concept of a single cell being able to reconstitute the entire blood system was not proven until 1977, when a group of researchers in Toronto was able to show stable reconstitution of both the myeloid and the lymphoid lineage after transplantation of cells from one via chromosome-aberrations identified stem cell clone (Abramson *et al.*, 1977). Since then, many aspects of these cells have been studied to understand the basic biological functions of HSCs, like self-renewal and maintenance, differentiation capacity, lineage contribution, or quiescence and activation. Today, HSCs are highly clinically relevant, since these cells are transplanted in stem cell transplantations as treatments in many blood related diseases, leukemias amongst others. However, isolating sufficient numbers of transplantable cells remains challenging. Approaches to isolate and expand HSCs *ex vivo* before transplantation are being established (Wilkinson *et al.*, 2019; Kobayashi *et al.*, 2019), yet, are not applicable in the clinic so far.

### *1.1.1. Hematopoietic stem cells and development*

Hematopoiesis occurs in distinct waves during embryonic development at several different sites of the embryo. Prior to the formation of stem cells and before the establishment of the circulatory system, a subset of specialized mesodermal precursor cells migrate to the yolk sac and initiate embryonic red blood cell production at embryonic day (E) 7.5 (Mikkola and Orkin, 2006). Circulation of blood cells that supply the growing embryo and later development of definitive hematopoiesis, relies on an intact circulatory system. In parallel to the development of the mesodermal precursor cells, the vascular system develops and the first heartbeat can be detected at E8.5. This initial part of the circulatory system is called vitelline circulation, connecting the dorsal aorta, the yolk sac, and the heart (Mikkola and Orkin, 2006). Shortly after, a second vascular route develops, called umbilical circuit. After fusion of the placental chorionic plate with the allantois, a mesoendodermal appendage which functions as an

excretory and respiratory outlet for the embryo (Caprioli *et al.*, 1998; Caprioli *et al.*, 2001), umbilical vessels are formed from the allantoic mesoderm (Downs and Harmann, 1997; Mikkola and Orkin, 2006), connecting the dorsal aorta to the placental vascular network and the fetal liver subsequently (Mikkola and Orkin, 2006).

During this first primitive streak of hematopoiesis, progenitor cells with erythroid, macrophage, and myeloid potential are formed, leading to the production of different myeloid cells in the embryo. These progenitor cells migrate to the fetal liver at E10.5 where they reside until at least E16.5. The majority of these primitive cells will then be replaced by HSC-derived cells. However, some macrophages derived from these primitive embryonic progenitors are still present in the adult, suggesting self-renewal capacity of fetal-derived macrophages (Gomez Perdiguero *et al.*, 2015) (Figure 1.1.1 A).

Definitive HSCs are defined by their engraftment capability in adult tissues and equal potency to adult BM HSCs. First emergence of definitive HSCs is observed at E10.5 in the aorta-gonad-mesonephros (AGM) region (Muller *et al.*, 1994; Medvinsky and Dzierzak, 1996), more specifically the dorsal aorta and the vitelline and umbilical arteries of the mid-gestation embryo (de Bruijn *et al.*, 2000). The mesodermal germ layer, which contains the dorsal aorta, the genital ridge, and the mesonephros derives the AGM. The genital ridge later forms the gonads, and the mesonephros gives rise to the kidneys. This region extends from anterior to posterior limbs of E9.5 to E12.5 embryos (de Bruijn *et al.*, 2000; Medvinsky *et al.*, 2011; Gao *et al.*, 2018) and HSCs are generated from the hemogenic endothelium within the AGM. Since this is three days after primitive erythrocytes appearance in the yolk sac, a common ancestor is unlikely (Dzierzak and Speck, 2008). It is therefore suggested that the definitive hematopoietic progenitor-stem cells arise through an independent process compared to primitive erythroid progenitors. A subset of endothelial cells in the AGM of the embryo is activated through a hematopoietic transcriptional program during a process called endothelial-to-hematopoietic transition (EHT). Cells of the so-called hemogenic endothelium undergo major morphological changes, break away from neighboring endothelial cells and adopt a hematopoietic fate (Ottersbach, 2019) (Figure 1.1.1 B).

From E10.5, definitive HSCs are also found in the yolk sac, placenta, and fetal liver. While it has been ruled out that *de novo* formation of definitive HSCs occurs in the fetal liver (Johnson and Moore, 1975), this is not yet clear for the placenta (Gekas *et al.*, 2005). Both yolk sac and placenta do contribute to the HSC pool in the fetal liver, but it is not clear whether this is through *de novo* generation or an expansion of pre-existing AGM derived cells (Dzierzak and Speck, 2008).

The placenta harbors a favorable microenvironment for HSCs during development. The placenta is formed from two parts, the chorion and the allantois. Both parts are formed during early gastrulation, but initially develop independently of one another (Downs, 2002). The

slightly earlier developing chorion is comprised of an ectodermal part that rapidly expands as well as a mesodermal part that is less proliferative (Hernandez-Verdun, 1974; Ellington, 1987; Downs, 2002). The allantois on the other hand, originates in the epiblast (Gardner *et al.*, 1985; Downs, 2002) and is of mesodermal origin (Bonnevie, 1950; Downs, 2002). At approximately E8.5, the allantois, which is now expanded and highly vascularized, becomes attached to the chorion, forming the chorio-allantoic placenta (Downs, 2002). The placental vascular compartment of the fetus arises from the allantoic mesoderm, whereas the maternal components arise from the maternal vasculature and cells that line the uterus, so-called uterine decidual cells (Rossant and Cross, 2001). After chorio-allantoic fusion, folds in the chorion mark sites where fetal placental blood vessels grow in from the allantois to form the fetal components of the placental vasculature network (Rossant and Cross, 2001). Trophoblast cells start to branch and create a structure called the labyrinth. The maternal blood enters into small spaces of the labyrinth, ensuring material exchange between fetal and maternal blood systems. Subsequently, connection of the fetal placental vasculature to the umbilical artery and veins supplies the rest of the embryo with those materials (Rossant and Cross, 2001).

First definitive HSCs are found in the placenta around the same time as in the AGM region. It remains unclear where these cells originate. Studies have suggested limited numbers of HSCs in the umbilical artery, which like the placenta is derived from the allantoic mesoderm. It is possible that the allantoic mesoderm gives rise to HSCs and that *de novo* hemogenic activity extends into the placenta (Gekas *et al.*, 2005; Gekas *et al.*, 2010; Dieterlen-Lièvre *et al.*, 2010). Additionally, the placenta is connected to the dorsal aorta of the AGM region via the umbilical artery and since at no time point during development, large numbers of transplantable HSCs are found in the AGM, an expansion of immature HSCs from the AGM in other organs like the placenta is likely as well (Gekas *et al.*, 2005). In contrast to AGM and yolk sac, a large expansion of HSCs in the placenta can be seen at E12.5-13.5. During the third trimester, HSC numbers in the placenta decline while an expansion is seen in the fetal liver suggesting the migration of the HSCs from the placenta to the fetal liver via the umbilical vein (Ottersbach and Dzierzak, 2010). These kinetics are unique to the placenta and do not mimic activity in any other hematopoietic organ (Gekas *et al.*, 2005). Even though placental and fetal liver HSCs share similar surface marker expression, HSCs in either of the organs display unique functional differences. Unlike fetal liver HSCs, placental HSCs, whilst being pluripotent, do not promote definitive myelo-erythroid differentiation (Gekas *et al.*, 2005; Mikkola and Orkin, 2006). A role for the placenta as a lymphoid organ has also been suggested (Mikkola and Orkin, 2006) (Figure 1.1.1 C).

Another open question during development hematopoiesis is how the yolk sac contributes to the HSC pool in the fetal liver. Previous studies could show a colonization of HSCs from the yolk sac to the fetal liver starting at E12.5 (Kumaravelu *et al.*, 2002). Previous to fetal liver

colonization, between E8 and E10, the yolk sac only contains immature cells that are, however, capable of contributing to adult hematopoiesis upon transplantation into newborn mice and maturation (Toles *et al.*, 1989; Yoder and Hiatt, 1997; Yoder *et al.*, 1997; Kumaravelu *et al.*, 2002; Medvinsky *et al.*, 2011). The primary origin of these cells, however, remains unclear. A recent publication of Ganuza *et al.*, (2018) describes that while the yolk sac contains few precursors capable of maturing into definitive HSCs, it does not generate robust definitive HSC activity (Ganuza *et al.*, 2018). This would indicate that the yolk sac does not form *de novo* HSCs.

During the last phase of hematopoietic development, HSCs migrate to the fetal liver, expand and home to the BM around birth. The fetal liver is the main embryonic site for HSC expansion. The fetal liver does not produce HSCs *de novo*, but it is seeded by circulating HSCs and other hematopoietic cells (Houssaint, 1981; Johnson and Moore, 1975; Mikkola and Orkin, 2006). Initially, myelo-erythroid progenitors are found in the fetal liver at E9.5, while first HSCs do not appear until E11.5 (Mikkola and Orkin, 2006). After E12.5, the fetal liver is the main hematopoietic organ until HSCs home to the BM around birth. Between E12.5 and E16.5, HSCs in the fetal liver expand up to 1000-fold and start to differentiate to mature blood cells (Bowie *et al.*, 2007b; Bowie *et al.*, 2006; Morrison *et al.*, 1995; Gao and Liu, 2018; Ema and Nakauchi, 2000; Gao *et al.*, 2018). After E16.5, the number of HSCs plateaus and then declines (Ema and Nakauchi, 2000; Gekas *et al.*, 2005; Morrison *et al.*, 1995; Mikkola and Orkin, 2006). From E17.5 on, first functional HSCs are found in the BM (Christensen *et al.*, 2004; Gekas *et al.*, 2005; Mikkola and Orkin, 2006). Single-lineage progenitor cells seed the fetal liver at all times during development to ensure efficient production of differentiated blood cells for the embryo. During early gestation, primarily erythroid progenitors accumulate in the fetal liver, whereas, during later stages of gestation, this changes and more myeloid and lymphoid progenitors are found. (Mikkola and Orkin, 2006). However, how the fetal liver as a niche supports HSC expansion and differentiation is not clear yet. This organ provides a microenvironment that promotes rapid expansion of HSCs contrary to the BM, where HSCs are mostly quiescent. Transplant experiments showed a competitive advantage of fetal liver HSCs over adult BM HSCs when transplanted into recipient mice (Harrison *et al.*, 1997; Morrison *et al.*, 1995; Rebel *et al.*, 1996; Mikkola and Orkin, 2006). Understanding of the fetal liver niche and its mechanisms of expansion might prove valuable for successful HSC expansion *in vitro* (Gao *et al.*, 2018). The migration from fetal liver to BM is accompanied by a shift from highly circulating fetal HSCs to mostly quiescent self-renewing adult HSCs conveyed by a change in surface marker expression, one of those being the transient down-regulation of CD34 around 7 weeks of age and probable establishment of homeostatic BM hematopoiesis (Ogawa *et al.*, 2001; Mikkola and Orkin, 2006).

Thus, from first generation of definitive HSCs at E10.5 in the AGM to HSC expansion in the fetal liver before birth, HSCs pass through several hematopoietic organs including the placenta and yolk sac. Different hematopoietic sites pose unique microenvironments that support different aspects of HSC development and maturation. Remaining key questions of HSC development are the unknown migratory path that HSCs take from AGM to the fetal liver as well as potential sites of *de novo* HSC generation other than the AGM.

However, during hematopoietic development, surface marker expression of progenitor cells and definitive HSCs is transient, making the identification of cellular origin and tracking of the path these cells take through hematopoietic sites without the development of new *in vivo* tracing techniques challenging.

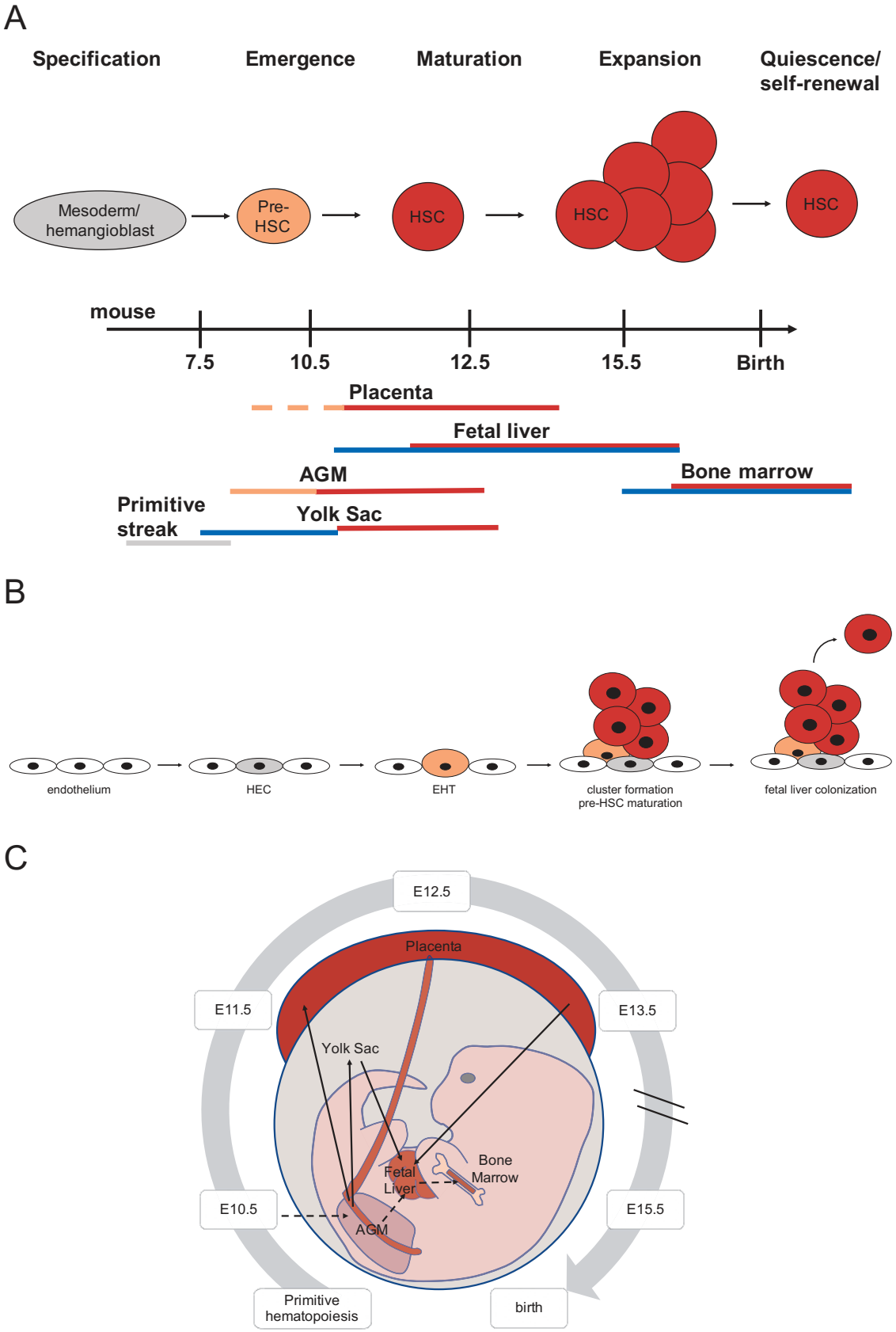


**Figure 1.1.1 Timeline of hematopoietic development.**
(A) Timeline of primitive and definitive hematopoiesis. Gray bars: primitive hematopoiesis from mesoderm/hemangioblast, blue bars: active hematopoietic differentiation, orange bars: pre-HSCs (broken orange bars: *de novo* HSC genesis not experimentally proven), red bars: presence of functional adult-type HSCs (adapted from Mikkola and Orkin, 2006). (B) Endothelial-to-hematopoietic transition (EHT), HEC: Hemogenic endothelial cells (adapted from Ottersbach, 2019). (C) Model of definitive HSC migration during development.

### *1.1.2. Functional assays for stem cells and progenitors*

In order to characterize and test functionality of HSCs, numerous *in vitro* and *in vivo* assays have been developed since Till and McCulloch (Till and McCulloch, 1961) first claimed the existence of this cell type in 1961. In this initial study, Till and McChulloch developed the first *in vivo* stem cell assay. They performed BM transplantation into irradiated recipient mice and quantified nodules or colonies of hematopoietic cells formed in the spleen of the recipient mice, a technique now called colony-forming unit-spleen (CFU-S). However, these cells colonizing in the spleen are not capable of long-term engraftment and the assay can therefore only be used to quantify short-term repopulating progenitor populations.

Today, *in vitro* assays are mainly used for a short-term readout of progenitor and stem cell function as *in vivo* assays are long-lasting, laborious and costly. Potential of progenitor cell populations is most commonly assessed by colony-forming unit (CFU) assays (Cashman *et al.*, 1983). Here, cells are cultured in semi-solid methylcellulose-based medium and the formation of defined colonies is observed after a certain period of time. Formation of mixed colonies containing all types of differentiated cells allows the retrospective identification of a multipotent progenitor as starting cell. Size and number of colonies is correlated to the potency of these progenitors. Other *in vitro* assays based on long-term BM cultures include the Cobblestone area forming assay (CAFC), where HSCs are cultured underneath a stromal layer and frequency of different hematopoietic cell subsets through cluster formation can be quantified (Ploemacher *et al.*, 1989) or the Long-term culture-initiating cell (LTC-IC) assay where cells are also grown on a stromal layer, but the endpoint is different to the CAFC. In the LTC-IC assay, the endpoint is the presence of progenitor cells with colony-forming potential (Sutherland *et al.*, 1989; van Os *et al.*, 2004). Both these assays have the ability to measure mouse primitive stem cell frequencies reliably *in vitro* (van Os *et al.*, 2004). Today, the LTC-IC is a well-established *in vitro* assay that relies on HSC self-renewal ability and differentiation capacity. This assay allows the detection of LTC-IC frequencies similar to HSCs quantified through *in vivo* transplantation assays (Woehrer *et al.*, 2013) and therefore serves as one of the best *in vitro* assays to investigate HSC potential.

To assess the function of HSCs, *in vivo* assays with long-term reconstitution ability as a read-out are the most robust and significant methods. The most frequently used *in vivo* assay to assess stem cell activity and function is transplantation, in which HSCs from donor mice are injected into lethally irradiated recipient mice. Since only HSCs are capable of reconstituting the entire hematopoietic system of the irradiated recipient mice indefinitely, this assay allows reliable investigation of long-term HSC reconstitution ability. Engraftment and long-term repopulation ability (LTRA) of donor HSCs is followed in the recipient through flow cytometry analysis of the blood over several months. To be able to differentiate between donor derived and recipient derived blood cells, one needs to be able to distinguish donor from recipient cells.

Different genetically modified systems can be used for this. One example is the use of mice with gene variations in the *Ptprc* gene which encodes the pan-hematopoietic surface marker CD45. C57Bl/6 (B6) mice carry the *Ptprc*$^{a}$ allele encoding the CD45.2 isoform of CD45 (in this study referred to as WT or WT CD45.2), whereas SJL mice carry the allele *Ptprc*$^{b}$ which encodes the isoform CD45.1. Backcrossing of B6 mice with SJL mice allowed the generation of a strain carrying the CD45.1 isoform on a B6 background (commonly referred to as B6.SJL-CD45.1, in this thesis referred to as WT CD45.1) (Shen *et al.*, 1985; Chisolm *et al.*, 2019). Either isoform can be specifically detected using monoclonal antibodies, allowing the discrimination between donor and recipient cells in transplantations. Additionally, through crossing of these strains, a third mouse line can be created carrying one allele of each *Ptprc* gene variation (here referred to as WT CD45.1/.2). This is useful in for example competitive transplantation studies were two different transplanted cell populations in addition to remaining recipient cells need to be distinguished.

HSCs have the potential to reconstitute the hematopoietic system over long periods of time, whereas multi-potent progenitors only reconstitute the system short to intermediate-term. This can be assayed through serial transplantation into secondary and tertiary recipients (Lemischka *et al.*, 1986). Variations of transplantation assays are used to investigate and compare stem cell frequencies of different genotypes, competitive advantage of HSCs of a specific genotype over a control population, or the clonal heterogeneity of a certain HSC pool. Limiting dilution assays allow the quantification of stem cell frequencies in a certain cell pool and the comparison of stem cell frequencies between different mouse genotypes. Here, lethally irradiated recipient mice are transplanted with different numbers of donor cells including a groups with very low cellular input. Analysis of the limiting number of cells required to successfully engraft and reconstitute the recipients permits the calculation of the frequency of HSCs in the starting cell pool (Szilvassy *et al.*, 1990; Taswell, 1984).

To compare the repopulating capacity of HSCs when in competition with HSCs of other genotypes, competitive transplantation assays are used (Harrison *et al.*, 1993). In this type of assay, cells from two different genotypes are transplanted together at a defined starting ratio into lethally irradiated recipients. Analysis of the repopulation of each genotype over time uncovers possible advantages in engraftment and repopulation capacity of one genotypic HSC over another.

More recently, single cell transplantation assays have been performed to uncover clonal heterogeneities on the level of the stem cells (Ema *et al.*, 2006; Dykstra *et al.*, 2007; Yamamoto *et al.*, 2013). Here, single HSCs are isolated and transplanted into lethally irradiated recipient mice. Analysis of engraftment efficiency and lineage output of a clonal hematopoietic system in the recipient over time permits retrospective characterization of the transplanted HSC.

### *1.1.3. Hematopoietic stem cell markers*

HSCs are of low abundance in the BM. Isolation is possible through marking specific surface antigens and detection of those via flow cytometry. Finding the most efficient marker strategy to enrich for these rare cells has been a long-lasting effort. In order to identify these surface markers, cells have to be isolated according to the potential markers and subsequently tested in functional assays to prove the enrichment for progenitors and stem cells. Already in the 1980s, it has been found that progenitors for certain mature blood lineages do not express specific lineage markers and therefore, excluding makers like B220 for the B cell lineage during isolation, could enrich for these progenitors (Muller-Sieburg *et al.*, 1986; Weissman and Shizuru, 2008). In 1988, Spangrude *et al*. were able to show that only hematopoietic cells expressing the surface antigen Stem cell antigen-1 (Sca-1) included HSCs (Spangrude *et al.*, 1988). Other identified markers include cKit (CD117) (Ogawa *et al.*, 1991; Morrison and Weissman, 1994), CD34 (Osawa *et al.*, 1996) and the so-called SLAM markers, including CD150 and CD48 amongst others. Together, these markers are used to further enrich for long-term repopulating HSCs (Kiel *et al.*, 2005) and allow to differentiate HSCs from downstream progenitors. Alternatively, using EPCR as an explicit HSC marker leads to similar engraftment and long-term repopulating capacity compared to this conventional marking strategy (Balazs *et al.*, 2006).

An alternative approach for stem cell identification was suggested by the Goodell lab, in which the DNA-dye Hoechst 33342 is used to identify HSCs as cells with high dye efflux and therefore low dye levels due to highly active membrane transport pumps in HSCs (Goodell *et al.*, 1996; Challen *et al.*, 2010). HSCs are mainly characterized by their functionality and not only by their surface phenotype. Upon inflammation or other stressors, surface marker expression can change and an isolation and identification solely based on surface markers needs to be carefully evaluated. In this thesis, highly enriched long-term repopulating adult HSCs under homeostasis are defined by $Lin^{-}Sca\text{-}1^{+}cKit^{+}CD150^{+}CD48^{-}CD34^{-}EPCR^{high}$.

During embryonic development, definitive HSCs change their surface marker expression gradually. Defining a single strategy to identify definitive HSCs during all stages of development is therefore not possible. Thus, marker strategies need to be adopted depending on the time-point of analysis. The earliest marker during embryonic development for hematopoiesis in general is the surface integrin CD41 (Ferkowicz *et al.*, 2003). Originally only used as a marker for the megakaryocytic lineage, CD41 was found to play a wider role during murine ontogeny (Mikkola *et al.*, 2003) and was identified as a marker for the onset of both primitive and definitive hematopoiesis (Ferkowicz *et al.*, 2003). From E9 yolk sac on, CD34 expression marks early HSCs throughout development until expression is lost in HSCs several weeks after birth (Ogawa *et al.*, 2001). The pan-hematopoietic marker CD45 only appears on

HSCs during late AGM stages (North *et al.*, 2002). Furthermore, CD48 is absent from HSCs throughout development and can therefore be used as a negative selection marker. Another SLAM marker, CD150 is only expressed on HSCs after the placenta stage and cannot be used for isolation of early definitive HSCs (McKinney-Freeman *et al.*, 2009). Moreover, cKit marks all HSC populations and can be used as early as E9 (Yoder *et al.*, 1997) (Figure 1.1.2).

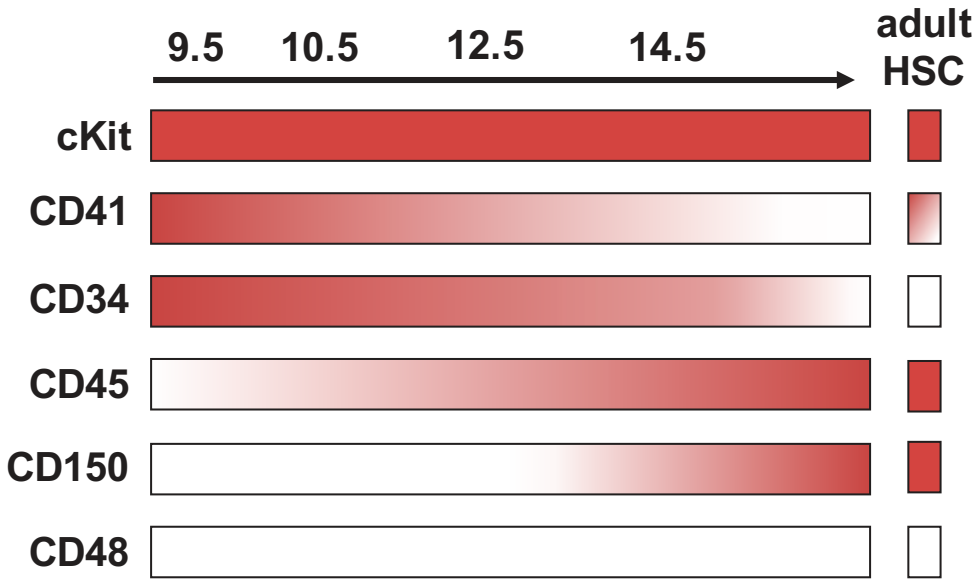


**Figure 1.1.2 Surface marker expression of definitive HSCs during development** and in the adult (adapted from McKinney-Freeman *et al.*, 2009).

### *1.1.4. Hematopoietic hierarchy*

The classical model of hematopoiesis describes a multi-potent self-renewing stem cell at the top of the hierarchy, and after multiple steps of differentiation, eventually giving rise to all types of mature blood cells. This suggests that cells while differentiating lose their lineage potential resulting in a tree-like hierarchy with defined branching points (Akashi *et al.*, 2000; Kondo *et al.*, 1997; Haas *et al.*, 2018). Most mature cells of the hematopoietic system are short-lived. The immediate demand to replenish lost cells due to injury, inflammation, or infection is initially met by progenitor populations with multi-, oligo-, or uni-potent potential. At the apex of the hematopoietic hierarchy, hematopoietic stem cells (HSCs) reside. These cells are long lived, show long-term self-renewal, and are capable of reconstituting all lineages of the hematopoietic system (multi-potent). HSCs give rise to multi-potent progenitors (MPPs) who give rise to more committed progenitors who then in turn give rise to mature blood cells (Orkin and Zon, 2008). However, HSCs at the top of the hierarchy only divide and differentiate infrequently. The majority of the time, these cells are in quiescence to ensure perpetuation of the hematopoietic system over a life-time.

Traditional views of the hematopoietic system describe a linear and stepwise differentiation of HSCs via MPPs towards more restricted oligo- and uni-lineage progenitors and eventually

mature blood cells (Kondo *et al.*, 1997; Akashi *et al.*, 2000)(Figure 1.1.3 A). However, more recent single-cell studies suggest that already the pool of HSCs is more heterogenous than originally thought and that hematopoiesis does not occur in a stepwise differentiation, but rather during a continuous gradual differentiation process (Buenrostro *et al.*, 2018; Velten *et al.*, 2017; Macaulay *et al.*, 2016; Zhang *et al.*, 2018). Even the most potent HSCs have now been suggested to already display biases towards certain lineage outcomes. At early time-points during differentiation, a cell can still change its commitment. The further a cell moves down the differentiation hierarchy, the more irreversible its state and lineage commitment becomes (Velten *et al.*, 2017; Carrelha *et al.*, 2018)(Figure 1.1.3 B).

Furthermore, the classical tree-like branched hierarchy suggests the differentiation from HSCs to mature blood cells via different progenitors. However, several independent studies have shown that certain mature blood lineages, like the megakaryocytic lineage, can already separate at the level of the HSCs suggesting a direct differentiation from HSCs to megakaryocytes (Woolthuis and Park, 2016; Notta *et al.*, 2016; Månsson *et al.*, 2007; Sanjuan-Pla *et al.*, 2013; de Sauvage *et al.*, 1996; Carrelha *et al.*, 2018; Zhang *et al.*, 2018; Yamamoto *et al.*, 2013; Haas *et al.*, 2015).

These studied also allowed the identification and revision of previous progenitor and stem cell populations. Previously only sub-categorized into long-term (LT) and short-term (ST) HSCs, newer studies also identified an intermediate-term (IT) HSCs, characterized by a self-renewal capacity hierarchically between LT- and ST-HSCs (Yamamoto *et al.*, 2013; Benveniste *et al.*, 2010; Zhang *et al.*, 2018). Moreover, the MPP compartment can now be divided into several different MPPs with differential lineage commitment (Wilson *et al.*, 2008; Pietras *et al.*, 2015; Zhang *et al.*, 2018).

Even though it is possible to dissect and enrich for different lineage-biased HSCs or MPPs based on surface marker expression of for example CD150 (Beerman *et al.*, 2010; Challen *et al.*, 2010; Morita *et al.*, 2010; Dykstra *et al.*, 2007; Sieburg *et al.*, 2006; Haas *et al.*, 2018; Wilson *et al.*, 2008) or CD41 in case of megakaryocytic-primed HSCs (Gekas and Graf, 2013; Haas *et al.*, 2015; Yamamoto *et al.*, 2018), the identification and dissection of the heterogeneity of the HSC pool was only possible with sophisticated single cell technologies. Most HSCs are able to differentiate into all blood lineages, however, only a small subset of HSCs displays a balanced lineage output (Haas *et al.*, 2018). The majority of HSCs display biases towards a certain lineage. Bulk analysis of this pool would not be able to distinctly identify specific lineage-biased HSCs (Carrelha *et al.*, 2018; Sanjuan-Pla *et al.*, 2013; Yamamoto *et al.*, 2013; Haas *et al.*, 2018).

Overall, these studies along with *in silico* reconstruction of developmental trajectories independent of defined surface markers indicate lineage commitment already early during the process of differentiation and the gradual acquiring of lineage-committed transcriptomic states

rather than distinct intermediate progenitor cell populations (Karamitros *et al.*, 2018; Macaulay *et al.*, 2016; Nestorowa *et al.*, 2016; Pina *et al.*, 2012; Tusi *et al.*, 2018; Velten *et al.*, 2017; Haas *et al.*, 2018). In addition, single cell assays allow tracing the lineage-fate of a single HSC over time and subsequent fate-mapping of these cells. These methods apply different marking strategies of HSCs (viral transduction or barcoding) and single cell transplantation or RNA sequencing to follow the offspring of a specific HSC clone over time and analyze its behavior (Rodriguez-Fraticelli *et al.*, 2018; Busch *et al.*, 2015). Thus, the traditional view of the hematopoietic hierarchy believed the HSC pool to be homogenous, however, these newly defined models uncovered heterogeneity at the level of stem cells not only in regards to lineage commitment.

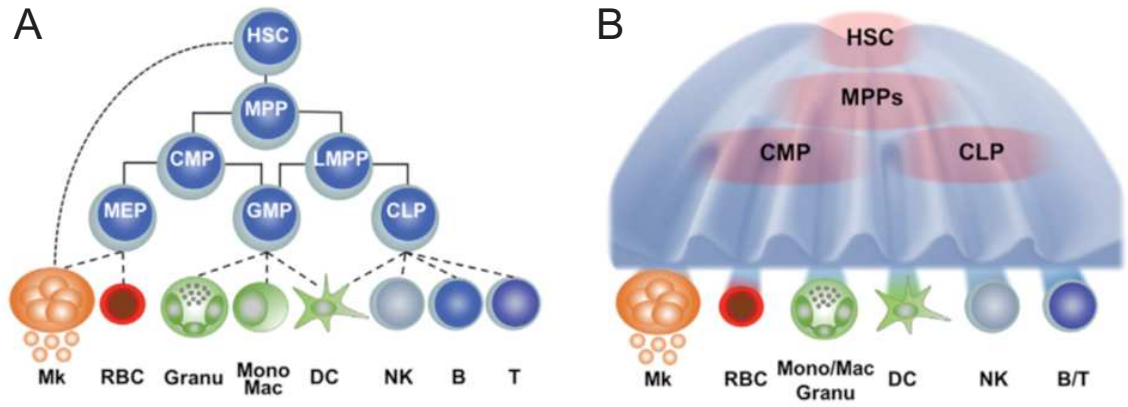


**Figure 1.1.3 Models of the hematopoietic hierarchy.**
(A) Traditional view of the hematopoietic hierarchy. (B) Continuous model of the hematopoietic hierarchy (adapted from Haas *et al.*, 2018).

### *1.1.5. HSC heterogeneity*

Even though heterogeneity within the pool of cells at the apex of the hematopoietic hierarchy has been discussed for decades, its functionality remained poorly understood (Jones *et al.*, 1990; Spangrude, 1992; Sieburg *et al.*, 2006; Dykstra *et al.*, 2007). Since then, heterogeneity in repopulation kinetics (Sieburg *et al.*, 2006; Muller-Sieburg *et al.*, 2012; Benz *et al.*, 2012), self-renewal abilities (Ema *et al.*, 2014), cell cycle status (Wilson *et al.*, 2008), and multi-lineage differentiation output (Verovskaya *et al.*, 2013; Haas *et al.*, 2015; Yamamoto *et al.*, 2018; Carrelha *et al.*, 2018) have been shown (Crisan and Dzierzak, 2016), suggesting not one cell type at the top of the hematopoietic hierarchy, but rather a heterogenous pool of phenotypically similar cells with differential functions, molecular characteristics, and cellular composition.

Certain specific subtypes of HSCs can be targeted with refined surface markers and defined transcriptional lineage-priming programs have been suggested (Haas *et al.*, 2015; Yamamoto *et al.*, 2013; Wilson *et al.*, 2008; Cabezas-Wallscheid *et al.*, 2014). Mechanisms causing or maintaining HSC heterogeneity include location in the bone marrow niche, endogenous

reporter expression, differing responsiveness to signaling pathways, epigenetic heterogeneity, or segregation of cell fate determinants (Crisan and Dzierzak, 2016; Haas *et al.*, 2018). Additionally, age of the hematopoietic system has been indicated to play a role. Some HSC subtypes cannot be found in the young hematopoietic system, however, seem to make up a large population in the aged system (Yamamoto *et al.*, 2018).

A distinct embryonic origin or different developmental microenvironments are also possible causes of HSC heterogeneity. Already cells isolated from the fetal liver display heterogeneity in regards to lineage output (Benz *et al.*, 2012; Crisan and Dzierzak, 2016), proposing an origin for this heterogeneity earlier during development. Moreover, fetal HSCs show differences in self-renewal properties over the developmental time course and compared to BM derived adult HSCs (Harrison *et al.*, 1997; Bowie *et al.*, 2007a; Crisan and Dzierzak, 2016). Only a small subset of gene signatures are shared between developing HSCs of the AGM and the adult BM definitive HSCs (Zhou *et al.*, 2016). Definitive HSCs migrate through different hematopoietic organs during fetal development. Each organ forms a unique microenvironment to the developing cells and might be at least partially responsible to establish certain heterogeneities. Intrinsic gene regulatory programs have been shown to play a role in HSC subtype appearance or behavior. Fetal liver-derived HSCs and BM-derived HSCs express specific transcription factors. For example, the transcription factor SOX17 is required for the maintenance of neonatal but not adult HSCs (He *et al.*, 2011; Kim *et al.*, 2007).

Another possibility is, that already during the earliest steps of HSC development, when early hematopoietic cells are formed from endothelial precursors, heterogeneity is established. Moreover, HSC generation from different cells-of-origin might contribute to the growing heterogeneity (Gekas et al., 2005; Gekas et al., 2010). It is widely accepted that at least a part of definitive HSCs are formed in the AGM region. Yet, other sites of *de novo* formation of HSCs cannot be completely excluded at this point. In the placenta, for example, high numbers of HSCs are found during development. It is controversial if these high numbers can be achieved alone through migration and expansion of AGM HSCs or if indeed the placenta or other surrounding tissues like the umbilical artery or the allantoic mesoderm harbor definitive HSC formation capabilities (Gekas et al., 2005; Ottersbach and Dzierzak, 2010; Dieterlen-Lièvre et al., 2010). Since definitive HSCs may be formed at different sites of the embryo during development, this spatial separation alone might already be a factor for the development of diverse HSC subtypes.

### 1.2. Hematopoietic stem cell niche

After birth, HSC primarily reside in the BM where the HSC pool and functioning hematopoiesis are maintained. In 1978, Schofield first hypothesized the existence of such a microenvironment in the BM that preserves the reconstituting ability of stem cells following Till and McCulloch's first stem cell experiments in the spleen (Schofield, 1978; Morrison and Scadden, 2014). Before, it had been shown that stromal and bone cells indeed impacted on HSCs (Dexter *et al.*, 1977; Lord *et al.*, 1975) and that heterologous cells were capable of regulating HSCs *in vivo* (Calvi *et al.*, 2003; Park *et al.*, 2012; Zhang *et al.*, 2003). Since then, many studies have focused on identifying components of the BM niche and understanding its complexity. Imaging of HSCs within the BM showed that the stem cells frequently localized adjacent to blood vessels, mostly sinusoidal vessels, indicating HSC maintenance in perivascular niches by endothelial or perivascular cells (Kiel *et al.*, 2005; Kiel *et al.*, 2007b; Sugiyama *et al.*, 2006; Morrison and Scadden, 2014). Following transplantation into irradiated recipients, however, HSCs mainly localized close to arteriolar vessels near the endosteum (Lo Celso *et al.*, 2009; Kiel *et al.*, 2007a; Morrison and Scadden, 2014). This might be partially due to sinusoid disruption during irradiation and arteriolar vessels being preserved (Hooper *et al.*, 2009; Morrison and Scadden, 2014).

The first heterologous cells shown to influence HSCs were the osteoblastic cells (Calvi *et al.*, 2003; Zhang *et al.*, 2003; Morrison and Scadden, 2014), yet, this might not be a direct effect. It is more likely that bone or bone-forming progenitors are able to promote maintenance or formation of HSC niches through recruitment of vasculature to the BM (Morrison and Scadden, 2014). Moreover, osteolineage cells elaborate cytokines and extracellular matrix (ECM) proteins and therefore regulate HSC function indirectly (Morrison and Scadden, 2014). Another critical cell type of the perivascular niche given the close location of HSCs to blood vessels, are the stromal cells. Multi-potent mesenchymal stem or stromal cells (MSCs) are a highly heterogenous pool of cells that surround blood vessels throughout the BM and are defined by their lineage differentiation into osteoblasts, adipocytes, and chondrocytes (Caplan, 1991; Friedenstein *et al.*, 1974; Park *et al.*, 2012). Through expression of genes like cytokine chemokine (C-X-C motif) ligand 12 (CXCL12) or stem cell factor (SCF), these cells mediate HSC maintenance and retention (Pinho *et al.*, 2013; Mendelson and Frenette, 2014).

Endothelial cells (ECs) are another cell type actively contributing to the perivascular BM niche. ECs promote HSC maintenance (Li *et al.*, 2004a; Morrison and Scadden, 2014) and BM sinusoidal ECs have been shown to support long-term reconstituting HSC expansion *in vitro* (Butler *et al.*, 2010; Kobayashi *et al.*, 2010; Morrison and Scadden, 2014). *In vivo*, ECs may regulate HSC directly and indirectly through synthesis of multiple factors like SCF that promote HSC maintenance and localization (Morrison and Scadden, 2014).

MSCs and ECs may be main contributors to the BM perivascular niche, but many other cell types are likely to directly or indirectly regulate this niche. Other cell types contributing to the niche include non-myelinating Schwann cells (Yamazaki *et al.*, 2011), osteoclasts (Adams *et al.*, 2006; Kollet *et al.*, 2006; Mansour *et al.*, 2012), sympathetic nerve cells (Katayama *et al.*, 2006; Méndez-Ferrer *et al.*, 2008), or other hematopoietic cells like macrophages (Chow *et al.*, 2011; Winkler *et al.*, 2010; Morrison and Scadden, 2014) (Figure 1.2.1).

More recently, specialized niches have been suggested within the BM for distinct types of HSCs and progenitor cells. Each unique niche might be shaped by multiple cell types, regulating HSCs differentially (Ding and Morrison, 2013). Moreover, HSC heterogeneity might in part be due to cellularly distinct niches. However, defining and identifying certain niche components with surface markers for imaging or flow cytometry remains challenging.

Imaging of the BM in particular remains challenging until today. Penetration of the bone without disturbing the underlying BM morphology poses a technical difficulty. Moreover, the complexity and heterogeneity of the BM niche make it difficult to specifically identify cellular subtypes and cell-cell interactions with the restriction of conventional filters and microscopes.

Even though to this day, more comprehensive overviews of the complexity of the niche are available through more sophisticated imaging techniques, like intravital microscopy and custom-build machines combining confocal and 2-photon microscopy (Lo Celso *et al.*, 2009) or 3-dimensional multicolor confocal imaging with multiplexing of up to 8 colors to identify rare cell types (Coutu *et al.*, 2018) in combination with reporter mouse models, and single cell transcriptomics data sets (Baccin *et al.*, 2020), the exact impact the niche or certain components and cells of the niche have on HSCs is not fully understood. HSCs behave differently *in vitro* and *in vivo*. The bone marrow microenvironment plays a big role in maintaining and mediating stem cell function and attempts to modulate artificial niches *in vitro* have made progress over the years, but have not been successful in mediating the same HSC function as *in vivo* (Torisawa *et al.*, 2014; Lim *et al.*, 2018). Further investigation is needed to be able to maintain and fully functionally characterize HSCs *in vitro*.

Upon hematopoietic stress, HSCs are activated, proliferate, and differentiate in order to replenish the lost cells of the hematopoietic system. Intrinsic mechanisms, micro-environmental interactions, and communication with surrounding cells have been shown to be involved in this HSC regulation and the following recovery of the system (Mendelson and Frenette, 2014). During homeostasis, the BM is the main niche for HSCs, however, other extramedullary sites of hematopoiesis exist and blood formation in sites like the spleen, the liver, the lymph nodes, or even sites like the heart, the adrenal glands, kidney, the pleural cavity or others can occur under various circumstances (Yamamoto *et al.*, 2016). Often, extramedullary hematopoiesis is however associated with hematological disorders like MPNs

(Craig *et al.*, 2004; Yamamoto *et al.*, 2016) or stromal abnormalities (Sohawon *et al.*, 2012; Yamamoto *et al.*, 2016).

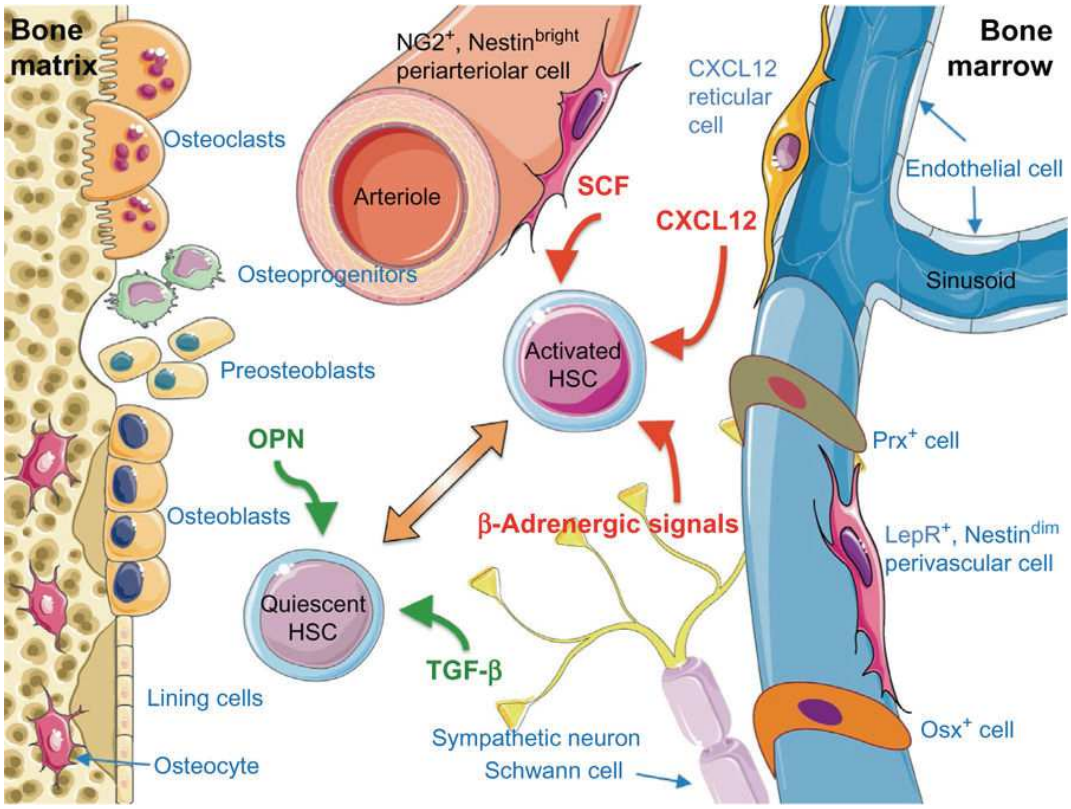


**Figure 1.2.1 Simplified model of the BM niche** with growth factors, cytokines, morphogens, ECM proteins, and adhesion molecules that regulate HSC behavior (Yu and Scadden, 2016).

### *1.2.1. Extracellular matrix*

Not only cellular components of the BM niche are involved in mediating the response to hematopoietic stress. The extracellular matrix (ECM) in the BM and cell adhesion proteins also play an important role both during the stress response as well as during regeneration (Lam *et al.*, 2011; Nakamura-Ishizu *et al.*, 2012; Mendelson and Frenette, 2014; Uckelmann *et al.*, 2016). The BM microenvironment contains a variety of ECM components categories like collagens, proteoglycans, and glycoproteins. These ECM molecules are not only mere supportive scaffolds in the BM, but are also involved in processes like cell adhesion, cell migration and homing, binding and presentation of cytokines, and regulation of cell growth (Klein, 1995). HSCs regulation and maintenance within the BM is mediated through both intrinsic and extrinsic cues and HSCs directly interact and adhere to niche surroundings, both cellularly and extracellularly, through expression of surface receptors like integrins (Ellis and Tanentzapf, 2010). The ECM-HSC interaction, however, is not only mediated from the side of the ECM to the HSCs, but HSCs themselves are also able to remodel their own niche in response to certain signals (Gattazzo *et al.*, 2014; Domingues *et al.*, 2017; Uckelmann *et al.*, 2016).

The ECM is indispensable for homeostatic maintenance of HSCs and functioning hematopoiesis. Under homeostasis, ECM molecules known to play a role in HSC regulation include Osteopontin (OPN, encoded by Spp1), Tenascin-C (TNC), Periostin (Postn), and Thrombospondin (Thbs1) (Domingues *et al.*, 2017; Klein, 1995). OPN plays a critical role for attraction, retention, and negative regulation of HSC proliferation and differentiation within the endosteal region of the bone marrow through interaction with integrins expressed on the surface of HSCs (Grassinger *et al.*, 2009; Domingues *et al.*, 2017). The glycoprotein TNC has been shown to affect several processes of HSC regulation like migration, homing, adhesion, lineage commitment, or reconstitution potential also through the integrin-ECM axis (Nakamura-Ishizu *et al.*, 2012; Ellis *et al.*, 2013; Domingues *et al.*, 2017). Postn has been shown to also play a role in regulation of HSC proliferation and quiescence (Khurana *et al.*, 2016; Cheng *et al.*, 2000; Domingues *et al.*, 2017). Thbs1 has been shown to be an adhesive ligand for developing hematopoietic cells (Klein, 1995).

During hematopoietic stress, HSCs are activated and start to proliferate to replenish lost blood cells. The role of the ECM in this process remains unclear. Previous data from our group identified the ECM adaptor protein Matrilin-4 (Matn4) as an important player in the stress-induced activation of HSCs. Highly expressed in long-term HSCs, Matn4 conferred a resistance to baseline stress stimuli. However, during acute stress, Matn4 is down-regulated, therefore releasing its protection, and allowing HSCs to proliferate. Part of this process is regulated through autocrine or intracellular mechanisms in the HSCs via the chemokine receptor CXCR4 (Uckelmann *et al.*, 2016). However, it is unlikely that only one component of the ECM mediates this HSC stress response and other ECM components will need to be studied for further understanding of this process.

## 1.3. HSCs under Stress

Hematopoietic stress like blood loss, inflammation, infection, chemotherapy, or radiation causes a rapid depletion of mature blood cells. These cells are replenished by the subsequent activation, proliferation and differentiation of HSCs. Moreover, emergency mechanisms at the highest level of the HSCs are in place to replenish lost cells rapidly without the need to differentiate via MPPs and other progenitors (Haas *et al.*, 2015). Previously, it has been thought that the HSCs get activated indirectly through feedback signals caused by the mature blood cell depletion. However, within the last decade, it has become clear that HSCs can also be directly activated through pro-inflammatory cytokines and participate in the primary immune response to both acute and chronic infections (Pietras, 2017).

### *1.3.1. Interferons*

One of those pro-inflammatory cytokines capable of activating HSCs directly is interferon (IFN). First discovered in 1957 (Isaacs and Lindenmann, 1957; Isaacs *et al.*, 1957; Lindenmann *et al.*, 1957), IFNs can be subcategorized into type I (IFN$\alpha$ and IFN$\beta$ and other species specific IFNs), type II (IFN$\gamma$), and type III (IFN$\lambda$) interferons, depending on their specific signaling receptors and pathways (Pestka *et al.*, 1987; Pestka *et al.*, 2004; Platanias, 2005). Once bound to its receptor, type I IFNs induce a phosphorylation cascade including Janus kinases (JAKs), tyrosine kinases (TYKs), and signal transducer and activators of transcription (STATs). Phosphorylated STATs in-turn relocate to the cell nucleus, bind to an Interferon-stimulated response element (ISRE) and transcription of Interferon-stimulated genes (ISGs) is induced (Darnell *et al.*, 1994; van Boxel-Dezaire *et al.*, 2006; Platanias, 2005). Type II and III IFNs signal through similar pathways as type I IFNs, but in the case of type II IFNs this does not include TYKs (Platanias, 2005; Sadler and Williams, 2008) (Figure 1.3.1). Additionally to the classical JAK-STAT pathway, it has been shown that IFNs are able to signal through a multitude of other pathways, including the p38-MAPK pathway (Li *et al.*, 2004b) or the PI3K/mTOR pathway (Lekmine *et al.*, 2003).

Production of type I IFN is possible by almost any cell type in the body when stimulated through transmembrane or cytosolic receptors (Trinchieri, 2010). Cytosolic receptors are activated upon recognition of viral or other autologous nucleic acids (Kawai and Akira, 2010; Trinchieri, 2010). Certain cell types, macrophages and dendritic cells (DCs) among others, rely on signaling through so-called pattern-recognition receptors (PRRs), one of those being the Toll-like receptors (TLRs), to produce type I IFN. These receptors in-turn detect pathogen-associated molecular patterns (PAMPs), particles of foreign pathogens, and induce an innate immune response (Kawai and Akira, 2010).

Initially thought to mainly have pro-inflammatory and immunomodulating effects, IFN$\alpha$ and other IFNs also display a variety of anti-inflammatory properties (Tilg and Peschel, 1996;

Boscá *et al.*, 2000; Mühl and Pfeilschifter, 2003). Both properties can be of therapeutic use in the treatment of chronic inflammatory diseases (Borden *et al.*, 2007; Benveniste and Qin, 2007) or certain types of cancers and myeloproliferative neoplasms (MPNs) (Hasselbalch and Holmstrom, 2019; Borden *et al.*, 2007; Kujawski and Talpaz, 2007). However, these conflicting properties can cause serious side effects. Pro-inflammatory effects of IFN$\alpha$ have been suggested to induce type I diabetes (Stewart *et al.*, 1993; Tilg and Peschel, 1996), cause development of acute arthritis (Kiely and Bruckner, 1994; Tilg and Peschel, 1996) or worsen autoimmune diseases (Gutterman, 1994; Tilg and Peschel, 1996).

Initially, it was believed that IFN$\gamma$, the only type II IFN, was exclusively produced by certain subsets of T cells and natural killer (NK) cells (Bach *et al.*, 1997; Young, 1996; Schroder *et al.*, 2004). However, it has been shown that type II IFN can also be produced and secreted by B cells and professional antigen-presenting cells (APCs), such as monocytes/macrophages and DCs (Harris *et al.*, 2000; Frucht *et al.*, 2001; Gessani and Belardelli, 1998). Macrophages induce an innate immune response through activation of TLRs and downstream signaling cascades. IFN$\gamma$ has been reported to play a role in priming macrophages for an improved response to bacterial infections (Jurkovich *et al.*, 1991; Lorsbach *et al.*, 1993; Schroder *et al.*, 2004).

Upon viral or bacterial infection, interferons are released, activation of an immune response is mediated, and infected cells are cleared. Regarding the impact of this response on HSCs, contradictory results have been reported (Boettcher and Manz, 2017). While it has been shown that IFN$\alpha$ and IFN$\gamma$ can induce quiescent HSCs to enter cell cycle (Essers *et al.*, 2009; Sato *et al.*, 2009; Baldridge *et al.*, 2010), others claim an anti-proliferative effect of IFN$\gamma$ on HSCs (de Bruin *et al.*, 2013). Moreover, different effects of IFN on HSCs *in vitro* and *in vivo* have been reported, suggesting other factors or the bone marrow microenvironment in addition to IFN being involved in the activation (Pietras *et al.*, 2014; Boettcher and Manz, 2017; Prendergast Á *et al.*, 2017; Essers *et al.*, 2009; Uckelmann *et al.*, 2016). Additionally, the effect IFN on HSCs is dependent on time (Demerdash *et al.*, in preparation; Essers *et al.*, 2009), dependent on acute, multiple, or chronic IFN exposure, and dependent on IFN dose (Essers *et al.*, 2009; Walter *et al.*, 2015; Baldridge *et al.*, 2010). During the inflammatory response, activated HSCs display immediate transcriptomic changes that are reversible once the HSCs go back to quiescence, however, long-term epigenetic changes or an epigenetic memory have been suggested (de Laval *et al.*, 2020).

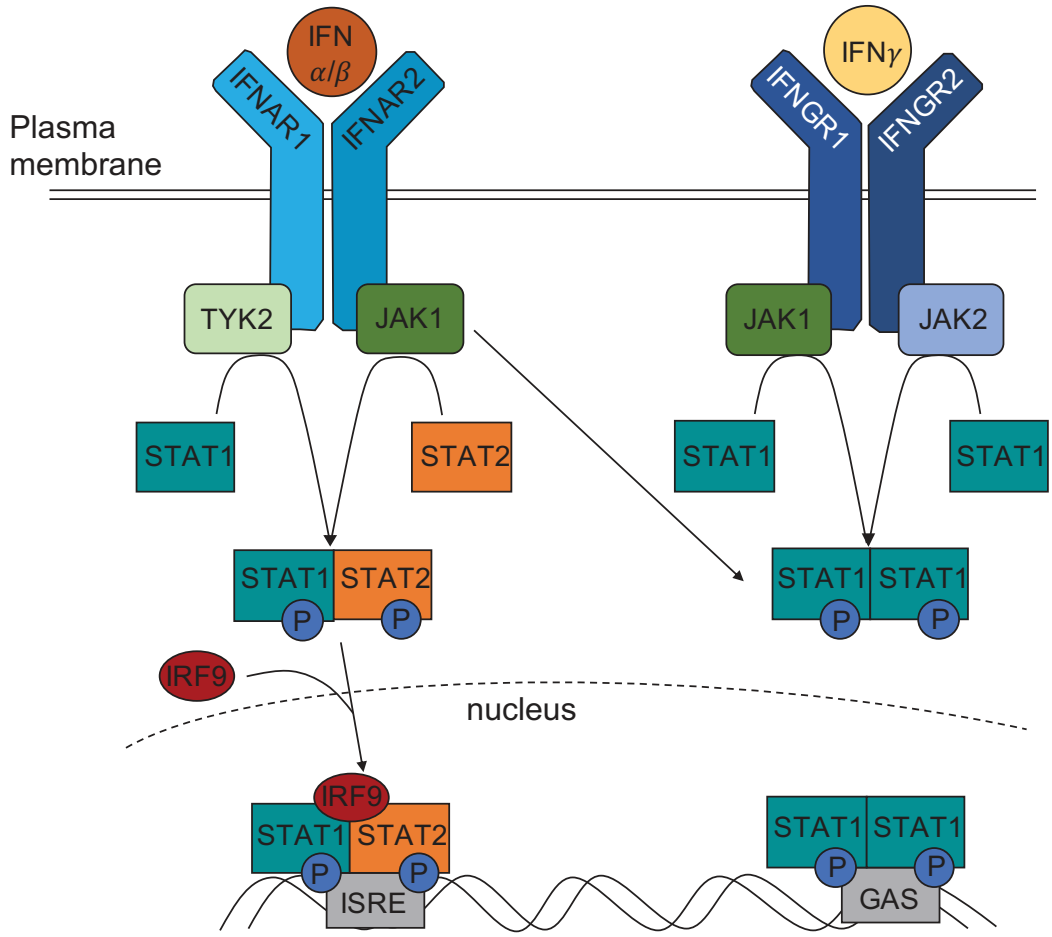


**Figure 1.3.1 Model of type I, II, and III IFN inflammatory signaling pathways through IFNAR and IFNGR** (adapted from Baldridge *et al.*, 2010).

### *1.3.2. Interferon-stimulated genes*

Upon pathogen detection, production and release of Interferons, neighboring cells sense the cytokines and in-turn induce the expression of ISGs. In brief, IFNs bind to their respective receptors which in-turn leads to conformational changes that induces phosphorylation of JAK and STATs followed by interaction with IFN regulatory factor (IRF) 9 to form the ISG factor 3 complex. This complex translocates to the nucleus, binds ISRE upstream of ISGs in the genome and induces the transcription of ISGs (Levy *et al.*, 1989; Kanno *et al.*, 1993; Levy *et al.*, 1988; Darnell, 1997; Schneider *et al.*, 2014). Several hundred ISGs are known to be induced upon binding of type I IFN to its receptor and the downstream signaling cascade (Der *et al.*, 1998; de Veer *et al.*, 2001). And yet, only few of these genes are directly linked to mediating an antiviral state (de Veer *et al.*, 2001; Schoggins *et al.*, 2011). The majority of ISGs seem to only mediate a response to viral infections indirectly, for example by encoding PRRs for the detection of viral components or transcription factors resulting in increased IFN production (Sadler and Williams, 2008).

The downstream response to detection of IFN is rapid. This is due to a baseline supply of most key players of the pathway without the need to produce large amounts before responding.

Interestingly, many of these signal-transducing proteins like JAK2 or STAT1/2 are ISGs themselves and are increasingly produced during infections and therefore reinforce the IFN response (Schneider *et al.*, 2014). ISG activity is complex and covers a wide range of different functions. Known direct or indirect functions include targeting pathogen life cycle, cell-cell communication, return to cellular homeostasis, and induction of apoptosis (Schneider *et al.*, 2014).

Following successful clearance of the infection, cellular desensitization to IFN is necessary to prepare the cells for a novel insult. Certain cell-intrinsic mechanisms are in place including receptor endocytosis (Coccia *et al.*, 2006). Cell-extrinsic mechanisms include inhibition of JAK-STAT signaling pathway through ISG-mediated desensitization (Schneider *et al.*, 2014).

ISGs are important antiviral effectors and IFN-based therapies have been used in the clinical to treat a number of viral infections. One family of viral restriction factors are the IFITM (IFN-inducible transmembrane) proteins (Huang *et al.*, 2011; Schneider *et al.*, 2014). Ifitms were some of the earliest identified ISGs (Friedman *et al.*, 1984; Bailey *et al.*, 2014). Ifitms are induced by both type I and II IFNs, however, have been shown to be expressed in most cells at basal levels (Friedman *et al.*, 1984; Huang *et al.*, 2011). Even though most members of the family display viral restriction properties, each member displays selectivity towards certain viruses. For example, IFITM1 effectively inhibits SARS-coronavirus, Ebola and Marburg, whereas IFITM3 has been shown to be most efficient against influenza A virus (Huang *et al.*, 2011). Cellular localization has been suggested as a factor in mediating these specificities. IFITMs are enriched in late endosomes and lysosomes and consistently, viruses that require transit to these compartments are most effected by IFITMs (Feeley *et al.*, 2011; Schneider *et al.*, 2014). Viruses that enter at the cell surface are not as affected by IFITMs (Feeley *et al.*, 2011). However, IFITM3 has been shown to also restrict infection with a nonenveloped virus (Anafu *et al.*, 2013). Several models have been suggested for the mechanisms of viral restriction of IFITMs. One suggests the alteration of kinetics of endosome acidification, which might lead to increased nonspecific protease activity and potentially explain the inhibition of both enveloped and non-enveloped viruses (Schneider *et al.*, 2014). Other models suggest inhibition by changing physical properties of membranes such as curvature or fluidity (Li *et al.*, 2013; Schneider *et al.*, 2014). Other examples of ISGs with known antiviral effects include members of the tripartite motif (TRIM) family, murine myxovirus resistance 1 (Mx1), genes involved in the OAS-RNaseL pathway or tetherin (encoded by Bst2) (Schneider *et al.*, 2014).

Thus, out of the hundreds of ISGs identified so far, most do not show direct antiviral activity, but might rather play an indirect role during the inflammatory response or even a role independent of the clearance of infection or inflammation.

### *1.3.3. Interferons during steady-state hematopoiesis*

Even though IFNs and ISGs play an important role during the fight against infections, it has been shown that also during homeostasis, basal levels of inflammatory signals are present. On the one hand, it is important to provide a baseline of ISG expression to be able to mediate a viral response more rapidly. On the other hand, the baseline inflammatory signaling might be due to the constant inflammatory stimulation deployed by latent bacteria and viruses of the microbiome (King and Goodell, 2011).

In recent years, not only was it shown that inflammatory signaling directly impacts on and regulates HSCs during infection (Essers *et al.*, 2009; Baldridge *et al.*, 2010), but also that HSCs and other tissue stem cells are highly resistant to viral infections, a phenomenon that has been indicated to be mediated through high basal levels of intrinsic ISGs expression in these cells (Wu *et al.*, 2018). Differentiated cells provide low baseline levels of ISG expression in order to activate response pathways quickly upon infection (Schneider *et al.*, 2014). In stem cells, this might not be the case. It is possible that the higher baseline of ISG expression in multipotent cells is a mechanism to avoid viral infection altogether. In addition to high ISG expression, stem cells seem to rely on other IFN-independent antiviral resistance mechanisms including RNA interference and epigenetic repression (Maillard *et al.*, 2013; Wu *et al.*, 2019b).

It has become clear that ISG signatures in stem cells potentially have a different function and underlying mechanisms than in differentiated cells. To improve the understanding of general HSC biology, investigation of ISG signatures in stem cells is therefore of great interest. Moreover, high baseline ISG expression in stem cells is not restricted to the hematopoietic system. Starting from embryonic stem cells, this high expression has also been observed in neuronal stem cells, and pancreatic stem cells amongst others (Wu *et al.*, 2018), suggesting specific stem cell-related functions of these signatures.

Recent data from our group also confirmed this in the hematopoietic system. The more undifferentiated the hematopoietic cell population, the higher the baseline ISG signature (Figure 1.3.2 A). Interestingly, using ISG expression as variables recapitulated the traditional hematopoietic hierarchy in a principal component analysis (PCA) (Figure 1.3.2 B). To investigate this difference in ISG levels in the hematopoietic system we used two independent reporter mouse models for homeostatic type I IFN response genes (IFITM3-eGFP) and more general type I IFN signaling (ISRE-eGFP), respectively (Figure 1.3.2 C) to recapitulate the expression data in WT mice. Both mouse models showed high reporter expression in HSCs with a decrease in reporter intensity upon differentiation (Figure 1.3.2 D). In the first mouse model, an eGFP was inserted into the gene locus near the promotor region of the antiviral response gene IFITM3 (Lange *et al.*, 2008). During the response to infection, activation of an IFN-stimulated response element (ISRE) leads to transcription and expression of ISGs. The second mouse model, in which eGFP was cloned upstream of the ISRE element, therefore

served as a more general IFN signaling model. Limiting dilution experiments with these mouse models underlined the powerful indicator of ISG activity for stemness. Upon transplantation of IFITM3-eGFP$^{hi}$ or IFITM3-eGFP$^{lo}$ lineage-negative cells, 1 in 260 IFITM3-eGFP$^{hi}$ cell showed successful engraftment in mice versus only 1 in every 15,000 IFITM3-eGFP$^{lo}$ cells. In the ISRE-eGFP model, this was even more pronounced with 1 in every 50 cells of ISRE-eGFP$^{hi}$ transplanted lineage-negative cells being able to engraft in the recipient mouse (Figure 1.3.2 E).

Systematic analysis of known components of the type I IFN signaling pathway showed that the homeostatic IFN baseline is mediated at least in part through HSPC intrinsic IFNAR and STAT1 signaling. Comparing ISG expression in HSCs of WT and several different knock-out (KO) mice showed a significant down-regulation of ISGs upon knock-out of IFN signaling pathway components and tumor-necrosis factor receptor 1 and 2 (TNFR1/2) and up-regulation of ISGs upon knock-out of pattern-recognition receptor (PRR) pathway components. This data suggested that the lack of PRRs like STING or MyD88 leads to a compensation through up-regulation of type I IFN signaling. Analysis of competitive chimeras of 50% wildtype cells and 50% IFNAR$^{-/-}$ or STAT1$^{-/-}$ cells revealed that IFN signaling pathway deficient HSCs still down-regulate ISG expression even though extrinsic signals from WT HSCs remain present, suggesting HSC intrinsic regulation (Figure 1.3.2 F) (Hirche *et al,* in preparation).

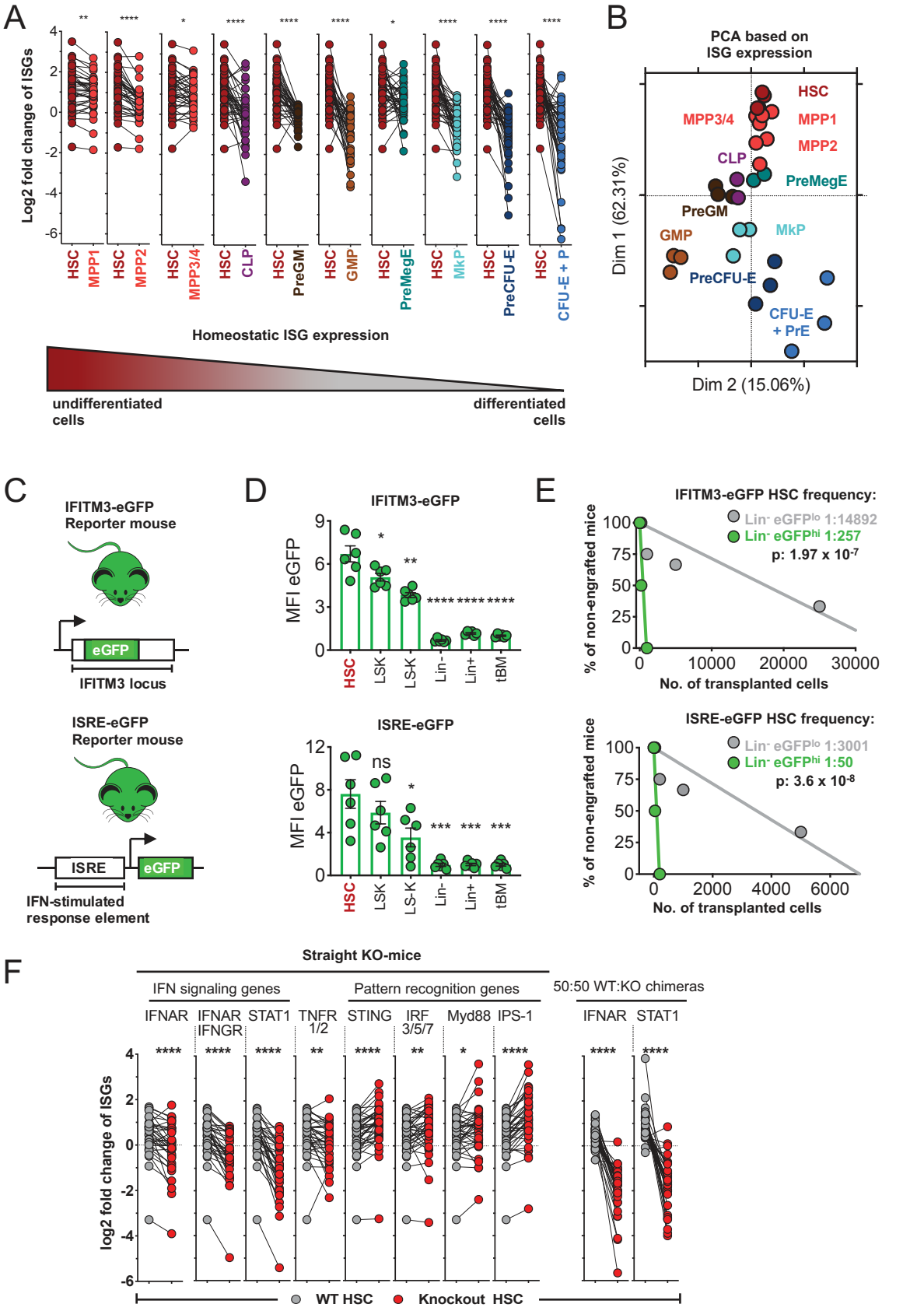


**Figure 1.3.2 Homeostatic IFN signaling baseline corresponds with hematopoietic differentiation and is mediated through cell intrinsic IFNAR /STAT1 signaling pathways.**
(A) Transcriptional profiling of 40 ISGs in stem and progenitor cells, n = 3 per cell type, mean expression values relative to cKit$^+$ progenitors are indicated and corresponding genes are connected by lines. (B) Principle component analysis of cell populations of (a) with ISGs as variables (left panel) and comparative schematic illustration of the hematopoietic differentiation hierarchy (right panel). (C) Illustration of IFITM3-eGFP (upper panel) and ISRE-eGFP

(lower panel) reporter mouse models. (D) Quantification of mean fluorescence intensity (MFI) of IFITM3-eGFP cell populations (upper panel) and ISRE-eGFP cell populations (lower panel) n = 6 per experiment. Dashed lines serve as reference to mean MFI of HSCs. (E) Limiting dilution of IFITM3-eGFP$^{low}$ (eGFP$^{lo}$) and IFITM3-eGFP$^{high}$ (eGFP$^{hi}$) (upper panel), or ISRE-eGFP$^{lo}$ and ISRE-eGFP$^{hi}$ (lower panel) lineage-negative bone marrow cells. Cell numbers indicated were transplanted and engraftment (cut-off at 1%) was assessed 12 weeks post transplantation, n = 3-4 mice per cell number. (F) Transcriptional profiling of ISGs in HSCs of wildtype (wt) and straight knockout mice (left panel), or of wt and knockout HSCs from 50:50 wt:knockout bone marrow chimeras (right panel), n = 3 per mouse genotype, mean expression values relative to wt cKit$^{+}$ progenitors are indicated and corresponding genes are connected by lines. If not indicated otherwise, data are represented as mean and standard error of the mean, and statistics were calculated by a two-tailed student's t test (ns, not significant; * $p \leq 0.05$; ** $p \leq 0.01$; *** $p \leq 0.001$; **** $p \leq 0.0001$) (Hirche *et al.,* in preparation).

### *1.3.4. IFN signaling heterogeneity and inheritance from HSCs to mature cells*

In recent years it has become clear that the pool of HSCs is heterogeneous (see 1.1.5 HSC heterogeneity) in regards to cell cycle status, lineage commitment and output, and self-renewal ability amongst others. In the immune system the importance of heterogeneity of cellular response upon viral infection has long been acknowledged. For example, IFN signaling is not induced in all virus-infected cells and not all cells actively contribute to clearance of the infection (Talemi and Hofer, 2018; Leviyang and Griva, 2018; Rand *et al.*, 2012; O'Neal *et al.*, 2019). However, most of these studies rely on mathematical modeling to understand the stochasticity of the IFN-mediated antiviral response. How this heterogeneity is established and maintained on a biological level, remains unclear. Most studies also do not take into consideration a potential role for HSCs in maintaining heterogeneity of the immune response. The previous data from our lab suggest, that heterogeneity in IFN signaling plays an important role in HSCs. In the previously discussed reporter mouse models, in addition to an inter-cell type specific heterogeneity of the reporter with higher expression in undifferentiated cells, reporter expression was also heterogeneous within one cell type. Analyzing different cellular compartments of the hematopoietic system always showed that only part of the cells expressed high levels of the reporter while others did not, even though these cells were otherwise phenotypically the same (Figure 1.3.3 A, left panel). Surprisingly, this reporter level status was stably inherited upon transplantation of HSCs to all downstream progeny, including mature blood cells. Reporter-high expressing HSCs generated an exclusively reporter-high expressing hematopoietic system upon transplantation and reporter-low expressing HSCs vice versa. Stable inheritance of this reporter status was shown until tertiary transplantation in both reporter mouse models (data here only shown from IFITM3-eGFP mice, selected cell types, and primary transplantation) (Figure 1.3.3 A, right panel, Figure 1.3.3 B).

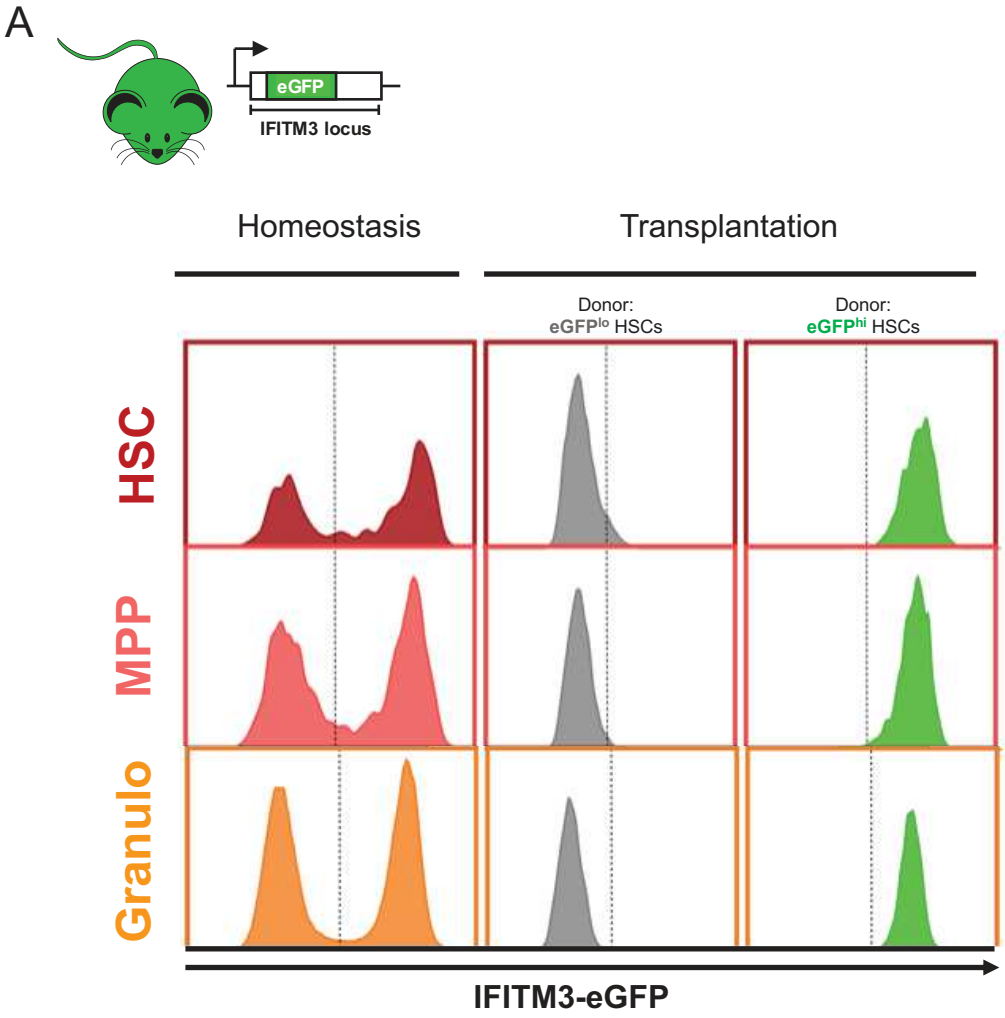


**Figure 1.3.3 IFN priming is stably inherited throughout hematopoiesis.**
30 IFITM3_low and IFITM3_high Lin$^-$Sca1$^+$cKit$^+$CD150$^+$CD48$^-$CD34$^-$EPCR$^+$ LT-HSCs were transplanted into lethally irradiated mice WT mice. (A) 12 weeks post transplantation, IFITM3-eGFP expression was determined in indicated populations, and compared to homeostatic IFITM3 expression (HSC: Lin$^-$Sca-1$^+$cKit$^+$ (LSK) CD150$^+$CD48$^-$, MPP: LSK CD150$^+$CD48$^+$, Granulocytes (Granulo): B220$^-$CD4/8$^-$CD11b$^+$Gr1$^+$). (B) 12 weeks post transplantation, IFITM3-eGFP$^{hi}$ cells deriving from IFITM3-eGFP$^{hi}$ or IFITM3-eGFP$^{lo}$ LT-HSCs cells were quantified (HSC: LSK CD150$^+$CD48$^-$, MPP: LSK CD150$^+$CD48$^+$, PreGM: Lin$^-$Sca-1$^-$cKit$^+$ (LS$^-$K) CD16/32$^-$CD150$^-$CD105$^-$, GMPs: LS$^-$K CD16/32$^+$, PreMegE: LS$^-$K CD16/32$^-$CD150$^+$CD105$^-$ , CFU-E + Pre Ery: LS$^-$K CD16/32$^-$CD150$^-$CD105$^+$, Granulocytes: B220$^-$CD4/8$^-$CD11b$^+$Gr1$^+$, B cells: B220$^+$, T cells: CD4/8$^+$) (Hirche *et al.,* in preparation).

# 2. AIM OF THE THESIS

During hematopoietic stress, IFNs and ISGs play an important role in mediating the stress response of the hematopoietic system. However, it has also been shown that IFNs and ISGs are present and expressed in the hematopoietic cells at baseline even without inflammation or infection. Baseline IFN signaling in these cells is heterogenous both between cell types as well as within a defined cell type. This thesis aims to uncover three major aspects of this baseline IFN signaling heterogeneity.

Stably present already in hematopoietic cells isolated from embryos during late gestation, the first aim of this thesis is to uncover the origin of IFN signaling heterogeneity during embryonic, hematopoietic development (**aim 1**) to give further insights into the preservation and regulation of this heterogeneity.

Our data strongly indicated that IFN signaling heterogeneity is stably inherited from stem cells to downstream progeny. However, why this heterogeneity is needed in different compartments of the hematopoietic system remains unclear. Therefore, the second aim of my thesis is to reveal the function of IFN signaling heterogeneity at the level of the stem cells as well as in differentiated cells (**aim 2**). These experiments will also be crucial to understand the implications this heterogeneity has in the development, maintenance, or treatment of hematological malignancies.

In order to target IFN signaling heterogeneity as a tool during the treatment of malignancies, it is important to understand how this baseline signaling is established and mediated at the molecular level. The third aim of this study is hence to uncover the mechanisms behind mediation and maintenance of IFN signaling heterogeneity in the hematopoietic system (**aim 3**).

In addition, in the final part of my thesis I aimed to better understand the role of the extracellular matrix (ECM) in the stress-induced activation of HSCs (**aim 4**). Previous data from our group revealed Matrilin-4 as a key player in mediating the HSC response to inflammatory stress (Uckelmann *et al.*, 2016). Here, we aimed to further analyze the interaction of the ECM and HSCs upon inflammatory stress in order to improve the understanding of HSC activation and interaction with the niche under stress.

In summary, the general aim of my thesis is to understand the establishment, maintenance and role of IFN signaling heterogeneity in the hematopoietic system as well as the HSC stress response. Uncovering these aspects of hematology will have far reaching implications in the understanding of general biological processes of stem cells and the immune system in health, disease, and upon infection.

# 3. RESULTS

## 3.1. The origin of interferon signaling heterogeneity in the hematopoietic system

### *3.1.1. IFN signaling heterogeneity in E13.5 fetal liver cells*

Recent studies showed that inflammatory signaling not only regulate differentiation and proliferation of adult HSCs, but that different inflammatory cytokines also play an active role during embryonic HSC emergence and maturation. For example, IL6 secreted by HSC-independent myeloid cells significantly impacts on HSC generation through Notch-mediated IL6R activation in zebrafish (Tie *et al.*, 2019). Similarly, activation of Notch and NF-$\kappa$B signaling through TNF$\alpha$/TNFR2 (Espin-Palazon *et al.*, 2014) and IFN$\gamma$ signaling downstream of Notch signaling (Sawamiphak *et al.*, 2014) regulate definitive HSC emergence and fate in zebrafish. During maturation of definitive HSCs in the mouse embryo, HSCs found in the AGM display lower levels of IFN$\alpha$-mediated Jak-Stat1 signaling compared to fetal liver HSCs (Kim *et al.*, 2006). Additionally, mouse embryos lacking IFN signaling were shown to have significantly fewer AGM HSPCs (Li *et al.*, 2014), however adult mice lacking IFN signaling do not show any changes in functional HSCs, suggesting that the lower number of AGM HSPCs during development is corrected later on. Given that IFN signaling has been shown to affect definitive HSCs number and function during embryonic development, it is likely that IFN signaling heterogeneity is also already established here.

In the adult hematopoietic system, IFN signaling heterogeneity is stably maintained at the level of HSCs and inherited over hundreds of generations to downstream progeny. To investigate the origin of this heterogeneity, we decided to investigate IFN signaling during the development of the hematopoietic system in the embryo. First, fetal liver cells from E13.5 IFITM3-eGFP reporter embryos were analyzed. In this mouse model, an eGFP was inserted into the gene locus of the antiviral response gene IFITM3 near the promotor region (Lange *et al.*, 2008). After E12.5, the fetal liver is the main hematopoietic organ until around E16.5 when migration to the BM starts (Ema and Nakauchi, 2000; Gekas *et al.*, 2005; Mikkola and Orkin, 2006). Analysis at E13.5 allows the investigation of an already rapidly expanding pool of HSCs while these cells are not migrating to the BM yet. This data was compiled by Simon Haas and Christoph Hirche from our group and formed the basis for my PhD study.

In the adult, heterogenous levels of ISG expression were seen under homeostasis and transplantation of IFITM3-eGFP$^{hi}$ or -eGFP$^{lo}$ HSCs showed a stably maintenance of this reporter status in the recipient mice. To analyze if fetal HSCs are already capable of maintaining their reporter status and inherit this to downstream mature blood cells, lineage$^-$ cKit$^+$ (LK) hematopoietic stem and progenitor cells (HSPCs) were isolated from E13.5 IFITM3-

eGFP fetal livers, separated according to reporter-high (eGFP$^{hi}$) and -low (eGFP$^{lo}$) expressing cells, and transplanted into lethally irradiated adult recipients (Figure 3.1.1 A). 12 weeks post transplantation, eGFP-reporter status was analyzed in donor-derived cell populations (Figure 3.1.1 B). Comparable to results obtained from transplantation experiments with adult stem cells, mice transplanted with reporter-high expressing HSPCs, exclusively gave rise to blood cells with high reporter expression and vice versa. Even though the reporter-high expressing cells displayed some heterogeneity in the degree of reporter expression, nevertheless, these cells always expressed the reporter at higher levels than cells generated by the initially reporter-low expressing fetal liver cells (Figure 1.3.3 B). The lack of reporter expression in B and T cells is the result of IFITM3 not being expressed in these cell types.

In conclusion, this experiment showed that IFN signaling heterogeneity was already present in HPSCs in the E13.5 fetal liver and additionally, can again be stably transplanted into adult recipients. To further investigate the origin of this heterogeneity, it was therefore necessary to analyze IFN signaling heterogeneity during earlier stages of hematopoietic development.

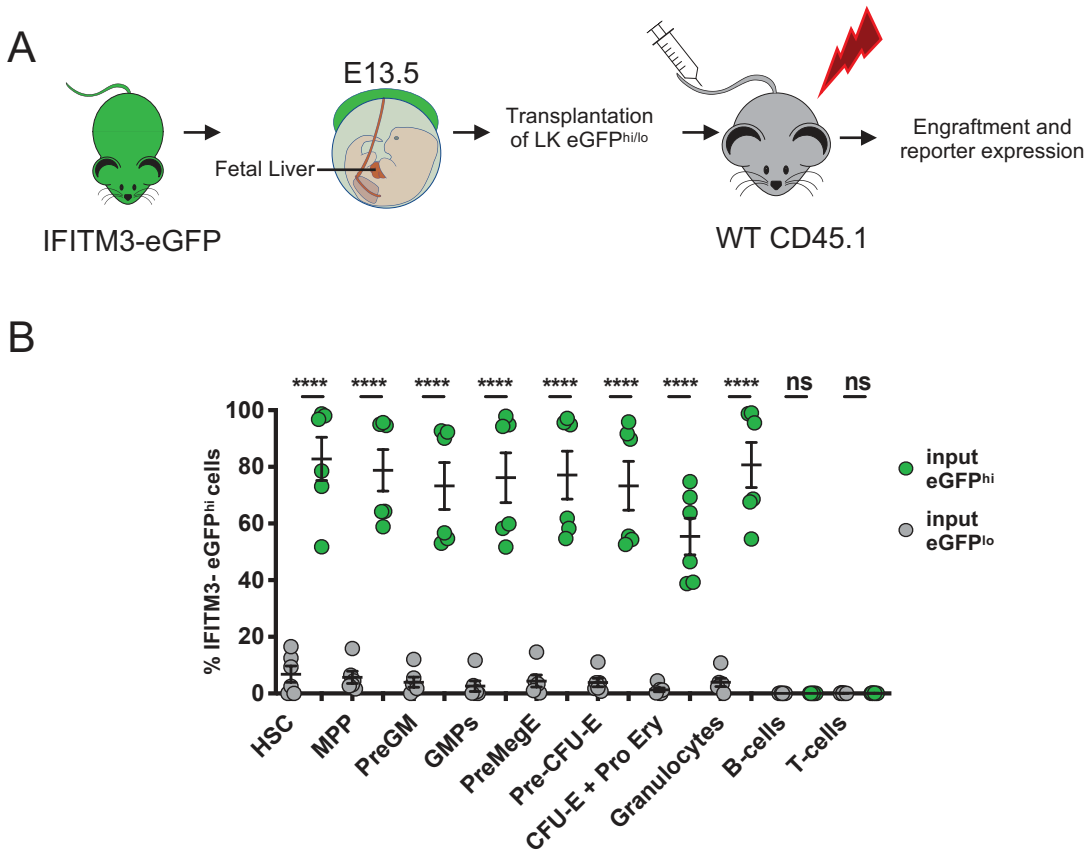


**Figure 3.1.1 At 13.5, IFITM3-eGFP fetal liver cells already display IFN signaling heterogeneity**.
(A) Schematic overview of the experimental setup: E13.5 fetal liver cells were isolated from pregnant IFITM3-eGFP reporter mice, Lin$^-$cKit$^+$ (LK) eGFP$^{hi/lo}$ cells were isolated with flow cytometry and transplanted with supporting cells into lethally irradiated adult recipients. (B) 12 weeks post transplantation, IFITM3-eGFP$^{hi}$ cells derived from transplanted IFITM3-eGFP$^{hi}$ or IFITM3-eGFP$^{lo}$ LK cells were quantified (HSC: Lin$^-$Sca-1$^+$cKit$^+$ (LSK) CD150$^+$CD48$^-$, MPP: LSK CD150$^+$CD48$^+$, PreGM: Lin$^-$Sca-1$^-$cKit$^+$ (LS$^-$K) CD16/32$^-$CD150$^-$CD105$^-$, GMPs: LS$^-$K CD16/32$^+$, PreMegE: LS$^-$K CD16/32$^-$CD150$^+$CD105$^-$ , CFU-E + Pre Ery: LS$^-$K CD16/32$^-$CD150$^-$CD105$^+$, Granulocytes: B220$^-$CD4/8$^-$CD11b$^+$Gr1$^+$, B cells: B220$^+$, T cells: CD4/8$^+$).

### *3.1.2. The level of ISG expression is organ and cell type specific during hematopoietic development*

To investigate the origin of IFN signaling heterogeneity in the hematopoietic system, we first analyzed IFN signaling in the different embryonic organs that harbor hematopoietic cells during development. HSPCs in the E13.5 fetal liver cells already showed stable IFN signaling heterogeneity. Thus, we decided to investigate IFN signaling heterogeneity one developmental day earlier.

First, hematopoietic cells were isolated from E12.5 embryos to test the expression of the different published markers for HSPCs on cells isolated from the different hematopoietic organs. The goal was to find a set of markers, which can be used uniformly to isolated HSPCs from different organs at this time point. E12.5 as an initial time point was chosen, because this allowed us to isolate efficient numbers of HSPCs from AGM, yolk sac, placenta, and fetal liver. Earlier time points would not allow for an efficient isolation of cells from the fetal liver, whereas at later developmental time points, all HSPCs will have migrated from the AGM to the other sites. Cells were isolated from all four of those organs of E12.5 IFITM3-eGFP embryos (Figure 3.1.2 A) to confirm that our cells of interest were present in all analyzed organs, even though, only few remaining HSCs were found in the AGM at this time point (Figure 3.1.2 B).

To be able to target and isolate definitive HSCs from first appearance (E10.5) in the AGM to arrival in the fetal liver (E13.5) with the same marking strategy, we decided to test the marker combination $CD48^{-}CD41^{+}cKit^{+}CD34^{+}$. CD41 is a marker that marks the initiation of definitive hematopoiesis and is expressed from E8.5 on in the yolk sac and from E9.5 on in the vitelline and umbilical vessels, shortly before the onset of definitive hematopoiesis. Expression of CD41 on HSPCs in the embryo can be detected until late fetal liver stages, when expression in HSCs is decreased. $CD41^{+}$ isolated embryonal cells give rise to various definitive colony types, including mixed colonies in *in vitro* colony-forming assays (Mikkola *et al.*, 2003), suggesting hematopoietic multi-lineage potential. In the adult hematopoietic system, CD41 expression is restricted to a stem-like megakaryocyte-committed progenitor and myeloid-bias HSCs (Haas *et al.*, 2015; Gekas and Graf, 2013) and mature cells of the megakaryocytic lineage. cKit serves as a global HSC marker that can be used at all times during development as well as the adult for isolation (North *et al.*, 2002; McKinney-Freeman *et al.*, 2009). Co-expression with CD34 has been suggested to further enrich for definitive hematopoietic stem cell activity, however, this is exclusive for murine hematopoietic development. In the adult mouse, long-term repopulating HSCs are found in the $CD34^{-}$ population (Ogawa et al., 2001, Mikkola et al., 2003). CD48 is a member of the SLAM family receptors and can be used to negatively mark HSCs both during development and through adult hematopoiesis (Kim *et al.*, 2006; Kiel *et al.*, 2005; Mikkola and Orkin, 2006). Thus, to test the gating, $CD48^{-}CD41^{+}cKit^{+}CD34^{+}$ cells (from here on called $cKit^{+}CD34^{+}$ or HSCs) and a control population of $CD48^{-}CD41^{+}cKit^{-}CD34^{-}$ blood

cells (from here on called cKit$^-$CD34$^-$ or blood cells) were isolated from different organs. The control population only expresses CD41 and therefore still includes hematopoietic cells with various progenitor potential (Ferkowicz *et al.*, 2003), but lacks stem cell potential due the exclusion of cKit and CD34 expression.

Definitive HSCs and blood cells were detectable in all four organs using this gating strategy (Figure 3.1.2 B) and further analysis was performed using these markers. The level of IFITM3-eGFP-reporter expression, here quantified as mean fluorescent intensity (MFI), showed significant organ-specific differences when compared to AGM. AGM reporter expression was always used as a baseline here, since HSCs isolated from this organ represent the most immature developmental stage of definitive HSCs compared to the other organs. Even though all of these cells display characteristics of definitive HSCs, those found in the AGM have not matured, migrated, and expanded to the extend cells from the other organs have. MFI was used as a mean to analyze overall reporter expression in these cells. A separation of IFITM3-eGFP$^{hi}$ and IFITM3-eGFP$^{lo}$ cells at this time point of development was not possible. Bi-modality of the reporter was seen in E13.5 fetal liver cells and is maintained in the adult system, yet not in E12.5 embryos.

HSCs isolated from placenta and fetal liver expressed the reporter significantly lower than those from AGM. In the blood cells, expression of the reporter is significantly lower than AGM in all isolated organs. (Figure 3.1.2 C). Sca-1 is a surface antigen most commonly known as a marker for adult HSCs (Spangrude *et al.*, 1988). However, Sca-1 is also an ISG and was used as a reference to assess ISG expression during the isolation of the cells. Interestingly, Sca-1 expression also showed organ-specific patterns. While Sca-1 expression in HSCs from the yolk sac and fetal liver was still significantly lower than in HSCs from the AGM, HSCs from the placenta expressed Sca-1 at significantly higher levels (Figure 3.1.2 D, left panel). Expression of Sca-1 in yolk sac and fetal liver blood cells again was significantly lower than AGM cells. Expression of Sca-1 in either cells of the placenta here did not significantly change from AGM cells (Figure 3.1.2 D, right panel). Comparing the reporter expression in HSCs (cKit$^+$CD34$^+$) with the expression in blood cells (cKit$^-$CD34$^-$) showed significant differences in both reporter expression (Figure 3.1.2 E) as well as Sca-1 expression (Figure 3.1.2 F). Regardless of the organ of isolation, HSCs always showed significantly higher expression of the reporter. The same holds true for Sca-1 expression, with the exception of fetal liver where no significant difference in Sca-1 expression were observed between the cell types. In conclusion, expression of the Ifitm3-eGFP reporter and Sca-1 are specific to organ of isolation and depending on the isolated cell type. The data suggests HSCs to have higher baseline IFN signaling than blood cells and overall, placenta HSCs to have the highest Sca-1 expression.

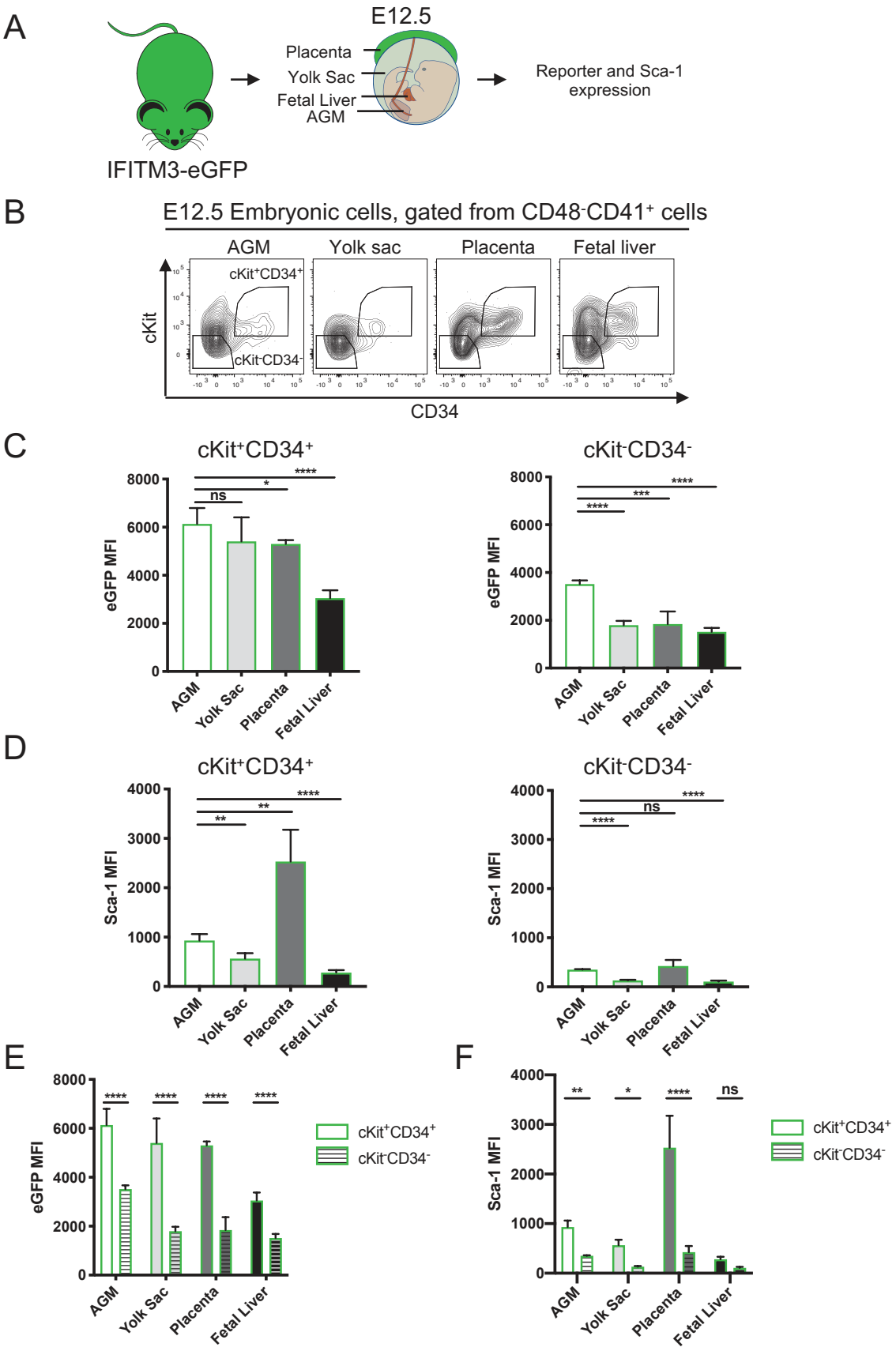


**Figure 3.1.2 HSC isolated from different embryonal organs at E12.5 show differential ISG expression.**
(A) Schematic overview of the experimental setup: E12.5 embryos were isolated from pregnant IFITM3-eGFP reporter mice. Embryonal organs were digested, HSCs ($CD48^-CD41^+cKit^+CD34^+$) and other blood cells ($CD48^-CD41^+cKit^-CD34^-$) were sorted, and eGFP and Sca-1 mean fluorescent intensity (MFI) was analyzed. (B) Example gating of embryo-derived HSCs and blood cells from four embryonal organs at E12.5. (C) MFI of the IFITM3-eGFP reporter was compared between HSCs ($cKit^+CD34^+$) and blood cells ($cKit^-CD34^-$) from different organs. (D) MFI of

Sca-1 was compared between between HSCs ($cKit^+CD34^+$) and blood cells ($cKit^-CD34^-$) from different organs. (E) MFI of the IFITM3-eGFP reporter was compared between HSCs ($cKit^+CD34^+$) and blood cells ($cKit^-CD34^-$). (F) MFI of Sca-1 was compared between HSCs ($cKit^+CD34^+$) and blood cells ($cKit^-CD34^-$).
Unpaired t-test analysis was performed comparing control cells and HSCs. In case of multiple comparisons, p-values were corrected by the Benjamini-Hochberg method with FDR = 5% (*, $p<0.05$, **, $p<0.01$, ***, $p<0.001$, ****, $p<0.0001$, ns, not significant). Mean ± SD, $n\geq3$.

To confirm these findings independent of the reporter system, the same analysis was performed using E12.5 wildtype (WT) embryos (Figure 3.1.3 A). Sca-1 fluorescent intensity was analyzed in HSCs ($cKit^+CD34^+$) and blood cells ($cKit^-CD34^-$) from different organs and compared to the level of Sca-1 in AGM. AGM is used as a baseline here, because this organ harbors the earliest confirmed definitive HSCs starting from E10.5. It is also likely that cells isolated from the AGM later during development did not migrate through other hematopoietic sites yet and might therefore be characterized as most immature definitive HSCs. Similar to the results in the IFITM3-eGFP reporter mice, the level of Sca-1 was exclusive for each organ and each cell type (Figure 3.1.3 B). Comparing the levels of Sca-1 in HSCs to blood cells showed higher levels in Sca-1, however, this was only significant in placenta (Figure 3.1.3 C). Moreover, placenta-derived HSCs showed much higher levels of Sca-1 than HSCs in any other organ or compared to blood cells.

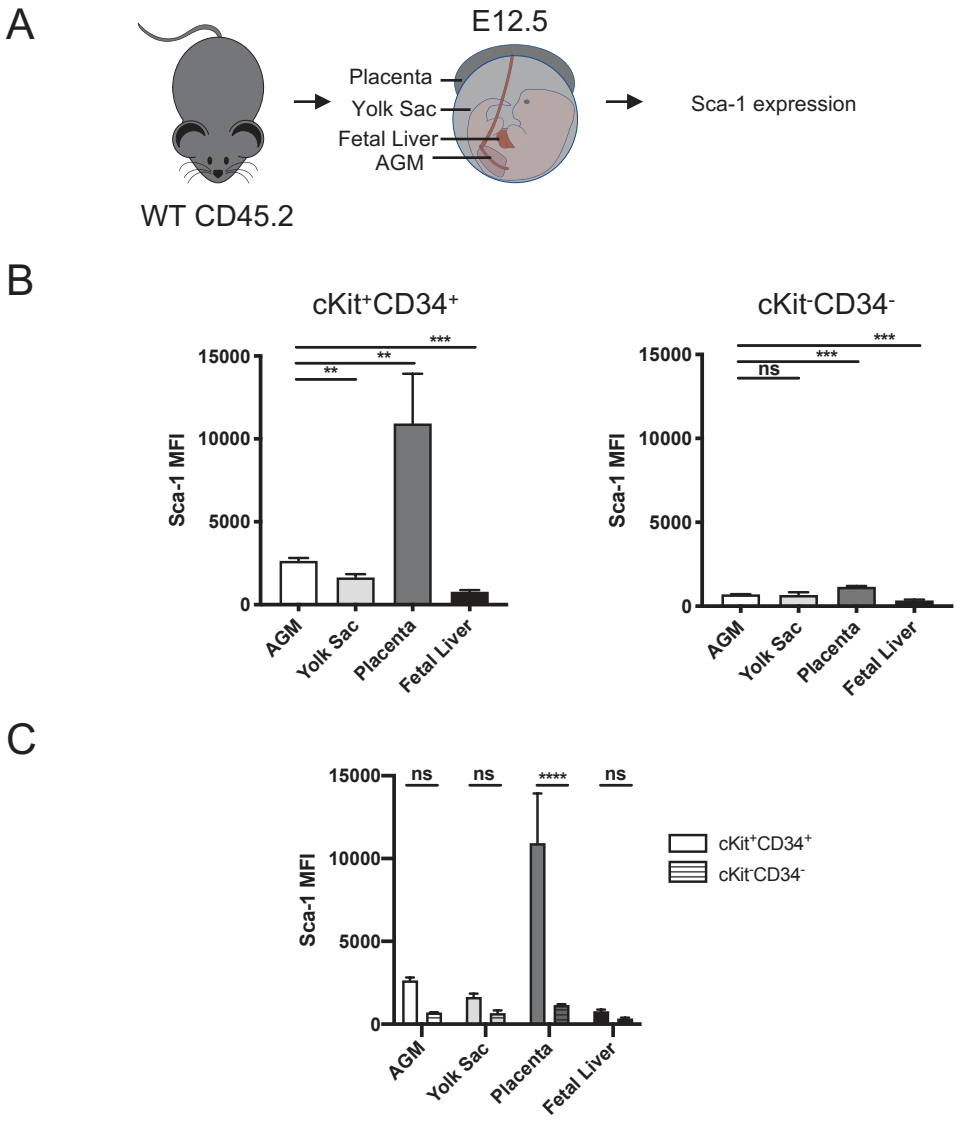


**Figure 3.1.3 Embryo-derived HSCs of WT mice show higher Sca-1 expression than blood cells at E12.5.**
(A) Schematic overview of the experimental setup: E12.5 embryos were isolated from pregnant WT mice. Embryonal organs were digested, HSCs ($CD48^-CD41^+cKit^+CD34^+$) and blood cells ($CD48^-CD41^+cKit^-CD34^-$) were sorted, and Sca-1 fluorescent intensity was analyzed. (B) MFI of the Interferon-stimulated gene (ISG) Sca-1 was compared between organs. (C) MFI of ISG Sca-1 was compared in HSCs and blood cells isolated from different organs.
Unpaired t-test analysis was performed. In case of multiple comparisons, p-values were corrected by the Benjamini-Hochberg method with FDR = 5% (*, p<0.05, **, p<0.01, ***, p<0.001, ****, p<0.0001, ns, not significant). Mean ± SD, n≥3.

Thus, these data suggest that at E12.5, organ and cell type specific ISG patterns exist. However, in this initial experiment, merely the expression of the two ISGs Ifitm3 and Sca-1 were analyzed. To be able to draw more general conclusions on ISG expression in the hematopoietic cells, analysis of larger sets of ISGs was necessary. Again, HSCs and blood cells from E12.5 WT embryos were isolated via flow cytometry and after RNA extraction and reverse transcription, the expression of a set of 42 ISGs was analyzed through qPCR. The set of 42 ISGs was chosen based on microarray analysis comparing BM HSCs of PBS- and IFN-treated adult WT mice. The 42 ISGs were amongst the most differentially expressed genes in the HSCs of the IFN-treated group. Relative fold change was calculated with normalization to

a separately sorted $CD48^{-}CD41^{-}$ negative population from AGM cells. This population is undefined by surface markers and includes any cells isolated from this organ to represent baseline IFN signaling independent of cell type. Results from the yolk sac are not shown here. Previously, it was not clear if yolk sac derived progenitors contribute to definitive hematopoiesis, which is why we initially included this organ in the analyses. However, recent findings from researchers in the lab of Shannon McKinney-Freeman (Ganuza *et al.*, 2018) describe the lack of repopulating potential of cells isolated from the yolk sac, suggesting no HSC activity or contribution to adult hematopoiesis from this organ. Here, we wanted to understand the origin of IFN signaling heterogeneity, which in the adult is stably present at HSC level. Since cells from the yolk sac do not contribute to this HSC pool and engraftment of yolk sac-derived cells in later experiments proved to be challenging, analysis from now on was mainly focused on other developmental organs.

As already suggested by the data from Ifitm3 and Sca-1, comparing HSCs and blood cells within each organ (Figure 3.1.4 A) showed differential expression of ISGs. In the AGM, overall ISG expression was significantly higher in HSCs than in blood cells, however, placenta and fetal liver did not show significant differences between blood cells and HSCs. Even though comparing the two cell populations within each organ did not show a specific pattern of ISG expression, comparing the expression between organs did again reveal a clear pattern (Figure 3.1.4 B). Regardless of blood cells or HSCs, the overall expression of the ISGs was always significantly higher in cells from the placenta compared to cells from AGM or fetal liver (Figure 3.1.4 B).

Next, we investigated if these patterns were time specific or independent of developmental time point. Thus, HSCs were isolated from AGM, placenta, and fetal liver of WT embryos from E10.5 to E13.5. At all analyzed times, HSCs from the placenta exhibited the overall highest expression of ISGs (Figure 3.1.4 C), indicating that this ISG pattern is not time point but rather organ specific. Calculating the median expression (median of relative fold change) of all analyzed ISGs confirmed these results (Figure 3.1.4 D). At all analyzed time points, median relative expression of the ISGs was highest in HSCs from the placenta compared to HSCs from the AGM or fetal liver. These data showed that the high IFN signaling in the placenta was not only mediated by a few exceptionally highly expressed ISGs, but that the baseline ISG signaling overall was higher.

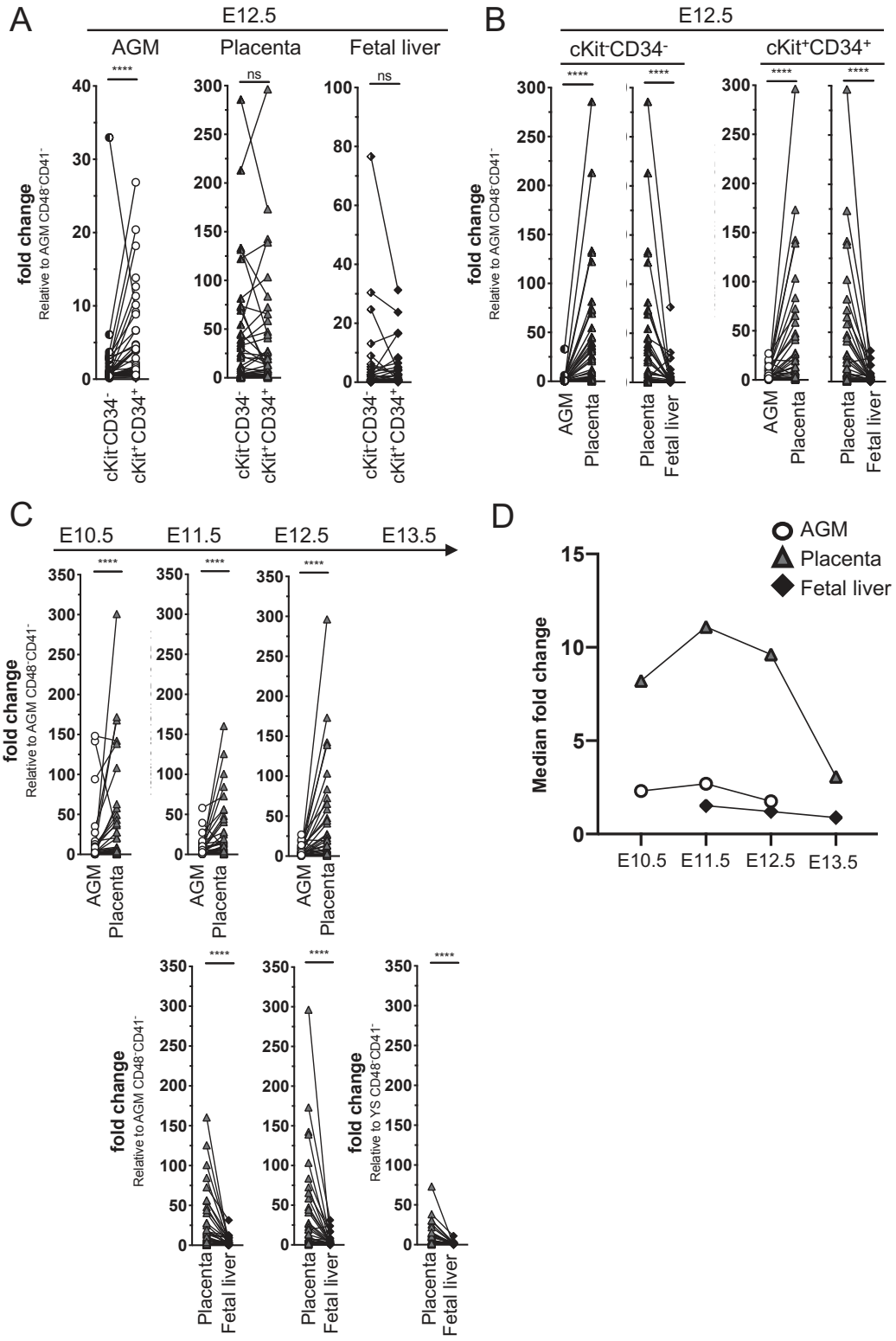


**Figure 3.1.4 ISG expression of embryo-derived HSCs of WT mice show differences depending on organ, cell type, and timepoint of isolation.**

(A) Fold change expression of 42 ISGs by qRT-PCR of blood cells ($CD48^-CD41^+cKit^-CD34^-$) and HSCs ($CD48^-CD41^+cKit^+CD34^+$) from E12.5 wildtype embryonal organs, relative to $CD48^-CD41^-$ cells from AGM, which includes hematopoietic and non-hematopoietic cells. (B) Fold change expression of 42 ISGs relative to $CD48^-CD41^-$ cells from AGM by qRT-PCR. Comparison of HSCs and blood cells between different organs at E12.5. (C) Fold change expression of ISGs relative to $CD48^-CD41^-$ cells from AGM (E10.5-E12.5) or yolk sac (E13.5) by qRT-PCR of HSCs ($CD48^-CD41^+cKit^+CD34^+$) of E10.5-E13.5 wildtype embryonal organs. (A-C) Each symbol represents expression of a single ISG. (D) Median of fold change of expression of ISGs over time.

Sdha, Oaz1, and Actin-beta were used as reference genes. Statistical test was performed as Wilcoxon matched-pairs signed rank test. (*, $p<0.05$, **, $p<0.01$, ***, $p<0.001$, ****, $p<0.0001$, ns, not significant), $n\geq3$.

After consulting with developmental hematologists, we realized that the previously used gating strategy for embryo-derived definitive HSCs ($CD48^-CD41^+cKit^+CD34^+$) only enriches for hematopoietic stem cell activity and does not represent a stringent gating for HSCs. Therefore, an alternative marking strategy for a higher enrichment of definitive embryo-derived HSCs was tested. Instead of CD34 as a positive marker for HSCs, CD45 was tested. In the adult system, CD45 is used as a pan-hematopoietic marker. In the embryo, CD45 has been shown to be exclusively expressed in $CD41^+$ cells, but its expression on these cells appears 1 to 2 days later than CD41 (Mikkola *et al.*, 2003). Even though hematopoietic activity can be found in both $CD45^-$ and $CD45^+$ cells in combination with other markers, CD45 can be used as a marker for definitive hematopoiesis (North *et al.*, 2002; Mikkola *et al.*, 2003). Previously, the $cKit^-CD34^-$ blood cell population was not very well defined and most likely included a large variety of different cell types, both hematopoietic and non-hematopoietic. Already early during development, cKit expression can be used as a marker for stem cell activity and a new reference population consisting of $cKit^-CD45^+$ cells will be used in this new panel. This population still includes $CD45^+$ hematopoietic cells, but excludes stem cells, and will from now on be called blood cells. The panel was once more tested on E12.5 embryos and identifiability of the cell populations from all four organs of interest was confirmed (Figure 3.1.5 A). Further, Sca-1 expression was again successfully utilized as control marker for HSCs compared to the Sca-1 low control cells (Figure 3.1.5 B).

The previous time course experiment was repeated (see Figure 3.1.4) to analyze ISG expression of embryonal organs over time. At E12.5, HSCs ($cKit^+CD45^+$) from all organs showed trends towards higher Sca-1 expression compared to blood cells ($cKit^-CD45^+$). Additionally, both HSCs and blood cells from the placenta showed trends towards higher Sca-1 expression compared to cells from the other organs at E12.5 (data not shown). More importantly, however, comparing the expression of the set of 42 ISGs in the HSC population between the organs recapitulated the results seen with the previous HSC marking strategy. HSCs from the placenta again showed again the highest expression of ISGs at all analyzed time points compared to cells from the AGM or fetal liver (Figure 3.1.5 C) and median relative expression of all ISGs was again highest in HSCs from the placenta over time (Figure 3.1.5 D). One difference in the results from the two gating strategies was the median expression in cells from the fetal liver. Previously, fetal liver cell median expression was overall lowest, however with the new gating, fetal liver cell median expression is higher than in AGM cells and only slightly lower than in placenta cells.

In conclusion, regardless of the specific gating used for HSCs during development, cells derived from the placenta displayed the highest overall expression of ISGs at all analyzed time points. The data thus suggested an organ specific baseline level of IFN signaling during hematopoietic development.

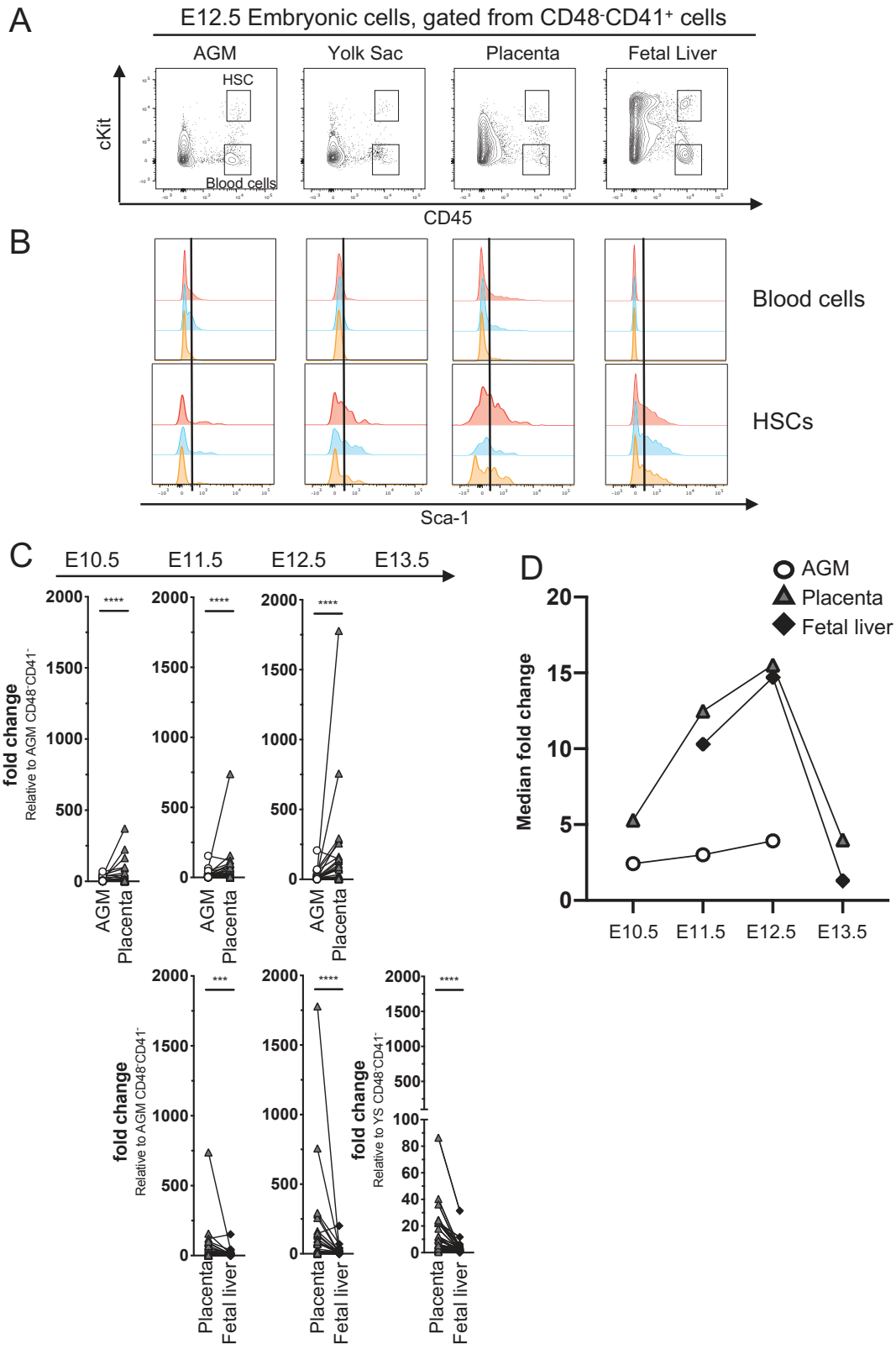


**Figure 3.1.5 ISG expression of HSCs isolated from embryonal organs of WT mice using different markers show differences depending on organ and cell type.**
(A) Example gating of WT E12.5 HSCs (CD48$^-$CD41$^+$cKit$^+$CD45$^+$) and blood cells (CD48$^-$CD41$^+$cKit$^-$CD45$^+$) from four different embryonal organs. (B) Example histograms of Sca-1 expression of HSCs and blood cells. (C) Fold change expression of ISGs relative to CD48$^-$CD41$^-$ cells from AGM (E10.5-E12.5) or yolk sac (E13.5) by qRT-PCR of HSCs (CD48$^-$CD41$^+$cKit$^+$CD45$^+$) of E10.5-E13.5 WT embryonal organs. Each symbol represents expression of a single ISG. (D) Median of fold change of expression of ISGs over time.
Sdha, Oaz1, and Actin-beta were used as reference genes. Statistical test was performed as Wilcoxon matched-pairs signed rank test. (*, p<0.05, **, p<0.01, ***, p<0.001, ****, p<0.0001, ns, not significant), n≥3.

### *3.1.3. ISG expression during hematopoietic development can inherited to mature blood cells*

During hematopoietic development, IFN signaling heterogeneity in HSCs was specific for each embryonal site and stable over the duration of development. In the adult, this heterogeneity was also stable following transplantation of HSCs and inherited to the reconstituted blood system in the recipient. Next, we wanted to investigate if IFN signaling heterogeneity in HSCs present in developmental organs is maintained upon transplantation of these HSCs. Thus, cells from E12.5 IFITM3-eGFP reporter embryonal organs (CD45.2) were transplanted into lethally irradiated adult WT recipient mice (CD45.1) to analyze how the baseline IFN signaling heterogeneity behaves upon engraftment in an adult microenvironment (Figure 3.1.6 A). Since experiments with sorted HSCs ($cKit^+CD34^+$) did not show successful engraftment in adult recipients (data not shown), here total cell suspension of the entire organ were transplanted. All cells isolated from one organ type were pooled, however, upon transplantation, recipient mice received the amount of cells equivalent to one organ (1 embryonic equivalent (1ee)). For AGM and placenta, 1ee was transplanted. To normalize for the expansion of cells in the fetal liver and therefore much higher cell numbers and thus also HSCs found in this organ, for fetal liver 0.05ee was transplanted.

4 weeks post-transplantation, the peripheral blood of the recipient mice was analyzed and number of CD45.2 cells was quantified to determine if engraftment was successful (Figure 3.1.6 B). The cut off for successful engraftment was set at 1% CD45.2+ cells found in the blood. Mice transplanted with cells derived from the AGM showed overall lowest engraftment. At E12.5, few HSCs are left in the AGM and in addition, these HSCs might be developmentally at an earlier stage than HSCs found in the placenta or fetal liver. Nonetheless, five mice showed stable engraftment at more than 1% engrafted cells. Most mice transplanted with either placenta or fetal liver cells engrafted successfully at levels ranging from 1% to around 60% CD45.2+ engrafted cells (Figure 3.1.6 B).

Mice showing successful engraftment were further analyzed for eGFP-reporter expression in CD45.2+ granulocytes (Figure 3.1.6 C). Recipients transplanted with cells derived from the AGM, did not express high levels of the Ifitm3-eGFP-reporter in granulocytes. Contrary, the majority of mice reconstituted with cells from the placenta, showed high numbers of Ifitm3-eGFP-reporter-expressing granulocytes. In this group few mice expressed the reporter in low cell numbers, but this was still not as low as the 0% reporter-expressing cell result in the mice transplanted with AGM cells. This difference was significant according to an unpaired non-parametric rank comparison test (Mann-Whitney). The pool of mice that received cells from the fetal liver showed a mix of different reporter expression phenotypes. Some mice showed high percentage of Ifitm3-eGFP-reporter-expressing granulocytes, comparable to mice transplanted with placenta-derived cells. Other recipient mice showed no Ifitm3-eGFP-

reporter-expressing cells, comparable to the results in mice transplanted with AGM derived cells. Few mice in the fetal liver cell transplanted group showed intermediate percentage of Ifitm3-eGFP-reporter-expressing cells (Figure 3.1.6 C). Overall, the baseline IFN signaling heterogeneity observed in the different developmental hematopoietic organs was maintained upon transplantation and conserved in differentiated cells of the transplanted adult recipients.

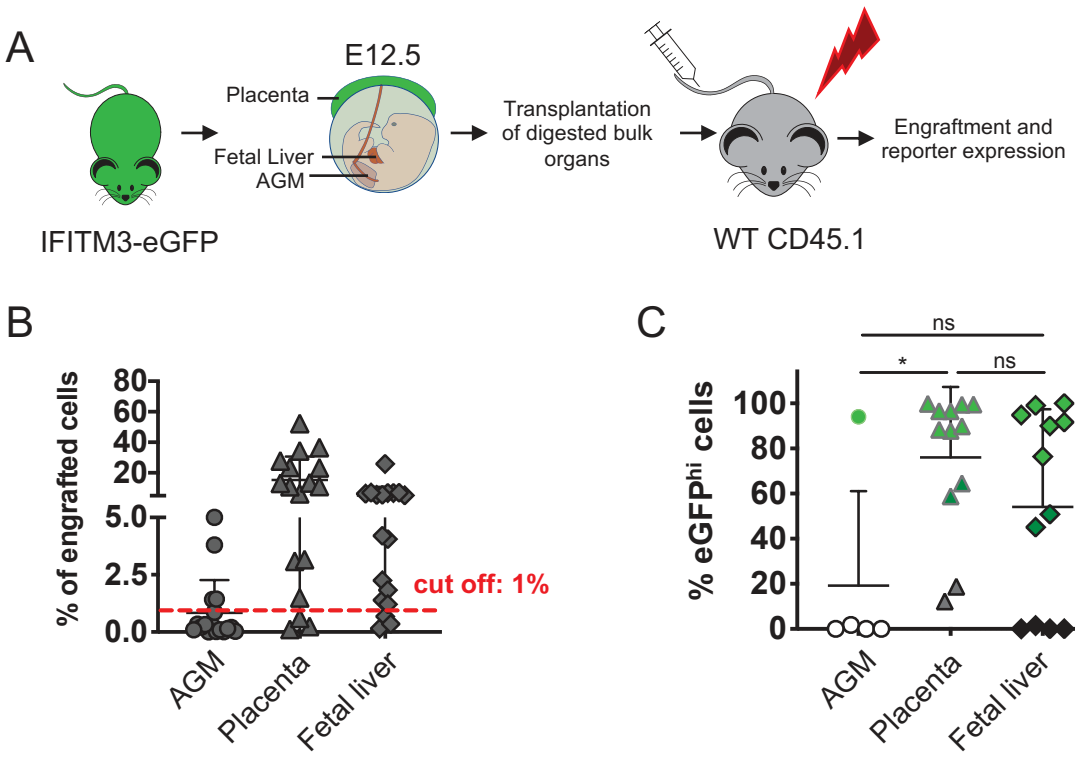


**Figure 3.1.6 IFITM3-eGFP-reporter expression status of HSCs in embryonal organs is stable upon transplantation into adult mice.**
(A) Schematic overview of the experimental setup: E12.5 embryos were isolated from pregnant IFITM3-eGFP reporter mice. Embryonal organs were digested and transplanted into lethally irradiated adult WT mice (CD45.1) through tail vein injection at 1 embryonal equivalent (1ee) for AGM and placenta and 0.05ee for fetal liver. 4 weeks post transplantation, engraftment of transplanted cells and IFITM3-eGFP reporter expression was analyzed. (B) Analysis of engraftment 4 weeks post transplantation as percentage of CD45.2 cells. Cut off for successful engraftment is set at 1%. (C) Quantification of IFITM3-eGFP reporter-expressing granulocytes of successfully transplanted mice. Unpaired t-test analysis was performed. In case of multiple comparisons, p-values were corrected by the Benjamini-Hochberg method with FDR = 5% (*, $p<0.05$, ns, not significant).
Each symbol represents one recipient mouse (circle: AGM-cell transplanted, triangle: placenta-cell transplanted, diamond: fetal liver-cell transplanted).

In order to study whether baseline IFN signaling heterogeneity in HSCs in embryonal organs is inheritable and to analyze the biological relevance of the findings in the reporter mice, E12.5 WT embryonal cells from different developmental hematopoietic organs were transplanted into lethally irradiated adult recipients. Again, a cell suspension of the whole embryonal organ was transplanted (Figure 3.1.7 A). The number of transplanted cells for placenta and fetal liver remained the same (placenta: 1ee, fetal liver: 0.05ee). However, to increase the engraftment efficiency of AGM-derived cells, 2ee were transplanted for this organ. Additionally, a higher number of recipients were transplanted with AGM cells.

After 4 weeks, peripheral blood of recipient mice was analyzed for engrafted cells. Successful engraftment was again defined as more than 1% CD45.2+ blood cells being found in the CD45.1+ recipient (Figure 3.1.7 B). Increasing the amount of AGM cells transplanted did only partially increase engraftment efficiency of this organ. In the AGM group, only 5 out of 12 recipient mice showed stable engraftment. However, the mice that did show engraftment, showed overall higher engraftment than in the previous experiment with the reporter mice (Figure 3.1.6 B). Further analysis was only performed with mice that showed stable engraftment. 5 and 12 weeks after the transplantation, CD45.2+ B cells were sorted from the peripheral blood of the recipient mice and relative ISG expression was calculated following RNA extraction and qPCRs.

5 weeks post transplantation, ISG expression was significantly higher in B cells isolated from placenta-transplanted mice compared to AGM-transplanted mice showing inheritance of the initial baseline ISG expression present in HSCs in embryonal organ to mature blood cells produced by these HSCs in the recipient mice (Figure 3.1.7 C). Compared to AGM-transplanted mice, fetal liver-transplanted mice also showed significantly higher ISG expression in B cells albeit not as high as placenta cells. At 12 weeks post-transplant (data not shown), this pattern is maintained, however, less significantly. Even though the expression of individual ISGs was widely spread compared to AGM baseline, the median expression of all analyzed ISGs at 5 weeks post transplant was significantly higher in B cells in placenta-transplanted mice compared to B cells in AGM-transplanted mice. At 12 weeks, this trend is maintained, though not significantly. Fetal liver-derived B cells showed intermediate median expression of ISGs compared to AGM and placenta (Figure 3.1.7 D).

In summary, these data showed stable IFN signaling heterogeneity in HSCs in embryonal organs that is transplantable into an adult microenvironment and inherited from stem cells to downstream progeny.

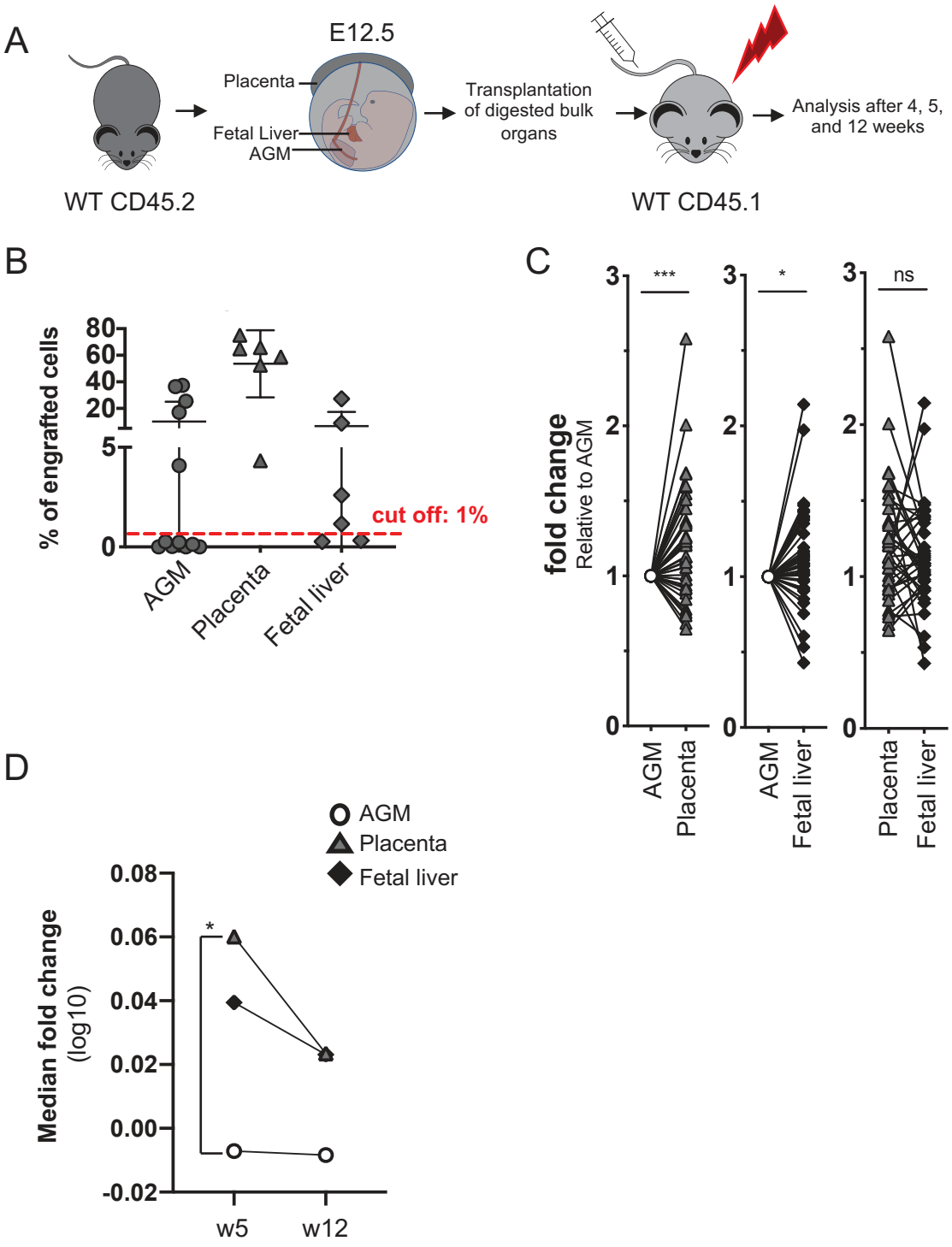


**Figure 3.1.7 Baseline ISG status of HSCs in embryonal organs is stable upon transplantation into adult mice and inherited to mature blood cells.**
(A) Schematic overview of the experimental setup: E12.5 embryos were isolated from pregnant WT mice (CD45.2). Embryonal organs were digested and transplanted into lethally irradiated adult WT mice (CD45.1) through tail vein injection at 1 embryonal equivalent (1ee) for placenta, 2ee for AGM, and 0.05ee for fetal liver. 4 weeks post transplantation, engraftment of transplanted cells was analyzed. 5 and 12 weeks post transplantation, mature cells (in this case $B220^+$ B cells) were sorted from peripheral blood. (B) Analysis of engraftment 4 weeks post transplantation as percentage of CD45.2 cells. Cut off for successful engraftment is set at 1%. (C) Fold change expression of 42 ISGs relative to AGM cells by qRT-PCR was calculated. Only data from 5 weeks post transplantation shown here. Sdha, Oaz1, and Actin-beta were used as reference genes. Each symbol represents expression of a single ISG from at least three replicates. Statistical test was performed as Wilcoxon matched-pairs signed rank test. (*, $p<0.05$, **, $p<0.01$, ***, $p<0.001$, ****, $p<0.0001$, ns, not significant), $n\geq3$. (D) Median (log10) of fold change of expression of ISGs over time. Unpaired t-test analysis was performed (*, $p<0.05$).
Circle: AGM-cell transplanted, triangle: placenta-cell transplanted, diamond: fetal liver-cell transplanted.

### *3.1.4. Developmental baseline IFN signaling is mediated by differential expression of ISGs*

Our findings suggest stable differences in baseline IFN signaling during hematopoietic development. Overall, baseline IFN signaling in HSCs in the placenta is highest over the course of development compared to baseline IFN signaling in HSCs in the AGM or fetal liver. However, this baseline expression is mediated through the expression of different ISGs depending on time of analysis, organ, or definition of the HSCs through different gating strategies.

Using cKit$^+$CD34$^+$ as a marker for HSCs, in AGM, baseline IFN signaling was mainly mediated through higher expression of Plac8, Trim30, and Ifitm1 at earlier time points (E10.5 and E11.5) and solely Trim30 at E12.5. In contrast, in placenta, the ISGs Rsad2 and Tgtp were amongst the most highly expressed ISGs at all analyzed time points. Other highly expressed ISGs in placenta included Sca-1 and Isg20, however, only at certain time points. Fetal liver HSCs displayed the most heterogenous ISG expression over time. At E11.5, Trim30 was most highly expressed in fetal liver. At E12.5, however, Isg20 was the ISG expressed at highest levels, whereas at E13.5, Sca-1 was expressed most highly (Figure 3.1.8 A).

Using cKit$^+$CD45$^+$ as a marker for HSCs (Figure 3.1.8 B), HSCs in the AGM showed similar ISGs being highly expressed compared to the other gating. Plac8 and Trim30 again were amongst the ISGs with the highest expression over time. In the HSCs in the placenta, however, no overlap amongst the most highly expressed ISGs could be seen when comparing the gating strategies. ISGs most highly expressed in cKit$^+$CD45$^+$ HSCs in the placenta included Sp100, Oas3, Oas2, and Oas1g at different time points of development. In the fetal liver, cKit$^+$CD45$^+$ HSCs expressed Plac8, Oas3, Trim30, Oas1g, and at 13.5 also Dhx58 at the high levels, but again not showing much overlap to the other gating strategy. One ISG showing overlap between cKit$^+$CD34$^+$ and cKit$^+$CD45$^+$ HSCs as well as between organs was Trim30. This ISG was amongst the most highly expressed for both gating strategies in AGM and fetal liver, however not in placenta.

Whereas the IFN signaling baseline in cKit$^+$CD34$^+$ HSCs was mediated by expression of a wide variety of ISGs like Rsad2 and Sca-1, in cKit$^+$CD45$^+$ HSCs, higher expression of genes related to the Oas-family played a larger role in mediating the IFN signaling baseline. Overall, differences in baseline IFN signaling during hematopoietic development is mediated through a variety of ISGs that is dependent on hematopoietic organ, time point of development and cell type. Thus, this data suggests that regulation of ISG expression in these cells is regulated through specific intrinsic transcriptional mechanisms rather than conserved extrinsic cues.

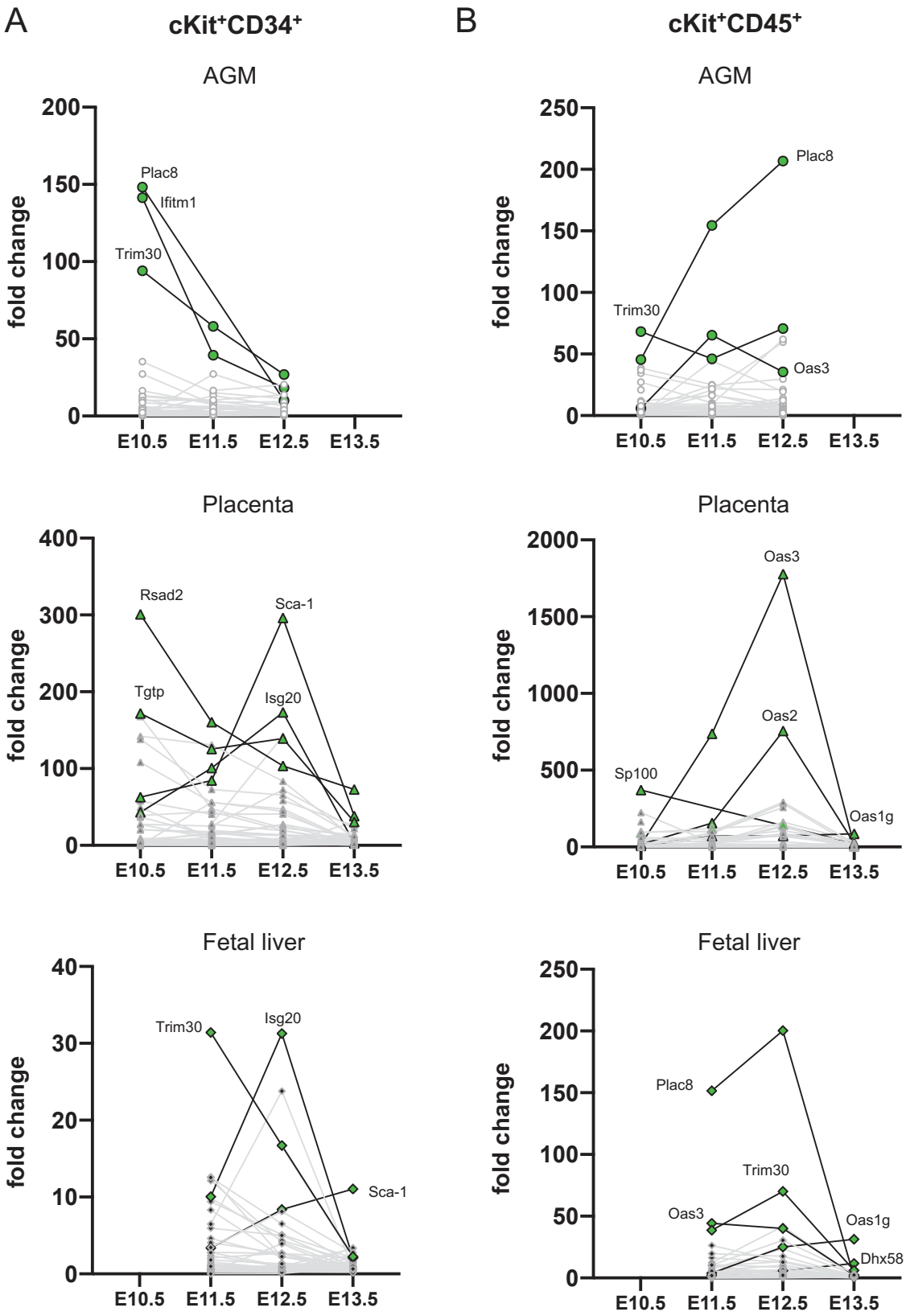


**Figure 3.1.8 Baseline ISG status of embryonal organs is mediated by a variety of different ISGs.**
(A) Fold change expression of ISGs in cKit$^+$CD34$^+$ WT HSCs over time relative to CD48$^-$CD41$^-$ cells from AGM (E10.5-E12.5) or yolk sac (E13.5) by qRT-PCR. (B) Fold change expression of ISGs in cKit$^+$CD45$^+$ WT HSCs over time relative to CD48$^-$CD41$^-$ cells from AGM (E10.5-E12.5) or yolk sac (E13.5) by qRT-PCR.
Sdha, Oaz1, and Actin-beta were used as reference genes. Each symbol represents expression of a single ISG. Example ISGs are highlighted in green.

### *3.1.5. At E10.5, ISRE-eGFP-expressing cells can be identified in the AGM*

Definitive HSCs first arise in the AGM around E10.5 of development. However, at this time point, baseline IFN signaling seems to already be present. Isolation of cells with flow cytometry previous to this time point is only possible when knowing which cells to target. Since E10.5 HSCs already show low levels of IFN signaling, it is likely that this baseline signaling originates prior to E10.5 in more immature cells. In order to study this independently of defined surface markers, AGMs of ISRE-eGFP reporter mice were fixed as whole mounts, trimmed, and chemically cleared for microscopy imaging (Yokomizo *et al.*, 2012) (Figure 3.1.9 A). Initially, E10.5 AGMs were prepared to test the procedure and confirm the presence of reporter-expressing cells. In E10.5 ISRE-eGFP AGMs, ISRE-eGFP-expressing cells were successfully identified using the described protocol (Figure 3.1.9 B). Thus, further analysis using this protocol will be performed to investigate ISRE-eGFP-reporter expressing cells at different time points during development previous to and after E10.5. In combination with defined surface markers that mark cells both during definitive hematopoiesis and before, like CD41 or cKit, it will potentially be possible to identify cells of the same cell type that either express or do not express the ISRE-eGFP-reporter and to detect the origin of the separation of cells with high and low IFN signaling baselines during hematopoietic development.

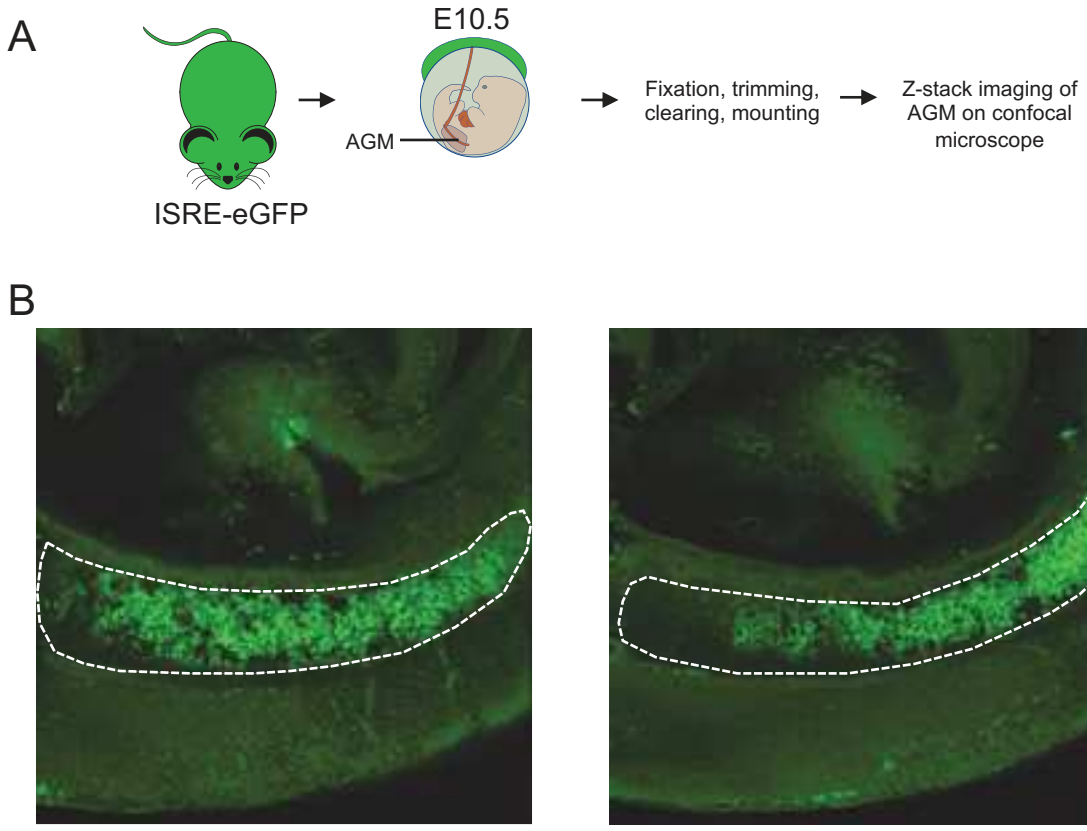


**Figure 3.1.9 ISRE-eGFP-reporter-expressing cells can be found in AGM of E10.5 ISRE-eGFP mice.**
(A) Schematic overview of the experimental setup: E10.5 ISRE-eGFP AGMs were isolated, fixed, trimmed, cleared, and mounted according to Yokomizo *et al.*, 2012. Z-stack images were recorded on LSM 710 (Zeiss) at a magnification of 20x. (B) Visualization of E10.5 ISRE-eGFP AGM whole mounts showing reporter-expressing cells in bright green. AGM region is outlined with white dashes. Left and right panel are two consecutive images of the same AGM sample.

### *3.1.6. Embryonal stem cells show high baseline IFN signaling*

Even though imaging is one option to study early hematopoietic development and the origin of IFN signaling heterogeneity, closing the gap between the earliest development of hematopoietic cells to the onset of definitive hematopoiesis in the AGM and potentially other hematopoietic organs, will be of further interest. Analysis of embryonal stem cells (ESCs) allows the investigation of early hematopoietic commitment in an *in vitro* system which could be useful to supplement data gained from *in vivo* systems.

ESC lines of both ISG reporter mouse lines were created with the help of the transgene service of the DKFZ in order to additionally study IFN signaling in an *in vitro* model system. In order to use these ESC lines as an additional model system to study IFN signaling heterogeneity, the baseline of homeostatic IFN signaling in these cell lines needed to be quantified. Baseline IFN signaling, here quantified by reporter expression, in the ESC lines was high compared to *in vivo* data (see Figure 3.1.5 B). To establish if this high baseline was due to a high unperturbed expression of the reporter or rather due to culture conditions or the handling of the cells, a number of test experiments were performed. Regardless of media conditions, time points of analysis after splitting cells or number of seeded cells after splitting, the IFN baseline signaling remained high. This confirmed that culture conditions and handling of the cells did not significantly influence the baseline IFN signaling (data not shown).

To study the origin of IFN signaling heterogeneity in this system, ISRE-eGFP ESCs were incubated in specialized media to form embroid bodies (EB, Figure 3.1.10 B) and differentiated into the hematopoietic lineage using a defined differentiation media (Pearson *et al.*, 2008) and at different time points during the differentiation process, samples were analyzed for reporter expression as a readout for baseline IFN signaling. Undifferentiated ESCs do not express the megakaryocyte marker CD41, but are high in cKit due to their stem cell character. Upon hematopoietic differentiation, cells start to express CD41. The culture conditions do not support a full differentiation to mature blood cells, but rather a differentiation from ESCs to certain hematopoietic progenitor populations, which is why cKit expression remains high (Figure 3.1.10 A). Over the time of differentiation, reporter expression only marginally changed. Cells that remained $cKit^{-}CD41^{-}$ even after 6 days in differentiation media showed a significant increase in ISRE-eGFP signal. Cells that differentiated and started to express cKit and CD41 did not significantly change their reporter expression levels compared to starting conditions in this process (Figure 3.1.10 C). Further analysis will need to be performed to characterize the $cKit^{-}CD41^{-}$ cells remaining during the differentiation protocol. However, the data suggest that either IFN signaling is starting high in ESC and is then at one point between ESC and HSC decreased in part of the cells, or the ESC lines do not fully represent the *in vivo* events.

A precise time point of the origin of IFN signaling heterogeneity could not be answered with this experimental setup, however, further experimental optimization like culturing cells longer

to achieve differentiation to further downstream populations might allow a conclusion about IFN signaling during the shift from progenitor populations to fully differentiated hematopoietic cells. The *in vitro* system lacks microenvironmental signals that the cells usually are exposed to *in vivo*. Due to the lack of these signals, a representation of the development *in vivo* might not be possible in this *in vitro* system.

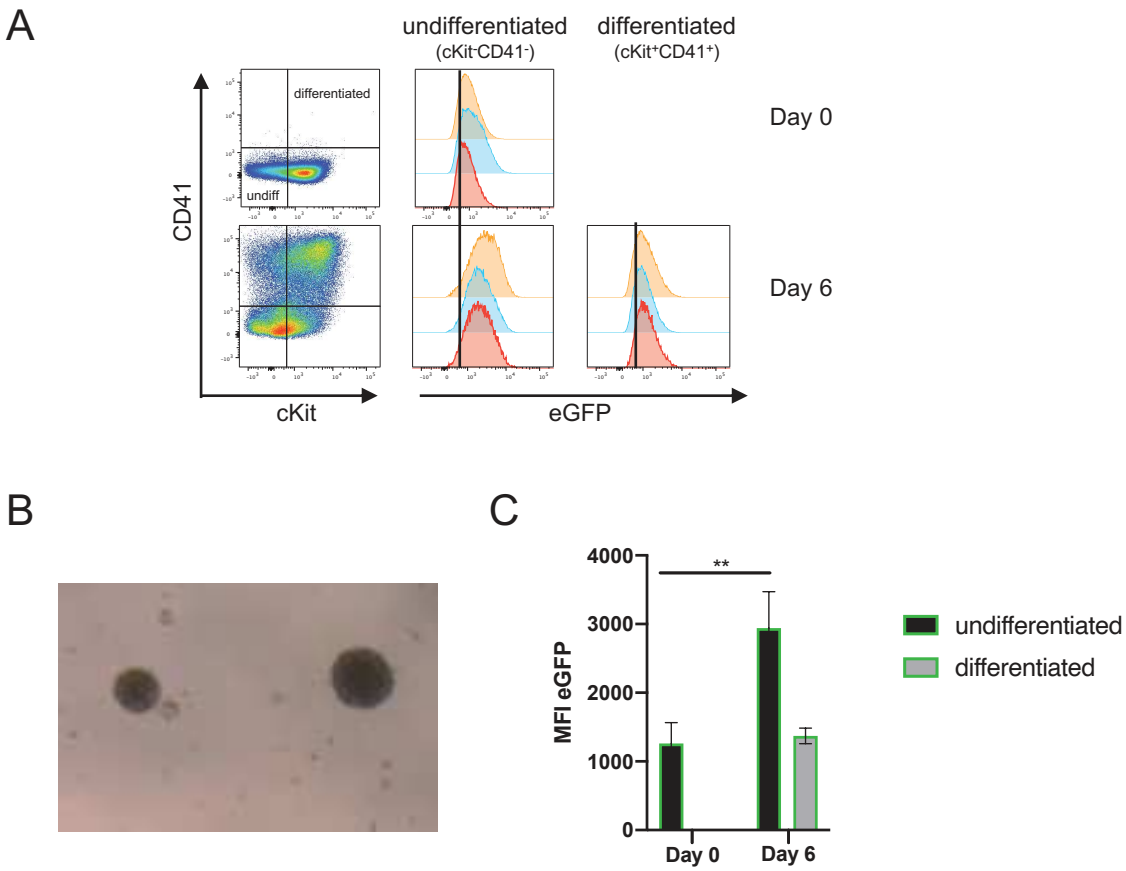


**Figure 3.1.10 *in vitro* differentiation of ISRE-eGFP ESCs towards hematopoietic fate.**
(A) Example gatings and histograms of three ISRE-eGFP ESC clones 0 and 6 days after culture in a defined differentiation media and visualization of differentiation through cKit and CD41 surface marker expression. Undifferentiated (undiff) cells: cKit$^-$CD41$^-$, differentiated cells: cKit$^+$CD41$^+$. (B) Example image of embroid body (EB) formation after 60 h of culture in EB media. (C) MFI of ISRE-eGFP reporter of three ESC clones 0 and 6 days after culture in defined differentiation media. Unpaired t-test analysis was performed (**, $p<0.01$). Mean ± SD, n=3.

In summary, our data suggest that IFN signaling heterogeneity originates during embryonic development. As early as E10.5 (Figure 3.1.4 C-D, Figure 3.1.5 C-D), differences in baseline expression of ISGs could be detected in HSCs at different hematopoietic sites in the embryo. Two different surface marker strategies to identify HSCs in the embryo showed that regardless of the specific cell population identified within the organs or expression of specific ISGs, the general IFN or ISG signature remained comparable. These differences in baseline signaling were stable upon transplantation (Figure 3.1.6 C, Figure 3.1.7 C-D) and inherited from embryonic HSCs to mature blood cells (Figure 3.1.7).

Interestingly, placenta showed the highest baseline IFN signaling during all analyzed time points of development. We hypothesize that in the placenta, the cells are in need of higher IFN baseline, which might serve as protection against pathogens, cytokines, or general immune signals from the maternal side of the placenta. No other embryonic organ is as exposed to signals from the mother as the placenta and the embryo is in need of an additional protective barrier to develop uninterruptedly. Whether these cells migrate from the AGM to the placenta and increase the signaling baseline there or these cells are newly formed in the placenta, remains to be investigated. Moreover, the IFN signaling heterogeneity within the fetal liver and subsequently in the adult, could potentially be explained by different paths the cells take throughout the embryo. HSCs are formed in the AGM, however, the exact path these cells take before ending up in the fetal liver, is still not fully understood.

### 3.2. The function of interferon signaling heterogeneity in the hematopoietic system

We could show that IFN signaling heterogeneity is stably present in both the embryo and the adult hematopoietic system. However, why this is the case remains poorly understood. Even though the IFN signaling heterogeneity is already established at the stem cell level and inherited to downstream progeny, it is possible that this does not have a function in all levels of the hematopoietic system. To increase our understanding of the function of IFN signaling heterogeneity, experiments on embryonal cells as well as adult HSCs and mature cell populations were performed.

#### 3.2.1. *In embryonal organs, HSCs allow decreased viral entry compared to blood cells* in vitro

During hematopoietic development, embryonic organs show differences in baseline IFN signaling. In the past, several ISGs have been implicated to have antiviral effects. Some of these effects include an active role during viral entry (Schneider *et al.*, 2014). To assess if baseline IFN signaling plays a role in viral entry during hematopoietic development, HSCs ($cKit^+CD34^+$) and blood cells ($cKit^-CD34^-$) of E12.5 WT embryonal organs were analyzed after *in vitro* infection with two different viruses.

In the adult, MCMV has been shown to induce long-term HSC cell cycle entry upon acute infection and a sustained inflammatory milieu upon non-acute infection in both IFNAR-dependent and -independent manner (Hirche *et al.*, 2017) and was used here to analyze if baseline IFN signaling plays a role in viral entry. Equal cell numbers of digested AGM, placenta, and fetal liver were infected *in vitro* with either a herpesvirus (murine cytomegalovirus (MCMV-3DR)) or a lentiviral construct (LeGO iC2), both containing an mCherry-reporter as a marker for identification. The lentiviral construct LeGO iC2 was used to compare infectibility of two independent viruses. 24 hours post infection, viral entry into HSCs and blood cells was quantified using flow cytometry (Figure 3.2.1 A). Due to limited virus availability, this experiment was only performed using two replicates per experimental group. Results should consequently only be seen as preliminary and additional experiments need to be performed to draw solid conclusions.

Blood cells generally showed higher frequency of mCherry signal 24 hours post infection compared to HSCs following infection with either virus (Figure 3.2.1 B), however, this was not significant in cells from the placenta. Following treatment with MCMV, AGM-derived blood cells showed significantly increased viral entry compared to HSCs. Yet, this trend was not seen following MCMV infection of cells from the placenta or fetal liver, where the reporter frequencies in HSCs and blood cells showed no significant difference. These data suggest virus-dependent differences in infectibility and protection towards viral entry of certain viruses in these organs. Comparing cells from the different organs, AGM derived cells generally

showed trends towards higher mCherry frequencies compared to placenta and fetal liver derived cells in either cell population (Figure 3.2.1 C), which was not significant in all populations. This data suggests increased viral entry in the presence of a lower IFN baseline. Moreover, after LeGO virus infection, almost no virus could be detected in embryonal HSCs. This data suggests differences in viral entry depending on organ, cell population, as well as virus type. However, experiments have to be repeated to be able to draw solid conclusions.

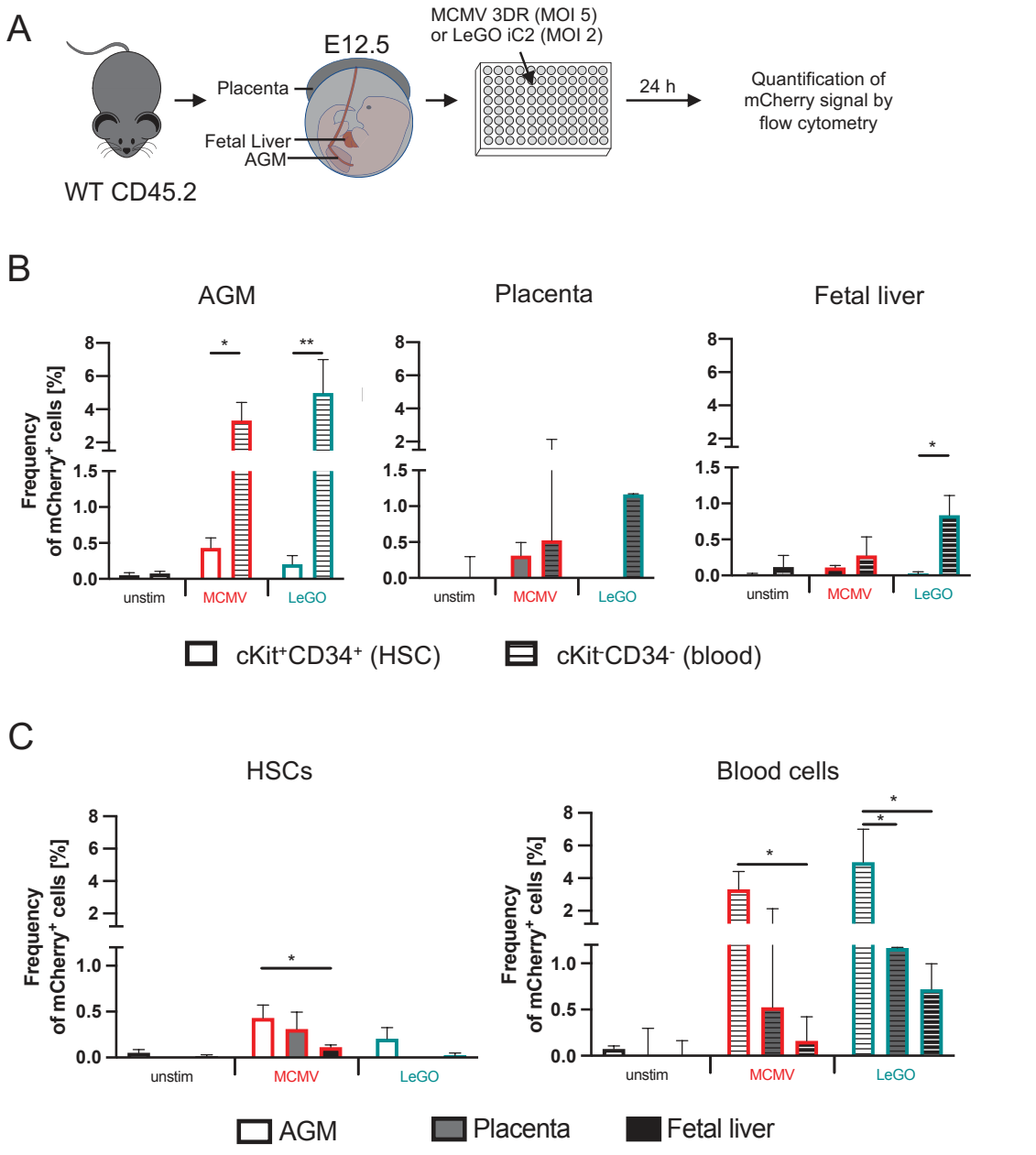


**Figure 3.2.1 Decreased viral entry in HSCs derived from E12.5 WT embryonal organs compared to blood cells.**
(A) Schematic overview of the experimental setup: E12.5 WT embryonal organs were isolated and digested as described previously. Defined cell numbers were plated into 96-well plates and infected with MCMV or LeGO virus containing an mCherry reporter. 24 hours post infection, viral entry was quantified in HSCs ($cKit^+CD34^+$) and blood cells ($cKit^-CD34^-$) with flow cytometry. (B) Frequency of $mCherry^+$ cells in HSCs compared to blood cells in AGM, placenta, and fetal liver. (C) Frequency of $mCherry^+$ cells in HSCs (left panel) and blood cells (right panel) compared between organs.
MCMV infected cells are marked in red, LeGO infected cells are marked in tourquise. Unpaired t-test analysis was performed. In case of multiple comparisons, p-values were corrected by the Benjamini-Hochberg method with FDR = 5% (*, $p<0.05$, **, $p<0.01$). Mean ± SD, n=2.

### *3.2.2. Transplanted chimeras show higher sensitivity to viral infection compared to control animals*

Upon infection or treatment, cells from both reporter statuses sensed IFN, as shown by an increase in reporter expression, however, reporter-low expressing cells responded less and importantly, always remained lower compared to reporter-high-expressing cells. Upon clearance of the infection, both subtypes of cells returned to their initial baseline (data not shown) (Hirche *et al.*, in preparation).

To functionally assess how a hematopoietic system that only produces cells of one type of baseline IFN signaling responds to a systemic infection, chimeras were created and after a period of recovery from irradiation and transplantation, infected with a herpesvirus. Hematopoietic stem and progenitor cells (HSPCs, LSK) from ISRE-eGFP mice were transplanted into lethally irradiated WT recipients to create mice with a hematopoietic system only consisting of $eGFP^{hi}$ cells, $eGFP^{lo}$ cells, or an unfractioned system containing both $eGFP^{hi}$ and $eGFP^{lo}$ cells. After a 26 week recovery period, recipients were systemically infected with MCMV. Over a period of 5 days, mice were monitored daily to track weight loss and overall well-being. 5 days post infection (dpi), blood, BM, spleen, and liver were analyzed and compared to MCMV infected, but not irradiated or transplanted control mice (Figure 3.2.2 A). Originally, this experiment was set up to compare how the hematopoietic systems reacted to a systemic viral infection if only $eGFP^{hi}$ or $eGFP^{lo}$ cells were present and potentially uncover differences in functionality of these cells. Surprisingly, monitoring these mice after the infection showed, that even after 26 weeks of recovery was not sufficient for full recovery of the irradiated and transplanted mice, since these mice showed a much more severe reaction to the virus than their non-irradiated and -transplanted counterparts. Even though the infected control group also lost weight, the drop in weight was significantly higher in all the infected transplanted groups compared to the MCMV infected control group, which was not irradiated and transplanted (Figure 3.2.2 B). At 5 dpi, the transplanted animals reached the defined endpoint of 20% weight loss compared to the starting weight and the experiment was stopped. Comparing the composition of mature cells in the blood showed that even the PBS treated animals of the transplanted groups showed significant differences in the frequency of B and T cells, possibly still recovering from irradiation and transplantation (Figure 3.2.2 C). Moreover, in the transplanted groups HSCs entered active cell cycle stronger upon MCMV infection than HSCs in the control group, shown by decreased frequency of HSCs in G0 compared to PBS treated HSCs. 5 dpi, the control animals infected with MCMV already recovered, as cell cycle activity was not significantly changed compared to the PBS treated group (Figure 3.2.2 D).

Nonetheless, there were differences between the experimental groups in the frequency of HSCs (here defined as $Lin^{-}Sca\text{-}1^{+}CD150^{+}CD48^{-}CD34^{-}$, due to changes in cKit signal upon MCMV; data not shown) in the BM, the total number of HSCs per leg, as well as the changes

in eGFP fluorescent intensity (Figure 3.2.2 E-G). Whether these differences are due to the differential stages of recovery post infection or an actual effect of the baseline IFN signaling in the hematopoietic system between the transplanted groups is not clear yet.

Thus, a conclusion on the function of IFN signaling heterogeneity in the hematopoietic system could not be drawn from this experimental setup due to irradiation and transplantation side effects. Further assessment of the experimental approach to investigate the function and role of cells with exclusively high or low IFN signaling baseline independently will be necessary.

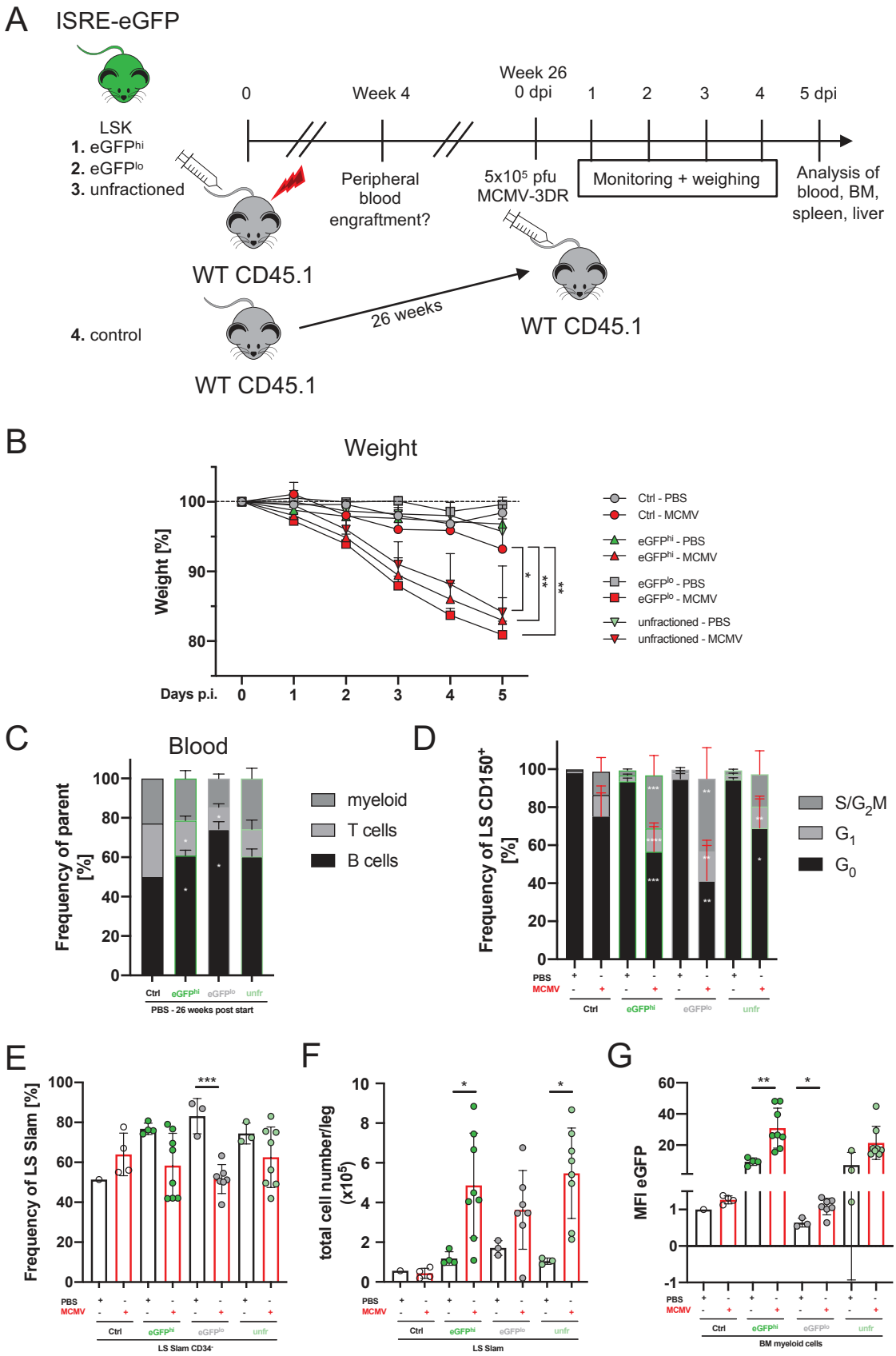


**Figure 3.2.2 Delayed recovery of the hematopoietic system of chimeras generated from ISRE-eGFP HSPCs following irradiation and transplantation.**
(A) Schematic overview of the experimental setup: Lethally irradiated WT CD45.1 mice were transplanted with 2000 HPSCs (LSK cells) of ISRE-eGFP mice selected according to eGFP$^{hi}$, eGFP$^{lo}$, and independent of reporter expression, here termed unfractionated. Recipient mice and a group of age-matched non-irradiated and non-transplanted WT CD45.1 mice (control) were left to recover for 26 weeks. Mice were then i.v. injected with PBS or

$5x10^5$ pfu MCMV-3DR and response to the systemic infection was monitored for 5 days. 5 days post infection (dpi), blood, BM, spleen, and liver were analyzed with flow cytometry to assess differences in response to an infection of a hematopoietic system lacking heterogeneous IFN signaling. (B) Weight loss curve following systemic infection. (C) Flow cytometric analysis of mature cells (B cells: $B220^+$, T cells: $CD4/8^+$, myeloid: $B220^-CD4/8^-CD11b^+Gr1^+$) in peripheral blood of PBS treated mice 5 dpi. (D) Cell cycle analysis of LS $CD150^+$ cells following PBS or MCMV-3DR treatment after 5 days ($G_0$: $Ki67^-Hoechst^{lo}$, $G_1$: $Ki67^+Hoechst^{lo}$, $S/G_2M$: $Ki67^+Hoechst^{hi}$) via flow cytometry. (E) Flow cytometric analysis of LT-HSCs (LS $CD150^+CD48^-CD34^-$) cell frequency in the BM following PBS or MCMV-3DR treatment after 5 days. (F) Analysis of total BM LS Slam cell numbers 5 dpi via flow cytometry. (G) Analysis of reporter expression (MFI) 5 dpi in myeloid cells ($B220^-CD4/8^-CD11b^+Gr1^+$) isolated from BM via flow cytometry. Unpaired t-test analysis was performed. In case of multiple comparisons, p-values were corrected by the Benjamini-Hochberg method with FDR = 5% (*, $p<0.05$, **, $p<0.01$, ***, $p<0.001$, ****, $p<0.0001$). Mean ± SD, $n\geq3$ (with exception of PBS treated control group).

### *3.2.3. Function of IFN signaling heterogeneity in mature blood cells*

During an infection or inflammation, HSCs are not the main responding cells. Even though HSCs are able to directly sense released cytokines like IFN (Essers *et al.*, 2009), their high IFN baseline might limit their response or even make them resistant to certain viral infections and protect them from exhaustion (Wu *et al.*, 2018). Upon an infection, a large variety of innate and adaptive immune cells are activated to clear the body from pathogens. T cells are one of the main essential players mediating this response and IFN has been shown to enhance the T cell response through stimulation of dendritic cells and therefore serves as a link between the innate and adaptive immune response (Le Bon and Tough, 2002; Le Bon *et al.*, 2003). Large numbers of T cells are generated in the thymus, a primary lymphoid organ, during early periods of life and start to differentiate and are exported to the periphery. Newly generated T cells that exit the thymus are only semi-mature and only acquire full maturity several days later (Yang and Bell, 1992; Hosseinzadeh and Goldschneider, 1993; Sprent, 1993). Once migrated to secondary lymphoid organs like the lymph nodes, T cells remain inactive or in interphase for a prolonged time up to several months. This is in contrast to T cells found in the spleen, where cells show rapid turnover of only several days (Claesson *et al.*, 1974; Sprent, 1993). During homeostasis, a background level of T cell proliferation in the secondary lymphoid organs has been suggested to make up for death of long-lived cells, as the generation of new T cells from the thymus is low, but not absent, in adults (Shortman *et al.*, 1990; Sprent, 1993). Mature $CD4^+$ and $CD8^+$ T cells in young animals are mostly naïve and only express low levels of CD44. Upon antigen contact, naïve T cells generate large numbers of cells expressing higher levels of CD44 that engage in immune responses (Sprent *et al.*, 2008). Most of these cells are lost again upon elimination of the infection and only a small portion survives to become long-lived memory T cells (Sprent and Tough, 1994; Jameson, 2005; Sprent *et al.*, 2008). Small numbers of these memory T cells are, however, also found in non-immunized animals, which are termed memory-phenotype (MP) T cells (Sprent and Surh, 2011). In young mice, only about 10-20% of these $CD44^{hi}$ T cells are memory T cells, however, in older mice, form the majority (Sprent *et al.*, 2008). Within the population of $CD44^{hi}$ memory T cells, a larger fraction expresses high levels of the surface marker CD62L (central memory T cells (CM T cells)), mediating a resting phenotype and allowing the cells to recirculate through lymph nodes and spleen, similar to naïve T cell which are also $CD62L^{hi}$. A smaller fraction of $CD44^{hi}$ memory T cells does not express CD62L and are partially-activated effector cells (effector memory T cells (EM T cells)) (Sprent *et al.*, 2008). T cells show strong reactivity to foreign antigens, however, are mostly tolerant to self antigens. In rare cases of response to tissue-specific antigens, this response is usually repressed by $CD4^+CD25^+$ T regulatory (Treg) cells to avoid autoimmune diseases (Liston and Rudensky, 2007; Sakaguchi and Sakaguchi, 2005; Sprent *et al.*, 2008).

In recent years, the BM has been in discussion as a site that harbors antigen-independent proliferation and recirculating memory CD8 T cells to sustain long-term systemic immunity (Parretta *et al.*, 2005; Becker *et al.*, 2005; Di Rosa, 2016b). However, contrasting findings have been reported regarding the activation, proliferation, and migratory capability of these cells (Di Rosa, 2016a; Alp and Radbruch, 2016; Di Rosa, 2016b).

One of our hypothesis on the role of baseline IFN signaling heterogeneity in the hematopoietic system is that the heterogeneity is established at the level of the HSCs to stably provide heterogeneity to short living, differentiated cells. To investigate this hypothesis, possible functional differences in differentiated cells were investigated in ISRE-eGFP reporter mice. Mature cell compartments (B, T, and myeloid cells) were analyzed under homeostasis to define a baseline output of differentiated cell subtypes in ISRE-eGFP$^{hi}$ and ISRE-eGFP$^{lo}$ cells (data only shown for T cells).

In the hematopoietic stem cell and progenitor compartment, the ratio of ISRE-eGFP$^{hi}$ to ISRE-eGFP$^{lo}$-expressing cells is close to 1, 50% of HSPCs are ISRE-eGFP$^{hi}$ and 50% of HSPCs are ISRE-eGFP$^{lo}$ (data not shown). To confirm if this was also true for different subpopulations of the mature cell compartment, the T cell compartment of ISRE-eGFP mice was analyzed. These experiments were performed together with a Master student, Johanna Kohl geb. Mörs, under my supervision. Under homeostasis, different T cell subsets derived from the spleen of ISRE-eGFP mice display an approximate ratio of 50% of ISRE-eGFP$^{hi}$- and ISRE-eGFP$^{lo}$-expressing cells with few exceptions in the spleen. CD4$^+$ central memory (CM, CD62L$^+$CD44$^+$) T cells had significantly fewer ISRE-eGFP$^{lo}$ cells, while CD8$^+$ effector memory (EM, CD62L$^-$ CD44$^+$) T cells had significantly more ISRE-eGFP$^{lo}$ cells (Figure 3.2.3 A). Even though the ratio of the different reporter-expressing cells was similar, overall reporter expression, here measured by MFI, changed between the specific subpopulations of T cells. MFI here was normalized to all CD4$^+$ cells of the spleen. CD4$^+$ EM and CD4$^+$ Treg cells expressed the ISRE-eGFP reporter at higher intensities than CD4$^+$ naïve T cells (CD62L$^+$CD44$^-$), and within the CD8+ T cell compartment, CM T cells showed significantly higher intensities of the ISRE-eGFP reporter compared to EM T cell (Figure 3.2.3 B).

During an infection, T cells are activated following antigen presentation and start to secrete cytokines to eliminate foreign pathogens. Initially, eGFP expression in splenic T cells of ISRE-eGFP mice was analyzed 24 hours post pI:C treatment *in vivo* to assess if changes in reporter expression are subpopulation-specific. ISRE-eGFP expression increased overall following pI:C (Figure 3.2.3 C), however, the frequency of ISRE-eGFP$^{hi}$ to ISRE-eGFP$^{lo}$ cells did not change (Figure 3.2.3 D), which is in accordance with previous data from our group on HSCs and other hematopoietic cells following pI:C treatment (data not shown). One exception here are the CD8$^+$ EM T cells. In this compartment upon pI:C treatment, MFI of the ISRE-eGFP-reporter did not increase significantly (Figure 3.2.3 C) and the frequency of ISRE-eGFP$^{lo}$

cells increased significantly while the frequency of ISRE-eGFP$^{hi}$ cells subsequently decreased (Figure 3.2.3 D). Already under homeostasis, the CD8$^{+}$ EM T cell compartment was composed of significantly more ISRE-eGFP$^{lo}$ cells, which indicated differences compared to other T cell compartments.

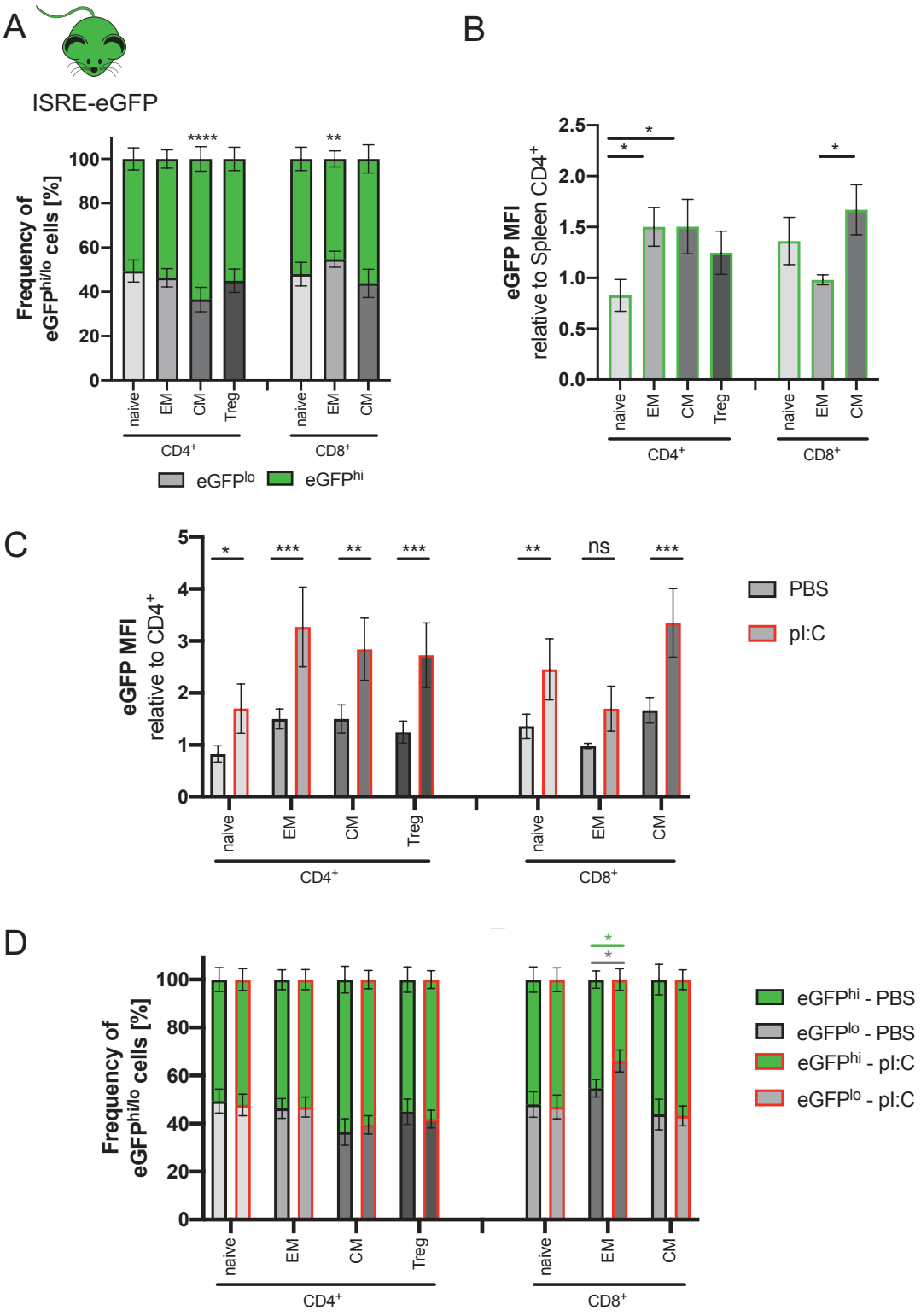


**Figure 3.2.3 ISRE-eGFP$^{hi/lo}$ T cell frequency and intensity in the spleen during steady-state and inflammation *in vivo* did not change significantly in most T cell populations.**
(A) Flow cytometric analysis of the frequency of ISRE-eGFP in CD4$^+$ and CD8$^+$ naïve, effector memory (EM), central memory (CM) and regulatory (Treg) T cells (naïve: CD62L$^+$CD44$^-$, EM: CD62L$^-$CD44$^+$, CM: CD62L$^+$CD44$^+$, Treg: CD4$^+$CD25$^+$) isolated from the spleen. (B) MFI of ISRE-eGFP reporter in CD4$^+$ and CD8$^+$ T cells from the spleen normalized to MFI of total CD4$^+$ cells of the spleen. (C) MFI of ISRE-eGFP in CD4$^+$ and CD8$^+$ naïve, EM, CM and Treg T cells isolated from the spleen 24 hours post i.p. pI:C injection. (D) Flow cytometric analysis of the frequency of ISRE-eGFP in CD4$^+$ and CD8$^+$ naïve, EM, CM and Treg T cells isolated from the spleen 24 hours post i.p. pI:C injection.
Unpaired t-test analysis was performed. In case of multiple comparisons, p-values were corrected by the Benjamini-Hochberg method with FDR = 5% (*, p<0.05, **, p<0.01, ***, p<0.001, ****, p<0.0001, ns: not significant). Mean ± SD, n≥3.

Next, *in vitro* T cell activation of ISRE-eGFP$^{hi}$ and ISRE-eGFP$^{lo}$ cells was investigated. CD4$^{+}$ and CD8$^{+}$ naïve T cells (CD62L$^{+}$CD44$^{-}$) were sorted from the spleen of ISRE-eGFP mice according to reporter expression and activated *in vitro* by presentation of CD3/CD28-coated beads (ThermoFisher; Dynabeads™ Mouse T-Activator CD3/CD28 for T-Cell Expansion and Activation). Activation was then analyzed through flow cytometry after 48-72 hours of culture by quantification of Lag3 and PD-1 surface marker expression (Workman *et al.*, 2002; Freeman *et al.*, 2000; Grosso *et al.*, 2009). Proliferation of these cells was also analyzed using Cell Trace Violet (ThermoFisher, CellTrace™ Violet Cell Proliferation Kit; CTV). Overall, ISRE-eGFP$^{hi}$ cells remained high after culture and sorted ISRE-eGFP$^{lo}$ cells maintained a low IFN signaling baseline indicating that basal levels of IFN signaling were not affected by the culture conditions (Figure 3.2.4 A).

During activation, surface marker expression of T cell subsets changes (Sallusto *et al.*, 2004), which was also observed in our experiment. During the culture and activation, the T cells lost most of their naïve character and surface marker expression of CD44 and CD62L changed towards EM and CM T cells. While both ISRE-eGFP$^{hi}$ and ISRE-eGFP$^{lo}$ sorted T cell populations started to express CD44 at high levels and therefore lost their naïve character, depending on reporter expression, different levels of CD62L were expressed, leading to different frequencies of phenotypic EM and CM T cells. Significantly more ISRE-eGFP$^{lo}$ cells expressed CD62L at lower levels and therefore significantly higher frequencies of EM T cells compared to ISRE-eGFP$^{hi}$ cells were observed. On the other hand, more of ISRE-eGFP$^{hi}$ cells expressed high levels of CD62L and therefore showed significantly higher frequencies of phenotypic CM T cells. It cannot be excluded yet if these cells, albeit phenotypically EM and CM T cells, functionally behaved like EM or CM T cells (Figure 3.2.4 B). Therefore, following analysis of the T cell activation was performed on all CD4$^{+}$ and CD8$^{+}$ cells regardless of their CD44/CD62L phenotype. T cell activation was generally low as most cells remained Lag3$^{-}$PD-1$^{-}$. Interestingly, after 48-72 hours of incubation with activation beads nearly all ISRE-eGFP$^{hi}$ cells remained non-activated (Lag3$^{-}$PD-1$^{-}$). Merely few started to express Lag3. Even though many ISRE-eGFP$^{lo}$ cells also remained Lag3$^{-}$PD-1$^{-}$, significantly more started to express either PD-1 or Lag3 alone or in combination suggesting more efficient activation of these cells (Figure 3.2.4 C).

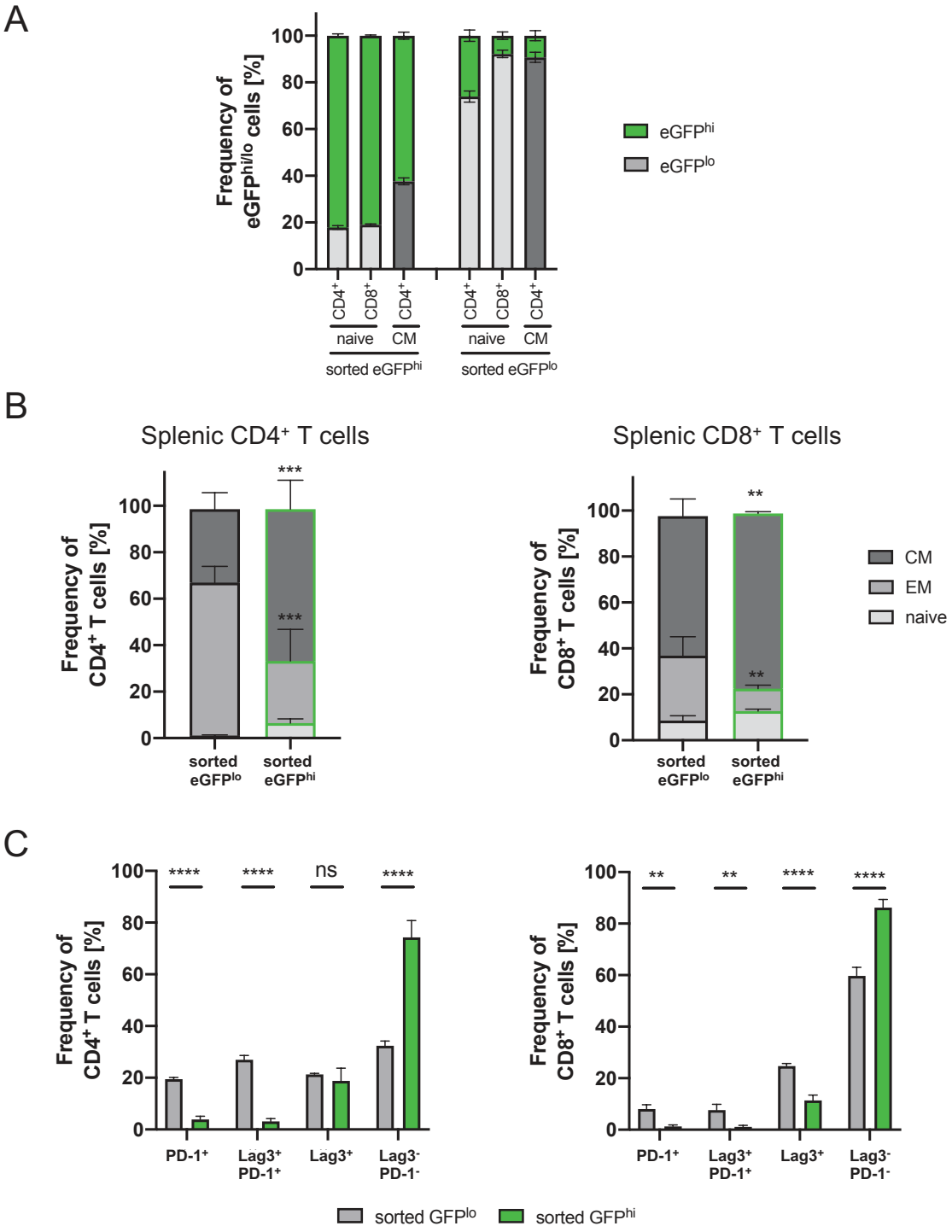


**Figure 3.2.4 ISRE-eGFP T cell frequency after cultivation and activation *in vitro* showed differential activation of ISRE-eGFP$^{hi}$ and -eGFP$^{lo}$ T cells.**
(A) Flow cytometric analysis of the frequency of ISRE-eGFP in CD4$^+$ and CD8$^+$ naïve, and central memory (CM) T cells (naïve: CD62L$^+$CD44$^-$, CM: CD62L$^+$CD44$^+$) isolated from the spleen after 48-72 hours in culture. (B) Frequency of CD4$^+$ (left panel) and CD8$^+$ (right panel) T cell subpopulations of sorted naïve ISRE-eGFP$^{hi/lo}$ T cells from the spleen after 48-72 hours in culture. (C) Frequency of activated T cells of sorted CD4$^+$ (left panel) and CD8$^+$ (right panel) naïve ISRE-eGFP$^{hi/lo}$ T cell from the spleen after 48-72 hours of CD3/CD28 antigen stimulation *in vitro*.
Unpaired t-test analysis was performed. In case of multiple comparisons, p-values were corrected by the Benjamini-Hochberg method with FDR = 5% (*, p<0.05, **, p<0.01, ***, p<0.001, ****, p<0.0001). Mean ± SD, n≥3.

Proliferation analysis showed that around 75% of all cells were proliferating and that the frequency of proliferating cells was not significantly different between ISRE-eGFP$^{hi}$ and ISRE-eGFP$^{lo}$ cells (Figure 3.2.5 A). Moreover, the division index (average number of cell divisions including non-divided cells) (Figure 3.2.5 B) and proliferation index (total number of divisions divided by number of cells that divided) (Figure 3.2.5 C) were not significantly changed between any of the analyzed cell types. These results indicate that there is no difference in proliferation of ISRE-eGFP$^{hi}$ or ISRE-eGFP$^{lo}$ T cells after *in vitro* culture even though ISRE-eGFP$^{hi}$ cells did not express activation markers.

Thus, our data suggests that most T cell subpopulations express similar levels of ISRE-eGFP$^{hi}$ and -eGFP$^{lo}$ cells which is stable upon inflammation, with few exceptions. Following *in vitro* stimulation of the T cells with CD3/CD28, ISRE-eGFP$^{hi}$ and -eGFP$^{lo}$ T cells showed differences in the efficiency of activation, leading to the hypothesis that there are indeed differences in the function of immune cells with high or low IFN signaling baseline. Even though ISRE-eGFP$^{hi}$ T cells were activated less efficiently than ISRE-eGFP$^{lo}$ T cells, this was not reflected in the proliferation of these cells.

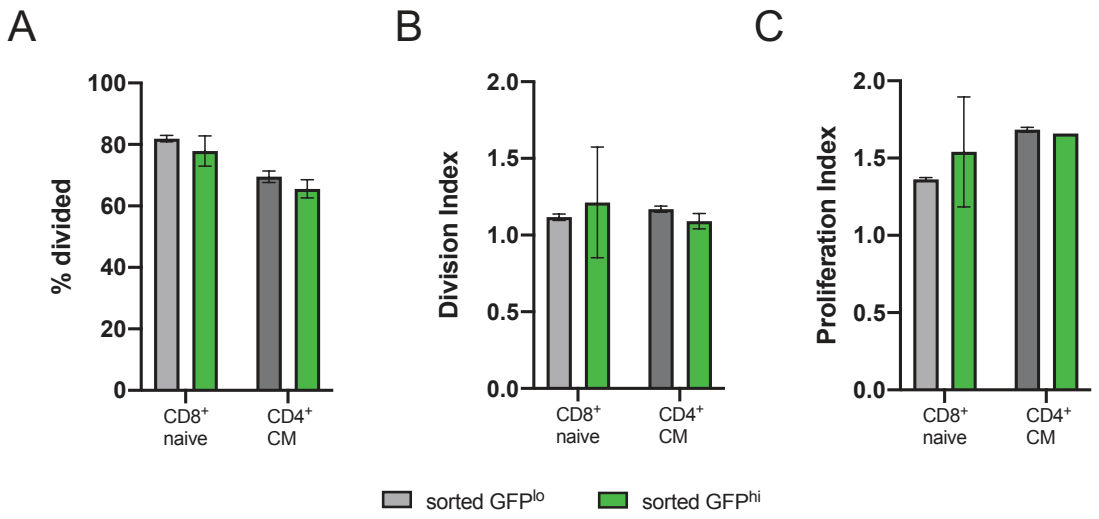


**Figure 3.2.5 Proliferation analysis of T cells isolated from ISRE-eGFP mice showed no differences comparing ISRE-eGFP$^{hi}$ or ISRE-eGFP$^{lo}$ T cells after cultivation and activation *in vitro*.**
Flow cytometric analysis of cell trace violet (CTV, ThermoFisher, CellTrace™ Violet Cell Proliferation Kit) signal in ISRE-eGFP$^{hi/lo}$ CD4$^+$ and CD8$^+$ naïve, and central memory (CM) T cells (naïve: CD62L$^+$CD44$^-$, CM: CD62L$^+$CD44$^+$) isolated from the spleen after 48-72 hours in culture and CD3/CD28 antigen stimulation normalized to CTV signal baseline before culture. (A) Percentage of cells that divided. (B) Divison Index: Average number of cell divisions of all cells (including non-divided cells). (C) Proliferation Index: Total number of divisions divided by number of cells that divided (not including non-divided cells).
The proliferation modeling tool from FlowJo software (Tree Star) was used for analysis here. Mean ± SD, n≥3.

### 3.3. Mechanisms of interferon signaling heterogeneity

IFN signaling heterogeneity was shown to be stable both during hematopoietic development as well as in the adult hematopoietic system. Even though mediated from the level of the stem cells to downstream progeny, the function of this heterogeneity might play a larger role at the level of mature blood cells in the adult. However, the mechanisms how this heterogeneity is established and maintained, remained unknown. In this part of the project, DNA methylation patterns in the hematopoietic system were studied in collaboration with a PhD student from the group of Daniel Lipka (Section of Translational Cancer Epigenomics, Department of Translational Medical Oncology, Stefan Fröhling, DKFZ, NCT), Jens Langstein. DNA methylation analysis was chosen, because chromatin based changes, like DNA methylation are important regulators of gene expression and DNA methylation is one of the main mechanisms implicated in regulating epigenetic memory in the immune system (D'Urso and Brickner, 2014). Many other epigenetic mechanisms are known, however, making use of the knowledge of how epigenetic memory is mediated in the immune system gave us a starting point for the analysis of mechanisms mediating and maintaining IFN signaling heterogeneity in the hematopoietic system.

#### *3.3.1. IFITM3-eGFP reporter mice show differences in DNA methylation based on reporter status*

Phenotypically, there is no big difference in how cells isolated from both reporter and WT mice behave. No changes in cell cycle status, differentiation capacity, surface marker expression, or transplantability could be detected between cells isolated from either reporter model (data not shown). The only difference between these cells is indicated by reporter status. In the following, we studied whether epigenetic variations, in particular differential DNA methylation patterns, in cells with higher or lower reporter expression could mediate the heterogeneity in reporter expression. HSCs and cKit$^+$-cells from adult IFITM3-eGFP, ISRE-eGFP, and WT mice were sorted and DNA methylation analysis of the Ifitm3 locus was performed after bisulfite-treatment of isolated DNA, allowing discrimination between methylated and unmethylated cytosines in a CpG dinucleotide context. Several regions within the Ifitm3 locus that span multiple CpG sites were amplified by PCR and analyzed by mass spectrometry (MassARRAY®, Agena Biosciences) to quantify methylation states. For Ifitm3, amplicon 3 was located across exon 1 close to the 5' gene start site of Ifitm3 near the inserted GFP and the respective promotor region, whereas amplicon 7 was located across exon 2 close to the 3' end of the gene. Both amplicons did, however, also cover introns and regions of the gene body (Figure 3.3.1 A, B).

CpG sites in cKit$^+$-cells and HSCs from WT mice displayed only low methylation levels in amplicon 3, however where partially methylated (around 50%) in amplicon 7. ISRE-eGFP cells

showed a similar pattern, regardless of reporter status. IFITM3-eGFP cells, however, displayed differences in methylation levels depending on their eGFP-expression status. HSCs and cKit$^{+}$-cells with low eGFP reporter expression were fully methylated at this locus, whereas cells that showed high expression of the reporter were only partially methylated, suggesting that DNA methylation levels at this locus could impact eGFP reporter and Ifitm3 gene expression (Figure 3.3.1 C). In previous data, cells from IFITM3-eGFP and ISRE-eGFP mice always behaved similarly. These differences in DNA methylation showed the first significant differences between the two reporter mouse lines. Even though Ifitm3 is also under the regulation of the ISRE, in ISRE-eGFP mice, the eGFP reporter is not directly located within the Ifitm3 gene like it is in the IFITM3-eGFP mice. It is possible that the insertion of the reporter into the gene locus disrupts DNA methylation patterns usually observed at this locus. This might also explain why Ifitm3 methylation in the ISRE-eGFP mice, where no reporter is present within the locus, was more similar to WT patterns.

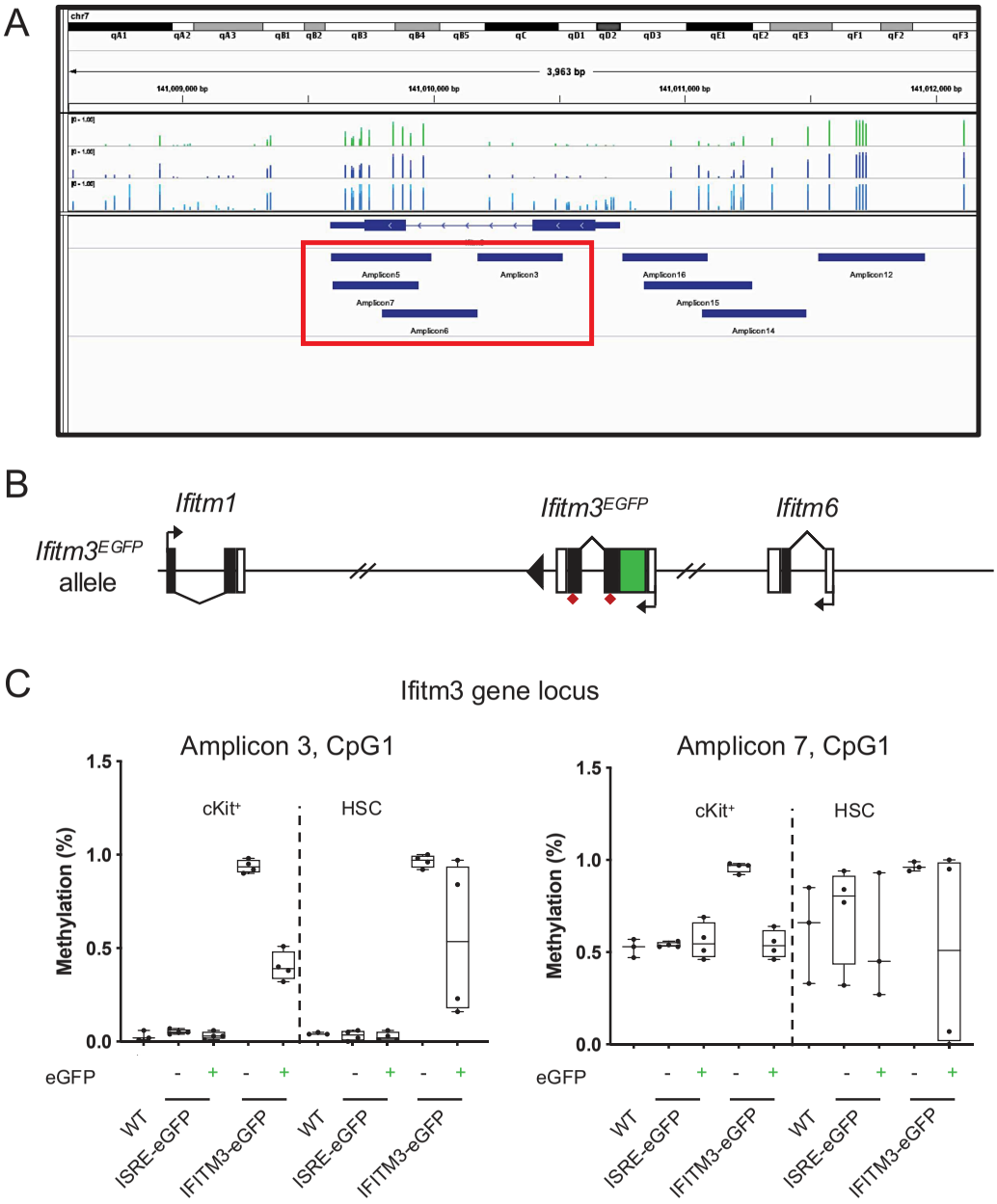


**Figure 3.3.1 DNA methylation analysis of the Ifitm3 locus shows differential methylation levels in the two reporter mouse lines.**
(A) Schematic overview of the Ifitm3 gene locus on mouse chromosome 7 with highlighted analyzed amplicons. (B) Schematic overview of the eGFP insertion into the Ifitm3 gene locus (adapted from Lange *et al.*, 2008). (C) MassArray® results of DNA methylation levels at the Ifitm3 locus of cKit$^+$ cells and HSCs isolated by reporter expression where applicable from WT, ISRE-eGFP, and IFITM3-eGFP mice. CpG 1 of amplicon 3 is shown in the left panel, CpG 1 of amplicon 7 is shown in the right panel.

### *3.3.2. During development, differences in IFN signaling baseline in embryonal organs might partially be mediated by differences in DNA methylation*

During development, differences in IFN signaling baseline could be shown comparing different embryonal hematopoietic sites. In placenta and fetal liver, this higher baseline was able to inhibit entry of specific viruses, whereas a low baseline in AGM was not able to do so.

To investigate if this baseline is mediated through differences in DNA methylation in these cells, E12.5 IFITM3-eGFP embryonal cells from AGM, placenta, and fetal liver were separately transplanted into adult recipients. 16 weeks post transplantation, DNA methylation was analyzed in B cells isolated from peripheral blood (Figure 3.3.2 A). No significant differences could be seen in the DNA methylation patterns between mice transplanted with cells from either organ. However, AGM-derived B cells showed a trend towards higher methylation compared to fetal liver or placenta-derived cells in amplicon 3 and 7 (Figure 3.3.2 B, upper panel). This trend was not detected in amplicon 5 (Figure 3.3.2 B, lower panel).

In summary, DNA methylation might partially be responsible for mediating IFN signaling heterogeneity both in the adult and during development, however, more experiments investigating DNA methylation patterns as well as investigation of other epigenetic mechanisms will need to be performed in order to show potential significant differences and confirm the observed trends or uncover novel epigenetic mechanisms regulating IFN signaling heterogeneity.

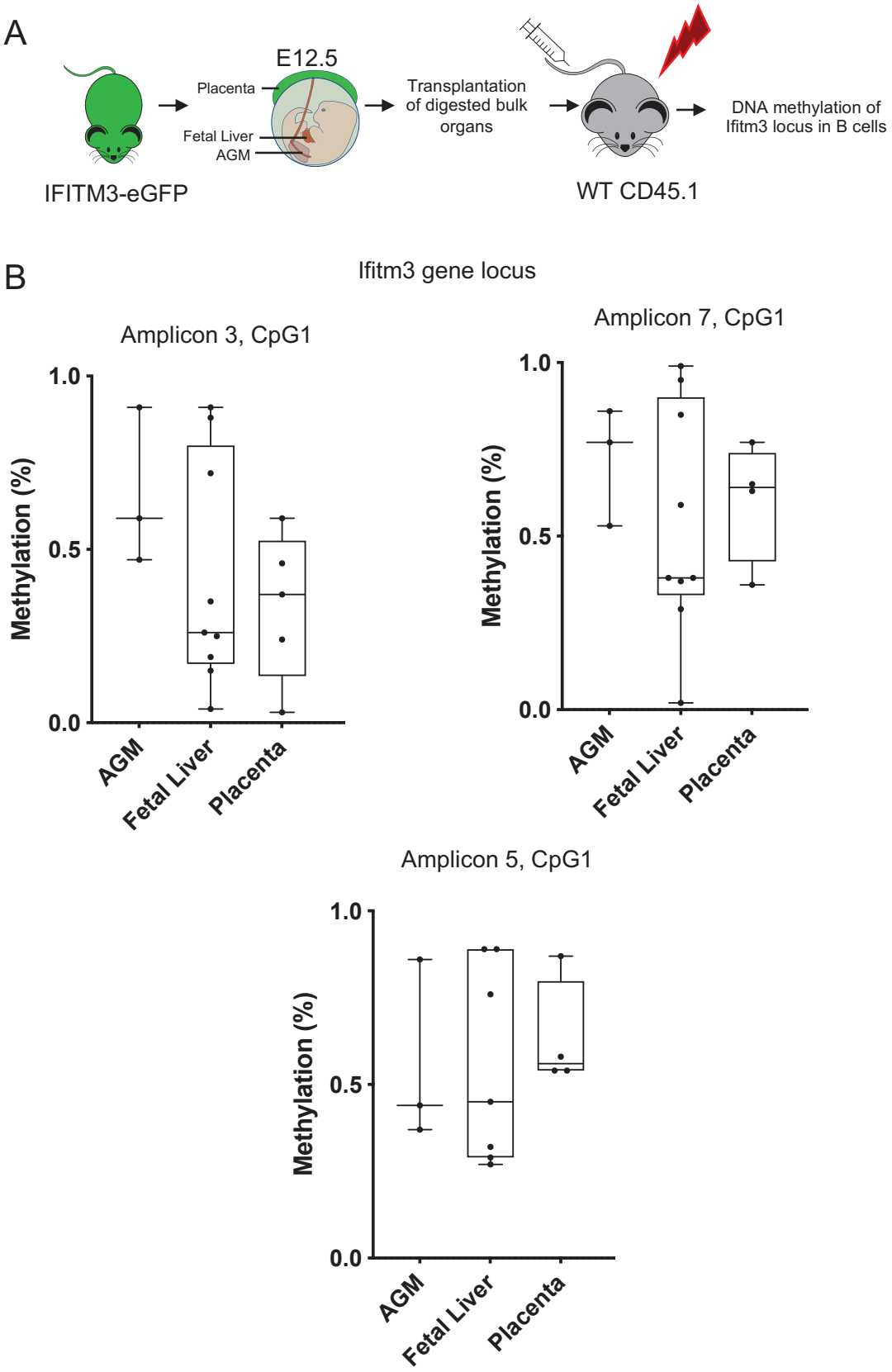


**Figure 3.3.2 Ifitm3 locus of mature blood cells post transplantation of embryonal organs shows different levels of DNA methylation depending on organ source of transplanted cells.**
(A) Schematic overview experimental setup. AGM, placenta, and fetal liver cells were isolated from E12.5 IFITM3-eGFP embryos, digested, and transplanted into lethally irradiated adult CD45.1 WT recipients. 16 weeks post transplantation, B cells were sorted from engrafted mice and analyzed for DNA methylation levels. (B) MassArray® results of DNA methylation levels at the Ifitm3 locus of B cells isolated from recipients transplanted with AGM-, placenta-, or fetal liver derived cells from E12.5 IFITM3-eGFP embryos. CpG 1 of amplicon 3 is shown in the upper left panel, CpG 1 of amplicon 7 is shown in the upper right panel, CpG 1 of amplicon 5 is shown in the lower panel.

### 3.4. The role of the extracellular matrix in the stress-induced activation of HSCs

The ECM is an important component of the bone marrow. However, the role and function of the ECM in stressed hematopoiesis remains largely unknown. Recently, our group identified the ECM adaptor protein Matn4 as a player in the stress-induced activation of HSCs (Uckelmann *et al.*, 2016). This is an example of HSCs actively contributing to changes in their microenvironment through the expression of ECM components. In different cancer models, this has already been described in more detail. As example, metastasizing cells have been shown to create their own microenvironment in distant organs by expression of ECM components (Oskarsson *et al.*, 2011; Lapin *et al.*, 2017). The ECM and the bone marrow microenvironment play an important role during the activation, proliferation, but also migration of HSCs and studying other ECM components in the setting of stress hematopoiesis is of large interest to further understand HSC biology in both health and disease.

Here, we investigated several ECM components, known to play a role in HSC maintenance and function, under various different hematopoietic stress treatments.

#### *3.4.1. Spp1 expression is higher in LT-HSCs compared to committed progenitors and down-regulated upon inflammatory stress*

To identify additional ECM components with a potential role in the response of HSCs during hematopoietic stress, we analyzed gene expression of several ECM components in WT LK $CD150^{+}CD48^{-}$ HSPCs upon treatment with the IFN-mimetic polyinosinic:polycytidylic acid (pI:C) and found Spp1 to be significantly down-regulated in LK $CD150^{+}CD48^{-}$ HSPCs 24 hours post pI:C treatment (Figure 3.4.1 A). Analysis of different hematopoietic cell compartments showed that Spp1 expression is higher in LT-HSCs, here defined as LSK $CD150^{+}CD48^{-}$ $CD34^{-}$, compared to more committed progenitors like common-myeloid progenitors (CMPs), granulocyte-macrophage progenitors (GMPs), or megakaryocyte-erythroid progenitors (MEPs), albeit not significant. Mature blood cells express Spp1 at varying levels (Figure 3.4.1 B). Spp1 down-regulation upon inflammatory stress in HSPCs LK $CD150^{+}CD48^{-}$ cells was restricted to the transcriptional level. Immunofluorescent staining with anti-Spp1 antibody even showed an increase in SPP1 protein levels in HSPCs LK $CD150^{+}CD48^{-}$ cells (Figure 3.4.1 C).

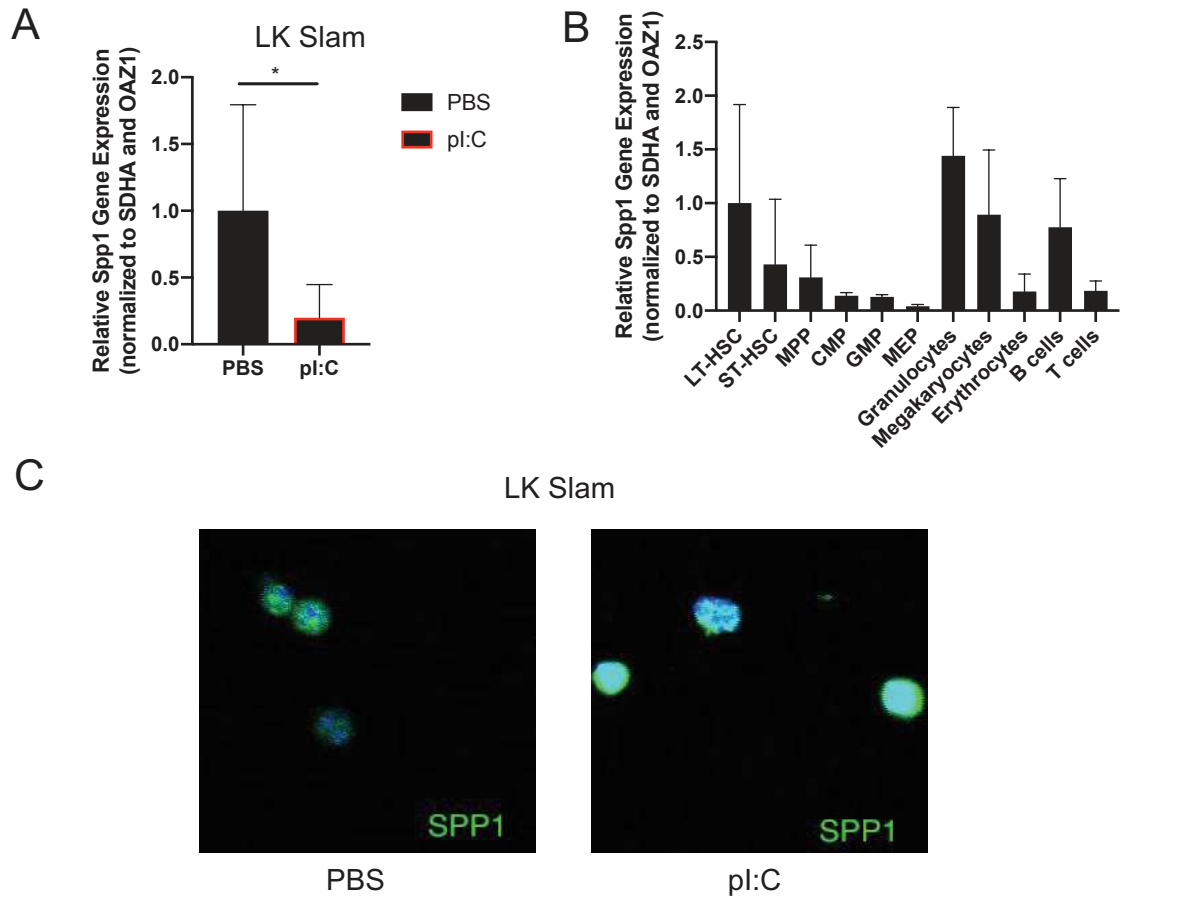


**Figure 3.4.1 Upon inflammatory stress, Spp1 expression in HSCs changes.**
(A) Relative gene expression of Spp1 in WT LK Slam (Lin$^-$cKit$^+$ CD150$^+$CD48$^-$) cells upon 24 hours of PBS or pI:C treatment *in vivo*. (B) Relative gene expression of Spp1 in the hematopoietic system compared to expression in LT-HSCs. (LT-HSCs: Lin$^-$Sca-1$^+$cKit$^+$ (LSK) CD150$^+$CD48$^-$CD34$^-$, ST-HSCs: LSK CD150$^+$CD48$^-$CD34$^+$, MPP: LSK CD150$^+$CD48$^+$, CMP: Lin$^-$Sca-1$^-$cKit$^+$ (LS$^-$K) CD34$^+$CD16/32$^{lo}$, GMP: LS$^-$K CD34$^+$CD16/32$^{hi}$, MEP: LS$^-$K CD34$^-$ CD16/32$^{lo}$, Granulocytes: B220$^-$CD4/8$^-$CD11b$^+$Gr1$^+$, Megakaryoctes: CD41$^+$, Erythrocytes: Ter119$^+$, B cells: B220$^+$, T cells: CD4/8$^+$). (C) Immunofluorescent staining of WT LK Slam (LK CD150$^+$CD48$^-$) cells upon 24 hours of PBS or pI:C treatment *in vivo* analyzed on a confocal microscope. (A-B) Sdha and Oaz1 were used as reference genes. Unpaired t-test analysis was performed. In case of multiple comparisons, p-values were corrected by the Benjamini-Hochberg method with FDR = 5% (*, p<0.05, **, p<0.01, ***, p<0.001, ****, p<0.0001). Mean ± SD, n≥3.

### *3.4.2. Spp1 deficient progenitors show increased colony formation in secondary CFUs*

After identification of Spp1 as a potential ECM component playing a role in stress-induced HSC activation, mice lacking Spp1 ($Spp1^{-/-}$) were analyzed. All ECM-deficient mice used in the following sections were kindly provided by the group of Thordur Oskarsson at DKFZ/HI-STEM. Initial analysis was performed to characterize the hematopoietic system of these mice under homeostasis. $Spp1^{-/-}$ mice showed a slight but significant increase in total LSK number in the BM (Figure 3.4.2 A, right panel). However, mature lineage output was mostly normal with only a slight reduction in $Ter119^{+}$ cells in the BM of the $Spp1^{-/-}$ mice (Figure 3.4.2 B, right panel). Peripheral blood composition was not significantly altered (Figure 3.4.2 B, left panel) and cell cycle activity of the $Spp1^{-/-}$ mice did not show any changes compared to WT mice (Figure 3.4.2 C). Additionally to flow cytometric analysis, peripheral blood parameters were analyzed using a Hemavet 950 (Drew Scientific). The hematocrit (HCT) was significantly decreased in $Spp1^{-/-}$ mice (Figure 3.4.2 D), however did not vary considerably form normal range. None of the other parameters were significantly changed (data not shown).

Next, colony forming potential was analyzed to assess expansion, differentiation, and progenitor potential of BM cells lacking Spp1. BM cells isolated from $Spp1^{-/-}$ mice did not show differential colony forming unit (CFU) counts during primary colony formation, however, increased number of colony formation was observed after secondary plating of primary colonies (Figure 3.4.2 E). This indicated an increased number of progenitor cells and a retention of progenitor potential in mice lacking Spp1 when pushed to proliferation *in vitro*.

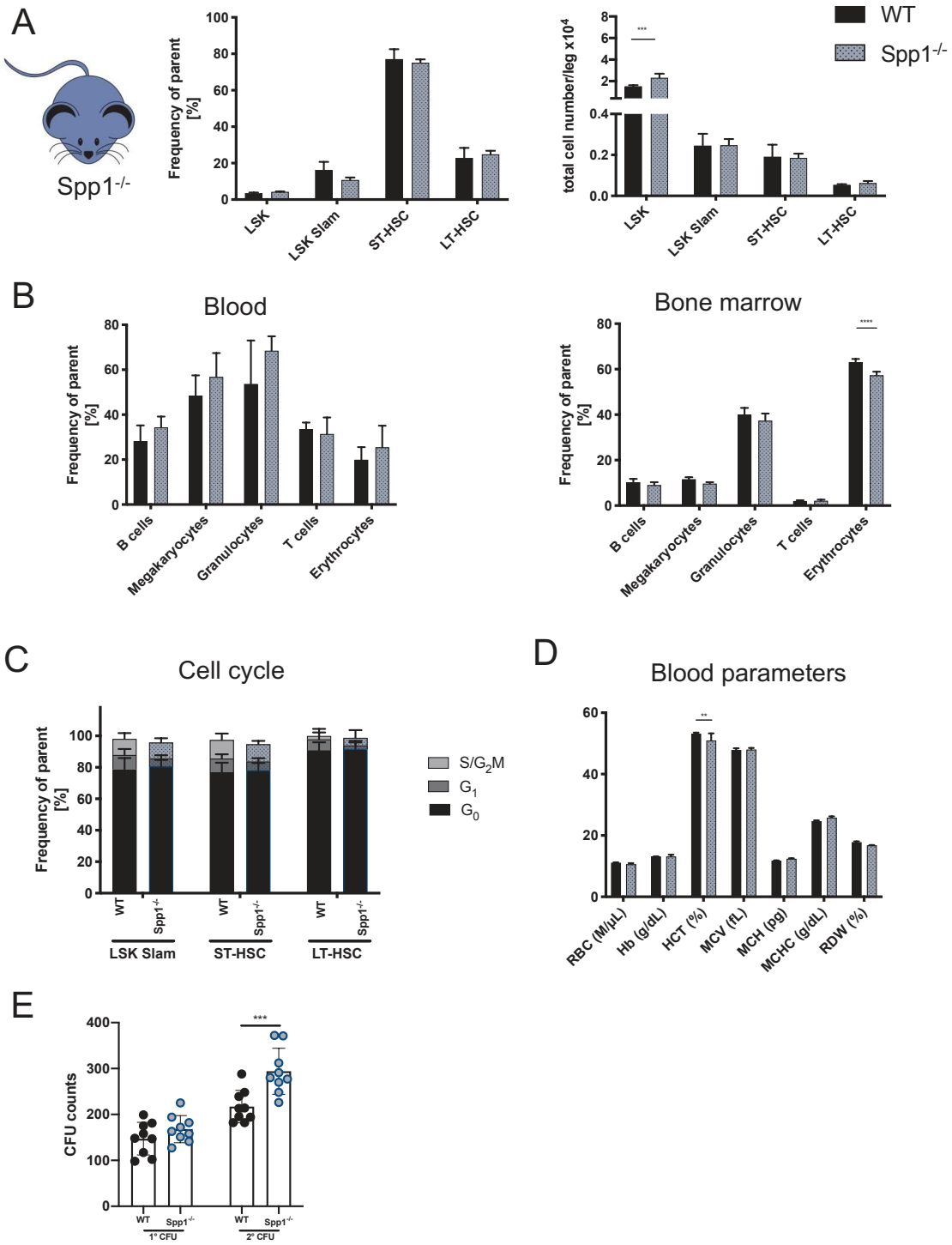


**Figure 3.4.2 The hematopoietic system of Spp1$^{-/-}$ mice only shows minor differences compared to WT mice under homeostasis.**

(A) Frequencies (left panel) and total cell numbers (right panel) of the HSPC compartment of WT and Spp1$^{-/-}$ mice assessed by flow cytometry (LSK: Lin$^-$Sca-1$^+$cKit$^+$, LSK Slam: LSK CD150$^+$CD48$^-$, ST-HSCs: LSK CD150$^+$CD48$^-$CD34$^+$, LT-HSCs: LSK CD150$^+$CD48$^-$CD34$^-$). (B) Frequencies of the differentiated cell compartment in blood (left panel) and bone marrow (right panel) of WT and Spp1$^{-/-}$ mice (B cells: B220$^+$, Megakaryocytes: CD41$^+$, Granulocytes: B220$^-$CD4/8$^-$CD11b$^+$Gr1$^+$, T cells: CD4/8$^+$, Erythrocytes: Ter119$^+$). (C) Cell cycle analysis of HSC compartment ($G_0$: Ki67$^-$Hoechst$^{lo}$, $G_1$: Ki67$^+$Hoechst$^{lo}$, S/$G_2$M: Ki67$^+$Hoechst$^{hi}$). (D) Analysis of peripheral blood parameters of WT and Spp1$^{-/-}$ mice assessed through Hemavet. Units are given for each individual parameter in brackets in the x-axis (RBC: red blood cell count, Hb: Hemoglobin, HCT: hematocrit, MCV: mean corpuscular volume, MCH: mean corpuscular hemoglobin, MCHC: mean corpuscular hemoglobin concentration, RDW: red cell distribution width). (E) Analysis of 1° and 2° Colony-forming unit (CFU) of total bone marrow cells of WT and Spp1$^{-/-}$ mice after 7 days of culture.

Unpaired t-test analysis was performed. In case of multiple comparisons, p-values were corrected by the Benjamini-Hochberg method with FDR = 5% (*, p<0.05, **, p<0.01, ***, p<0.001, ****, p<0.0001). Mean ± SD, n≥3.

### *3.4.3. Spp1$^{-/-}$ mice show improved recovery following inflammatory stress*

Spp1 has been shown to play a critical role for the attraction and retention of HSCs in the BM. A negative regulatory role in HSC proliferation and differentiation via interaction with HSC surface integrins has also been suggested (Grassinger *et al.*, 2009). Mere lack of this ECM molecule did not show significant differences in the hematopoietic system, however, under homeostasis, HSCs are mainly quiescent and HSC-ECM interaction might not be of importance to maintain this state. Upon inflammatory stress, HSCs are activated, start to cycle and possibly change their location within the niche to reestablish homeostasis. A disruption of the proper interaction to the niche might cause defects in these processes. In WT mice, treatment pI:C lead to a down-regulation of Spp1 gene expression in HSCs on the one hand (Figure 3.4.1 A). On the other hand, microscopic analysis of the protein expression of SPP1 showed an increase of SPP1 on the surface of HSCs following *in vivo* pI:C treatment (Figure 3.4.1 C). We thus tested the response of Spp1$^{-/-}$ HSCs to pI:C. In WT mice, pI:C treatment lead to a significant decrease in the frequency of megakaryocyte-erythroid progenitors (MEP), however, treatment of Spp1$^{-/-}$ mice did not show this reduction, suggesting either a defect in the response to pI:C or an improved recovery following the treatment (Figure 3.4.3 A, right panel). Furthermore, pI:C treatment of Spp1$^{-/-}$ mice showed a significant reduction in the frequency of myeloid restricted pre-granulocyte-macrophage progenitors (Pre-GM) after 24 hours, which was not observed in WT mice (Figure 3.4.3 A, left panel).

Chemotherapeutic treatment causes massive hematopoietic defects and induces an inflammatory response. The response to the chemotherapeutic 5-fluorouracil (5-FU) was therefore analyzed in Spp1$^{-/-}$ mice. The only difference in response following this treatment compared to WT mice was a lack of granulocyte depletion in the BM. In WT mice, 5-FU treatment lead to a rapid loss of granulocytes in the BM after 8 days, yet, in Spp1$^{-/-}$ mice, granulocyte frequencies remained almost unaffected following treatment, again suggesting a possible improved recovery (Figure 3.4.3 B).

To further analyze the kinetics of the inflammatory response and the recovery phase , Spp1$^{-/-}$ mice were treated with pI:C between 6 and 72 hours. In contrast to WT, Spp1$^{-/-}$ Pre-GM showed a gradual decrease following treatment with the lowest frequency 24 hours after the treatment. Following the 24 hour mark, a rapid recovery could be seen (Figure 3.4.3 C, left panel). WT MEPs were not significantly changed following pI:C, however, data in Spp1$^{-/-}$ mice indicate a higher frequency of MEPs after pI:C treatment. During the time course, Spp1$^{-/-}$ MEPs were significantly increased already 6 hours after treatment, reaching their highest frequency after 12 hours. From 24 to 72 hours, MEP frequencies decreased again, but where still slightly elevated after 72 hours (Figure 3.4.3 C, right panel).

During inflammatory stress, HSCs are activated and start to proliferate to replenish lost blood cells. The time course analysis showed that 6 hours after pI:C treatment, Spp1$^{-/-}$ LT-HSC

frequencies were significantly reduced and after 12 hours almost completely depleted. At the 24 hour time point, frequencies had started to recover. A comparison to a WT time course treatment will need to be done to uncover possible changes in the kinetics of the response of ECM-deficient cells following hematopoietic stress (Figure 3.4.3 D, left panel). Cell cycle analysis after pI:C treatment showed that Spp1$^{-/-}$ LT-HSCs exit $G_0$ around 12 hours and remain activated until 48 hours after treatment were changes in $G_0$ are significant. 72 hours post pI:C, cells start to return to quiescence with an increase in frequency of cells again in $G_0$ (Figure 3.4.3 D, right panel).

This time line is in accordance with the response of WT HSCs to pI:C treatment (data not shown). Thus, our data indicates only minor differences in the inflammatory response mainly at the level of progenitor cells of Spp1$^{-/-}$ mice compared to WT mice.

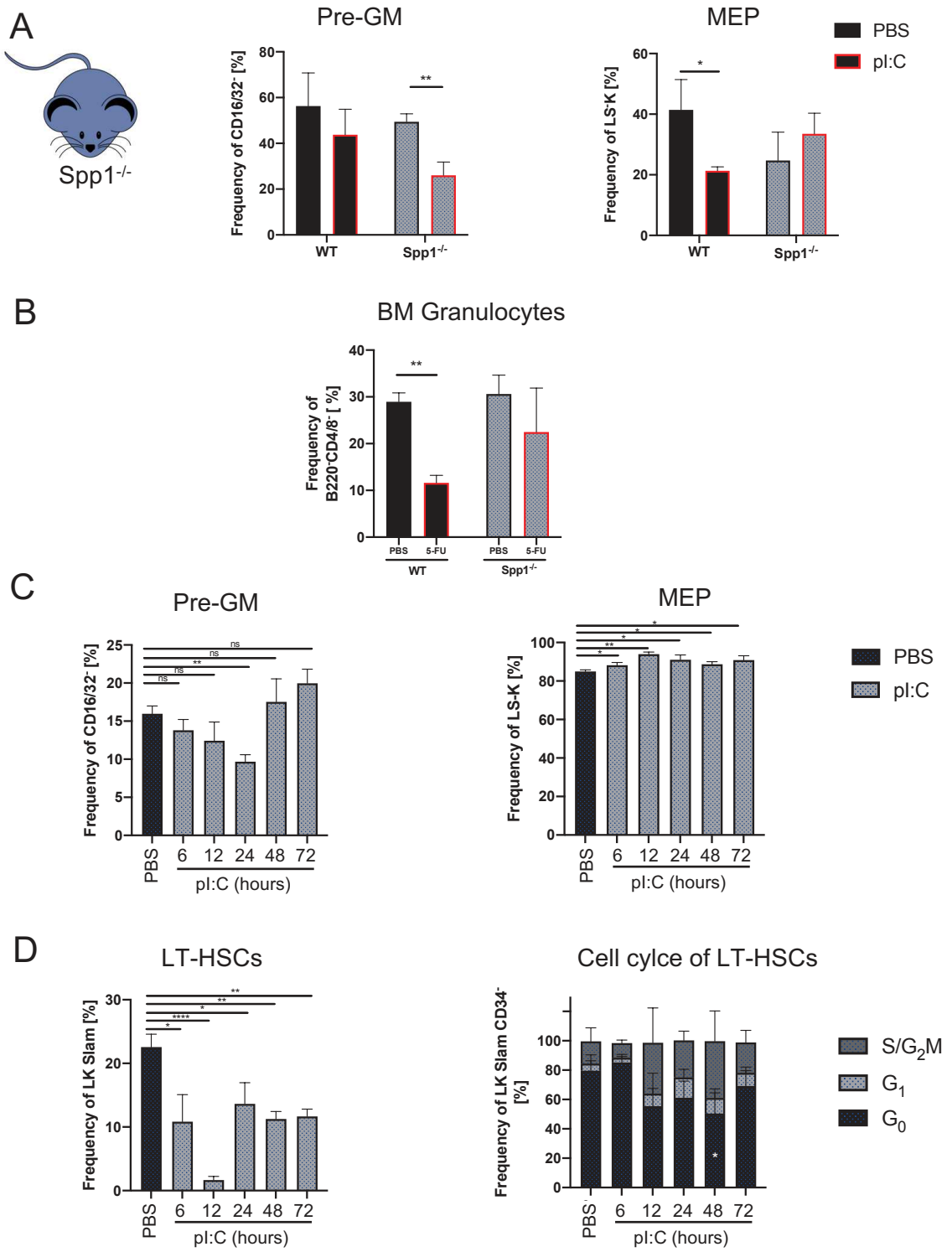


**Figure 3.4.3 Response to inflammatory stress of Spp1$^{-/-}$ mice to inflammatory stress only shows minor differences on the level of progenitor cells compared to WT mice.**
(A) Flow cytometric analysis of Pre-GM (Lin$^-$Sca-1$^-$cKit$^+$ (LS$^-$K) CD41$^-$CD16/32$^-$CD150$^-$CD105$^-$) and MEP (LS$^-$K CD16/32$^-$CD34$^-$) of WT and Spp1$^{-/-}$ mice after 24 hours of *in vivo* PBS or pI:C treatment. (B) Flow cytometric analysis of BM Granulocytes (B220$^-$CD4/8$^-$CD11b$^+$Gr1$^+$) of WT and Spp1$^{-/-}$ mice after 8 days of *in vivo* PBS or 5-FU treatment. (C) Flow cytometric analysis Pre-GM (LS$^-$K CD41$^-$CD16/32$^-$CD150$^-$CD105$^-$) and MEP (LS$^-$K CD16/32$^-$CD34$^-$) cells of Spp1$^{-/-}$ mice after 6, 12, 24, 48, or 72 hours of *in vivo* pI:C treatment compared to PBS treatment. (D) Flow cytometric analysis LT-HSCs (LK CD150$^+$CD48$^-$CD34$^-$) and cell cycle activity ($G_0$: Ki67$^-$Hoechst$^{lo}$, $G_1$: Ki67$^+$Hoechst$^{lo}$, S/$G_2$M: Ki67$^+$Hoechst$^{hi}$) of LT-HSCs of Spp1$^{-/-}$ mice after 6, 12, 24, 48, or 72 hours of *in vivo* pI:C treatment compared to PBS treatment.
Unpaired t-test analysis was performed. In case of multiple comparisons, p-values were corrected by the Benjamini-Hochberg method with FDR = 5% (*, p<0.05, **, p<0.01, ***, p<0.001, ****, p<0.0001). Mean ± SD, n≥3.

### *3.4.4. Mice lacking the ECM component Postn do not show any defects in mature lineage output under homeostasis*

In addition to Spp1, we also investigated the ECM component Postn. Under homeostasis, Postn has been shown to play a role in regulation of HSC proliferation and potential (Domingues *et al.*, 2017) and we thus wanted to investigate if Postn also played a role in the stress-induced activation of HSCs. Similar to $Spp1^{-/-}$ mice, $Postn^{-/-}$ mice displayed some smaller differences in the hematopoietic stem cell compartment like decreased LSK $CD150^{+}CD48^{-}$ frequencies in the BM compared to WT mice (Figure 3.4.4 A). Nevertheless, output of mature blood cells in the BM and peripheral blood was mostly normal (Figure 3.4.4 B), indicating a compensation by progenitor populations downstream of HSCs. Cell cycle activity of $Postn^{-/-}$ HSCs was also comparable to WT HSCs (Figure 3.4.4 C).

Blood analysis of $Postn^{-/-}$ mice revealed a significant increase in the mean corpuscular volume (MCV) compared to WT mice (Figure 3.4.4 D). Other blood parameters were within normal range.

BM cells isolated from $Postn^{-/-}$ mice formed significantly more colonies during the first round of the colony forming unit (CFU) assay compared to WT BM. However, significantly fewer colonies were produced by the $Postn^{-/-}$ progenitors 8 days after re-plating of primary colonies. These data would indicate only an increased short term progenitor potential (Figure 3.4.4 E). Even though significantly less in number, $Postn^{-/-}$ cells formed larger colonies compared to WT (data not shown), potentially indicating different cell types within the colony and therefore different progenitor potential of $Spp1^{-/-}$ BM cells compared to WT cells. Thus, our data shows only minor differences in the hematopoietic system of $Postn^{-/-}$ mice compared to WT mice under homeostasis and potential differences in progenitor potential when hematopoietic cells are pushed to differentiation *in vitro*.

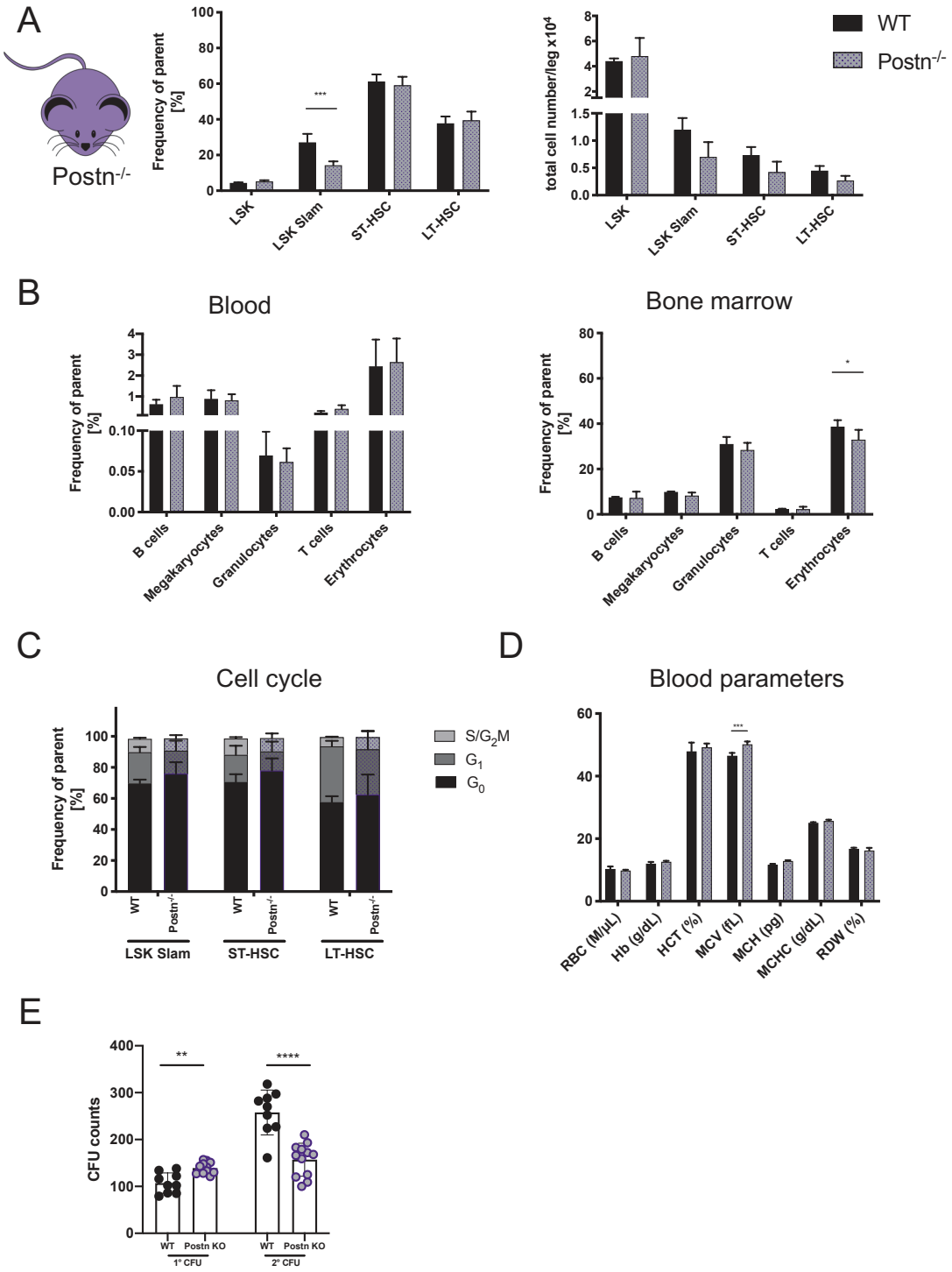


**Figure 3.4.4 Hematopoietic system of Postn$^{-/-}$ mice only showed minor differences compared to WT under homeostasis.**

(A) Frequencies (left panel) and total cell numbers (right panel) of the HSPC compartment of WT and Postn$^{-/-}$ mice assessed by flow cytometry (LSK: Lin$^-$Sca-1$^+$cKit$^+$, LSK Slam: LSK CD150$^+$CD48$^-$, ST-HSCs: LSK CD150$^+$CD48$^-$CD34$^+$, LT-HSCs: LSK CD150$^+$CD48$^-$CD34$^-$). (B) Frequencies of the differentiated cell compartment in blood (left panel) and bone marrow (right panel) of WT and Postn$^{-/-}$ mice (B cells: B220$^+$, Megakaryoctyes: CD41$^+$, Granulocytes: B220$^-$CD4/8$^-$CD11b$^+$Gr1$^+$, T cells: CD4/8$^+$, Erythrocytes: Ter119$^+$). (C) Cell cycle analysis of HSC compartment ($G_0$: Ki67$^-$Hoechst$^{lo}$, $G_1$: Ki67$^+$Hoechst$^{lo}$, S/$G_2$M: Ki67$^+$Hoechst$^{hi}$). (D) Analysis of peripheral blood parameters of WT and Postn$^{-/-}$ mice assessed through Hemavet. Units are given for each individual parameter in brackets in the x-axis (RBC: red blood count, Hb: Hemoglobin, HCT: hematocrit, MCV: mean corpuscular volume, MCH: mean corpuscular hemoglobin, MCHC: mean corpuscular hemoglobin concentration, RDW: red cell distribution width). (E) Analysis of 1° and 2° Colony-forming unit (CFU) of total bone marrow cells of WT and Postn$^{-/-}$ mice after 7 days of culture.

Unpaired t-test analysis was performed. In case of multiple comparisons, p-values were corrected by the Benjamini-Hochberg method with FDR = 5% (*, p<0.05, **, p<0.01, ***, p<0.001, ****, p<0.0001). Mean ± SD, n≥3.

### *3.4.5. Postn$^{-/-}$ HSCs perform better than WT HSCs in a competitive transplantation*

Even though Postn$^{-/-}$ mice showed normal output of differentiated cells, variations in cell frequencies in the stem cell compartment could indicate functional differences of HSCs in these mice. Thus, we performed competitive transplantation experiments to test the repopulating ability of Postn$^{-/-}$ HSCs in competition with WT HSCs in the same microenvironment. Repopulation of transplanted BM cells of Postn$^{-/-}$ mice was analyzed in competition with WT cells. Postn$^{-/-}$ (CD45.2) and WT (CD45.1/.2) BM cells were transplanted at a 50:50 ratio into lethally irradiated recipients (CD45.1) and engraftment was followed over time. (Figure 3.4.5 A). As a control, WT CD45.2 and WT CD45.1/.2 cells were competitively transplanted to normalize for repopulation differences in WT isotypes (data not shown). Already 4 weeks post transplantation, Postn$^{-/-}$ blood cells significantly outcompeted WT blood cells. This competitive advantage of the Postn$^{-/-}$ cells increased over time and was stable upon retransplanted into secondary recipients (Figure 3.4.5 B). This data indicates that Postn$^{-/-}$ HSCs perform better than WT HSCs in a competitive environment and repopulate more efficiently than WT HSCs. This could point to differential regulation of the homing, engraftment, expansion, or maintenance of Postn$^{-/-}$ HSCs. This and long-term effects of this increased proliferative stress on the HSCs will need to be further investigated. Further experiments will focus on characterizing the hematopoietic system of these mice following treatment with other cytokines to study their response to different forms of inflammatory stimuli. Additionally, homing capacity of ECM-deficient HSCs compared to WT cells will be studied.

Overall, ECM-deficient mice do not show any obvious defects in the hematopoietic system under homeostasis. Some differences in response and recovery following hematopoietic stress could be shown and further analysis will need to be performed to uncover the mechanisms and consequences these have on the hematopoietic system.

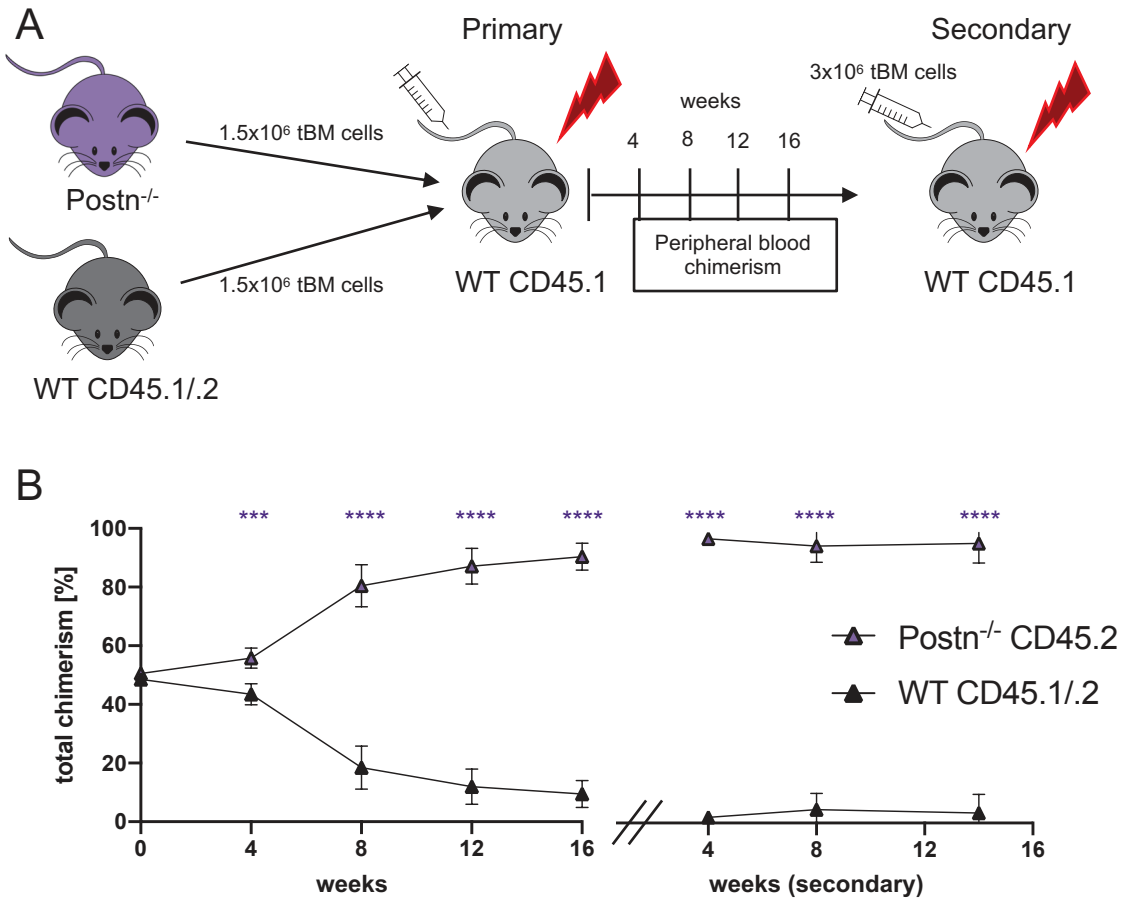


**Figure 3.4.5 Postn$^{-/-}$ HSCs have competitive repopulation advantage over WT HSCs.**
(A) Schematic overview of the experiment. Postn$^{-/-}$ and WT tBM cells are mixed 50:50 and transplanted into lethally irradiated CD45.1 WT mice. Peripheral blood chimerism is analyzed over time. After 16 weeks, tBM cells or primary recipients are transplanted into secondary recipients and again, peripheral blood chimerism is analyzed over time. (B) Peripheral blood chimerism of Postn$^{-/-}$ (CD45.2) and WT (CD45.1/.2) over time analyzed by flow cytometry. Unpaired t-test analysis was performed (*, $p<0.05$, **, $p<0.01$, ***, $p<0.001$, ****, $p<0.0001$). Mean ± SD, $n\geq3$.

# 4. DISCUSSION

## 4.1. The origin of interferon signaling heterogeneity during embryonic development of the hematopoietic system

During hematopoietic development, different embryonic sites pose as niches for the formation, maturation, and expansion of HSCs. Each site has a distinct microenvironment favorable for the HSC at different time points of development (Gekas *et al.*, 2005). One of those sites is the placenta. Even though it has been shown before that fetal B cell precursors are present in the placenta (Melchers, 1979), its role and function during hematopoietic development has not been investigated until much later and the placenta as one of the embryonic organs of hematopoietic development has only been recognized in the early 2000s (Alvarez-Silva *et al.*, 2003; Gekas *et al.*, 2005). Today, it is accepted that the placenta does indeed function as a hematopoietic organ, however, its full potential and role as an HSC-supportive niche is still fairly unknown.

In the adult hematopoietic system, a baseline of homeostatic IFN signaling mediated by baseline expression of ISGs is critical to ensure a rapid response during an infection and proper clearance of foreign pathogens from the system to allow recovery. This baseline of IFN signaling, however, is highly heterogenous both within one cell type as well as between different cell types.

In this study, we uncovered that during definitive hematopoietic development, placenta-derived cells displayed the highest overall IFN signaling baseline at all times compared to other embryonic sites (Figure 4.1.1 A). The placenta faces a unique status during development as it is the only organ with direct interaction of mother and embryo. Proper placental development is crucial and malformation of this organ often leads to embryonic lethality and pregnancy loss (Rossant and Cross, 2001; Gekas *et al.*, 2005). Here, the fetus is supplied with oxygen and nutrients, which also poses the risk of pathogen exposure from the maternal side. Cells residing in this organ during development might therefore need increased protection against infections or in case of infection, a heightened response to inflammatory cues. High IFN signaling baseline in the placenta potentially serves as a protection barrier to ensure uninterrupted and correct development of rare definitive HSCs that will establish and maintain the entire adult blood system during the lifetime of an organism.

Already in the fetal liver, however, HSCs display heterogenous levels of the IFN signaling baseline, which means, that not all of these cells established a higher baseline during development. Our data so far supports the hypothesis that once a baseline level of IFN signaling is established, the baseline remains stable over time, differentiation, and transplantation. This leads to the assumptions that either not all cells migrating through the

placenta established a high baseline after all, that some cells did in fact not migrate through the placenta during development but rather directly from AGM or via the yolk sac to the fetal liver, or that cells with an originally high baseline contrary to previous data lost their level of baseline IFN signaling to make up the pool of fetal liver-derived HSCs with low IFN signaling baseline. Additionally, it cannot be excluded from our data that the placenta is a site of *de novo* HSC formation or that immature progenitors migrate to the placenta from sites of primitive hematopoiesis like the allantoic mesoderm that houses the hemangioblast (Huber *et al.*, 2004) and only mature to definitive HSCs in the placenta (Mikkola *et al.*, 2005). Moreover, cellular kinetics could play a role. Cells only temporarily passing through the placenta potentially would not mediate a higher IFN signaling baseline unlike cells that are generated in the placenta or reside there longer (Figure 4.1.1 B).

In conclusion, we identified the placenta as an embryonic niche that provides cells with high basal IFN signaling during hematopoietic development, which potentially protects migrating cells against invading pathogens from the maternal system. Investigation of IFN signaling in HSCs of the embryo following embryo transfer into mice with differential IFN signaling compared to the embryo and treatment of pregnant mice with recombinant IFN or broad spectrum antibiotics will help to better understand the role of maternal IFN signaling on general embryo development as well as the developing IFN signaling.

Close proximity of maternal and fetal hematopoietic system in the placenta poses the question, if maternal IFN signaling affects the development of IFN signaling heterogeneity in the embryo or if this signaling in the embryo develops independently. Moreover, the placenta is a niche for developing definitive HSCs, however, if placental endothelial cells or other cells of the niche, like stromal cells, directly or indirectly impact on the HSCs and IFN signaling remains to be investigated. Different HSC locations within the placental niche potentially have divers effects on establishing IFN signaling levels, which could be addressed using imaging approaches. Whole organ imaging of reporter mice in combination with HSC staining will allow specific identification of the location of HSCs with higher IFN signaling within the organ. Hematopoietic activity has been suggested in the placental labyrinth, the chorionic plate, as well as different nearby vessels (Azevedo Portilho *et al.*, 2016; Ottersbach and Dzierzak, 2005; Sasaki *et al.*, 2010; Rhodes *et al.*, 2008; Bertrand *et al.*, 2005; Azevedo Portilho and Pelajo-Machado, 2018). One caveat of this approach is the proper identification of HSCs during development. Even though we were able to isolate cells starting from E10.5 with our defined HSCs surface marker schemes, it was not proven that these cells were in fact all functional definitive HSCs. At this early timepoint of development, specific identification of definitive HSCs with surface markers for flow cytometry or imaging remains challenging, however, usage of the IFN signaling

reporter mouse systems will allow the identification of cells with increased IFN signaling levels independent of a specific cell type.

The placenta is not only the major organ of nutrient exchange between fetal and maternal systems, but also an endocrine organ (Linzer and Fisher, 1999; Ottersbach and Dzierzak, 2010). A number of hormones are produced from placental trophoblast cells, some of which have been known to influence vascularization of the placenta (Ma *et al.*, 1997; Ng *et al.*, 1994; Ottersbach and Dzierzak, 2010). Moreover, a direct influence of these hormones on hematopoiesis has also been reported (Linzer and Fisher, 1999; Ottersbach and Dzierzak, 2010). Hormone production in the placental niche and exposure of HSCs and other hematopoietic cells to these hormones potentially alters the function of these cells and their IFN signaling baseline. To test this, cells isolated from other embryonal organs could be exposed to hormones *in vitro* to analyze potential changes in IFN signaling levels and compare the levels to those of the cells from the placenta.

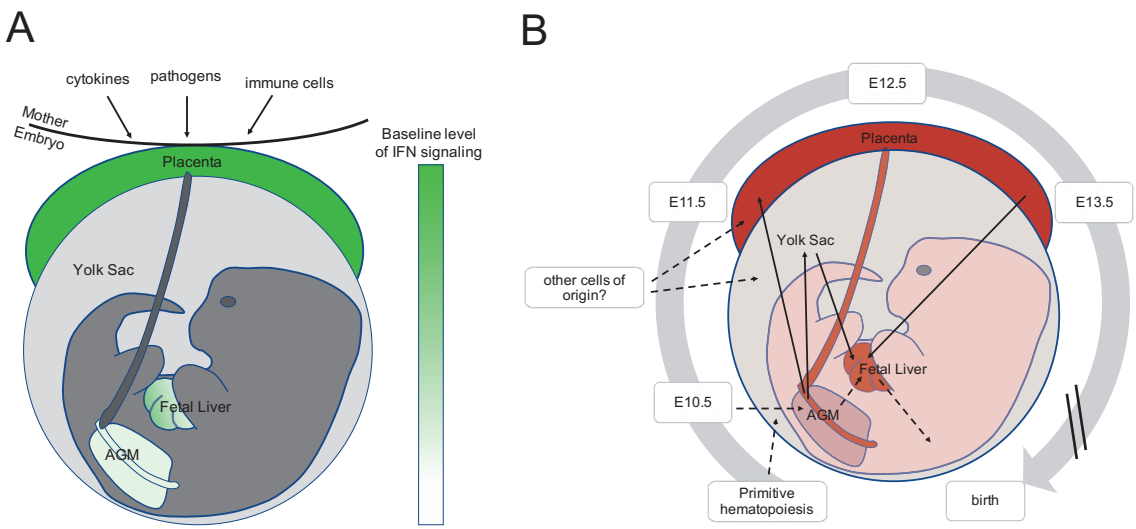


**Figure 4.1.1 Models** of (A) IFN signaling heterogeneity during development of definitive HSCs and (B) potential paths of definitive HSCs during hematopoietic development.

Throughout these experiments, fetal liver cells showed the most heterogeneity in regards to IFN signaling levels and these cells showed the highest susceptibility to changes in the experimental setup. Whereas AGM- and placenta-derived mature blood cells displayed either low or high basal ISG levels, respectively, levels of fetal liver-derived mature blood cells ranged from anywhere as low as AGM to as high as the highest placenta levels, mimicking the phenotype seen in the adult system. Thus, the data would suggest that previous to the migration to the fetal liver, cells with higher and lower IFN signaling baseline are established and together form the heterogenous pool of cells found in the fetal liver prior to birth and that is maintained in the adult system.

In this thesis, we were able to show differential ISG expression during hematopoietic development, however, basal IFN signaling was already established at the earliest time point investigated (E10.5). Our data and that of others (Wu *et al.*, 2018) indicate that ESCs express high levels of ISGs. Additionally, data from our group also showed that tissue-resident macrophages that do not originate from HSCs (Gomez Perdiguero *et al.*, 2015; Schulz *et al.*, 2012) express higher levels of ISGs than macrophages differentiated from an HSC-origin (Itani *et al.*, in preparation). These findings indicate that before the emergence of definitive hematopoiesis, IFN signaling is generally high. However, when the first definitive HSCs emerge in the AGM, these cells only show low levels of ISG expression. HSCs are found in the placenta only slightly later than in the AGM, where the cells again express higher levels of ISGs, leading to the question if all cells initially display high levels of IFN signaling during primitive hematopoiesis and only a subset of cells loose the high baseline with the onset of definitive hematopoiesis. It is also possible that primitive or immature HSCs with high IFN signaling seed the placenta from an unknown origin and maintain high basal levels in this organ whereas newly formed definitive HSCs in the AGM do not maintain this higher baseline. Overall, this data indicates that the origin of IFN signaling heterogeneity during hematopoietic development precedes the onset of definitive hematopoiesis in the AGM.

Further insight into the cells of origin of this heterogeneity is of interest and could be achieved through improved imaging techniques. This will include co-staining with known developmental hematopoiesis and endothelial markers at earlier developmental stages to try to identify the earliest reporter-expressing cells. Additionally, new preparation and staining protocols will be tested to optimize the procedure. The current protocol includes a trimming step that is necessary to decrease the depth of the embryo, allowing the microscope objective proper focus. This is not ideal since trimming risks to damage the area of interest in the embryo. Other protocols like the iDISCO protocol (Renier *et al.*, 2014) achieved imaging without trimming. However, this will need to be tested on embryos younger than E10.5.

Additionally to improved imaging approaches, further optimization of the culture and analysis of ESC lines *in vitro* will allow the investigation of IFN signaling during early hematopoietic

development which will be a valuable addition to data generated *in vivo*. Differentiation from ESCs to definitive HSCs occurs through various steps from mesodermal cells, or pre-HSCs, that commit to the hematopoietic lineage and then give rise to HSCs (Matsumoto *et al.*, 2009). Identification of these mesodermal cells was shown in embryoid bodies of an *in vitro* co-culture system of ESCs and OP9 cells that included an inducible HOXB4 expression system (Kyba *et al.*, 2002; Matsumoto *et al.*, 2009). This culture system supports the differentiation of pre-HSCs to an intermediate cell populations here termed embryonic HSCs with only low engraftment efficiency in the adult and it is proposed that these embryonic HSCs then give rise to definitive or adult type HSCs (Matsumoto *et al.*, 2009). In my thesis, focus was on the analysis of definitive HSCs in regards to their IFN signaling. However, since at E10.5, differences in baseline IFN signaling are already established, analysis of intermediate stages of hematopoietic development previous to the emergence of definitive HSCs will be of interest. During the development from ESCs to the definitive HSCs found in the AGM, IFN signaling baseline is reduced, however, at which cellular stage this occurs or which mechanisms are in play, is not known yet. The proposed co-culture system potentially allows investigation IFN signaling during primitive hematopoietic development independently of *in vivo* mouse models to support future findings.

Clinically, this could have an important impact. In regenerative medicine, manipulation of induced pluripotent stem cells (iPSCs) has been used to generate mature cells of different tissues (Takahashi *et al.*, 2007; Matsumoto *et al.*, 2009; Shi *et al.*, 2017), however, generation of efficient numbers of HSCs *in vitro* has not been successful so far. Optimization of *in vitro* culture systems of ESCs in combination with more detailed analysis of IFN signaling during primitive hematopoietic development could potentially contribute to improving current protocols of immunotherapy. If a manipulation of IFN signaling or interference with establishment of IFN signaling heterogeneity is possible *in vitro*, HSCs or other hematopoietic cells with the desired IFN signaling baseline could be generated and introduced to patients with abnormal IFN signaling. For example during autoimmunity, IFN signaling imbalance and abnormal expression of ISGs contributes to disease progression (Trinchieri, 2010). Introduction of *in vitro*-manipulated hematopoietic cells could reestablish balanced IFN signaling.

In the adult hematopoietic system, basal IFN signaling mediated through expression of ISGs is maintained at the stem cell level and inherited upon differentiation. A stem cell with a high baseline will produce mature cells with a higher baseline relative to other mature cells (Hirche *et al.*, in preparation). During hematopoietic development, the different embryonic sites display unique basal ISG levels. After transplantation of embryonal cells into adult recipients, these baselines were maintained in the mature blood cells. It is important that IFN signaling heterogeneity is established during hematopoietic development. Once definitive HSCs are generated, matured, and homed to the BM upon birth, there is likely no *de novo* formation of HSCs in the adult. The HSC pool is maintained and replenished through self-renewal of already existing HSC. It is therefore important that all crucial functions of HSCs including basal IFN signaling levels are already established during development and maintained throughout life.

We did not succeed in successful engraftment of stringently isolated embryonal HSCs into adult recipients. It is possible that these still fairly immature cells cannot withstand the stress of flow cytometric isolation and HSC activity might be diminished after this procedure. Alternatively, successful homing to the adult bone marrow might pose a challenge. Definitive HSCs are defined by their ability to engraft an adult recipient, however, this is only possible if the cells successfully home to the bone marrow. Transplantation efficiency of definitive HSCs from early time points of development before their final expansion in the fetal liver might be improved when cells are injected into fetal livers of neonatal recipients rather than through tail vein injection into adult recipients. Further transplant experiments might give additional insights into the exact cells that mediated differential IFN signaling heterogeneity.

High basal ISG expression is conserved in multiple different tissue stem cells, including HSCs, mesenchymal stem cells (MSCs), neuronal stem cells, and pancreatic stem cells, however, each tissue site displays a distinct pattern of highly expressed ISGs (Wu *et al.*, 2018). Additionally, a published data set comparing BM-derived with placental MSCs confirmed distinct ISG expression patterns for cells isolated from each analyzed tissue (Roson-Burgo *et al.*, 2014, Wu *et al.*, 2018). Our data strengthened these findings in embryonal tissues isolated during hematopoietic development. Although the overall IFN signaling baseline of HSCs derived from AGM and placenta did not change significantly between differently defined HSCs, progenitor cells, or general blood cells, these baselines were not always mediated through differential expression of the same ISGs. Most ISGs that are highly expressed in these embryonal HSCs have known antiviral or -bacterial functions (Wang *et al.*, 2015; Huang *et al.*, 2011; Steinbusch *et al.*, 2019; Carlow *et al.*, 1998; Weiss *et al.*, 2018; Stepp *et al.*, 2017; Lee *et al.*, 2019; Leisching *et al.*, 2019), however, functions independent of viral response have also been suggested. Examples of other known functions during tissue homeostasis include a

role for Oas1g in the estrogen dependent pathways in rat mammary gland physiology (Maia *et al.*, 2008), a role of Plac8 in trophoblast invasion and migration during placental development (Chang *et al.*, 2018) or as identification markers that enrich for certain cell populations (Natale *et al.*, 2017; Spangrude *et al.*, 1988). More recently, several of these ISGs have been implicated to play a role in different forms of cancer and increased expression often correlated with further disease progression and poorer overall outcome (Li *et al.*, 2019; Jia *et al.*, 2018; Tang *et al.*, 2020). The panel of ISGs used in this study was defined using microarray data of adult HSCs after *in vivo* recombinant IFN$\alpha$ treatment. Differentially expressed genes were identified and subsequently used as ISGs to investigate IFN signaling under homeostasis. ISG expression patterns are, however, dependent on isolated tissue, developmental stage of the cells, and external stimuli. Defining an ISG panel less biased to HSCs and independently of IFN treatment will help to further investigate IFN signaling heterogeneity during unperturbed hematopoiesis. This indicates that even though all of these genes are stimulated upon IFN and may play a role in the response to infections, most of these ISGs additionally have other functions during homeostasis and when regulated abnormally, can lead to the development of malignancies.

Overall, during hematopoietic development, HSCs migrate through different embryonic sites. Each site models a unique microenvironment for the maturation and expansion of these cells and therefore, depending on the site, the cells are exposed to distinct microenvironmental cues. Furthermore, our data showed distinct ISG expression patterns depending on the surface marker definition of cells isolated from the same tissue, which indicates cell intrinsic regulation of these ISG expression patterns.

HSCs sense microenvironmental changes and need to adapt to those. However, at the same time, those cells need to be protected from exposure to pathogens or other harming stimuli. Maintenance of a properly functioning HSC pool is crucial for survival and intrinsic regulation of ISG expression provides a way to ensure protection. Competitive transplantations of cells derived from organs of different IFN signaling baselines into the same recipient microenvironment allows the investigation of cell intrinsic and extrinsic effects. Definitive HSCs start to express CD45 during late AGM stages (North *et al.*, 2002) and usage of the CD45.1/.2 system permits identification of donor-derived cells from for example AGM or placenta. If donor-derived cells retain their IFN signaling baseline regardless of the presence of cells with differential baseline or effects of the niche, cell intrinsic regulation of the establishment of the baseline is likely. One limitation of this experimental setup is the difference in engraftment efficiency of cells from different embryonic sites. In this study, E12.5 embryonic organ cells were transplanted. This is not the ideal timepoint to study AGM-derived HSCs. Placenta-derived HSCs are in the peak of expansion at this point and will most certainly outcompete

AGM-derived cells rapidly when transplanted together. In order to analyze donor-derived cells from both AGM and placenta in a competitive setting, an earlier timepoint like E11.5 will be beneficial.
We already know that from fetal liver stage of development on, cells with varying baselines co-exist in the same niche throughout adulthood. Maintenance of the baseline therefore is not affected by the presence and signals of cells with a different baseline. During development, however, cells in the AGM mainly display low levels of IFN signaling initially, whereas cells in placenta show a higher baseline. Analysis before these cells would naturally meet might give new insights into the initial establishment of IFN signaling heterogeneity.

In conclusion, we were able to identify differential IFN signaling baselines in embryonic sites of hematopoietic development that are mediated through the expression of distinct ISG patterns. Our data indicates that the origin of IFN signaling heterogeneity precedes that of the development of definitive hematopoiesis and additional experiments during primitive hematopoietic development, for example through imaging or in ESC cultures, will be necessary to identify the exact origin of IFN signaling heterogeneity during hematopoietic development.
A possible branching point for the separation of cells with high and low IFN signaling baseline is EHT, when cells commit to hematopoietic fate from the hemogenic endothelium. This occurs in the AGM, but also other embryonic sites like the placenta or the yolk sac contain hemogenic endothelium (Ottersbach and Dzierzak, 2005; Gekas *et al.*, 2010; Hirschi, 2012). However, it has not been proven yet if the progeny of these hemogenic endothelial cells from other embryonic sites fully mature to cells with definitive multilineage and self-renewal potential like adult type HSCs. If this is indeed the case, HSCs with high IFN signaling baseline potentially arise from hemogenic endothelium in the placenta whereas those with low IFN signaling baseline possibly arise in the AGM (Figure 4.1.2 A). A split of the different populations is also possible at several later stages during EHT in one embryonic site (Figure 4.1.2 B) or once EHT has occurred and cells migrate through different embryonic sites (Figure 4.1.2 C). Following EHT, immature or pre-HSCs mature to definitive HSCs and different signals during maturation could lead to a pool of definitive HSCs with differential IFN signaling baselines.
The question arises how separately developing HSCs are phenotypically so similar in the adult. In the adult hematopoietic system, even though cells with different IFN signaling baselines exist and potentially have different functions upon infection or inflammation, the HSCs otherwise perform and behave similarly which would favor a separation of the populations late stage during development.

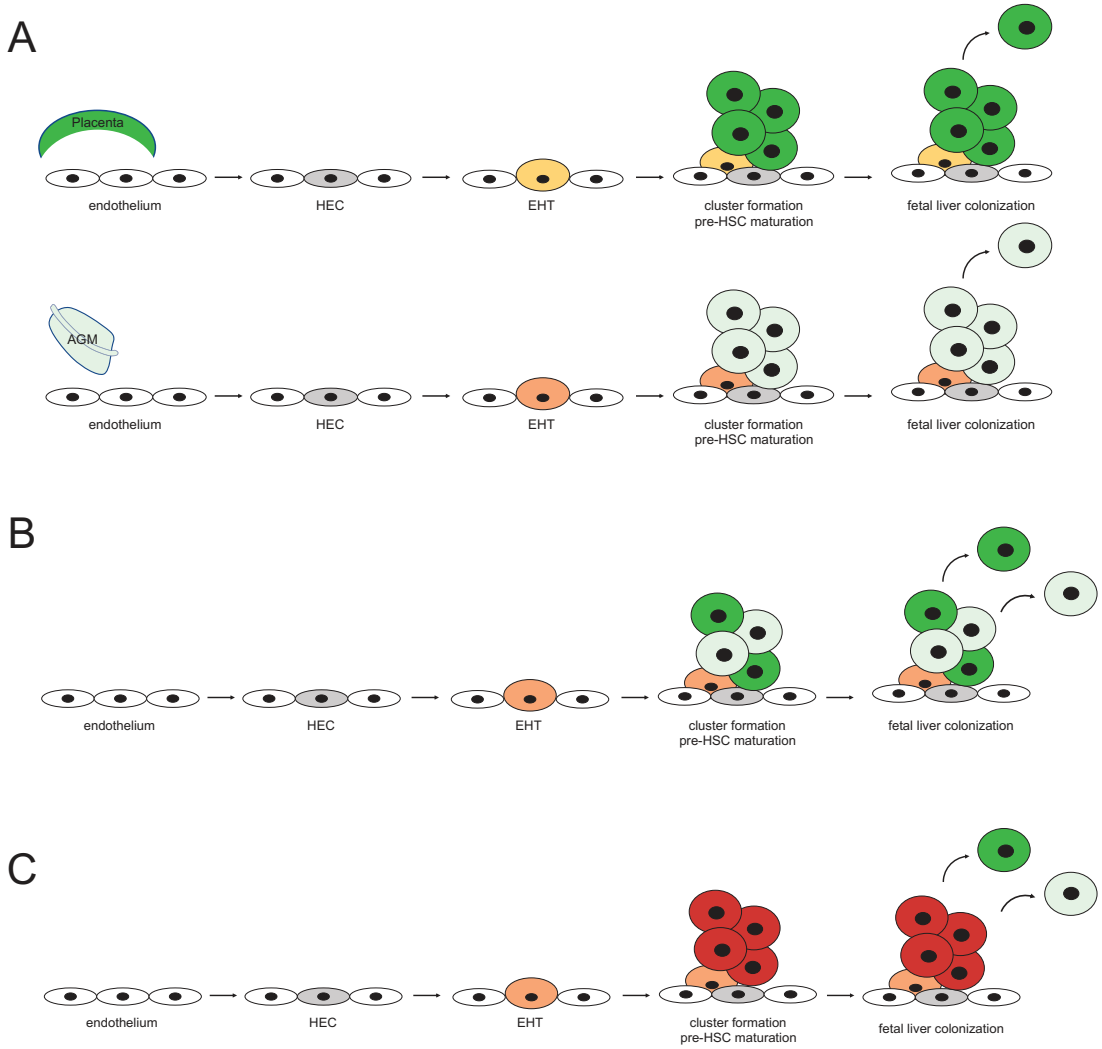


**Figure 4.1.2 Models of possible branching points of IFN signaling heterogeneity.**
(A) Independent development of high and low IFN signaling baseline in different locations. (B) Development of cells with high and low IFN signaling baseline during EHT. (C) Development of one type of cell during EHT and later development of differential IFN signaling baselines for example by migration through different embryonic sites (adapted from Ottersbach, 2019).

### 4.2. The function of interferon signaling heterogeneity during hematopoietic development and in the adult hematopoietic system

During infections, immune cells are recruited rapidly to clear foreign pathogens and infected cells from the system and reintroduce homeostasis. It is important to not completely deplete the immune system during this process and heterogeneity in cellular response might be one factor to prevent exhaustion. Decreased basal levels of IFN signaling in mice lacking IFNAR show abnormalities in splenic NK cells, B lymphocytes, as well as myeloid cells (Hwang *et al.*, 1995; Swann *et al.*, 2007; Gough *et al.*, 2012) and KO of the IFN$\beta$ gene in mice lead to an increased susceptibility to more severe chronic inflammation (Teige *et al.*, 2003; Gough *et al.*, 2012). HSC homeostasis and proper niche function has been shown to be reliant on constitutive IFN (Essers *et al.*, 2009; Sato *et al.*, 2009), but increased levels of IFN, either by an overproduction or prolonged IFN treatment, leads to the exhaustion of the HSC niche (Sato *et al.*, 2009), showing that balanced levels of IFN and IFN signaling are necessary to ensure long-term maintenance and function of the hematopoietic system. Heterogeneity in baseline IFN signaling through differential ISG expression within one cell type creates several layers of the inflammatory signaling and provides the hematopoietic system the possibility to have cells with different levels of susceptibility and different response kinetics to external insults.

IFN signaling heterogeneity is already established during hematopoietic development and maintained in the adult system. Under homeostasis, adult HSCs and other tissue stem cells express ISGs at high levels (Hirche *et al.*, in preparation, Wu *et al.*, 2018). Even though HSCs can directly sense and respond to IFN and actively start proliferation (Essers *et al.*, 2009; Baldridge *et al.*, 2010), these cells show increased viral resistance (Wu *et al.*, 2018; Maillard *et al.*, 2013). HSCs participate in the antiviral response by providing increased output of differentiated cells while protecting themselves from infection at the same time. Whether the heterogeneity in IFN signaling baseline within this cell pool directly causes functional differences on the stem cell level or if this heterogeneity is only established here in order to be inherited to mature cells that actively clear infections, remains to be investigated. Moreover, it is not clear if the heterogeneity is more important during development and if so, in which cells, in the adult, or in both. We therefore aimed to investigate the function of IFN signaling heterogeneity in different cell types during embryonic development and in the adult system.

Our data indicates that higher baseline expression of ISGs in embryonal organs confers a protection against the entry of certain viruses. Previous data from the adult hematopoietic system, however, also showed that upon inflammatory stress or viral infection, cells with higher IFN signaling baseline, upregulated the expression of ISGs more significantly than those cells with lower initial baseline (Hirche *et al.*, in preparation). We hypothesize that a high baseline of ISG expression allows the cells to activate further transcription of these genes more rapidly

and more efficiently than other cells, leading to a faster response and subsequent lower infection.

HSCs display varying levels of basal IFN signaling and in the adult, so do mature blood and immune cells. During development, we could show definitive HSCs that displayed different levels of IFN signaling which led to differential viral infectibility. However, how differences in baseline IFN signaling affect immune cells during development, was not addressed yet. Previous to the emergence of definitive HSCs, progenitor cells are formed in the developing embryo with erythroid, macrophage and myeloid potential (Gomez Perdiguero *et al.*, 2015). Most mature cells differentiated from these progenitors are later replaced by HSC-derived cells. However, some primitive streak immune cells persist in the adult as tissue-resident cells that are maintained independently of HSCs. Data from our group showed higher baseline IFN signaling in tissue-resident cells compared to their HSC-derived counterparts (Itani *et al.*, in preparation) leading to the question of the function of the IFN signaling baseline in these cells both during development and in the adult. So called tissue-resident B1a cells, found in the peritoneal cavity of adult mice, for example, serve as a mediator between the innate and adaptive immune system (Baumgarth, 2011; Beaudin and Forsberg, 2016). These tissue-resident cells have been shown to play an important role during the rapid response to neonatal infections, however, are also related to the development of autoimmunity (Baumgarth, 2011; Duan and Morel, 2006; Beaudin and Forsberg, 2016). Initially during development, proper protection of the embryo against infections and insults is of utmost importance, and potentially mediated by the generally high IFN signaling in early developmental immune cells. To decrease the risk of autoimmunity and autoinflammatory diseases, however, establishment of a balance in highly reactive cells and those that react less or slower would be crucial. Replacement of most of these tissue-resident cells with an overall high IFN signaling baseline with HSC-derived cells could be one way to secure this balance. Further analysis of the IFN signaling of immune cells that developed before the emergence of HSCs and those that differentiated from definitive HSCs during different timepoints of development phenotypically via flow cytometry as well as functionally following cytokine or viral stimulation will improve the understanding of the importance of IFN signaling heterogeneity and provide insights into those cells where the heterogeneity is most important.

During hematopoietic development, functional differences in cells with a higher or lower IFN signaling baseline could be shown following viral infection. However, since the IFN signaling heterogeneity is stably maintained throughout adulthood, it is likely that the heterogeneity also has a function there. Experiments to study the function of IFN signaling heterogeneity in the hematopoietic system of adult mice following viral infection, failed to produce results. Through irradiation and transplantation, mice were created that lacked IFN signaling heterogeneity with

hematopoietic systems either having a high or low IFN signaling baseline. These mice as well as control mice were then systemically infected with MCMV, but all experimental mice displayed heightened response to the virus compared to control mice that were not irradiated or transplanted, indicating an incomplete recovery of the hematopoietic system of experimental mice.

This data is in concurrence with a recently published study of Calvi *et al*. (2019) showing persistent and progressive deficits in the hematopoietic stem cell compartment in both the acute and delayed phases up to 26 weeks following different doses of sublethal external total body irradiation in combination with injection of soluble $^{137}$Cesium. Changes in the bone marrow microenvironment following radiation injury appeared to also affect long-term recovery of HSCs (Calvi *et al.*, 2019; Doan *et al.*, 2013). These findings pose a challenge to modern stem cell research. The most frequently used assays to determine stem cell function are various forms of transplantation assays. Even though the transplanted cells of interest are not directly exposed to radiation, the successful recovery of the bone marrow niche of the recipient mice post irradiation is crucial to investigate homeostatic HSC biology. Furthermore, it cannot be excluded that the transplantation procedure itself leads to delayed effects on homeostasis. Lethal irradiation, in the clinic often in combination with chemotherapy, is the state-of-the-art method to condition recipients for HSC transplantation. The hematopoietic system of the recipient is thereby completely depleted, enabling introduction and engraftment of donor cells. During the time it takes for the donor cells to engraft and reestablish a hematopoietic system, recipients are at great risk of severe infections amongst other complications. Use of mice immunodeficient mice (e.g. NOD *scid* gamma (NSG) mice (Shultz *et al.*, 2005)) has been successful to study the human hematopoietic system through xenograft transplantations (McIntosh *et al.*, 2015), however, use of these mice for general mouse-to-mouse transplantation assays is impractical due to their severe immunodeficiency and high susceptibility to opportunistic infections.

In recent years, great focus has therefore been to develop other methods of conditioning decreasing the risk of immunosuppression and rejection of donor cells by the recipients. One promising method is the depletion of certain hematopoietic cells with antibodies prior to transplantation (George *et al.*, 2019). Antibody-depletion of recipient's HSCs and immune cells without the need of further conditioning might allow investigation of IFN signaling heterogeneity function independent of radiation-induced long-term side effects. Investigation of the function of IFN signaling heterogeneity without the need of transplantation assays altogether would be ideal, however, so far, there is no *in vivo* system that allows the analysis of a hematopoietic system that lacks heterogeneity and only displays high or low baseline IFN signaling.

One of our approaches to study IFN signaling during hematopoietic development is the treatment of pregnant mice with either recombinant IFN or broad spectrum antibiotics and

subsequent analysis of the IFN signaling baseline in the embryos. A possible outcome of these treatments is the skewing towards a higher or lower baseline in the embryo, respectively. According to our previous data, once a baseline is established, it is maintained for life and analysis of these embryos once adulthood is reached potentially provides a model system to further study the function of IFN signaling heterogeneity in the adult without transplantation assays. However, the hematopoietic system of these mice will need to be carefully characterized to uncover developmental or functional homeostatic defects before exposure to secondary insults like a systemic infection.

IFN signaling heterogeneity is stably inherited from HSCs to all downstream populations, however, so far it has not been clear if this heterogeneity also has a function in all these populations. It is possible that differences in basal IFN signaling levels are established and maintained at the stem cell level, yet only displays an active function on the level of the mature blood cells. Within the $CD8^+$ T cell compartment, both effector memory (EM) and central memory (CM) T cells are found in the spleen at certain times (Samji and Khanna, 2017). $CD8^+$ CM T cells have a higher proliferative potential than EM T cells (Sallusto *et al.*, 2004; Samji and Khanna, 2017). In a model proposed by Lanzavecchia and Sallusto (2000), EM T cells display more rapid effector functions compared to CM T cells. According to the model, EM T cells provide a protective memory, where the cells migrate to inflamed peripheral tissues and show immediate effector functions. CM T cells, on the other hand, provide a reactive memory, home to T cell areas of secondary lymphoid organs. CM T cells have little to no effector function, but are able to proliferate and differentiate to effector cells in response to antigen stimulation (Lanzavecchia and Sallusto, 2000). CM T cells therefore need a longer period of reactivation whereas EM T cells are able to respond immediately (Sallusto *et al.*, 2004).
Our results suggest a link between basal IFN signaling and $CD8^+$ T cell effector function. ISRE-eGFP $CD8^+$ EM T cells displayed an overall lower IFN signaling baseline mediated through a higher frequency of ISRE-eGFP$^{lo}$ cells compared to CM T cells. Upon inflammation, the overall baseline remained low in $CD8^+$ EM T cells due to a further increase in ISRE-eGFP$^{lo}$ cells. These data indicate that a lower IFN signaling baseline mediates an advantage towards rapid and immediate T cell effector functions.
Lag3 is a negative regulator during expansion of activated primary T cells and establishment of the memory T cell pool. Maintenance of T cell homeostasis is critical and relies on negative regulation of T cell activation and expansion (Workman *et al.*, 2004; Workman and Vignali, 2003; Grosso *et al.*, 2009). Whilst Lag3 expression on naïve $CD8^+$ T cells is low, the expression increases upon activation in response to antigen stimulation (Workman *et al.*, 2002; Grosso *et al.*, 2009) and it has been suggested that Lag3 plays an important functional role on CD8 T cells by maintaining a tolerogenic state. Inhibition of Lag3 has been shown to reverse this

state and partially restore effector function (Grosso *et al.*, 2009). Similar to Lag3, transient upregulation of PD-1 on activated T cells negatively regulates their function (Freeman *et al.*, 2000; Grosso *et al.*, 2009) and PD-1 expression is sustained at high levels on chronically activated and nonfunctional CD8 T cells after viral infection (Barber *et al.*, 2006; Day *et al.*, 2006; Grosso *et al.*, 2009). Analysis of different Lag3/PD-1 expressing T cell subpopulations has shown that CD8 T cells expressing PD-1 at the highest level are not capable of producing IFN$\gamma$ and therefore mediate lytic function. Moreover, cells that produce the highest levels of cytokines co-express Lag3, which suggests distinct functional characteristics of different T cell subpopulations with those expressing high levels of Lag3 being the most responsive (Grosso *et al.*, 2009). Additionally, as PD-1 expression levels increase, effector function of these T cells decreases. However, even though Lag3 and PD-1 are supposedly negative regulators of T cell function, PD-1/Lag3 double positive cells are more functional effector T cells compared to Lag3$^{-}$PD-1$^{int}$ CD8 T cells (Grosso *et al.*, 2009). Antibody-mediated blockage of PD-1 or more recently Lag3 amongst other co-inhibitory molecules has been successfully applied as immunotherapy against several different cancers (Woo *et al.*, 2012; Matsuzaki *et al.*, 2010; Wu *et al.*, 2019a) or chronic inflammation or infection (Anderson *et al.*, 2016; Barber *et al.*, 2006; Lichtenegger *et al.*, 2018). Immune checkpoint inhibition initiates a T cell response directed against tumor-associated antigens and reverses checkpoint mediated T cell exhaustion.

Our data showed that most ISRE-eGFP$^{hi}$ T cells did not express Lag3 or PD-1 after CD3/CD28 antigen stimulation *in vitro*, however, ISRE-eGFP$^{lo}$ T cells were able to express both PD-1 and Lag3 suggesting negative regulatory function of ISRE-eGFP$^{lo}$ rather than -eGFP$^{hi}$ T cells. One of the proposed roles of Lag3 is the maintenance of a tolerogenic T cell state to prevent T cell exhaustion and chronic activation. Upregulation of Lag3 expression in a small fraction of ISRE-eGFP$^{hi}$ T cell could indicate that even though these cells might not be fully activated, protection from exhaustion is still ensured. On the other hand, further increase of PD-1 expression in ISRE-eGFP$^{lo}$ T cells might also indicate reduced effector function of these cells compared to ISRE-eGFP$^{hi}$ cells and lack of Lag3 and PD-1 expression in ISRE-eGFP$^{hi}$ cells might indicate enhanced T cell activity in cells with a higher IFN signaling baseline.

It has been shown that one of the mechanisms responsible for resistance to immunotherapies, including blockage of PD-1, is related to type I IFN signaling (Jacquelot *et al.*, 2019). IFNAR signaling induced the expression of nitric oxide synthase 2 (NOS2) in tumor bearing mice which was associated with the reduction of intratumor cytotoxic T cells, increased Tregs and myeloid cells leading to an acquired resistance to anti-PD-1 antibody-based therapy (Jacquelot *et al.*, 2019). Furthermore, during a clinical trial on melanoma patients, differentially-expressed transcripts between responders and non-responders to anti-PD-1 antibody treatment showed a higher expression of several IFN-related genes in the tumors of non-responders implicating type I IFN signaling in poor response to immune checkpoint blockade (Jacquelot *et al.*, 2019).

In our study, *in vitro* T cell activation through antigen coated beads showed that regardless of $CD8^+$ or $CD4^+$, ISRE-eGFP$^{hi}$ T cells mostly remained inactive ($Lag3^-PD\text{-}1^-$) after incubation and only few cells had started to express Lag3. Almost no ISRE-eGFP$^{hi}$ cells expressed PD-1 or both markers at the same time. ISRE-eGFP$^{lo}$ T cells were activated more efficiently than ISRE-eGFP$^{hi}$ cells. ISRE-eGFP$^{lo}$ T cells expressed PD-1 alone, Lag3 alone, or both markers in combination after *in vitro* activation. Low expression of PD-1 of ISRE-eGFP$^{hi}$ T cells after antigen stimulation in our data could indicate another possible mechanism of resistance to immune checkpoint inhibition besides high Nos2 expression. If PD-1 is not expressed on the surface of the activated T cells, it might be more challenging to target these cells with anti-PD-1 antibody during immunotherapy to induce increased immune response.
Taken all data into account suggests distinct functional characteristics of ISRE-eGFP$^{hi}$ and ISRE-eGFP$^{lo}$ T cells, however, further investigation into the exact roles or effector functions of each subset during homeostasis, infection, inflammation, or cancer, is needed.

It is unlikely that IFN signaling heterogeneity only has a function in one mature cell type and investigation of other fully differentiated and immune cells of the hematopoietic system like B cells, NK cells, dendritic cells (DCs), neutrophils, macrophages, or other myeloid cells will allow a broader understanding of the impact of this signaling heterogeneity on the immune and hematopoietic system. These cells are major players during innate and adaptive immune response and IFN signaling heterogeneity in these cells potentially provides a more effective, faster response, or the ability to respond with a wider variety of mechanisms to foreign pathogens or inflammatory cues.
On the other hand, it is possible that IFN signaling heterogeneity does in fact not play a direct role in all immune cells, but rather an indirect role. For example, one mechanism to activate B cells during the antigen-dependent phase of B cell development is through interaction with T cells and T cell-dependent antigens (Bonilla and Oettgen, 2010). If IFN signaling heterogeneity plays a direct role during the activation of T cells, a function on B cells is potentially only indirect. Moreover, due to the vast number of interactions between the cell types of the immune system, both direct and indirect functions of IFN signaling heterogeneity on the level of these cells is possible.
Additionally, some of these terminally differentiated immune cells have the same precursor, monocytes. Monocytes are a heterogenous cell population and are classified into classical, intermediate, and nonclassical monocytes depending on surface marker expression (Anbazhagan *et al.*, 2014; Sprangers *et al.*, 2016) with the three cell types displaying distinct functions. Under homeostasis, tissue macrophages and DCs do not rely on the recruitment of monocytes for renewal, however, during inflammation, monocytes contribute to these immune cell populations (Sprangers *et al.*, 2016). Monocytes are recruited to inflammatory sites in

response to IFN where they differentiate into inflammatory macrophages and DCs (Askenase *et al.*, 2015; Sprangers *et al.*, 2016). However, prolonged immune response by these cells can lead to tissue damage, further inflammatory cascades or autoimmunity (Zimmermann *et al.*, 2012; Croxford *et al.*, 2015; Sprangers *et al.*, 2016). In patients with chronic inflammatory and fibrotic liver disease, intermediate monocytes accumulate as a consequence of increased recruitment of these cells from circulation and also differentiation of classical monocytes in response to the inflammation in the liver (Liaskou *et al.*, 2013; Sprangers *et al.*, 2016). Additionally, in juvenile idiopathic arthritis patients, increased phosphorylation of STAT1 and/or STAT3 has been shown in classical monocytes following IFN$\gamma$ stimulation (Throm *et al.*, 2018). The knowledge of the putative role of the different monocyte populations as distinct precursors during inflammation is still limited (Sprangers *et al.*, 2016), but of great interest for therapeutic targeting. Analysis of IFN signaling baselines in these different populations of monocytes as well as the fully differentiated down-stream populations under homeostasis and inflammation could provide important insight into the function of these cells and potentially further explain their contribution to chronic inflammatory or autoimmune diseases.
In conclusion, our data indicate functional differences in cells with high and low IFN signaling baseline in T cells, however, further investigation in these and other cell types of the immune system is important to understand the full effect of IFN signaling heterogeneity on the level of the immune cells under homeostasis and in response to infection or inflammation.

A balanced response to inflammatory signals is crucial to a long-term maintenance of the immune system. In healthy individuals, following successful clearance of foreign pathogens by initiating an inflammatory response, homeostasis is re-established. To prepare cells for a novel insult, cellular desensitization to IFN is necessary (Schneider *et al.*, 2014). Constitutive IFN production and secretion is crucial for an efficient response to infection, however, defective regulation of homeostatic IFN signaling can lead to the emergence of various autoinflammatory – or immune diseases (Muskardin and Niewold, 2018; Gough *et al.*, 2012; Kretschmer and Lee-Kirsch, 2017). If IFN production or signaling is dysregulated, autoimmune disorders including systemic lupus erythematosus (SLE), rheumatoid arthritis, or inflammatory bowel disease can develop (Schneider *et al.*, 2014; Ronnblom, 2011; Duan *et al.*, 2019). Serum IFN$\alpha$ levels in patients with SLE vary and are even normal in about half of the patients (Niewold *et al.*, 2007; Muskardin and Niewold, 2018) and abnormal inflammatory response is manifested through increased expression if type I IFN-regulated genes (Bennett *et al.*, 2003; Trinchieri, 2010) in certain immune cells. This heterogeneity leads to differences in molecular pathogenesis of SLE and disease severity (Baechler *et al.*, 2003; Muskardin and Niewold, 2018).

High levels of IFN signaling and development of certain hematological malignances are closely linked. Diseases that have been shown to be affected by high levels of IFN signaling are myeloproliferative neoplasms (MPNs) and certain cancers including chronic myeloid leukemia (CML). MPNs are a group of clonal hematopoietic disorders characterized by aberrant proliferation of one or more mature functional blood elements and progressive BM fibrosis (Spivak *et al.*, 2003; Dunbar *et al.*, 2017). Even though chronic inflammation can lead to development of early stage MPNs and subsequent leukemic transformation, treatment with IFN has shown success (Hasselbalch and Holmstrom, 2019; Borden *et al.*, 2007; Kujawski and Talpaz, 2007) and even lead to minimal residual disease in some patients (Hasselbalch and Holmstrom, 2019).

Our data shows IFN signaling heterogeneity, which has important implications for clinical applications. Understanding how IFN signaling heterogeneity is maintained under homeostasis and which functions this has in healthy individuals, will allow a translation to diseases that are affected by differences in basal IFN signaling. In SLE as well as other rheumatic diseases, high basal IFN signaling levels have been correlated with a more severe diseases. Manipulating basal IFN signaling levels in patients with a worse prognosis could lead to an improved outcome. IFN signaling heterogeneity is not only found between certain individuals or cell types, but also within one cell type. Reprogramming of certain subsets of immune cells that display abnormal IFN signaling could lead to a reversal to homeostasis.

Moreover, analysis of basal IFN signaling levels in MPNs might indicate which cells are responsible for a leukemic transformation in these diseases. Understanding through which mechanisms development of MPNs are promoted or identifying at what time point during development abnormal IFN signaling is introduced would allow for a more specific clinical approach.

Upon aging, the immune system is not as strong and efficient as in young individuals leading to increased deaths of older people following for example viral infections, like influenza A viral infection, which has been linked to defects in IFN production and activation of pathways inducing ISG expression (Molony *et al.*, 2017). Further analysis of the significance and function of IFN signaling heterogeneity upon aging and potential defects in mediating a balanced immune response will be of great interest.

Overall, understanding the function of IFN signaling heterogeneity during hematopoietic development, in the adult hematopoietic system, and upon aging in health, infection, and disease will allow targeting of specific aspects of the pathway to improve response to infections, inhibit development of certain diseases, improve existing treatments or develop new treatment approaches.

### 4.3. The mechanisms of interferon signaling heterogeneity

DNA methylation is one of main epigenetic mechanisms of gene regulation and has been shown to be involved in the pathogenesis of several autoimmune disorders (Chen *et al.*, 2019; Imgenberg-Kreuz *et al.*, 2018; Imgenberg-Kreuz *et al.*, 2016; Hedrich and Tsokos, 2011). But also in the healthy hematopoietic system, DNA methylation as well as other post-translational modifications play an important role in regulating IFN signaling and orchestrating IFN-mediated host immune response (Chen *et al.*, 2017).

DNA methylation analysis in IFITM3-eGFP and ISRE-eGFP mice gave conflicting results and a conclusion about the exact mechanisms that regulate IFN signaling heterogeneity could not be drawn. In IFITM3-eGFP mice, Ifitm3 gene locus is disrupted by the insertion of an eGFP, however, this targeted mutation does not affect normal development of these mice (Lange *et al.*, 2008). In ISRE-eGFP mice, eGFP is regulated by an IFN responsive promotor (Tovey *et al.*, 2006), but does not interrupt the ISRE locus (see Figure 3.3.1B). Previous data from our group showed a significant overlap in results obtained from IFITM3-eGFP and ISRE-eGFP mice. However, DNA methylation analysis displayed that in IFITM3-eGFP mice, DNA methylation levels in the Ifitm3 locus were dependent on reporter expression whereas in ISRE-eGFP mice, this was not the case and DNA methylation of the Ifitm3 locus was independent of reporter expression. Insertion of the eGFP might cause changes in DNA methylation levels at this locus and thereby masks any changes in methylation levels that could be due to IFN signaling heterogeneity. In ISRE-eGFP mice, distinction between cells with high or low eGFP expression did not show any differences in DNA methylation levels leading to the assumption that IFN signaling heterogeneity in these mice is, if at all, only to some extent mediated through DNA methylation patterns.

DNA methylation analysis of other ISG loci that are not affected by eGFP insertion will help understand if DNA methylation is indeed one of the mechanisms responsible for IFN signaling heterogeneity. If other loci of ISGs also do not show differences in DNA methylation patterns regardless of IFN signaling levels like the Ifitm3 locus in the ISRE-eGFP mice, IFN signaling heterogeneity is likely not mediated through differences in DNA methylation and variations observed in the IFITM3-eGFP mice are a results of eGFP insertion. In that case, further analysis will have to focus on investigating other epigenetic mechanisms to uncover how IFN signaling heterogeneity is established.

Other epigenetic mechanisms regulating gene function in the immune system include further post-translational modifications like phosphorylation, ubiquitination, or acetylation (Zhou *et al.*, 2017). However, regulation through noncoding RNAs like long noncoding RNAs or microRNAs has also been suggested (Vigneau *et al.*, 2003; Dorhoi *et al.*, 2013; Fenimore and H, 2016). Analysis of other mechanisms known to be involved in the regulation of IFN signaling or mechanisms of epigenetic memory in general might give insight into which mechanisms are

responsible for the regulation of the signaling heterogeneity. A variety of epigenetic mechanisms mediate gene expression and epigenetic memory affects the responsiveness of organisms to repeated environmental cues or stimuli over long periods of time. Epigenetic memory is defined as stable propagation of a change in gene expression that can be induced by developmental or environmental cues (D'Urso and Brickner, 2014). This memory can be mediated through multiple mechanisms that often lead to chromatin-based changes like DNA methylation, histone modifications, or incorporation of variant histones (Suganuma and Workman, 2011; D'Urso and Brickner, 2014). There are different types of epigenetic memories, depending on when and how the memory is established. Cellular memory occurs during early development, when tissue specific transcription factors mediate and establish different transcriptional programs. These programs are then maintained over many cell divisions through histone methylation (Kiefer, 2007; Bantignies *et al.*, 2003; D'Urso and Brickner, 2014). Environmental stimuli lead to changes in transcription. Transcriptional memory is defined by a qualitatively or quantitatively altered responsiveness of cells and organisms to a repeated stimuli that is mediated by epigenetically heritable mechanisms. If a gene was previously expressed following a stimuli, reactivation and more robust transcriptional response of this gene can be influenced by changes in chromatin structure (Brickner *et al.*, 2007; Gialitakis *et al.*, 2010; D'Urso and Brickner, 2014). For example, in humans, the class II major histocompatibility gene *HLA-DRA* is induced by IFN$\gamma$. This induction is much faster when the cells have already been exposed to IFN$\gamma$ previously. This memory is stable over several mitotic generations. Here, dimethylation of histone H3 on lysine 4 (H3K4) in the promoter of *HLA-DRA* is the responsible mechanism (Gialitakis *et al.*, 2010; D'Urso and Brickner, 2014).

A third type of epigenetic memory is the transgenerational memory which is characterized by a memory in gene expression over several generations (Jablonka and Raz, 2009; D'Urso and Brickner, 2014). This can lead to phenotypic differences between genetically identical organisms through genomic imprinting and epigenetic modifications (Bartolomei and Ferguson-Smith, 2011; D'Urso and Brickner, 2014). If a parent is exposed to certain environmental factors, this can also influence the physiology, morphology, and health of the offspring through epigenetic modifications like cytosine methylation, chromatin structure, but also through RNA populations (Rando, 2012; D'Urso and Brickner, 2014).

Making use of the general knowledge of epigenetic memory could improve the understanding of the epigenetic mechanisms that mediate and stably maintain IFN signaling heterogeneity in the hematopoietic system. In the hematopoietic system, heterogenous behavior of HSCs like lineage or proliferation bias has been linked to epigenetic changes. Differences in DNA methylation and chromatin accessibility of HSC-specific enhancer and promotor regions of certain HSC clones were correlated to cellular behavior and functional output of these cells (Yu and Scadden, 2016).

Certain cells of the immune system display a memory to previous insults and are primed to respond more efficiently to recurring insults. Understanding the epigenetic mechanisms behind this will also improve the understanding of the memory of IFN signaling heterogeneity in HSCs. Memory T cells, for example, are part of the adaptive immune system and display transcriptional memory when encountered with the same antigen multiple times that is mediated through the chromatin environment like different histone modifications (Dunn *et al.*, 2015; Woodworth and Holloway, 2017). One example here is the H3 acetylation of the IFN$\gamma$ promoter following viral infection that is maintained from naïve T cells to $CD8^+$ memory T cells (Northrop *et al.*, 2006; Northrop *et al.*, 2008; Dunn *et al.*, 2015). However, a combination of different epigenetic modifications in the same genomic locus has been shown in ESCs that provide a regulatory mechanism that either rapidly activates or represses transcription based on the situation (Bernstein *et al.*, 2006; Cui *et al.*, 2009; Dunn *et al.*, 2015). Such “bivalent” loci also exist in memory T cells (Araki *et al.*, 2009; Dunn *et al.*, 2015).
Histone modifications are one way to change the chromatin environment. Other modifications include ATP-dependent chromatin remodeling complexes or histone variant exchange where canonical histones are replaced by variant forms (Weber and Henikoff, 2014; Dunn *et al.*, 2015). This can have an effect on nucleosome stability (Jin and Felsenfeld, 2007; Dunn *et al.*, 2015), disrupt chromatin structures (Chen *et al.*, 2013; Dunn *et al.*, 2015), or have indirect effects (Loyola *et al.*, 2006; Dunn *et al.*, 2015) and thereby mediate transcriptional memory.

Epigenetic memory in the immune system is mediated through interplay of several different mechanisms that provide multiple layers of regulation. Gene expression and transcriptional memory in other parts of the hematopoietic system likely follows a similar direction. Even though DNA methylation is one potential mechanisms mediating IFN signaling heterogeneity, analysis of other epigenetic mechanisms mentioned here will help entangle the complex regulatory network responsible for the establishment and maintenance of IFN signaling heterogeneity.

### 4.4. The role of the ECM in the stress-induced activation of HSCs

Even though the ECM in general is a widely studied structural component of the BM microenvironment (Choi and Harley, 2017; Discher *et al.*, 2009; Klein, 1995), its active role in HSC biology has not been focused on as much. During steady-state hematopoiesis, ECM molecules have been shown to actively participate in HSC proliferation, differentiation, migration, homing, lineage commitment through ECM-integrin interaction (Grassinger *et al.*, 2009; Nakamura-Ishizu *et al.*, 2012; Ellis *et al.*, 2013; Domingues *et al.*, 2017). During HSC activation upon inflammatory stress, a multitude of mechanisms are working simultaneously to ensure a proficient response and an efficient replenishment of lost blood cells while preventing the depletion of long-term HSCs. Once HSCs sense inflammatory signals, the cells start to proliferate (Essers *et al.*, 2009). The ECM provides structural support and plays a role in maintaining the HSC location in the niche. Upon stress, this ECM-HSC interaction changes and allows the HSCs to move to other niche locations within the BM or sites of extramedullary hematopoiesis (Yamamoto *et al.*, 2016). Moreover, intracellular HSC regulation of the expression of certain ECM components has been suggested. It is possible that HSCs thereby partially model their own microenvironment similar to certain metastasizing cancer cells that shape the microenvironment to colonize distant organs through autocrine expression of ECM components (Oskarsson *et al.*, 2011; Lapin *et al.*, 2017). This suggests both regulation of HSC activity through the ECM, but also vice versa regulation of the ECM through HSCs. Mobilized HSCs potentially send signals to or sense the ECM and are therefore able to home to different locations within the BM or return to their homeostatic location once the cells return to quiescence. The ECM, however, also receives signals from surrounding niche cells and indirect communication of niche cells and HSCs mediated through ECM components is likely. Within the BM niche, many different cell types, secreted factors, and the ECM are in constant exchange. Untangling complex direct and indirect communication and signals between those components is of great interest to improve hematopoietic recovery following injury or inflammation. However, understanding of the dual cross-talk between HSCs and the ECM upon inflammatory stress remains incomplete. Previous studies from our group (Uckelmann *et al.*, 2016) have shown that the ECM plays an indispensable direct role in the activation of HSCs upon inflammatory stress through Matn4-CXCR4 interaction.

Aim of this study was to investigate other ECM components and uncover potential roles during stress-induced HSC activation. Thus, we analyzed several different mouse lines lacking an ECM component known to play a role in normal HSC function. These KO mouse lines only displayed mild hematopoietic differences compared to WT mice and functional assays provided insight into the response of mice lacking an ECM component to inflammatory stimuli and competitive transplantation and therefore suggesting potential roles during hematopoietic stress. Further analysis of the mice after stimulation of an inflammatory response,

transplantations, treatment with integrin inhibitors, or a combination of these via flow cytometry, gene expression analysis, and microscopy, will help provide extended knowledge of the role of these ECM components in the stress-induced activation of HSCs.

Generation of mice that conditionally lack ECM components in HSCs through usage of for example of an HSC-specific Cre recombinase (*HSC-SCL-Cre*-ER$^T$ transgenic mice) (Gothert *et al.*, 2005) in combination with floxed ECM genes, will allow the investigation of the function of autocrine expression of ECM components during stress hematopoiesis. Nonetheless, analysis of mice lacking only one ECM component might not lead to a complete understanding of the interactions of HSCs and their microenvironment since the ECM is a complex network of components and an interaction between many factors is probable. Moreover, other components could possibly compensate for the lack of a single component.

A promising *in vitro* approach to investigate cell-ECM interaction more generally rather than single ECM component would be a high-throughput ECM microarray, which allows the analysis of the effect of a large library of a combination of ECM components or other soluble factors on stem cell functions (Anderson *et al.*, 2004; Peerani and Zandstra, 2010; Gattazzo *et al.*, 2014). Another approach to study the ECM employ the comprehensive proteomic characterization of *in vitro* stromal cell-derived ECM to analyze its protein composition (Ragelle *et al.*, 2017). Co-culture of activated HSCs through treatment with inflammatory cytokines *in vitro* together with MSCs and subsequent proteomics analysis of the ECM might allow the identification of further ECM components involved in the stress-induced activation of HSCs. In the context of other tissue stem cells, *in vitro* artificial scaffolds or organoid cultures have proven successful ways to study ECM-stem cell interaction (Kim *et al.*, 2013; Sato and Clevers, 2013). However, in the case of HSCs, this is more challenging as maintenance of HSCs *in vitro* is not yet possible for extended periods of time and proper HSC function relies on the interaction of many different factors like other cell types, extracellular components, and biophysical properties of the very specialized BM niche.

On the other hand, studying the interaction of cells and the ECM in *in vivo* systems is also challenging. Many ECM-cell interactions are mediated through the ECM-integrin axis. Rather than analyzing mice lacking specific ECM components, perhaps analysis the stress-induced activation of HSCs of mice lacking certain integrins either constitutively or conditionally on HSCs or other cell populations of the niche like MSCs will lead to better understanding of the mediation of signals from ECM to those cells *in vivo*.

Overall, it is undeniable that the BM microenvironment plays an important role during stress-induced activation of HSCs. However, to understand the whole picture and the dynamics of cells and extracellular components involved in this process, more comprehensive approaches like the examples given above are necessary and will provide valuable new information that can be translated to improve HSC maintenance or recovery upon stress. Moreover, this will also be relevant for improving the efficiency of expansion of HSCs *ex vivo* prior to stem cell transplantations to cure hematological malignancies.

# 5. MATERIALS AND METHODS

## 5.1. Materials

### *5.1.1. Antibodies*

Flow Cytometry

***Table 1*** *List of mouse antibodies for flow cytometry*

| Antigen | Label | Clone | Company |
|---|---|---|---|
| B220 | AlexaF700, APC-Cy7, eFluor488, APC, eFluor450 | RA3-6B2 | eBioscience, Invitrogen |
| CD4 | AlexaF700, PE, PE-Cy7, APC | GK1.5 | eBioscience, Invitrogen |
| CD8 | AlexaF700, PE, PE-Cy7, APC | 53-6.7 | eBioscience |
| CD11b | AlexaF700, PE-Cy5, APC | M1/70 | eBioscience, Invitrogen |
| CD16/32 | PE<br>APC | 93<br>2.4G2 | eBioscience,<br>BD |
| CD31 | eFluor450 | 390 | Invitrogen |
| CD34 | AlexaF700, PacificBlue | RAM34 | BD, eBioscience |
| CD41 | APC-eFluor780, PE-Cy7 | eBioMWReg30 | eBioscience |
| CD45 | APC | 30-F11 | eBioscience |
| CD45.1 | AlexaF700, PacificBlue | A20 | Biolegend |
| CD45.2 | AlexaF700, PacificBlue, PE-Cy7, APC | 104 | Invitrogen, Biolegend, eBioscience |
| CD48 | PE-Cy7, PE | HM48-1 | Biolegend, eBioscience |
| CD105 | eFluor450 | MJ7/18 | eBioscience, Invitrogen |
| CD117 (cKit) | BV711, PE-Cy5, PE, APC-eFluor780 | 2B8 | Biolegend, eBioscience |
| CD150 | PE-Cy5 | TC15-12F12.2 | Biolegend |
| Sca-1 (Ly6A) | PacificBlue,<br>APC-Cy7, PE-Cy5 | E13-161.7<br>D7 | Biolegend<br>BD, eBioscience |
| Gr-1 | AlexaF700, APC, PE | RB6-8C5 | eBioscience, Invitrogen |
| Ter119 | AlexaF700, APC | TER119 | Biolegend, eBioscience |
| ESAM | APC | 1G8/ESAM | Biolegend |
| VE-Cadherin | PE | 11D4.1 | BD |
| EPCR | PE | RMEPCR1560 | StemCell |
| Ki67 | PE-Cy7, APC | B56 | BD |
| Hoechst | | | Invitrogen |
| DAPI | | | ThermoFisher |
| 7AAD | | | LifeTechnologies |
| CD3 | FITC, BV510 | 17A2 | Biolegend |
| CD44 | BV421 | IM7 | eBioscience |
| CD62L | PE-Cy7 | MEL-14 | Biolegend |

| | | | |
|---|---|---|---|
| PD-1 | PE, APC | J43 | eBioscience, Invitrogen |
| Lag3 | APC-Cy7 | C9B7W | Invitrogen |
| CD25 | BV786 | PC61 | Biolegend |
| Efluor506 live/dead | 405/506nm | | ThermoFisher |

Immunofluorescence

***Table 2*** *List of antibodies for immunofluorescence*

| **Antigen** | **Species** | **Label** | **Company** |
|---|---|---|---|
| Spp1 | Rabbit anti-mouse | - | Rockland |
| - | Goat anti-rabbit | AlexaF488 | Cell signaling Technology |

### *5.1.2. Kits*

***Table 3*** *List of used kits*

| **Name** | **Company** | **Order no.** |
|---|---|---|
| SuperScript® VILO™ cDNA Synthesis Kit | Life Technologies | 11754250 |
| Arcturus® PicoPure® RNA Isolation Kit | Life Technologies | KIT0204 |
| DYNAL™ Dynabeads™ Untouched Kit for Mouse-CD4-cells | ThermoFisher | 11415D |
| CellTrace™ Violet Cell Proliferation Kit | ThermoFisher | C34557 |
| Dynabeads™ Mouse T-Activator CD3/CD28 for T-Cell Expansion and Activation | ThermoFisher | 11452D |
| QIAamp® DNA Micro Kit | QIAGEN | 56304 |
| EZ DNA Methlyation Kit | Zymo Research | D5001, D5002 |

### *5.1.3. qRT-PCR Primers*

***Table 4*** *List of qRT-PCR primers and sequences*

| **Gene** | **Primer** | **Sequence** |
|---|---|---|
| Reference genes | | |
| Sdha | fw | AAGTTGAGATTTGCCGATGG |
| Sdha | rev | TGGTTCTGCATCGACTTCTG |
| Oaz1 | fw | TTTCAGCTAGCATCCTGTACTCC |
| Oaz1 | rev | GACCCTGGTCTTGTCGTTAGA |
| Actin-beta | fw | CTAAGGCCAACCGTGAAAAG |
| Actin-beta | rev | ACCAGAGGCATACAGGGACA |
| | | |
| Interferon-stimulated genes (ISGs) | | |
| Agrn | fw | GTGCAGCACACCTACTCCTG |
| Agrn | rev | ACCATCCAGCAGGCTCTCT |
| Bst2 | fw | GAAGTCACGAAGCTGAACCA |
| Bst2 | rev | CCTGCACTGTGCTAGAAGTCTC |
| Ddx58 | fw | GAGAGTCACGGGACCCACT |
| Ddx58 | rev | CGGTCTTAGCATCTCCAACG |
| Dhx58 | fw | AGAGACGGTAGACAGAGGCAAG |

| | | |
|---|---|---|
| Dhx58 | rev | TCAGGGTTGTTACAGTCCAGTG |
| Dtx3l | fw | CAAGTTTGGAGGACCAGCA |
| Dtx3l | rev | TCCTTACTCAATGCCTTTTGC |
| Gbp6 | fw | CAGGAAGAAGGTTGAACAGGA |
| Gbp6 | rev | GCTCTGAAGGACATGATTTGC |
| H2-Eb1 | fw | CCTCCAGTGGCTTTGGTC |
| H2-Eb1 | rev | CTGCGTCCCGTTGTAGAAAT |
| H2-T10 | fw | CCTCAGATCTCTCAGCACCTG |
| H2-T10 | rev | CGGGTCACATGTGCCTTT |
| H2-T22 | fw | TGCTGCAGAAATACCTGGAA |
| H2-T22 | rev | TGCCTTTGGAGGGTCTGA |
| H2-T24 | fw | CATTCGGCAATACTACAACAGC |
| H2-T24 | rev | TGTGAACTGGAGGGTGTGAG |
| Ifi44 | fw | CTGATTACAAAAGAAGACATGACAGAC |
| Ifi44 | rev | AGGCAAAACCAAAGACTCCA |
| Ifitm1 | fw | GCTCCTCGACCACACCTCT |
| Ifitm1 | rev | TGACCCCAGTACAACCACCT |
| Ifitm3 | fw | AACATGCCCAGAGAGGTGTC |
| Ifitm3 | rev | ACCATCTTCCGATCCCTAGAC |
| Iigp2 | fw | GCCTGGATTGCAGTTTTGTAA |
| Iigp2 | rev | TCAAATTCTTTAACCTCAGGTGACT |
| Irf7 | fw | CTTCAGCACTTTCTTCCGAGA |
| Irf7 | rev | TGTAGTGTGGTGACCCTTGC |
| Irgb10 | fw | CCCTGAACATCGCTGTGAC |
| Irgb10 | rev | GGGCATTAATGAACGTGGAC |
| Irgm | fw | AAGGCCACTAACATCGAATCA |
| Irgm | rev | TGCCTTATCTCACTTAATACTCCTCA |
| Isg20 | fw | GCGCCTGCTACACAAGAAC |
| Isg20 | rev | CTGAGAGATTTTGTAGAGCTCCATT |
| Ly6a/Sca-1 | fw | TGGATTCTCAAACAAGGAAAGTAAAGA |
| Ly6a/Sca-1 | rev | ACCCAGGATCTCCATACTTTCAATA |
| Nampt | fw | GGCAGAAGCCGAGTTCAA |
| Nampt | rev | TGGGTGGGTATTGTTTATAGTGAG |
| Oas1g | fw | GCATCAGGAGGTGGAGTTTG |
| Oas1g | rev | GGCTTCTTATTGATACTACCATGACC |
| Oas2 | fw | TAGACCAGGCCGTGGATG |
| Oas2 | rev | GTTTCCCGGCCATAGGAG |
| Oas3 | fw | AACACTGGTACCGCCAGGT |
| Oas3 | rev | AGGAGCTCCAGGGCGTAG |
| Oasl1 | fw | GGCCAACCAGTGTCTGAAA |
| Oasl1 | rev | TGGATATCGGGTGCTCTCTT |
| Oasl2 | fw | AGGTGGCTGCAGAAGCTG |
| Oasl2 | rev | TGTTTCACTCTCACCTGAACATC |
| Plac8 | fw | CAGACCAGCCTGTGTGATTG |
| Plac8 | rev | TCCAAGACAAGTGAAACAAAAGG |

| | | |
|---|---|---|
| Rbm6 | fw | TTTCTCAGGGCAAAATGTCC |
| Rbm6 | rev | TGGGCCAGTCCTATAATCTTG |
| Rnf213 | fw | CAGCTCTTCGAACTGTGTGG |
| Rnf213 | rev | GGAACACAGACTCAGCAGTGG |
| Rsad2 | fw | GTGGACGAAGACATGAATGAAC |
| Rsad2 | rev | TCAATTAGGAGGCACTGGAAA |
| Samd9l | fw | TTGCAGAATGAGGAAACTGAAA |
| Samd9l | rev | AATGCATTTTGTGGGAATCG |
| Samhd1 | fw | CAAGCGGTCAGGATCAATAAA |
| Samhd1 | rev | TGAGCTGCTCTGCAAATTTCT |
| Scotin | fw | CTGTGGACCCTATTGCTGCT |
| Scotin | rev | GGGATCGAATTGTCTTCACC |
| Sp100 | fw | GAAACTCCACGAAACCCAAG |
| Sp100 | rev | AGATAGTCAAAAGAAGCAGTTCACAT |
| Stat1 | fw | TGAGATGTCCCGGATAGTGG |
| Stat1 | rev | CGCCAGAGAGAAATTCGTGT |
| Stat2 | fw | GGAACAGCTGGAACAGTGGT |
| Stat2 | rev | GTAGCTGCCGAAGGTGGA |
| Tgtp | fw | CCAGATCAAGGTCACCACTG |
| Tgtp | rev | GAGATGATTTTGCTTTCCCTTTT |
| Trafd1 | fw | GTGCTGCTGACGAGATTCTG |
| Trafd1 | rev | GAGAAGGGTTGCAGCTTGTC |
| Trim30 | fw | GAGCTGGAGGATCAGACAGAGT |
| Trim30 | rev | GTTGCAGGCTTAAGGACTGACT |
| Ube2l6 | fw | ATGCTCCTGCTGCCAGAC |
| Ube2l6 | rev | CTCCCTGGGGAAATCAATC |
| Usp18 | fw | TGACTCCGTGCTTGAGAGG |
| Usp18 | rev | CGGGAGTCCACAACTTCACT |
| Zbp1 | fw | CAGGAAGGCCAAGACATAGC |
| Zbp1 | rev | GACAAATAATCGCAGGGGACT |
| Znfx1 | fw | CTGTTGGCCATGAGACTGG |
| Znfx1 | rev | TCTGGCCACGCTGAGTCT |
| | | |
| ECM-related genes | | |
| Postn | fw | GCCACGAGGTGTCCTAGAAA |
| Postn | rev | CCTTCGCACCCTATCTCAAT |
| Spp1 | fw | GCCTGCACCCAGATCCTATA |
| Spp1 | rev | CTCCATCGTCATCATCATCG |

### *5.1.4. DNA Methylation primers for IFITM3 locus*

***Table 5*** *List of primers and sequences for DNA methylation*

| Description | Sequence |
|---|---|
| SQ001_Ifitm3_1_1_001_10F | aggaagagagTTTTTGTTTTTTAGTGTTGTTTTTG |
| SQ001_Ifitm3_1_1_001_T7R | cagtaatacgactcactatagggagaaggctAAAACTTCAAATTCACACACACCTT |
| SQ002_Ifitm3_1_2_001_10F | aggaagagagTTGTTTTTTAGTGTTGTTTTTGTTT |

| | |
|---|---|
| SQ002_Ifitm3_1_2_001_T7R | cagtaatacgactcactatagggagaaggctAAACAACCTCACCCTATATCTACCC |
| SQ003_Ifitm3_1_5_001_10F | aggaagagagTTGTGATTAATATGTTTAGAGAGGTGT |
| SQ003_Ifitm3_1_5_001_T7R | cagtaatacgactcactatagggagaaggctAAACAACCTCACCCTATATCTACCC |
| SQ004_Ifitm3_1_14_001_10F | aggaagagagTTTGGGTAGATGGAGTTTTAGGTTT |
| SQ004_Ifitm3_1_14_001_T7R | cagtaatacgactcactatagggagaaggctCTCCATCCTTTACCCTTCAATACTA |
| SQ005_Ifitm3_1_15_001_10F | aggaagagagATGGGGAGATGTAGTTTATAGGGAG |
| SQ005_Ifitm3_1_15_001_T7R | cagtaatacgactcactatagggagaaggctAATTATCAAATACACTTTATTAAATCCAC |
| SQ006_Ifitm3_1_21_001_10F | aggaagagagATGTTGAGGATTAAGGTGTTGATGT |
| SQ006_Ifitm3_1_21_001_T7R | cagtaatacgactcactatagggagaaggctAAAAATTCTAAAATCAAACTCTTCCAA |
| SQ007_Ifitm3_1_33_001_10F | aggaagagagAAGTGTATTTTATTGAATTTATTGTGG |
| SQ007_Ifitm3_1_33_001_T7R | cagtaatacgactcactatagggagaaggctTCTACCTATCAACTCCAAAACCACT |
| SQ008_Ifitm3_2_1_001_10F | aggaagagagTGTTTTTGTGAAGAATTTAAGAAAG |
| SQ008_Ifitm3_2_1_001_T7R | cagtaatacgactcactatagggagaaggctAATACTACAACCACTCTTTTTCCCTC |
| SQ009_Ifitm3_2_4_001_10F | aggaagagagGAGGGAAAAAGAGTGGTTGTAGTATT |
| SQ009_Ifitm3_2_4_001_T7R | cagtaatacgactcactatagggagaaggctCCCTTCCCTTTAAAAAACCAAC |
| SQ010_Ifitm3_2_8_001_10F | aggaagagagATTTGGTAATAGTTGGGTGTGTTTG |
| SQ010_Ifitm3_2_8_001_T7R | cagtaatacgactcactatagggagaaggctAAAAAATACCCAAAAAACCTCTCAC |
| SQ011_Ifitm3_2_9_001_10F | aggaagagagTTGGTAATAGTTGGGTGTGTTTGAT |
| SQ011_Ifitm3_2_9_001_T7R | cagtaatacgactcactatagggagaaggctAAAAAATACCCAAAAAACCTCTCAC |
| SQ012_Ifitm3_2_13_001_10F | aggaagagagGTGTGATTAATTATTGGATTTTGGT |
| SQ012_Ifitm3_2_13_001_T7R | cagtaatacgactcactatagggagaaggctCCTAAAAACTAAAACAACCCCAACT |
| SQ013_Ifitm3_2_14_001_10F | aggaagagagGTTGGTTTTTTAAAGGGAAGGG |
| SQ013_Ifitm3_2_14_001_T7R | cagtaatacgactcactatagggagaaggctATTTCTCAAAAATTTCCTTTTCCTAA |
| SQ014_Ifitm3_2_20_001_10F | aggaagagagTTGGTTTTATAGATAGGTGGGATGA |
| SQ014_Ifitm3_2_20_001_T7R | cagtaatacgactcactatagggagaaggctCATTTTATCTAAACTCTACCCCACAA |
| SQ015_Ifitm3_2_21_001_10F | aggaagagagATTGTGAATTAGGGGAATTTTTAGG |
| SQ015_Ifitm3_2_21_001_T7R | cagtaatacgactcactatagggagaaggctCCTCCCCATAAATAAAAAATAAACTCTA |
| SQ016_Ifitm3_2_29_001_10F | aggaagagagTTTGATGAAATTGTTTTGGG |
| SQ016_Ifitm3_2_29_001_T7R | cagtaatacgactcactatagggagaaggctTCATCCCACCTATCTATAAAACCAA |

## 5.2. Methods

### *5.2.1. Mouse strains*

All animal experiments were performed in agreement with the German Law for Protection of Animals and the National Institute of Health Guidelines for Care and Use of Laboratory Animals (DKFZ Organentnahme Nummer DKFZ355, TVA no.: G22-17, G106-18). Mice were housed in individually ventilated cages under specific pathogen-free conditions in the animal facility at the German Cancer Research Center, Heidelberg, Germany.

C57Bl/6 mice, referred to as wildtype (WT or WT CD45.2) mice, were purchased from Janvier Laboratories. B6.SJL-Ptprca-Pep3b-/BoyJ mice are referred to as WT CD45.1 mice, were bred in house, and used as indicated. WT CD45.1/.2 mice were obtained by crossing WT CD45.2 and WT CD45.1 mice. IFITM3-eGFP (Lange *et al.*, 2008), ISRE-eGFP (Tovey *et al.*, 2006), *Spp1*$^{-/-}$ (Liaw *et al.*, 1998) and *Postn*$^{-/-}$ (Oka *et al.*, 2007) mice are on a C57Bl/6 background.

### *5.2.2. Embryo dissection and cell preparation*

C57Bl/6 WT (CD45.2), IFITM3-eGFP, or ISRE-eGFP mice were used for timed matings. At embryonal (E) day 0.5, mated females are checked for a vaginal plug. If mating was successful, pregnant females are separated from males. At E10.5, E11.5, E12.5, and E13.5, embryos were isolated from pregnant females and dissected under a stereo microscope (Leica M165 FC, Leica microsystems) in petri dishes containing PBS with 10%v/v fetal calf serum (10% FCS) and 1% Penicillin/Streptomycin. Placenta, yolk sac, and aorta-gonad-mesonephros region (AGM) were isolated and digested in PBS containing organ-specific concentrations of Type I Collagenase (Sigma, Cat. C0130):

1 AGM: 0.2% in 500 µl PBS
1 Placenta: 0.125% in 500 µl PBS
1 Yolk Sac: 0.005% in 500 µl PBS

Organs were digested for 1.5 h at 37°C, dissociated with a pipette and filtered through 40 µm nylon filters (BD Biosciences).

Fetal liver was isolated, cells were suspended by pipetting up and down in PBS and filtered through 40 µm nylon filters.

Cells were washed with PBS and stained as described in 5.2.4 Fluorescence activated cell sorting.

### *5.2.3. Isolation of bone marrow, spleen, thymus and peripheral blood*

For isolation of adult BM cells for FACS-Sorting and flow cytometry experiments the tibiae, femora, sternum, coxae and vertebral column of a mouse were dissected. Bones were cleaned and crushed in RPMI-1640 medium (Sigma, Cat. R8758) supplemented with 2% FCS. The spleen and thymus were minced in RPMI with 2% FCS and cells suspended by pipetting up

and down. BM, spleen, and thymus cells were filtered through 40µm nylon filters. Viable cell numbers were determined using Vi-Cell Automated Cell Viability Analyzer (Beckman Coulter). If necessary, lineage depletion was performed. For the lineage depletion, BM cells were incubated with lineage antibodies recognizing CD4, CD8, CD11b, B220, Gr-1 and TER119 in RPMI with 2% FCS for 30 min on ice. After antibody incubation, the cells were washed and lineage positive cells were removed from the cell suspension using Dynabeads® Magnetic Beads (Invitrogen, Cat. 11415D). For all washing steps PBS with 2% FCS was used followed by a 5 minute centrifugation at 1600rpm, 4°C.

For FACS analysis of peripheral blood, 4-5 drops of blood were collected from the vena facialis (v. facialis) of each mouse into an EDTA coated tube. Blood cells were analyzed using the Hemavet 950 (Drew Scientific). For FACS analysis, erythrocytes were lysed with 1 ml of ACK lysing buffer according to manufacturer's instructions. Cells were washed with PBS and stained as described in 5.2.4 Fluorescence activated cell sorting.

### *5.2.4. Fluorescence activated cell sorting (FACS)*

Cell surface staining was performed in PBS supplemented with 2% FCS (PBS/2% FCS). Cells were incubated with antibodies for 30 min on ice. Embryonal organ cells were stained for HSCs and progenitors using CD48, CD41, cKit, CD34, or CD45.

Adult BM cells were stained for hematopoietic subsets using lineage antibodies (CD4, CD8, CD11b, Gr-1, B220 and TER119), cKit, Sca-1, CD150, CD48, EPCR and CD34. Committed progenitor cells were identified by staining with additional antibodies against CD16/32, CD41 and CD105. T cells were classified into different compartments using CD4, CD8, CD44, CD62L, and CD25. T cell activation was analyzed using Lag3 and PD-1. All cell suspensions were washed with PBS/2% FCS followed by a 5 min centrifugation at 1600rpm, 4°C, and filtered through a nylon mesh filter (40 µm). For flow cytometric analysis the LSRII or LSR Fortessa (BD Biosciences, San Jose, CA), equipped with a 350nm, 405nm, 488nm, 561nm, and 640nm laser were used. For flow cytometric cell sorting, Aria I, Aria II, and Fusion II (BD Biosciences, San Jose, CA) equipped with 355nm, 405nm, 488nm, 532nm, 561nm, and 640nm lasers were used. Data was analyzed using FlowJo software (Tree Star).

### *5.2.5. RNA isolation and Reverse Transcription*

For all samples for qRT-PCR analysis cells were directly FACS sorted into 100µl extraction buffer (Arcturus PicoPure Kit) and RNA was isolated with the PicoPure RNA isolation kit (Arcturus) according to manufacturer's instructions, including an RNAse free DNAse step to remove genomic DNA. RNA was reverse transcribed with the SuperScript VILO cDNA synthesis kit (Invitrogen) according to manufacturer's instructions.

### *5.2.6. Quantitative Real-time PCR (qRT-PCR)*

For quantitative real-time PCR (qRT-PCR) the Applied Biosystems ViiATM 7 RT-PCR System was used with 384-well plates. The amplification protocol consisted of an initial denaturation step of 95°C for 10 min followed by 40 cycles of 15 s 95°C and 60 seconds 60°C. Primers for qPCR reactions were designed with the Assay Design Center of the Universal Probe Library (Roche1) or Primer3 (Rozen and Skaletsky, 2000). Sequences of genes were obtained from ENSEMBL or NCBI. Sdha, Oaz1, and Actin-beta were used as housekeeping genes for normalization of gene expression. Relative gene expression was calculated by comparative ddCT-method.

### *5.2.7. Generation of embryonal organ and adult bone marrow chimeras*

For transplantation experiments with embryonal cells, E12.5 embryonal organs were isolated and digested as described before (5.2.2 Embryo dissection and cell preparation). For AGM, 1 or 2 embryonal equivalents (ee), for placenta 1ee, and for fetal liver 0.05ee were i.v. injected into lethally irradiated (2x500 rad) adult recipient mice. Embryonal cells were transplanted alongside $1x10^5$ CD45.1 total adult BM cells and $2x10^5$ adult splenocytes to support engraftment of fetal cells in an adult environment in 150 µl PBS.

For uniform chimeras of reporter mice, 2000 LSK cells of $eGFP^{hi}$, $eGFP^{low}$, or independent of reporter status (un-fractioned) were transplanted in 100-200 µl PBS with $1x10^5$ total BM cells of CD45.1/2 WT mice as support into lethally irradiated CD45.1 recipient mice (i.v. in 150 µL PBS).

For adult mixed BM chimeras, $1.5x10^6$ BM cells of each genotype (WT CD45.1./.2, $Postn^{-/-}$ (CD45.2)) were mixed prior to i.v. injection and a FACS analysis of the injected cells was performed to determine the input-ratio.

The blood chimerism was monitored by FACS analysis 4 weeks after transplantation and over time. To identify recipient and donor cells, mice with different CD45 isoforms, CD45.1 and CD45.2, which are expressed on most blood and BM cells and can be distinguished by specific FACS antibodies.

All mice were kept on antibiotic (Cotrim) containing water for 3 weeks post transplantation.

### *5.2.8. Secondary transplantation*

16-20 weeks post primary transplantation BM was isolated from primary recipients. $3x10^6$ cells were diluted in 100-200 µl PBS and i.v. injected into lethally irradiated secondary recipients. The blood chimerism was monitored by FACS analysis every 4 weeks after transplantation and where indicated, cells were isolated at different timepoints after transplantation from blood for further analysis.

### *5.2.9. In vitro culture of embryonic stem cells (ESC) on mouse embryonic fibroblasts (MEF)*

Protocols for *in vitro* culture and differentiation of ESCs to hematopoietic fate are based on and adapted from protocols by Pearson *et al.* (Pearson *et al.*, 2008). CF1-MEF feeder cells (Mitomycin-C treated, tebu-bio) were maintained on gelatine-coated (0.1% in water, STEMCELL) culture dishes in Dulbecco's Modified Eagle Medium (DMEM, 4.5 g/l D-Glucose, + 0.11 g/l Pyruvate, Gibco) supplemented with 10% heat-inactivated fetal bovine serum (FBS, Gibco), 1% Penicillin-Streptomycin (10.000 U/ml, Gibco) and 1% L-Glutamine (200 mM 100X, Gibco) hereafter referred to as MEF medium. All media components are filtered sterile. Supplied MEF tubes containing 2 $x10^6$ MEF cells are rapidly thawed, cells were gently added dropwise to pre-warmed MEF medium, washed, distributed over 3x 10.0 cm culture dishes or 3x 6-well culture plates and incubated overnight in a 5% $CO_2$ humidified incubator at 37°C. Two frozen mESC tubes (300 $x10^3$ cells/tube, clone #2, passage 2) were rapidly thawed and gently added dropwise to pre-warmed ES+LIF+2i medium containing DMEM KnockOut (4.5 g/L D-Glucose, Sodium Pyruvate, Gibco) supplemented with 1% heat-inactivated ESC FBS Qualified (Gibco), 1% Penicillin-Streptomycin (10.000U/ml, Gibco), 1% L-Glutamine (200mM 100X, Gibco), 3µM CHIR99021 (WNT pathway activator; Inhibits GSK3, STEMCELL), 1µM PD0325901 (MEK/ERK pathway inhibitor; Inhibits MEK, STEMCELL), 1µl/ml mouse recombinant leukemia inhibitory factor (LIF, maintains the mouse embryonic stem cell phenotype, STEMCELL), 1% MEM non-essential amino acid solution (100X, Gibco) and 0.001% 2-Mercaptoethanol (50 mM in Dulbecco's Phosphate Buffered Saline (DPBS), SigmaAldrich). All media components are filtered sterile. After 5 min centrifugation at 1200 rpm the supernatant is aspirated, the pellet thoroughly resuspended in ES+LIF+2i medium and the cells distributed on the MEF-seeded dishes. Approximately 600 $x10^3$ mESC are grown per 10 cm dish and fed daily with pre-warmed ES+LIF+2i medium. On day 1 post-seeding the mESC are gently washed with PBS prior to media change. On day 4 post-seeding (approximately 80% confluent) the cells are washed with PBS and incubated for 30-60 seconds at 37°C with Trypsin-EDTA (0,05%, Gibco). After adding ES+LIF+2i medium the cell clusters are thoroughly resuspended and singularized cells sub-cultured at max. $200x10^3$ cells/well (6-well gelatine-coated MEF-seeded culture plate).

### *5.2.10. Adaptation of in vitro culture conditions for ISRE-eGFP ESCs*

In the previously used ES+LIF+2i medium, FCS was substituted with KnockOut multi-species serum-replacement (Gibco). Another approach employed N2B27 culture medium without the use of MEF feeder cells. The medium contains DMEM/F12 (Nutrient Mixture F-12, Gibco) and Neurobasal medium (1x, Gibco) in a 1:1 ratio supplemented with 2% B27 (B-27 serum free supplement, Gibco), 1% Penicillin-Streptomycin (10.000U/ml, Gibco), 1% L-Glutamine

(200mM 100X, Gibco), 1% N2 (100X, serum free supplement, Gibco), 1.625µl/ml bovine serum albumin (BSA, 20%/PBS), 1µl/ml 2-Mercaptoethanol (50mM in Dulbecco's Phosphate Buffered Saline (DPBS), SigmaAldrich), 3µM CHIR99021 (STEMCELL), 1µM PD0325901 (STEMCELL) and 0.1µl/ml mouse recombinant LIF (STEMCELL). All media components are filtered sterile.

#### *5.2.11. In vitro differentiation of ISRE-eGFP ESCs toward hematopoietic fate*

Freshly cultured mESC (on MEF feeder cells in ES medium) are separated from the feeder layer by trypsin treatment followed by thorough resuspending to separate and singularize the cells. Subsequently the cell suspension is incubated for max. 40min in ultra-low T25 attachment flasks (Corning, SigmaAldrich) containing hypoxic (pre-conditioned in 5% $O_2$) embryoid body (EB) medium containing Iscove's Modified Dulbecco's Medium (IMDM, Gibco) supplemented with 15% heat-inactivated ESC FBS Qualified (Gibco), 1% Penicillin-Streptomycin (10.000U/ml, Gibco), 1% L-Glutamine (200mM 100X, Gibco), 50µg/ml ascorbic acid (antioxidant, STEMCELL), 200µg/ml Holotransferrin (iron source, SigmaAldrich), 4.5mM MTG (1-Thioglycerol, stimulates differentiation, SigmaAldrich) and 5% protein-free hybridoma medium (PFHM, growth stimulating, Gibco). All media components are filtered sterile. The procedure allows to obtain ESC from the supernatant while MEF remain attached to the T25 flasks. After centrifugation at 1200rpm for 5 min 75.000 ESC are resuspended in 7ml EB medium and cultured in new T25 flask for 60h under hypoxic conditions. Next, to induce differentiation a cytokine-mix of 3ml EB medium containing BMP4, Activin A, VEGF and FGF2 (all with a final concentration of 5ng/ml in $V_{total}$ = 10ml) is added. The cells are cultured under hypoxic conditions for another 60h. This results in the formation of macroscopically visible embryoid bodies (EB). After a media change (after 5 days (t = 120h): remove 8ml supernatant, centrifuge to remove debris, mix 7ml of conditioned supernatant with 5ml fresh EB medium) the EB are cultured for further 24h under hypoxic conditions. After 6 days (t = 144h), the EB are harvested by washing the spheres twice with PBS. So dissociate the EB 250µl NZ mix (500mg collagenase type IV (Gibco), 1g hyaluronidase type II (Gibco), 40.000U deoxyribonuclease type I and II (SigmaAldrich) dissolved in 50ml PBS) + 1ml PBS is added to the EB pellet at 37°C for 20 min (tube is swirled ever 5 min). The enzymatic activity is stopped by adding 8ml PBS followed by incubation for 1-2 min at RT. The cells are subsequently resuspended thoroughly and centrifuged at 1200rpm for 5 min. The final pellet is resuspended in 1ml PBS + 2% FCS and cells are washed and stained as described in section 5.2.4.

### *5.2.12. AGM whole mount staining and imaging*

For whole mount staining of the AGM, the protocol published by Yokomizo *et al.*, 2012 was used. For imaging, confocal microscope LSM 710 ConfoCor3 (Carl Zeiss Microscopy GmbH) equipped with a 405nm, 458nm, 488nm, 514nm, 561nm, 594nm, and 633nm laser was used. Image analysis was done using FIJI software (Schindelin *et al.*, 2012).

### *5.2.13. In vitro culture and viral infection of embryonal cells*

For analysis of viral entry into embryonal cells, E12.5 embryonal organs were isolated and digested as described above (5.2.2 Embryo dissection and cell preparation). In a 96-well plate, $3x10^5$ embryonal organ cells were plated in 100µl StemPro™-34 SFM (ThermoFisher, Cat.10639011) with supplements. Supplements include 10 µl/ml Penicilin/Streptomycin, 10 µl/ml L-Glutamine and 130 µl/5ml of a nutrient supplement. Murine Cytomegalovirus (MCMV-3DR) was added at an multiplicity of infection (MOI) of 5, the lentiviral construct (LeGO iC2) was added at MOI2 in 100 µl of StemPro + supplements. For unstimulated controls, 100 µl Stem Pro + supplements was added for a total volume of 200 µl per well. 24h after addition of the virus, cells were washed, stained, and analyzed by flow cytometry as described before (5.2.4 Fluorescence activated cell sorting).

### *5.2.14. CellTrace™ Violet and T cell activation assay*

Cells were isolated from BM, spleen, and thymus, stained for T cell markers and T cells were isolated by flow cytometry as described before (5.2.3 Isolation of bone marrow, spleen, thymus, and peripheral blood and 5.2.4 Fluorescence activated cell sorting). During FACS isolation, cells were collected in PBS/2% FCS and CellTrace™ Violet assay was performed according to CellTrace™ Violet Cell Proliferation Kit (Invitrogen, Cat# C34557, C34571). After resuspension of cells in pre-warmed culture medium, T cells were activated using Dynabeads™ Mouse T-Activator CD3/CD28 for T-Cell Expansion and Activation (ThermoFisher, 11452D) according to manufacturer's protocol. Cells were incubated for 3-4 days at 37°C, 5% $CO_2$, stained for T cell activation markers and analyzed by flow cytometry (5.2.4 Fluorescence activated cell sorting).

### *5.2.15. DNA-Methylation analysis*

Cells were isolated from BM and embryos, stained and isolated by flow cytometry as described before (sections 3 and 4). During isolation, cells were sorted into PBS/2% FCS and pelleted at 2000 rpm, 4°C for 10 mins. Supernatant was discarded, pellets were frozen in liquid nitrogen and stored at -80°C. DNA methylation analysis was performed by Jens Langstein from the group of Daniel Lipka (Section of Translational Cancer Epigenomics, Department of Translational Medical Oncology, Stefan Fröhling, DKFZ, NCT). Genomic DNA was purified

using QIAamp® DNA Micro Kit (QIAGEN, Cat# 56304) according to manufacturer's protocol and eluted in a volume 20µl. Bisulfite conversion was done using EZ DNA Methlyation Kit (Zymo Research, Cat# D5001 and D5002) according to manufacturer and bisulfite converted DNA eluted in a volume of 10-20µl depending on number of PCR amplicons. Bisulfite converted DNA is amplified through PCR using IFITM3 locus specific primers.

| **5 µl reaction** | |
|---|---|
| | [µL] |
| BT DNA | 1.00 |
| 10X buffer | 0.50 |
| dNTP (10mM ) | 0.10 |
| Primer mix (10 µM) | 0.10 |
| HotStar Taq (Qiagen, 5U/µl) | 0.04 |
| dd$H_2O$ | 3.26 |

The amplification protocol consisted of an initial denaturation step of 95°C for 15 min followed by 45 cycles of 30 sec 94°C, 30 sec 56°C, and 60 sec 72°C. Final cycle remained at 72°C for 10 min before holding at 4°C.

After confirmation of PCR products on agarose gel, samples were treated with shrimp alkaline phosphatase (SAP).

| SAP conditions + inactivation: 37°C for 20 min + 85°C for 5 min | | |
|---|---|---|
| Take 5 µl of the PCR product | | |
| Add 2 µl SAP mix: | 0.3 | µl SAP |
| | 1.7 | µl $H_2O$ |
| 7.0 µl Final Volume | | |

PCR products were then *in vitro* transcribed and desalted.

| *In vitro* transcription conditions: 37°Cx 180 min | | |
|---|---|---|
| take 2 µl of SAPed PCR | | |
| Add 5 µl i.v.T mix: | 3.21 | µl water |
| | 0.89 | µl 5X buffer |
| | 0.22 | µl T cleavage mix |
| | 0.22 | µl DTT |
| | 0.4 | µl T7 polymerase |
| | 0.06 | µl RNAseA |
| 7.0 µl Final Volume | | |

| Desalting: Shake plate with resin for 10', then speed at 3,000 RPM for 5 mins |
|---|
| 7 µl Cleavage rxn |
| 20 µl water |
| 6 mg resin per well |
| 27.0 µl Final Volume |

After desalting, samples were spotted onto MassARRAY® (Agena Biosciences) chips and run according to manufacturer's protocol.

### *5.2.16. Treatment of mice*

Mice were intraperitoneally (i.p.) injected with 5µg/g pI:C (Invivogen) or 100 µg/g 5-FU (Invivogen) or i.v. injected with $5x10^5$ PFU MCMV-3DR. All reagents were diluted in PBS.

### *5.2.17. Cell cycle analysis*

The cell cycle activity of HSCs and progenitors was assessed with a staining for the proliferation marker Ki67 and the DNA dye Hoechst. For this BM cells were stained for surface markers (5.2.4 Fluorescence activated cell sorting). After cell surface staining BM cells were fixed using BD Cytofix/Cytoperm™ Buffer, washed with 1x Permwash and stained with anti-Ki67 antibody coupled with PE-Cy7 or APC for 30 min at RT or overnight at 4°C. Cells were incubated with Hoechst 33342 (Molecular Probes) at 25 µg/ml for 10 min prior to FACS analysis.

### *5.2.18. Colony-Forming Assay*

BM cells were prepared and stained as described above. $3x10^4$ total BM cells were plated in 1 ml of Methocult 3434® (Stem Cell Technologies). Samples were plated in duplicates into 35 $mm^2$ tissue culture dishes and incubated in a humidified atmosphere at 37°C and 5% $CO_2$. Colonies consisting of >40 cells were counted using an inverted microscope at 7-8 days. After 8 days, colonies were isolated and $3x10^4$ cells re-plated. Newly formed colonies consisting of >40 cells were again counted using an inverted microscope at 7-8 days.

### *5.2.19. Immunofluorescence*

BM cells were isolated, lineage depleted and stained as described above. 2,000-5,000 primary sorted LK Slam ($Lin^-$ $cKit^+$ $CD150^+$ $CD48^-$) cells were centrifuged and pelleted cells resuspended in 30 µl PBS. This cell suspension was then spotted onto previously prepared adhesion slides (Marienfeld GmbH Nr. 0900000). Preparation of slides was according to manufacturer's instructions. Cell attachment to the slides was checked under the microscope after 5 min. Cells were fixed on the slides by incubation in ice-cold Methanol for 10 min at -20°C followed by an incubation in ice-cold Aceton for 5 min at -20°C.

For immunofluorescence staining, the adhered cells were first blocked with 20µl/well Block Aid Solution (Life Tech B10710) for 1-2 hours at RT or over-night at 4°C to reduce unspecific binding of antibodies.

15 µl/well of primary antibodies diluted in Block Aid Solution were then added to the well and incubated over-night at 4°C. Slides were washed twice for 10 min with PBS. Secondary

antibodies and DAPI (1:1000) (15 µl/well) diluted in Block Aid Solution were added and incubated for 1.5h at RT. The slides were washed 2x for 10 min in PBS. Cover slips were mounted onto the slides with ProLong Gold Anti-fade mounting medium (Invitrogen). For immunofluorescent analysis, confocal microscope LSM 710 ConfoCor3 (Carl Zeiss Microscopy GmbH) equipped with a 405nm, 458nm, 488nm, 514nm, 561nm, 594nm, and 633nm laser was used.

### *5.2.20. Statistical analysis*

For statistical analysis and graphical representation of data the GraphPad Prism® software version 8.0-8.4 was used. Statistical analysis was performed using an unpaired t-test if not indicated otherwise. In case of multiple comparisons, p-values were corrected by the Benjamini-Hochberg method with FDR = 5%. Statistical significance is indicated by * $p < 0.05$, ** $p < 0.01$, *** $p < 0.001$, and **** $p < 0.0001$.
Error bars indicate the standard deviation.

# 6. ABBREVIATIONS

| | |
|---|---|
| **5-FU** | 5-fluorouracil |
| **AGM** | Aorta-gonad mesonephros (region) |
| **APC** | Antigen-presenting cell |
| **BM** | Bone marrow |
| **CFU (-S)** | Colony-forming unit (-Spleen) |
| **CML** | Chronic myeloid leukemia |
| **CMP** | Common myeloid progenitor |
| **CpG** | Cytosine/guanine dinucloetide |
| **CTV** | CellTrace Violet |
| **CXCR4** | Chemokine-receptor 4 |
| **DC** | Dendritic cells |
| **DNA** | Desoxyribonucleic acid |
| **dpi** | Days post infection |
| **E.** | Embryonic day |
| **ECM** | Extracellular matrix |
| **ee** | Embryonic equivalent |
| **eGFP** | Enhanced green-fluorescent protein |
| **EHT** | Endothelial-to-hematopoietic transition |
| **EPCR** | Epithelial protein C receptor |
| **ESC** | Embryonal stem cell |
| **FACS** | Fluorescent-activated cell sorting |
| **FCS** | Fetal-calf serum |
| **GMP** | Granulocyte-macrophage-progenitor |
| **HSC** | Hematopoietic stem cell |
| **HSPC** | Hematopoietic stem and progenitor cell |
| **i.p.** | intraperitoneal |
| **i.v.** | intravenous |
| **IFITM** | IFN-inducible transmembrane protein |
| **IFN** | Interferon |
| **IFNAR** | Interferon-alpha receptor |
| **IRF** | IFN regulatory factor |
| **ISG** | Interferon-stimulated gene |
| **ISRE** | Interferon-stimulated response element |
| **JAK** | Janus kinase |
| **KO** | Knock-out |
| **LeGO** | Lentiviral gene ontology vector |
| **Lin** | Lineage (meaning markers specific for mature blood cell lineages) |
| **LT-HSC** | Long-term hematopoietic stem cell |
| **LTRA** | Long-term repopulation ability |
| **Matn4** | Matrilin-4 |
| **MCH** | Mean corpuscular hemoglobin |
| **MCMV** | Murine cytomegalovirus |
| **MCV** | Mean corpuscular volume |
| **MEP** | Megakaryocyte-erythroid progenitor |
| **MFI** | Mean fluorescent intensity |
| **MOI** | Multiplicity of infection |
| **MPN** | Myeloproliferative neoplasm |
| **MPP** | Multipotent progenitor |
| **MPV** | Mean platelet volume |
| **MSC** | Mesenchymal stem cell |
| **Mx1** | Myxovirus restitance 1 |
| **MyD88** | Myeloid differentiation primary response gene 88 |
| **NK** | Natural killer cells |
| **PAMP** | Pathogen-associated molecular pattern |
| **PBS** | Phosphate-buffered saline |
| **PCA** | Principal component analysis |
| **pI:C** | Polyinosinic:polycytidylic acid |
| **Postn** | Periostin |
| **Pre-GM** | Granulocyte and macrophage precursor |
| **PreMegE** | Megakaryocyte and erythrofyte precursor |
| **Pro-Ery** | Erythrocyte precursor |
| **PRR** | Pattern-recognition receptor |
| **q(RT)-PCR** | Quantitative (real time) polymerase chain reaction |
| **RDW** | Red cell distribution width |
| **RNA** | Ribonucleic acid |
| **Sca-1** | Stem cell antigen-1 |
| **SLAM** | lymphocyte activation molecule |
| **Spp1** | Osteopontin (also OPN) |
| **ST-HSC** | Short-term hematopoietic stem cell |
| **STAT** | Signal transducer and activator of transcription |
| **STING** | Stimulator of interferon genes |
| **Thbs1** | Thrombospondin |
| **TLR** | Toll-like receptor |
| **TNC** | Tenascin C |
| **TNFR1/2** | Tumor-necrosis factor receptor 1 and 2 |
| **TRIM** | Tripartite motif |
| **TYK** | Tyrosine kinase |
| **WT** | Wildtype (in this case C56Bl mice) |

# 7. LIST OF FIGURES

## 8. LIST OF TABLES

# 9. APPENDIX

## 9.1. Contributions

Starting, executing, and completing this thesis would not have been possible without the contribution of many people.

Many thanks to **Marieke Essers** who contributed greatly to the success of this thesis by helping to develop and further shape the project outline and providing guidance, support, discussions, and a great working environment.

**Simon Haas** and **Christoph Hirche** contributed immensely by providing crucial background data to this thesis. Experiments shown in the introduction relating to IFN signaling heterogeneity in the adult hematopoietic system as well as the transplantation of E13.5 IFITM3-eGFP fetal liver cells were performed by Simon and Christoph. Moreover, Christoph provided valuable support in setting up experimental procedures of the embryo experiments.

**Franziska Pilz**, **Andrea Kuck**, **Rebecca Weber**, **Jasmin Meier**, **Corinna Klein**, and **Adriana Przybylla** contributed through great technical support, including mouse maintenance, genotyping, antibody titration, and ordering of supplies and mice.

**Franziska Pilz** was a great support throughout the IFN signaling project and contributed on many levels including setup of timed matings, embryo dissection, and pipetting of qPCRs.

**Andrea Kuck** was a tremendous help in both the IFN signaling as well as the ECM project. Contributions included assisting with experiments as well as performing numerous experiments independently.

**Rebecca Weber** contributed through great technical support including qPCRs and CFU assays.

**Jonna Bloeme**, a summer student under my supervision, contributed to qPCR data of embryonal organs and preparation and imaging of embryo whole mounts.

**Johanna Kohl**, a Master student under my supervision, contributed greatly to the ESC and T cell experiments and performed several experiments independently.

**Abdul Rahman Itani**, a fellow PhD student in our group, contributed through support with embryo dissections and during sorting.

**Jens Langstein**, a PhD student in the group of Daniel Lipka and Stefan Fröhling, performed all DNA methylation analyses.

**Jasmin Meier** in the group of Thordur Oskarsson provided ECM KO mouse lines as well as ECM primers and antibodies.

Flow cytometric analysis and sorts were performed in the flow cytometry core facility of the DKFZ with the help of **Marcus Eich**, **Florian Blum**, **Klaus Hexel**, **Tobias Rubner**, and **Steffen Schmitt**.

Microscopic imaging was performed in the light microscopy core facility of the DKFZ with the help of **Manuela Brom** and **Felix Bestvater**.

Important support in mouse husbandry and irradiation was provided by all the **caretakers of the mouse facility**.

The DKFZ Transgen Service contributed through help with generation of ESC lines. A big thanks goes to **Frank van der Hoeven** and **Ulrich Kloz** for their support.

Great thanks to **Andreas Trumpp**, **Simon Haas**, **Christoph Hirche**, **Daniel Hübschmann**, **Daniel Lipka**, **Mick Milsom**, **Pablo Hernández Malmierca**, **Florian Grünschläger**, **Dominik Vonficht**, **Jude Al-Sabah**, **Marleen Büchler-Schäff**, **Andrea Barnert**, **Abdul Rahman Itani**, **Shubhankar Sood**, **Yasmin Demerdash**, **Sarah Geiger**, **Áine Prendergast,** and **Sandra Blaszkiewicz** for contributing through very helpful discussions, but also sharing of protocols and reagents, at different stages of my PhD.

Thank you to my thesis advisory committee, **Andreas Trumpp** and **Ingrid Lohmann** for important guidance and support throughout my thesis.

## 9.2. Acknowledgments

Firstly, a big thank you and a lot of gratitude goes to **Marieke Essers** for giving me the opportunity to work in your group, for being a great mentor, for supporting and guiding me throughout the many different projects of my thesis and for always believing in me. Working in the "Stress group" has been (and still will be) a great pleasure and it has been great seeing the group grow from at times only having two technicians and two PhD students to a group of 13 with people from many different backgrounds and expertise. You are able to create a friendly and familial working environment with room for each of us to explore and grow as scientist. Thank you.

A big thank you also goes to **Andreas Trumpp** for providing an excellent research environment at HI-STEM that allows great multi-disciplinary discussions and interactions. I am grateful to be able to work in such a supporting department with this extraordinary scientific infrastructure. Thank you also for many discussions and insightful comments around my PhD project at lab meetings, blood clubs, and TAC meetings.

Many thanks go **Andrea**, **Franzi**, **Rebecca**, **Corinna**, **Adriana**, **Jasmin** and all other HI-STEM technicians for great support for my PhD project specifically, but also generally for keeping the lab running throughout every situation. Your work is invaluable and the research would not be possible without you.

Thank you to **Dagmar**, **Erika**, and **Jan** for all your support with contracts, travels, or really anything bureaucratic surrounding the lab.

Thank you to all the DKFZ core facilities for providing excellent support throughout this thesis.
A special thanks goes to **Marcus**, **Flo**, **Klaus**, **Tobi**, and **Steffen** from the FACS core facility for making the long hours at the FACS a bit easier and helping with machine maintenance and startup, compensation, or turning off the machine at 7am after an all-nighter.
A big thank you also to all the animal caretakers for all the support with mouse monitoring, irradiation, timed matings, and general mouse maintenance.
Thank you **Manuela** and **Felix** from the microscopy core facility for great technical support at the microscope. Especially, if it involves trying to manually build a gadget to image my embryo whole mounts.
Thank you to **Frank** and **Uli** from the DKFZ Transgen Service for discussions and planning around embryo experiments and generation of ESC mouse lines.

**Chris**, thank you so much for introducing me to this project and trusting me to take over. Thank you for all the discussions and scientific input, but more importantly, thank you for becoming a great friend who shares my love for all the good things in life like volleyball, food, coffee, wine, and gin. Your birthday or Christmas parties were always fun and definitely memorable and it's been great seeing you flourish in Berlin. I am looking forward to the next (or first proper) visit.

**Simon**, I can't thank you enough for your support over the last years. Your encouragement when projects or experiments didn't work out was always greatly appreciated and made me feel more motivated to keep working hard. You are a great role-model for young scientist and it's been a pleasure seeing you grow from a PhD student to a confident and very successful scientist with your own group while always making time for a good party. Even though you were not directly part of the "Stress group" anymore, you were always willing to discuss projects, experiments, and results and provided and keep providing great input. Thank you for being a mentor and friend.

**Andrea**, thank you for everything. You, besides Marieke, are the only group member who has been there since day 1 of my PhD and have always been a great support. I am always amazed by your experience working in the lab and your ability to seemingly remember every single experiment you have ever done. You are a great person to have a round and I always enjoy chatting with you. Even though in the beginning of my PhD, we did not work together as much, it's been great working more and more together over the last 1-2 years and it's been a pleasure developing the ECM project together. It's great seeing you be so enthusiastic about new experiments and new methods. I am looking forward to a great collaboration on both the IFN as well as ECM story in the future. Thank you for being a great collegue and keeping the lab running.

**Franzi**, thank you for your great enthusiasm and motivation in and outside of the lab. Thank you for your support with many experiments and all things mouse. It's been great seeing you develop into a confident technician who does not shy away from new challenges. Sorry for making you do all those qPCRs, but I really do appreciate it. Thank you for all the delicious cakes and other foods you made for us over the years.

**Shub**, thank you for always being you. Through all your ups and downs, you always come out smiling. Thank you for great discussions, for your never ending thoughts regarding science, and for your ability to discuss basically anything with anyone. From when you first arrived to start your PhD to now, you have grown so much from a young not so independent fellow to a

confident (still very young) man who is taking more and more responsibility as a leader in our group and the DKFZ in general. Thank you.

**Yasmin**, I am very happy and grateful that you stayed for your PhD after your Master Thesis. Thank you for being a great member of our group, always super friendly, helpful, and hard working. Don't ever change and keep singing!

**Abdul**, thank you for all your help in the last year. You came into this project with great motivation and immediately started implementing your own ideas and came up with super interesting new approaches. Thank you for not only your technical support on experiments and sorts, but also your emotional (and nutritional) support. I love that once you set your mind to something, you don't give up. I am looking forward to many more international dinners.

**Johanna**, thank you for being an amazing Master student. You never complaint about having to come on the weekends to do cell culture, staying overnight at the sorter (thanks for the meatballs and potato salad), or long hours brooding over FlowJo in a tiny room with no windows. You are doing a really great job at planning the experiments and coming up with new angles to investigate which rewarded you with fantastic data sets. Thank you for your great contribution to my thesis and for being a fellow striped T-shirt lover.

**Sarah**, even though you only just joined the group, you have already integrated super nicely and have become an integral part of the stress group. Thank you for valuable input and discussions of the project and I am really looking forward to collaborating more in the future.

A massive thank you to the entire **stress group** (current and past) for a great working environment. It's always a pleasure to work with you and I love that we can all come together to do giant experiments and still get along at the end. You have all become really good friends. Thank you for many lunches, coffee breaks, dinners, stress outings (most of them at least), retreats, and discussions. The science has brought us together, but I think what will keep us connected the most in the end, are all the memories we made together. Thank you **Marieke**, **Sandra**, **Andrea**, **Áine**, **Simon**, **Chris**, **Franzi**, **Rebecca**, **Shub**, **Yasmin**, **Abdul**, **Johanna**, **Sarah**, **Luisa**, **Ramon**, **Rana**, **Can**, **Cecilia**, **Jonna**, **Jari**, and **Eline** for 4 great years and more to come.

Thank you, **Jens**, for all your help with the DNA methylation analysis. Your work provided an invaluable contribution to the project and the story would not be complete without it. Thank you also for critically reading the methylation part and helpful discussions around this.

Thank you to **Marleen**, **Andrea**, **Pablo**, **Domi**, and **Flo** for happily sharing protocols and expertise to parts of the project. Your input was highly appreciated and helped shape this story.

A big thank you also goes to the lunch group. Thank you **Pablo**, **Flo**, **Domi**, **Jude**, **Raphael**, all the many Haas Lab Master students, **stress people**, and all the others for many great lunch discussions on many different topics (some more interesting than others). And thank you for always asking the most important question: Coffee?

**Julius**, thank you for being a great friend from day 1 on. Thank you for all your support and discussions in the lab, but even more so outside of the lab. I cherish the many memories of watching soccer, barbecues, dinners, or playing beach volleyball. Even though this sometimes meant picking Goose poo off the sand at 9am on a Sunday morning. I admire your ability to become friends with everyone immediately and am super happy that I get to be one of them. Thank you.

Thank you **Megan**, **Sina**, **Tash**, **Jens**, **Marie**, **Markus**, **Mac**, **Manu** for all the dinners, barbecues, or wine hikes. Spending time outside of the lab with you is always great fun and I will happily help with moving or building IKEA furniture again, because I know you'd do the same for me (and it always involves liquid refreshments which of course helps). I am sad to see many of you leave Heidelberg, but that only means more places to visit for me.

Thank you to **Pia**, **Franzy**, **Sarah-Jane**, **Felix**, **Andrea**, **Andi**, **Jonas**, **Maija**, **Lisa**, **Sam**, and **Kristin** for providing an outlet outside of the lab through bouldering. Thank you for always supporting me and pushing me to work harder. If that's doing a pull-up or doing an experiment.

Thank you to **Marieke**, **Shub** and **Jens** for critically reading my thesis and for helpful discussions.

A big thank you to my **volleyball family** for being understanding of the long and sometimes unusual hours of research. That sometimes meant missing practice, but having committed to the responsibility of being part of a competitive team also helped to plan and execute experiments more efficiently. Thank you for a great environment and atmosphere on the team and for acting as a great relief to stressful lab work on many occasions.

An riesen Dankeschön geht an meine Freunde zu Hause. Ohne euch wäre ich nicht die Person, die ich heute bin. Danke an **Gina**, **Judith**, **Jana**, **Sören**, **Tobi**, **Jahnosch** und **Jan-Philipp** dafür, dass egal, wie lange wir uns nicht gesehen haben, wir immer gemeinsam durch dick und dünn gehen können. Und wenn wir uns sehen, ist eigentlich alles wie immer. Freundschaften, die ein ganzes Leben lang halten, sind selten, aber ich bin dankbar, dass ich euch habe und ich auch in den schwierigen und stressigen Zeiten immer auf euch zählen kann.

Das größte Dankeschön geht an meine **Familie**. Die letzten Jahre waren leider nicht immer einfach und schön, aber ich wusste, dass egal, was passiert, ihr mich immer in meinen Träumen und Zielen unterstützt. Danke dafür, dass ihr Verständnis habt, dass ich nicht so oft zu Hause war. Danke für die mentale Unterstützung wenn ein Experiment mal wieder länger gedauert hat oder nicht funktioniert hat. Danke, dass ihr immer gerne zu Besuchen nach Heidelberg gekommen seid, damit ich nicht so weit mit dem Zug fahren musste. Danke für die Hilfe bei diversen Umzügen durch halb Deutschland und beim Aufbauen von Möbeln, egal ob das auch mal darin endet, für mehrere Stunden aus der Wohnung ausgesperrt zu sein. Danke für viele gemeinsame Urlaube, trotz gebrochener Knochen. Danke für die Freiheit, in meinem Leben das machen zu können, was ich möchte. Danke für viele gemeinsame Zeiten und Ausflüge, die natürlich immer mit gutem Essen verbunden sind. Danke für die uneingeschränkte Unterstützung auf den vielen Stopps auf dem Weg zur Doktorarbeit.
So eine Arbeit ist nicht alleine möglich und ihr habt einen immensen Anteil an dieser geleistet. Danke **Mama**, **Papa**, **Henriette**, **Max**, **Oma Hilde**, **Renate**, **Jenni**, und an den Rest der Familie, egal ob blutsverwandt oder nicht.

# 10. REFERENCES

Abramson, S., Miller, R. G. and Phillips, R. A. (1977). The identification in adult bone marrow of pluripotent and restricted stem cells of the myeloid and lymphoid systems. J Exp Med *145*, 1567-79.

Adams, G. B., Chabner, K. T., Alley, I. R., Olson, D. P., Szczepiorkowski, Z. M., Poznansky, M. C., Kos, C. H., Pollak, M. R., Brown, E. M. and Scadden, D. T. (2006). Stem cell engraftment at the endosteal niche is specified by the calcium-sensing receptor. Nature *439*, 599-603.

Akashi, K., Traver, D., Miyamoto, T. and Weissman, I. L. (2000). A clonogenic common myeloid progenitor that gives rise to all myeloid lineages. Nature *404*, 193-7.

Alp, O. S. and Radbruch, A. (2016). The lifestyle of memory CD8(+) T cells. Nat Rev Immunol *16*, 271.

Alvarez-Silva, M., Belo-Diabangouaya, P., Salaun, J. and Dieterlen-Lievre, F. (2003). Mouse placenta is a major hematopoietic organ. Development *130*, 5437-44.

Anafu, A. A., Bowen, C. H., Chin, C. R., Brass, A. L. and Holm, G. H. (2013). Interferon-inducible transmembrane protein 3 (IFITM3) restricts reovirus cell entry. J Biol Chem *288*, 17261-71.

Anbazhagan, K., Duroux-Richard, I., Jorgensen, C. and Apparailly, F. (2014). Transcriptomic network support distinct roles of classical and non-classical monocytes in human. Int Rev Immunol *33*, 470-89.

Anderson, A. C., Joller, N. and Kuchroo, V. K. (2016). Lag-3, Tim-3, and TIGIT: Co-inhibitory Receptors with Specialized Functions in Immune Regulation. Immunity *44*, 989-1004.

Anderson, D. G., Levenberg, S. and Langer, R. (2004). Nanoliter-scale synthesis of arrayed biomaterials and application to human embryonic stem cells. Nat Biotechnol *22*, 863-6.

Araki, Y., Wang, Z., Zang, C., Wood, W. H., 3rd, Schones, D., Cui, K., Roh, T. Y., Lhotsky, B., Wersto, R. P., Peng, W.*, et al.* (2009). Genome-wide analysis of histone methylation reveals chromatin state-based regulation of gene transcription and function of memory CD8+ T cells. Immunity *30*, 912-25.

Askenase, M. H., Han, S. J., Byrd, A. L., Morais da Fonseca, D., Bouladoux, N., Wilhelm, C., Konkel, J. E., Hand, T. W., Lacerda-Queiroz, N., Su, X. Z.*, et al.* (2015). Bone-Marrow-Resident NK Cells Prime Monocytes for Regulatory Function during Infection. Immunity *42*, 1130-42.

Azevedo Portilho, N. and Pelajo-Machado, M. (2018). Mechanism of hematopoiesis and vasculogenesis in mouse placenta. Placenta *69*, 140-145.

Azevedo Portilho, N., Tavares Guedes, P., Croy, B. A. and Pelajo-Machado, M. (2016). Localization of transient immature hematopoietic cells to two distinct, potential niches in the developing mouse placenta. Placenta *47*, 1-11.

Baccin, C., Al-Sabah, J., Velten, L., Helbling, P. M., Grunschlager, F., Hernandez-Malmierca, P., Nombela-Arrieta, C., Steinmetz, L. M., Trumpp, A. and Haas, S. (2020). Combined single-cell and spatial transcriptomics reveal the molecular, cellular and spatial bone marrow niche organization. Nat Cell Biol *22*, 38-48.

Bach, E. A., Aguet, M. and Schreiber, R. D. (1997). The IFN gamma receptor: a paradigm for cytokine receptor signaling. Annu Rev Immunol *15*, 563-91.

Baechler, E. C., Batliwalla, F. M., Karypis, G., Gaffney, P. M., Ortmann, W. A., Espe, K. J., Shark, K. B., Grande, W. J., Hughes, K. M., Kapur, V.*, et al.* (2003). Interferon-inducible gene expression

signature in peripheral blood cells of patients with severe lupus. Proc Natl Acad Sci U S A *100*, 2610-5.

Bailey, C. C., Zhong, G., Huang, I. C. and Farzan, M. (2014). IFITM-Family Proteins: The Cell's First Line of Antiviral Defense. Annu Rev Virol *1*, 261-283.

Balazs, A. B., Fabian, A. J., Esmon, C. T. and Mulligan, R. C. (2006). Endothelial protein C receptor (CD201) explicitly identifies hematopoietic stem cells in murine bone marrow. Blood *107*, 2317-21.

Baldridge, M. T., King, K. Y., Boles, N. C., Weksberg, D. C. and Goodell, M. A. (2010). Quiescent haematopoietic stem cells are activated by IFN-gamma in response to chronic infection. Nature *465*, 793-7.

Bantignies, F., Grimaud, C., Lavrov, S., Gabut, M. and Cavalli, G. (2003). Inheritance of Polycomb-dependent chromosomal interactions in Drosophila. Genes Dev *17*, 2406-20.

Barber, D. L., Wherry, E. J., Masopust, D., Zhu, B., Allison, J. P., Sharpe, A. H., Freeman, G. J. and Ahmed, R. (2006). Restoring function in exhausted CD8 T cells during chronic viral infection. Nature *439*, 682-7.

Bartolomei, M. S. and Ferguson-Smith, A. C. (2011). Mammalian genomic imprinting. Cold Spring Harb Perspect Biol *3*.

Baumgarth, N. (2011). The double life of a B-1 cell: self-reactivity selects for protective effector functions. Nat Rev Immunol *11*, 34-46.

Beaudin, A. E. and Forsberg, E. C. (2016). To B1a or not to B1a: do hematopoietic stem cells contribute to tissue-resident immune cells? Blood *128*, 2765-2769.

Becker, T. C., Coley, S. M., Wherry, E. J. and Ahmed, R. (2005). Bone marrow is a preferred site for homeostatic proliferation of memory CD8 T cells. J Immunol *174*, 1269-73.

Beerman, I., Bhattacharya, D., Zandi, S., Sigvardsson, M., Weissman, I. L., Bryder, D. and Rossi, D. J. (2010). Functionally distinct hematopoietic stem cells modulate hematopoietic lineage potential during aging by a mechanism of clonal expansion. Proc Natl Acad Sci U S A *107*, 5465-70.

Bennett, L., Palucka, A. K., Arce, E., Cantrell, V., Borvak, J., Banchereau, J. and Pascual, V. (2003). Interferon and granulopoiesis signatures in systemic lupus erythematosus blood. J Exp Med *197*, 711-23.

Benveniste, E. N. and Qin, H. (2007). Type I interferons as anti-inflammatory mediators. Sci STKE *2007*, pe70.

Benveniste, P., Frelin, C., Janmohamed, S., Barbara, M., Herrington, R., Hyam, D. and Iscove, N. N. (2010). Intermediate-term hematopoietic stem cells with extended but time-limited reconstitution potential. Cell Stem Cell *6*, 48-58.

Benz, C., Copley, M. R., Kent, D. G., Wohrer, S., Cortes, A., Aghaeepour, N., Ma, E., Mader, H., Rowe, K., Day, C.*, et al.* (2012). Hematopoietic stem cell subtypes expand differentially during development and display distinct lymphopoietic programs. Cell Stem Cell *10*, 273-83.

Bernstein, B. E., Mikkelsen, T. S., Xie, X., Kamal, M., Huebert, D. J., Cuff, J., Fry, B., Meissner, A., Wernig, M., Plath, K.*, et al.* (2006). A bivalent chromatin structure marks key developmental genes in embryonic stem cells. Cell *125*, 315-26.

Bertrand, J. Y., Giroux, S., Golub, R., Klaine, M., Jalil, A., Boucontet, L., Godin, I. and Cumano, A. (2005). Characterization of purified intraembryonic hematopoietic stem cells as a tool to define their site of origin. Proc Natl Acad Sci U S A *102*, 134-9.

Boettcher, S. and Manz, M. G. (2017). Regulation of Inflammation- and Infection-Driven Hematopoiesis. Trends Immunol *38*, 345-357.

Bonilla, F. A. and Oettgen, H. C. (2010). Adaptive immunity. J Allergy Clin Immunol *125*, S33-40.

Bonnevie, K. (1950). New facts on mesoderm formation and proamnion derivatives in the normal mouse embryo. J Morphol *86*, 495-546.

Borden, E. C., Sen, G. C., Uze, G., Silverman, R. H., Ransohoff, R. M., Foster, G. R. and Stark, G. R. (2007). Interferons at age 50: past, current and future impact on biomedicine. Nat Rev Drug Discov *6*, 975-90.

Boscá, L., Bodelón, O. G., Hortelano, S., Casellas, A. and Bosch, F. (2000). Anti-inflammatory action of type I interferons deduced from mice expressing interferon beta. Gene Ther *7*, 817-25.

Bowie, M. B., Kent, D. G., Copley, M. R. and Eaves, C. J. (2007a). Steel factor responsiveness regulates the high self-renewal phenotype of fetal hematopoietic stem cells. Blood *109*, 5043-5048.

Bowie, M. B., Kent, D. G., Dykstra, B., McKnight, K. D., McCaffrey, L., Hoodless, P. A. and Eaves, C. J. (2007b). Identification of a new intrinsically timed developmental checkpoint that reprograms key hematopoietic stem cell properties. Proceedings of the National Academy of Sciences *104*, 5878-5882.

Bowie, M. B., McKnight, K. D., Kent, D. G., McCaffrey, L., Hoodless, P. A. and Eaves, C. J. (2006). Hematopoietic stem cells proliferate until after birth and show a reversible phase-specific engraftment defect. J Clin Invest *116*, 2808-16.

Brickner, D. G., Cajigas, I., Fondufe-Mittendorf, Y., Ahmed, S., Lee, P. C., Widom, J. and Brickner, J. H. (2007). H2A.Z-mediated localization of genes at the nuclear periphery confers epigenetic memory of previous transcriptional state. PLoS Biol *5*, e81.

Buenrostro, J. D., Corces, M. R., Lareau, C. A., Wu, B., Schep, A. N., Aryee, M. J., Majeti, R., Chang, H. Y. and Greenleaf, W. J. (2018). Integrated Single-Cell Analysis Maps the Continuous Regulatory Landscape of Human Hematopoietic Differentiation. Cell *173*, 1535-1548.e16.

Busch, K., Klapproth, K., Barile, M., Flossdorf, M., Holland-Letz, T., Schlenner, S. M., Reth, M., Hofer, T. and Rodewald, H. R. (2015). Fundamental properties of unperturbed haematopoiesis from stem cells in vivo. Nature *518*, 542-6.

Butler, J. M., Nolan, D. J., Vertes, E. L., Varnum-Finney, B., Kobayashi, H., Hooper, A. T., Seandel, M., Shido, K., White, I. A., Kobayashi, M.*, et al.* (2010). Endothelial cells are essential for the self-renewal and repopulation of Notch-dependent hematopoietic stem cells. Cell Stem Cell *6*, 251-64.

Cabezas-Wallscheid, N., Klimmeck, D., Hansson, J., Lipka, D. B., Reyes, A., Wang, Q., Weichenhan, D., Lier, A., von Paleske, L., Renders, S.*, et al.* (2014). Identification of regulatory networks in HSCs and their immediate progeny via integrated proteome, transcriptome, and DNA methylome analysis. Cell Stem Cell *15*, 507-522.

Calvi, L. M., Adams, G. B., Weibrecht, K. W., Weber, J. M., Olson, D. P., Knight, M. C., Martin, R. P., Schipani, E., Divieti, P., Bringhurst, F. R.*, et al.* (2003). Osteoblastic cells regulate the haematopoietic stem cell niche. Nature *425*, 841-6.

Calvi, L. M., Frisch, B. J., Kingsley, P. D., Koniski, A. D., Love, T. M., Williams, J. P. and Palis, J. (2019). Acute and late effects of combined internal and external radiation exposures on the hematopoietic system. Int J Radiat Biol *95*, 1447-1461.

Caplan, A. I. (1991). Mesenchymal stem cells. J Orthop Res *9*, 641-50.

Caprioli, A., Jaffredo, T., Gautier, R., Dubourg, C. and Dieterlen-Lièvre, F. (1998). Blood-borne seeding by hematopoietic and endothelial precursors from the allantois. Proc Natl Acad Sci U S A *95*, 1641-6.

Caprioli, A., Minko, K., Drevon, C., Eichmann, A., Dieterlen-Lièvre, F. and Jaffredo, T. (2001). Hemangioblast commitment in the avian allantois: cellular and molecular aspects. Dev Biol *238*, 64-78.

Carlow, D. A., Teh, S. J. and Teh, H. S. (1998). Specific antiviral activity demonstrated by TGTP, a member of a new family of interferon-induced GTPases. J Immunol *161*, 2348-55.

Carrelha, J., Meng, Y., Kettyle, L. M., Luis, T. C., Norfo, R., Alcolea, V., Boukarabila, H., Grasso, F., Gambardella, A., Grover, A.*, et al.* (2018). Hierarchically related lineage-restricted fates of multipotent haematopoietic stem cells. Nature *554*, 106-111.

Cashman, J., Henkelman, D., Humphries, K., Eaves, C. and Eaves, A. (1983). Individual BFU-E in polycythemia vera produce both erythropoietin dependent and independent progeny. Blood *61*, 876-84.

Challen, G. A., Boles, N. C., Chambers, S. M. and Goodell, M. A. (2010). Distinct hematopoietic stem cell subtypes are differentially regulated by TGF-beta1. Cell Stem Cell *6*, 265-78.

Chang, W. L., Liu, Y. W., Dang, Y. L., Jiang, X. X., Xu, H., Huang, X., Wang, Y. L., Wang, H., Zhu, C., Xue, L. Q.*, et al.* (2018). PLAC8, a new marker for human interstitial extravillous trophoblast cells, promotes their invasion and migration. Development *145*.

Chen, K., Liu, J. and Cao, X. (2017). Regulation of type I interferon signaling in immunity and inflammation: A comprehensive review. J Autoimmun *83*, 1-11.

Chen, P., Zhao, J., Wang, Y., Wang, M., Long, H., Liang, D., Huang, L., Wen, Z., Li, W., Li, X.*, et al.* (2013). H3.3 actively marks enhancers and primes gene transcription via opening higher-ordered chromatin. Genes Dev *27*, 2109-24.

Chen, S., Pu, W., Guo, S., Jin, L., He, D. and Wang, J. (2019). Genome-Wide DNA Methylation Profiles Reveal Common Epigenetic Patterns of Interferon-Related Genes in Multiple Autoimmune Diseases. Front Genet *10*, 223.

Cheng, T., Rodrigues, N., Dombkowski, D., Stier, S. and Scadden, D. T. (2000). Stem cell repopulation efficiency but not pool size is governed by p27(kip1). Nat Med *6*, 1235-40.

Chisolm, D. A., Cheng, W., Colburn, S. A., Silva-Sanchez, A., Meza-Perez, S., Randall, T. D. and Weinmann, A. S. (2019). Defining Genetic Variation in Widely Used Congenic and Backcrossed Mouse Models Reveals Varied Regulation of Genes Important for Immune Responses. Immunity *51*, 155-168.e5.

Choi, J. S. and Harley, B. A. (2017). Marrow-inspired matrix cues rapidly affect early fate decisions of hematopoietic stem and progenitor cells. Sci Adv *3*, e1600455.

Chow, A., Lucas, D., Hidalgo, A., Méndez-Ferrer, S., Hashimoto, D., Scheiermann, C., Battista, M., Leboeuf, M., Prophete, C., van Rooijen, N.*, et al.* (2011). Bone marrow CD169+ macrophages promote the retention of hematopoietic stem and progenitor cells in the mesenchymal stem cell niche. J Exp Med *208*, 261-71.

Christensen, J. L., Wright, D. E., Wagers, A. J. and Weissman, I. L. (2004). Circulation and chemotaxis of fetal hematopoietic stem cells. PLoS Biol *2*, E75.

Claesson, M. H., Ropke, C. and Hougen, H. P. (1974). Distribution of short-lived and long-lived small lymphocytes in the lymphomyeloid tissues of germ-free NMRI mice. Scand J Immunol *3*, 597-604.

Coccia, E. M., Uze, G. and Pellegrini, S. (2006). Negative regulation of type I interferon signaling: facts and mechanisms. Cell Mol Biol (Noisy-le-grand) *52*, 77-87.

Coutu, D. L., Kokkaliaris, K. D., Kunz, L. and Schroeder, T. (2018). Multicolor quantitative confocal imaging cytometry. Nat Methods *15*, 39-46.

Craig, C. E., Quaglia, A. and Dhillon, A. P. (2004). Extramedullary haematopoiesis in massive hepatic necrosis. Histopathology *45*, 518-25.

Crisan, M. and Dzierzak, E. (2016). The many faces of hematopoietic stem cell heterogeneity. Development *143*, 4571-4581.

Croxford, A. L., Lanzinger, M., Hartmann, F. J., Schreiner, B., Mair, F., Pelczar, P., Clausen, B. E., Jung, S., Greter, M. and Becher, B. (2015). The Cytokine GM-CSF Drives the Inflammatory Signature of CCR2+ Monocytes and Licenses Autoimmunity. Immunity *43*, 502-14.

Cui, K., Zang, C., Roh, T. Y., Schones, D. E., Childs, R. W., Peng, W. and Zhao, K. (2009). Chromatin signatures in multipotent human hematopoietic stem cells indicate the fate of bivalent genes during differentiation. Cell Stem Cell *4*, 80-93.

D'Urso, A. and Brickner, J. H. (2014). Mechanisms of epigenetic memory. Trends Genet *30*, 230-6.

Darnell, J. E., Jr. (1997). STATs and gene regulation. Science *277*, 1630-5.

Darnell, J. E., Jr., Kerr, I. M. and Stark, G. R. (1994). Jak-STAT pathways and transcriptional activation in response to IFNs and other extracellular signaling proteins. Science *264*, 1415-21.

Day, C. L., Kaufmann, D. E., Kiepiela, P., Brown, J. A., Moodley, E. S., Reddy, S., Mackey, E. W., Miller, J. D., Leslie, A. J., DePierres, C.*, et al.* (2006). PD-1 expression on HIV-specific T cells is associated with T-cell exhaustion and disease progression. Nature *443*, 350-4.

de Bruijn, M. F. T. R., Speck, N. A., Peeters, M. C. E. and Dzierzak, E. (2000). Definitive hematopoietic stem cells first develop within the major arterial regions of the mouse embryo. The EMBO Journal *19*, 2465-2474.

de Bruin, A. M., Demirel, O., Hooibrink, B., Brandts, C. H. and Nolte, M. A. (2013). Interferon-gamma impairs proliferation of hematopoietic stem cells in mice. Blood *121*, 3578-85.

de Laval, B., Maurizio, J., Kandalla, P. K., Brisou, G., Simonnet, L., Huber, C., Gimenez, G., Matcovitch-Natan, O., Reinhardt, S., David, E.*, et al.* (2020). C/EBPβ-Dependent Epigenetic Memory Induces Trained Immunity in Hematopoietic Stem Cells. Cell Stem Cell *26*, 793.

de Sauvage, F. J., Carver-Moore, K., Luoh, S. M., Ryan, A., Dowd, M., Eaton, D. L. and Moore, M. W. (1996). Physiological regulation of early and late stages of megakaryocytopoiesis by thrombopoietin. J Exp Med *183*, 651-6.

de Veer, M. J., Holko, M., Frevel, M., Walker, E., Der, S., Paranjape, J. M., Silverman, R. H. and Williams, B. R. (2001). Functional classification of interferon-stimulated genes identified using microarrays. J Leukoc Biol *69*, 912-20.

Der, S. D., Zhou, A., Williams, B. R. and Silverman, R. H. (1998). Identification of genes differentially regulated by interferon alpha, beta, or gamma using oligonucleotide arrays. Proc Natl Acad Sci U S A *95*, 15623-8.

Dexter, T. M., Allen, T. D. and Lajtha, L. G. (1977). Conditions controlling the proliferation of haemopoietic stem cells in vitro. J Cell Physiol *91*, 335-44.

Di Rosa, F. (2016a). Maintenance of memory T cells in the bone marrow: survival or homeostatic proliferation? Nat Rev Immunol *16*, 271.

Di Rosa, F. (2016b). Two Niches in the Bone Marrow: A Hypothesis on Life-long T Cell Memory. Trends Immunol *37*, 503-512.

Dieterlen-Lièvre, F., Corbel, C. and Salaün, J. (2010). Allantois and placenta as developmental sources of hematopoietic stem cells. Int J Dev Biol *54*, 1079-87.

Ding, L. and Morrison, S. J. (2013). Haematopoietic stem cells and early lymphoid progenitors occupy distinct bone marrow niches. Nature *495*, 231-5.

Discher, D. E., Mooney, D. J. and Zandstra, P. W. (2009). Growth Factors, Matrices, and Forces Combine and Control Stem Cells. Science *324*, 1673-1677.

Doan, P. L., Russell, J. L., Himburg, H. A., Helms, K., Harris, J. R., Lucas, J., Holshausen, K. C., Meadows, S. K., Daher, P., Jeffords, L. B.*, et al.* (2013). Tie2(+) bone marrow endothelial cells regulate hematopoietic stem cell regeneration following radiation injury. Stem Cells *31*, 327-37.

Domingues, M. J., Cao, H., Heazlewood, S. Y., Cao, B. and Nilsson, S. K. (2017). Niche Extracellular Matrix Components and Their Influence on HSC. J Cell Biochem *118*, 1984-1993.

Dorhoi, A., Iannaccone, M., Farinacci, M., Fae, K. C., Schreiber, J., Moura-Alves, P., Nouailles, G., Mollenkopf, H. J., Oberbeck-Muller, D., Jorg, S.*, et al.* (2013). MicroRNA-223 controls susceptibility to tuberculosis by regulating lung neutrophil recruitment. J Clin Invest *123*, 4836-48.

Downs, K. M. (2002). Early placental ontogeny in the mouse. Placenta *23*, 116-31.

Downs, K. M. and Harmann, C. (1997). Developmental potency of the murine allantois. Development *124*, 2769-80.

Duan, B. and Morel, L. (2006). Role of B-1a cells in autoimmunity. Autoimmun Rev *5*, 403-8.

Duan, L., Rao, X. and Sigdel, K. R. (2019). Regulation of Inflammation in Autoimmune Disease. J Immunol Res *2019*, 7403796.

Dunbar, A., Nazir, A. and Levine, R. (2017). Overview of Transgenic Mouse Models of Myeloproliferative Neoplasms (MPNs). Curr Protoc Pharmacol *77*, 14.40.1-14.40.19.

Dunn, J., McCuaig, R., Tu, W. J., Hardy, K. and Rao, S. (2015). Multi-layered epigenetic mechanisms contribute to transcriptional memory in T lymphocytes. BMC Immunol *16*, 27.

Dykstra, B., Kent, D., Bowie, M., McCaffrey, L., Hamilton, M., Lyons, K., Lee, S. J., Brinkman, R. and Eaves, C. (2007). Long-term propagation of distinct hematopoietic differentiation programs in vivo. Cell Stem Cell *1*, 218-29.

Dzierzak, E. and Speck, N. A. (2008). Of lineage and legacy: the development of mammalian hematopoietic stem cells. Nat Immunol *9*, 129-36.

Ellington, S. K. (1987). A morphological study of the development of the chorion of rat embryos. J Anat *150*, 247-63.

Ellis, S. J. and Tanentzapf, G. (2010). Integrin-mediated adhesion and stem-cell-niche interactions. Cell Tissue Res *339*, 121-30.

Ellis, S. L., Heazlewood, S. Y., Williams, B., Reitsma, A. J., Grassinger, J., Borg, J., Heazlewood, C. K., Chidgey, A. P. and Nilsson, S. K. (2013). The role of Tenascin C in the lymphoid progenitor cell niche. Exp Hematol *41*, 1050-61.

Ema, H., Morita, Y. and Suda, T. (2014). Heterogeneity and hierarchy of hematopoietic stem cells. Exp Hematol *42*, 74-82.e2.

Ema, H., Morita, Y., Yamazaki, S., Matsubara, A., Seita, J., Tadokoro, Y., Kondo, H., Takano, H. and Nakauchi, H. (2006). Adult mouse hematopoietic stem cells: purification and single-cell assays. Nat Protoc *1*, 2979-87.

Ema, H. and Nakauchi, H. (2000). Expansion of hematopoietic stem cells in the developing liver of a mouse embryo. Blood *95*, 2284-8.

Espin-Palazon, R., Stachura, D. L., Campbell, C. A., Garcia-Moreno, D., Del Cid, N., Kim, A. D., Candel, S., Meseguer, J., Mulero, V. and Traver, D. (2014). Proinflammatory signaling regulates hematopoietic stem cell emergence. Cell *159*, 1070-1085.

Essers, M. A., Offner, S., Blanco-Bose, W. E., Waibler, Z., Kalinke, U., Duchosal, M. A. and Trumpp, A. (2009). IFNalpha activates dormant haematopoietic stem cells in vivo. Nature *458*, 904-8.

Feeley, E. M., Sims, J. S., John, S. P., Chin, C. R., Pertel, T., Chen, L. M., Gaiha, G. D., Ryan, B. J., Donis, R. O., Elledge, S. J*., et al.* (2011). IFITM3 inhibits influenza A virus infection by preventing cytosolic entry. PLoS Pathog *7*, e1002337.

Fenimore, J. and H, A. Y. (2016). Regulation of IFN-gamma Expression. Adv Exp Med Biol *941*, 1-19.

Ferkowicz, M. J., Starr, M., Xie, X., Li, W., Johnson, S. A., Shelley, W. C., Morrison, P. R. and Yoder, M. C. (2003). CD41 expression defines the onset of primitive and definitive hematopoiesis in the murine embryo. Development *130*, 4393-403.

Ford, C. E., Hamerton, J. L., Barnes, D. W. and Loutit, J. F. (1956). Cytological identification of radiation-chimaeras. Nature *177*, 452-4.

Freeman, G. J., Long, A. J., Iwai, Y., Bourque, K., Chernova, T., Nishimura, H., Fitz, L. J., Malenkovich, N., Okazaki, T., Byrne, M. C*., et al.* (2000). Engagement of the PD-1 immunoinhibitory receptor by a novel B7 family member leads to negative regulation of lymphocyte activation. J Exp Med *192*, 1027-34.

Friedenstein, A. J., Chailakhyan, R. K., Latsinik, N. V., Panasyuk, A. F. and Keiliss-Borok, I. V. (1974). Stromal cells responsible for transferring the microenvironment of the hemopoietic tissues. Cloning in vitro and retransplantation in vivo. Transplantation *17*, 331-40.

Friedman, R. L., Manly, S. P., McMahon, M., Kerr, I. M. and Stark, G. R. (1984). Transcriptional and posttranscriptional regulation of interferon-induced gene expression in human cells. Cell *38*, 745-55.

Frucht, D. M., Fukao, T., Bogdan, C., Schindler, H., O'Shea, J. J. and Koyasu, S. (2001). IFN-gamma production by antigen-presenting cells: mechanisms emerge. Trends Immunol *22*, 556-60.

Ganuza, M., Chabot, A., Tang, X., Bi, W., Natarajan, S., Carter, R., Gawad, C., Kang, G., Cheng, Y. and McKinney-Freeman, S. (2018). Murine hematopoietic stem cell activity is derived from pre-circulation embryos but not yolk sacs. Nat Commun *9*, 5405.

Gao, S. and Liu, F. (2018). Fetal liver: an ideal niche for hematopoietic stem cell expansion. Sci China Life Sci *61*, 885-892.

Gao, X., Xu, C., Asada, N. and Frenette, P. S. (2018). The hematopoietic stem cell niche: from embryo to adult. Development *145*.

Gardner, R. L., Lyon, M. F., Evans, E. P. and Burtenshaw, M. D. (1985). Clonal analysis of X-chromosome inactivation and the origin of the germ line in the mouse embryo. J Embryol Exp Morphol *88*, 349-63.

Gattazzo, F., Urciuolo, A. and Bonaldo, P. (2014). Extracellular matrix: a dynamic microenvironment for stem cell niche. Biochim Biophys Acta *1840*, 2506-19.

Gekas, C., Dieterlen-Lievre, F., Orkin, S. H. and Mikkola, H. K. (2005). The placenta is a niche for hematopoietic stem cells. Dev Cell *8*, 365-75.

Gekas, C. and Graf, T. (2013). CD41 expression marks myeloid-biased adult hematopoietic stem cells and increases with age. Blood *121*, 4463-72.

Gekas, C., Rhodes, K. E., Van Handel, B., Chhabra, A., Ueno, M. and Mikkola, H. K. (2010). Hematopoietic stem cell development in the placenta. Int J Dev Biol *54*, 1089-98.

George, B. M., Kao, K. S., Kwon, H. S., Velasco, B. J., Poyser, J., Chen, A., Le, A. C., Chhabra, A., Burnett, C. E., Cajuste, D.*, et al.* (2019). Antibody Conditioning Enables MHC-Mismatched Hematopoietic Stem Cell Transplants and Organ Graft Tolerance. Cell Stem Cell *25*, 185-192.e3.

Gessani, S. and Belardelli, F. (1998). IFN-gamma expression in macrophages and its possible biological significance. Cytokine Growth Factor Rev *9*, 117-23.

Gialitakis, M., Arampatzi, P., Makatounakis, T. and Papamatheakis, J. (2010). Gamma interferon-dependent transcriptional memory via relocalization of a gene locus to PML nuclear bodies. Mol Cell Biol *30*, 2046-56.

Gomez Perdiguero, E., Klapproth, K., Schulz, C., Busch, K., Azzoni, E., Crozet, L., Garner, H., Trouillet, C., de Bruijn, M. F., Geissmann, F.*, et al.* (2015). Tissue-resident macrophages originate from yolk-sac-derived erythro-myeloid progenitors. Nature *518*, 547-51.

Goodell, M. A., Brose, K., Paradis, G., Conner, A. S. and Mulligan, R. C. (1996). Isolation and functional properties of murine hematopoietic stem cells that are replicating in vivo. J Exp Med *183*, 1797-806.

Gothert, J. R., Gustin, S. E., Hall, M. A., Green, A. R., Gottgens, B., Izon, D. J. and Begley, C. G. (2005). In vivo fate-tracing studies using the Scl stem cell enhancer: embryonic hematopoietic stem cells significantly contribute to adult hematopoiesis. Blood *105*, 2724-32.

Gough, D. J., Messina, N. L., Clarke, C. J., Johnstone, R. W. and Levy, D. E. (2012). Constitutive type I interferon modulates homeostatic balance through tonic signaling. Immunity *36*, 166-74.

Grassinger, J., Haylock, D. N., Storan, M. J., Haines, G. O., Williams, B., Whitty, G. A., Vinson, A. R., Be, C. L., Li, S., Sorensen, E. S.*, et al.* (2009). Thrombin-cleaved osteopontin regulates hemopoietic stem and progenitor cell functions through interactions with alpha9beta1 and alpha4beta1 integrins. Blood *114*, 49-59.

Grosso, J. F., Goldberg, M. V., Getnet, D., Bruno, T. C., Yen, H. R., Pyle, K. J., Hipkiss, E., Vignali, D. A., Pardoll, D. M. and Drake, C. G. (2009). Functionally distinct LAG-3 and PD-1 subsets on activated and chronically stimulated CD8 T cells. J Immunol *182*, 6659-69.

Gutterman, J. U. (1994). Cytokine therapeutics: lessons from interferon alpha. Proc Natl Acad Sci U S A *91*, 1198-205.

Haas, S., Hansson, J., Klimmeck, D., Loeffler, D., Velten, L., Uckelmann, H., Wurzer, S., Prendergast, A. M., Schnell, A., Hexel, K.*, et al.* (2015). Inflammation-Induced Emergency Megakaryopoiesis Driven by Hematopoietic Stem Cell-like Megakaryocyte Progenitors. Cell Stem Cell *17*, 422-34.

Haas, S., Trumpp, A. and Milsom, M. D. (2018). Causes and Consequences of Hematopoietic Stem Cell Heterogeneity. Cell Stem Cell *22*, 627-638.

Harris, D. P., Haynes, L., Sayles, P. C., Duso, D. K., Eaton, S. M., Lepak, N. M., Johnson, L. L., Swain, S. L. and Lund, F. E. (2000). Reciprocal regulation of polarized cytokine production by effector B and T cells. Nat Immunol *1*, 475-82.

Harrison, D. E., Jordan, C. T., Zhong, R. K. and Astle, C. M. (1993). Primitive hemopoietic stem cells: direct assay of most productive populations by competitive repopulation with simple binomial, correlation and covariance calculations. Exp Hematol *21*, 206-19.

Harrison, D. E., Zhong, R. K., Jordan, C. T., Lemischka, I. R. and Astle, C. M. (1997). Relative to adult marrow, fetal liver repopulates nearly five times more effectively long-term than short-term. Exp Hematol *25*, 293-7.

Hasselbalch, H. C. and Holmstrom, M. O. (2019). Perspectives on interferon-alpha in the treatment of polycythemia vera and related myeloproliferative neoplasms: minimal residual disease and cure? Semin Immunopathol *41*, 5-19.

He, S., Kim, I., Lim, M. S. and Morrison, S. J. (2011). Sox17 expression confers self-renewal potential and fetal stem cell characteristics upon adult hematopoietic progenitors. Genes Dev *25*, 1613-27.

Hedrich, C. M. and Tsokos, G. C. (2011). Epigenetic mechanisms in systemic lupus erythematosus and other autoimmune diseases. Trends Mol Med *17*, 714-24.

Hernandez-Verdun, D. (1974). Morphogenesis of the syncytium in the mouse placenta. Ultrastructural study. Cell Tissue Res *148*, 381-96.

Hirche, C., Frenz, T., Haas, S. F., Doring, M., Borst, K., Tegtmeyer, P. K., Brizic, I., Jordan, S., Keyser, K., Chhatbar, C.*, et al.* (2017). Systemic Virus Infections Differentially Modulate Cell Cycle State and Functionality of Long-Term Hematopoietic Stem Cells In Vivo. Cell Rep *19*, 2345-2356.

Hirschi, K. K. (2012). Hemogenic endothelium during development and beyond. Blood *119*, 4823-7.

Hooper, A. T., Butler, J. M., Nolan, D. J., Kranz, A., Iida, K., Kobayashi, M., Kopp, H. G., Shido, K., Petit, I., Yanger, K.*, et al.* (2009). Engraftment and reconstitution of hematopoiesis is dependent on VEGFR2-mediated regeneration of sinusoidal endothelial cells. Cell Stem Cell *4*, 263-74.

Hosseinzadeh, H. and Goldschneider, I. (1993). Recent thymic emigrants in the rat express a unique antigenic phenotype and undergo post-thymic maturation in peripheral lymphoid tissues. J Immunol *150*, 1670-9.

Houssaint, E. (1981). Differentiation of the mouse hepatic primordium. II. Extrinsic origin of the haemopoietic cell line. Cell Differ *10*, 243-52.

Huang, I. C., Bailey, C. C., Weyer, J. L., Radoshitzky, S. R., Becker, M. M., Chiang, J. J., Brass, A. L., Ahmed, A. A., Chi, X., Dong, L.*, et al.* (2011). Distinct patterns of IFITM-mediated restriction of filoviruses, SARS coronavirus, and influenza A virus. PLoS Pathog *7*, e1001258.

Huber, T. L., Kouskoff, V., Fehling, H. J., Palis, J. and Keller, G. (2004). Haemangioblast commitment is initiated in the primitive streak of the mouse embryo. Nature *432*, 625-30.

Hwang, S. Y., Hertzog, P. J., Holland, K. A., Sumarsono, S. H., Tymms, M. J., Hamilton, J. A., Whitty, G., Bertoncello, I. and Kola, I. (1995). A null mutation in the gene encoding a type I interferon receptor component eliminates antiproliferative and antiviral responses to interferons alpha and beta and alters macrophage responses. Proc Natl Acad Sci U S A *92*, 11284-8.

Imgenberg-Kreuz, J., Carlsson Almlof, J., Leonard, D., Alexsson, A., Nordmark, G., Eloranta, M. L., Rantapaa-Dahlqvist, S., Bengtsson, A. A., Jonsen, A., Padyukov, L*., et al.* (2018). DNA methylation mapping identifies gene regulatory effects in patients with systemic lupus erythematosus. Ann Rheum Dis *77*, 736-743.

Imgenberg-Kreuz, J., Sandling, J. K., Almlof, J. C., Nordlund, J., Signer, L., Norheim, K. B., Omdal, R., Ronnblom, L., Eloranta, M. L., Syvanen, A. C*., et al.* (2016). Genome-wide DNA methylation analysis in multiple tissues in primary Sjogren's syndrome reveals regulatory effects at interferon-induced genes. Ann Rheum Dis *75*, 2029-2036.

Isaacs, A. and Lindenmann, J. (1957). Virus interference. I. The interferon. Proc R Soc Lond B Biol Sci *147*, 258-67.

Isaacs, A., Lindenmann, J. and Valentine, R. C. (1957). Virus interference. II. Some properties of interferon. Proc R Soc Lond B Biol Sci *147*, 268-73.

Jablonka, E. and Raz, G. (2009). Transgenerational epigenetic inheritance: prevalence, mechanisms, and implications for the study of heredity and evolution. Q Rev Biol *84*, 131-76.

Jacobson, L. O., Simmons, E. L., Marks, E. K. and Eldredge, J. H. (1951). Recovery from radiation injury. Science *113*, 510-11.

Jacquelot, N., Yamazaki, T., Roberti, M. P., Duong, C. P. M., Andrews, M. C., Verlingue, L., Ferrere, G., Becharef, S., Vetizou, M., Daillere, R*., et al.* (2019). Sustained Type I interferon signaling as a mechanism of resistance to PD-1 blockade. Cell Res *29*, 846-861.

Jameson, S. C. (2005). T cell homeostasis: keeping useful T cells alive and live T cells useful. Semin Immunol *17*, 231-7.

Jia, Y., Ying, X., Zhou, J., Chen, Y., Luo, X., Xie, S., Wang, Q. C., Hu, W. and Wang, L. (2018). The novel KLF4/PLAC8 signaling pathway regulates lung cancer growth. Cell Death Dis *9*, 603.

Jin, C. and Felsenfeld, G. (2007). Nucleosome stability mediated by histone variants H3.3 and H2A.Z. Genes Dev *21*, 1519-29.

Johnson, G. R. and Moore, M. A. (1975). Role of stem cell migration in initiation of mouse foetal liver haemopoiesis. Nature *258*, 726-8.

Jones, R. J., Wagner, J. E., Celano, P., Zicha, M. S. and Sharkis, S. J. (1990). Separation of pluripotent haematopoietic stem cells from spleen colony-forming cells. Nature *347*, 188-9.

Jurkovich, G. J., Mileski, W. J., Maier, R. V., Winn, R. K. and Rice, C. L. (1991). Interferon gamma increases sensitivity to endotoxin. J Surg Res *51*, 197-203.

Kanno, Y., Kozak, C. A., Schindler, C., Driggers, P. H., Ennist, D. L., Gleason, S. L., Darnell, J. E., Jr. and Ozato, K. (1993). The genomic structure of the murine ICSBP gene reveals the presence of the gamma interferon-responsive element, to which an ISGF3 alpha subunit (or similar) molecule binds. Mol Cell Biol *13*, 3951-63.

Karamitros, D., Stoilova, B., Aboukhalil, Z., Hamey, F., Reinisch, A., Samitsch, M., Quek, L., Otto, G., Repapi, E., Doondeea, J*., et al.* (2018). Single-cell analysis reveals the continuum of human lympho-myeloid progenitor cells. Nat Immunol *19*, 85-97.

Katayama, Y., Battista, M., Kao, W. M., Hidalgo, A., Peired, A. J., Thomas, S. A. and Frenette, P. S. (2006). Signals from the sympathetic nervous system regulate hematopoietic stem cell egress from bone marrow. Cell *124*, 407-21.

Kawai, T. and Akira, S. (2010). The role of pattern-recognition receptors in innate immunity: update on Toll-like receptors. Nat Immunol *11*, 373-84.

Khurana, S., Schouteden, S., Manesia, J. K., Santamaria-Martinez, A., Huelsken, J., Lacy-Hulbert, A. and Verfaillie, C. M. (2016). Outside-in integrin signalling regulates haematopoietic stem cell function via Periostin-Itgav axis. Nat Commun *7*, 13500.

Kiefer, J. C. (2007). Epigenetics in development. Dev Dyn *236*, 1144-56.

Kiel, M. J., He, S., Ashkenazi, R., Gentry, S. N., Teta, M., Kushner, J. A., Jackson, T. L. and Morrison, S. J. (2007a). Haematopoietic stem cells do not asymmetrically segregate chromosomes or retain BrdU. Nature *449*, 238-42.

Kiel, M. J., Radice, G. L. and Morrison, S. J. (2007b). Lack of evidence that hematopoietic stem cells depend on N-cadherin-mediated adhesion to osteoblasts for their maintenance. Cell Stem Cell *1*, 204-17.

Kiel, M. J., Yilmaz, O. H., Iwashita, T., Yilmaz, O. H., Terhorst, C. and Morrison, S. J. (2005). SLAM family receptors distinguish hematopoietic stem and progenitor cells and reveal endothelial niches for stem cells. Cell *121*, 1109-21.

Kiely, P. D. and Bruckner, F. E. (1994). Acute arthritis following interferon-alpha therapy. Br J Rheumatol *33*, 502-3.

Kim, I., He, S., Yilmaz, O. H., Kiel, M. J. and Morrison, S. J. (2006). Enhanced purification of fetal liver hematopoietic stem cells using SLAM family receptors. Blood *108*, 737-44.

Kim, I., Saunders, T. L. and Morrison, S. J. (2007). Sox17 dependence distinguishes the transcriptional regulation of fetal from adult hematopoietic stem cells. Cell *130*, 470-83.

Kim, J., Sachdev, P. and Sidhu, K. (2013). Alginate microcapsule as a 3D platform for the efficient differentiation of human embryonic stem cells to dopamine neurons. Stem Cell Res *11*, 978-89.

King, K. Y. and Goodell, M. A. (2011). Inflammatory modulation of HSCs: viewing the HSC as a foundation for the immune response. Nat Rev Immunol *11*, 685-92.

Klein, G. (1995). The extracellular matrix of the hematopoietic microenvironment. Experientia *51*, 914-26.

Kobayashi, H., Butler, J. M., O'Donnell, R., Kobayashi, M., Ding, B. S., Bonner, B., Chiu, V. K., Nolan, D. J., Shido, K., Benjamin, L.*, et al.* (2010). Angiocrine factors from Akt-activated endothelial cells balance self-renewal and differentiation of haematopoietic stem cells. Nat Cell Biol *12*, 1046-56.

Kobayashi, H., Morikawa, T., Okinaga, A., Hamano, F., Hashidate-Yoshida, T., Watanuki, S., Hishikawa, D., Shindou, H., Arai, F., Kabe, Y.*, et al.* (2019). Environmental Optimization Enables Maintenance of Quiescent Hematopoietic Stem Cells Ex Vivo. Cell Rep *28*, 145-158.e9.

Kollet, O., Dar, A., Shivtiel, S., Kalinkovich, A., Lapid, K., Sztainberg, Y., Tesio, M., Samstein, R. M., Goichberg, P., Spiegel, A.*, et al.* (2006). Osteoclasts degrade endosteal components and promote mobilization of hematopoietic progenitor cells. Nat Med *12*, 657-64.

Kondo, M., Weissman, I. L. and Akashi, K. (1997). Identification of clonogenic common lymphoid progenitors in mouse bone marrow. Cell *91*, 661-72.

Kretschmer, S. and Lee-Kirsch, M. A. (2017). Type I interferon-mediated autoinflammation and autoimmunity. Curr Opin Immunol *49*, 96-102.

Kujawski, L. A. and Talpaz, M. (2007). The role of interferon-alpha in the treatment of chronic myeloid leukemia. Cytokine Growth Factor Rev *18*, 459-71.

Kumaravelu, P., Hook, L., Morrison, A. M., Ure, J., Zhao, S., Zuyev, S., Ansell, J. and Medvinsky, A. (2002). Quantitative developmental anatomy of definitive haematopoietic stem cells/long-term repopulating units (HSC/RUs): role of the aorta-gonad-mesonephros (AGM) region and the yolk sac in colonisation of the mouse embryonic liver. Development *129*, 4891-9.

Kyba, M., Perlingeiro, R. C. and Daley, G. Q. (2002). HoxB4 confers definitive lymphoid-myeloid engraftment potential on embryonic stem cell and yolk sac hematopoietic progenitors. Cell *109*, 29-37.

Lam, B. S., Cunningham, C. and Adams, G. B. (2011). Pharmacologic modulation of the calcium-sensing receptor enhances hematopoietic stem cell lodgment in the adult bone marrow. Blood *117*, 1167-75.

Lange, U. C., Adams, D. J., Lee, C., Barton, S., Schneider, R., Bradley, A. and Surani, M. A. (2008). Normal germ line establishment in mice carrying a deletion of the Ifitm/Fragilis gene family cluster. Mol Cell Biol *28*, 4688-96.

Lanzavecchia, A. and Sallusto, F. (2000). Dynamics of T lymphocyte responses: intermediates, effectors, and memory cells. Science *290*, 92-7.

Lapin, M., Tjensvoll, K., Oltedal, S., Javle, M., Smaaland, R., Gilje, B. and Nordgard, O. (2017). Single-cell mRNA profiling reveals transcriptional heterogeneity among pancreatic circulating tumour cells. BMC Cancer *17*, 390.

Le Bon, A., Etchart, N., Rossmann, C., Ashton, M., Hou, S., Gewert, D., Borrow, P. and Tough, D. F. (2003). Cross-priming of CD8+ T cells stimulated by virus-induced type I interferon. Nat Immunol *4*, 1009-15.

Le Bon, A. and Tough, D. F. (2002). Links between innate and adaptive immunity via type I interferon. Curr Opin Immunol *14*, 432-6.

Lee, W. B., Choi, W. Y., Lee, D. H., Shim, H., Kim-Ha, J. and Kim, Y. J. (2019). OAS1 and OAS3 negatively regulate the expression of chemokines and interferon-responsive genes in human macrophages. BMB Rep *52*, 133-138.

Leisching, G., Cole, V., Ali, A. T. and Baker, B. (2019). OAS1, OAS2 and OAS3 restrict intracellular M. tb replication and enhance cytokine secretion. Int J Infect Dis *80s*, S77-s84.

Lekmine, F., Uddin, S., Sassano, A., Parmar, S., Brachmann, S. M., Majchrzak, B., Sonenberg, N., Hay, N., Fish, E. N. and Platanias, L. C. (2003). Activation of the p70 S6 kinase and phosphorylation of the 4E-BP1 repressor of mRNA translation by type I interferons. J Biol Chem *278*, 27772-80.

Lemischka, I. R., Raulet, D. H. and Mulligan, R. C. (1986). Developmental potential and dynamic behavior of hematopoietic stem cells. Cell *45*, 917-27.

Leviyang, S. and Griva, I. (2018). Investigating Functional Roles for Positive Feedback and Cellular Heterogeneity in the Type I Interferon Response to Viral Infection. Viruses *10*.

Levy, D. E., Kessler, D. S., Pine, R. and Darnell, J. E., Jr. (1989). Cytoplasmic activation of ISGF3, the positive regulator of interferon-alpha-stimulated transcription, reconstituted in vitro. Genes Dev *3*, 1362-71.

Levy, D. E., Kessler, D. S., Pine, R., Reich, N. and Darnell, J. E., Jr. (1988). Interferon-induced nuclear factors that bind a shared promoter element correlate with positive and negative transcriptional control. Genes Dev *2*, 383-93.

Li, K., Markosyan, R. M., Zheng, Y. M., Golfetto, O., Bungart, B., Li, M., Ding, S., He, Y., Liang, C., Lee, J. C.*, et al.* (2013). IFITM proteins restrict viral membrane hemifusion. PLoS Pathog *9*, e1003124.

Li, W., Johnson, S. A., Shelley, W. C. and Yoder, M. C. (2004a). Hematopoietic stem cell repopulating ability can be maintained in vitro by some primary endothelial cells. Exp Hematol *32*, 1226-37.

Li, W., Li, F., Lei, W. and Tao, Z. (2019). TRIM30 modulates Interleukin-22-regulated papillary thyroid Cancer cell migration and invasion by targeting Sox17 for K48-linked Polyubiquitination. Cell Commun Signal *17*, 162.

Li, Y., Esain, V., Teng, L., Xu, J., Kwan, W., Frost, I. M., Yzaguirre, A. D., Cai, X., Cortes, M., Maijenburg, M. W.*, et al.* (2014). Inflammatory signaling regulates embryonic hematopoietic stem and progenitor cell production. Genes Dev *28*, 2597-612.

Li, Y., Sassano, A., Majchrzak, B., Deb, D. K., Levy, D. E., Gaestel, M., Nebreda, A. R., Fish, E. N. and Platanias, L. C. (2004b). Role of p38α Map Kinase in Type I Interferon Signaling. Journal of Biological Chemistry *279*, 970-979.

Liaskou, E., Zimmermann, H. W., Li, K. K., Oo, Y. H., Suresh, S., Stamataki, Z., Qureshi, O., Lalor, P. F., Shaw, J., Syn, W. K.*, et al.* (2013). Monocyte subsets in human liver disease show distinct phenotypic and functional characteristics. Hepatology *57*, 385-98.

Liaw, L., Birk, D. E., Ballas, C. B., Whitsitt, J. S., Davidson, J. M. and Hogan, B. L. (1998). Altered wound healing in mice lacking a functional osteopontin gene (spp1). J Clin Invest *101*, 1468-78.

Lichtenegger, F. S., Rothe, M., Schnorfeil, F. M., Deiser, K., Krupka, C., Augsberger, C., Schluter, M., Neitz, J. and Subklewe, M. (2018). Targeting LAG-3 and PD-1 to Enhance T Cell Activation by Antigen-Presenting Cells. Front Immunol *9*, 385.

Lim, H. K., Periasamy, P. and O'Neill, H. C. (2018). In Vitro Murine Hematopoiesis Supported by Signaling from a Splenic Stromal Cell Line. Stem Cells Int *2018*, 9896142.

Lindenmann, J., Burke, D. C. and Isaacs, A. (1957). Studies on the production, mode of action and properties of interferon. Br J Exp Pathol *38*, 551-62.

Linzer, D. I. and Fisher, S. J. (1999). The placenta and the prolactin family of hormones: regulation of the physiology of pregnancy. Mol Endocrinol *13*, 837-40.

Liston, A. and Rudensky, A. Y. (2007). Thymic development and peripheral homeostasis of regulatory T cells. Curr Opin Immunol *19*, 176-85.

Lo Celso, C., Fleming, H. E., Wu, J. W., Zhao, C. X., Miake-Lye, S., Fujisaki, J., Cote, D., Rowe, D. W., Lin, C. P. and Scadden, D. T. (2009). Live-animal tracking of individual haematopoietic stem/progenitor cells in their niche. Nature *457*, 92-6.

Lord, B. I., Testa, N. G. and Hendry, J. H. (1975). The relative spatial distributions of CFUs and CFUc in the normal mouse femur. Blood *46*, 65-72.

Lorsbach, R. B., Murphy, W. J., Lowenstein, C. J., Snyder, S. H. and Russell, S. W. (1993). Expression of the nitric oxide synthase gene in mouse macrophages activated for tumor cell killing. Molecular basis for the synergy between interferon-gamma and lipopolysaccharide. J Biol Chem *268*, 1908-13.

Loyola, A., Bonaldi, T., Roche, D., Imhof, A. and Almouzni, G. (2006). PTMs on H3 variants before chromatin assembly potentiate their final epigenetic state. Mol Cell *24*, 309-16.

Ma, G. T., Roth, M. E., Groskopf, J. C., Tsai, F. Y., Orkin, S. H., Grosveld, F., Engel, J. D. and Linzer, D. I. (1997). GATA-2 and GATA-3 regulate trophoblast-specific gene expression in vivo. Development *124*, 907-14.

Macaulay, I. C., Svensson, V., Labalette, C., Ferreira, L., Hamey, F., Voet, T., Teichmann, S. A. and Cvejic, A. (2016). Single-Cell RNA-Sequencing Reveals a Continuous Spectrum of Differentiation in Hematopoietic Cells. Cell Rep *14*, 966-977.

Maia, C. J., Socorro, S., Schmitt, F. and Santos, C. R. (2008). Characterization of oligoadenylate synthetase-1 expression in rat mammary gland and prostate: effects of 17beta-estradiol on the regulation of OAS1g in both tissues. Mol Cell Biochem *314*, 113-21.

Maillard, P. V., Ciaudo, C., Marchais, A., Li, Y., Jay, F., Ding, S. W. and Voinnet, O. (2013). Antiviral RNA interference in mammalian cells. Science *342*, 235-8.

Mansour, A., Abou-Ezzi, G., Sitnicka, E., Jacobsen, S. E., Wakkach, A. and Blin-Wakkach, C. (2012). Osteoclasts promote the formation of hematopoietic stem cell niches in the bone marrow. J Exp Med *209*, 537-49.

Månsson, R., Hultquist, A., Luc, S., Yang, L., Anderson, K., Kharazi, S., Al-Hashmi, S., Liuba, K., Thorén, L., Adolfsson, J.*, et al.* (2007). Molecular evidence for hierarchical transcriptional lineage priming in fetal and adult stem cells and multipotent progenitors. Immunity *26*, 407-19.

Matsumoto, K., Isagawa, T., Nishimura, T., Ogaeri, T., Eto, K., Miyazaki, S., Miyazaki, J., Aburatani, H., Nakauchi, H. and Ema, H. (2009). Stepwise development of hematopoietic stem cells from embryonic stem cells. PLoS One *4*, e4820.

Matsuzaki, J., Gnjatic, S., Mhawech-Fauceglia, P., Beck, A., Miller, A., Tsuji, T., Eppolito, C., Qian, F., Lele, S., Shrikant, P.*, et al.* (2010). Tumor-infiltrating NY-ESO-1-specific CD8+ T cells are negatively regulated by LAG-3 and PD-1 in human ovarian cancer. Proc Natl Acad Sci U S A *107*, 7875-80.

McIntosh, B. E., Brown, M. E., Duffin, B. M., Maufort, J. P., Vereide, D. T., Slukvin, II and Thomson, J. A. (2015). Nonirradiated NOD,B6.SCID Il2rgamma-/- Kit(W41/W41) (NBSGW) mice support multilineage engraftment of human hematopoietic cells. Stem Cell Reports *4*, 171-80.

McKinney-Freeman, S. L., Naveiras, O., Yates, F., Loewer, S., Philitas, M., Curran, M., Park, P. J. and Daley, G. Q. (2009). Surface antigen phenotypes of hematopoietic stem cells from embryos and murine embryonic stem cells. Blood *114*, 268-78.

Medvinsky, A. and Dzierzak, E. (1996). Definitive hematopoiesis is autonomously initiated by the AGM region. Cell *86*, 897-906.

Medvinsky, A., Rybtsov, S. and Taoudi, S. (2011). Embryonic origin of the adult hematopoietic system: advances and questions. Development *138*, 1017-31.

Melchers, F. (1979). Murine embryonic B lymphocyte development in the placenta. Nature *277*, 219-21.

Mendelson, A. and Frenette, P. S. (2014). Hematopoietic stem cell niche maintenance during homeostasis and regeneration. Nat Med *20*, 833-46.

Méndez-Ferrer, S., Lucas, D., Battista, M. and Frenette, P. S. (2008). Haematopoietic stem cell release is regulated by circadian oscillations. Nature *452*, 442-7.

Mikkola, H. K., Fujiwara, Y., Schlaeger, T. M., Traver, D. and Orkin, S. H. (2003). Expression of CD41 marks the initiation of definitive hematopoiesis in the mouse embryo. Blood *101*, 508-16.

Mikkola, H. K., Gekas, C., Orkin, S. H. and Dieterlen-Lievre, F. (2005). Placenta as a site for hematopoietic stem cell development. Exp Hematol *33*, 1048-54.

Mikkola, H. K. and Orkin, S. H. (2006). The journey of developing hematopoietic stem cells. Development *133*, 3733-44.

Molony, R. D., Nguyen, J. T., Kong, Y., Montgomery, R. R., Shaw, A. C. and Iwasaki, A. (2017). Aging impairs both primary and secondary RIG-I signaling for interferon induction in human monocytes. Sci Signal *10*.

Morita, Y., Ema, H. and Nakauchi, H. (2010). Heterogeneity and hierarchy within the most primitive hematopoietic stem cell compartment. J Exp Med *207*, 1173-82.

Morrison, S. J., Hemmati, H. D., Wandycz, A. M. and Weissman, I. L. (1995). The purification and characterization of fetal liver hematopoietic stem cells. Proc Natl Acad Sci U S A *92*, 10302-6.

Morrison, S. J. and Scadden, D. T. (2014). The bone marrow niche for haematopoietic stem cells. Nature *505*, 327-34.

Morrison, S. J. and Weissman, I. L. (1994). The long-term repopulating subset of hematopoietic stem cells is deterministic and isolatable by phenotype. Immunity *1*, 661-73.

Mühl, H. and Pfeilschifter, J. (2003). Anti-inflammatory properties of pro-inflammatory interferon-gamma. Int Immunopharmacol *3*, 1247-55.

Muller, A. M., Medvinsky, A., Strouboulis, J., Grosveld, F. and Dzierzak, E. (1994). Development of hematopoietic stem cell activity in the mouse embryo. Immunity *1*, 291-301.

Muller-Sieburg, C. E., Sieburg, H. B., Bernitz, J. M. and Cattarossi, G. (2012). Stem cell heterogeneity: implications for aging and regenerative medicine. Blood *119*, 3900-3907.

Muller-Sieburg, C. E., Whitlock, C. A. and Weissman, I. L. (1986). Isolation of two early B lymphocyte progenitors from mouse marrow: a committed pre-pre-B cell and a clonogenic Thy-1-lo hematopoietic stem cell. Cell *44*, 653-62.

Muskardin, T. L. W. and Niewold, T. B. (2018). Type I interferon in rheumatic diseases. Nat Rev Rheumatol *14*, 214-228.

Nakamura-Ishizu, A., Okuno, Y., Omatsu, Y., Okabe, K., Morimoto, J., Uede, T., Nagasawa, T., Suda, T. and Kubota, Y. (2012). Extracellular matrix protein tenascin-C is required in the bone marrow microenvironment primed for hematopoietic regeneration. Blood *119*, 5429-37.

Natale, B. V., Schweitzer, C., Hughes, M., Globisch, M. A., Kotadia, R., Tremblay, E., Vu, P., Cross, J. C. and Natale, D. R. C. (2017). Sca-1 identifies a trophoblast population with multipotent potential in the mid-gestation mouse placenta. Sci Rep *7*, 5575.

Nestorowa, S., Hamey, F. K., Pijuan Sala, B., Diamanti, E., Shepherd, M., Laurenti, E., Wilson, N. K., Kent, D. G. and Göttgens, B. (2016). A single-cell resolution map of mouse hematopoietic stem and progenitor cell differentiation. Blood *128*, e20-31.

Ng, Y. K., George, K. M., Engel, J. D. and Linzer, D. I. (1994). GATA factor activity is required for the trophoblast-specific transcriptional regulation of the mouse placental lactogen I gene. Development *120*, 3257-66.

Niewold, T. B., Hua, J., Lehman, T. J., Harley, J. B. and Crow, M. K. (2007). High serum IFN-alpha activity is a heritable risk factor for systemic lupus erythematosus. Genes Immun *8*, 492-502.

North, T. E., de Bruijn, M. F., Stacy, T., Talebian, L., Lind, E., Robin, C., Binder, M., Dzierzak, E. and Speck, N. A. (2002). Runx1 expression marks long-term repopulating hematopoietic stem cells in the midgestation mouse embryo. Immunity *16*, 661-72.

Northrop, J. K., Thomas, R. M., Wells, A. D. and Shen, H. (2006). Epigenetic remodeling of the IL-2 and IFN-gamma loci in memory CD8 T cells is influenced by CD4 T cells. J Immunol *177*, 1062-9.

Northrop, J. K., Wells, A. D. and Shen, H. (2008). Cutting edge: chromatin remodeling as a molecular basis for the enhanced functionality of memory CD8 T cells. J Immunol *181*, 865-8.

Notta, F., Zandi, S., Takayama, N., Dobson, S., Gan, O. I., Wilson, G., Kaufmann, K. B., McLeod, J., Laurenti, E., Dunant, C. F.*, et al.* (2016). Distinct routes of lineage development reshape the human blood hierarchy across ontogeny. Science *351*, aab2116.

Nowell, P. C., Cole, L. J., Habermeyer, J. G. and Roan, P. L. (1956). Growth and continued function of rat marrow cells in x-radiated mice. Cancer Res *16*, 258-61.

O'Neal, J. T., Upadhyay, A. A., Wolabaugh, A., Patel, N. B., Bosinger, S. E. and Suthar, M. S. (2019). West Nile Virus-Inclusive Single-Cell RNA Sequencing Reveals Heterogeneity in the Type I Interferon Response within Single Cells. J Virol *93*.

Ogawa, M., Matsuzaki, Y., Nishikawa, S., Hayashi, S., Kunisada, T., Sudo, T., Kina, T., Nakauchi, H. and Nishikawa, S. (1991). Expression and function of c-kit in hemopoietic progenitor cells. J Exp Med *174*, 63-71.

Ogawa, M., Tajima, F., Ito, T., Sato, T., Laver, J. H. and Deguchi, T. (2001). CD34 expression by murine hematopoietic stem cells. Developmental changes and kinetic alterations. Ann N Y Acad Sci *938*, 139-45.

Oka, T., Xu, J., Kaiser, R. A., Melendez, J., Hambleton, M., Sargent, M. A., Lorts, A., Brunskill, E. W., Dorn, G. W., 2nd, Conway, S. J.*, et al.* (2007). Genetic manipulation of periostin expression reveals a role in cardiac hypertrophy and ventricular remodeling. Circ Res *101*, 313-21.

Orkin, S. H. and Zon, L. I. (2008). Hematopoiesis: an evolving paradigm for stem cell biology. Cell *132*, 631-44.

Osawa, M., Hanada, K., Hamada, H. and Nakauchi, H. (1996). Long-term lymphohematopoietic reconstitution by a single CD34-low/negative hematopoietic stem cell. Science *273*, 242-5.

Oskarsson, T., Acharyya, S., Zhang, X. H., Vanharanta, S., Tavazoie, S. F., Morris, P. G., Downey, R. J., Manova-Todorova, K., Brogi, E. and Massague, J. (2011). Breast cancer cells produce tenascin C as a metastatic niche component to colonize the lungs. Nat Med *17*, 867-74.

Ottersbach, K. (2019). Endothelial-to-haematopoietic transition: an update on the process of making blood. Biochem Soc Trans *47*, 591-601.

Ottersbach, K. and Dzierzak, E. (2005). The murine placenta contains hematopoietic stem cells within the vascular labyrinth region. Dev Cell *8*, 377-87.

Ottersbach, K. and Dzierzak, E. (2010). The placenta as a haematopoietic organ. Int J Dev Biol *54*, 1099-106.

Park, D., Spencer, J. A., Koh, B. I., Kobayashi, T., Fujisaki, J., Clemens, T. L., Lin, C. P., Kronenberg, H. M. and Scadden, D. T. (2012). Endogenous bone marrow MSCs are dynamic, fate-restricted participants in bone maintenance and regeneration. Cell Stem Cell *10*, 259-72.

Parretta, E., Cassese, G., Barba, P., Santoni, A., Guardiola, J. and Di Rosa, F. (2005). CD8 cell division maintaining cytotoxic memory occurs predominantly in the bone marrow. J Immunol *174*, 7654-64.

Pearson, S., Sroczynska, P., Lacaud, G. and Kouskoff, V. (2008). The stepwise specification of embryonic stem cells to hematopoietic fate is driven by sequential exposure to Bmp4, activin A, bFGF and VEGF. Development *135*, 1525-35.

Peerani, R. and Zandstra, P. W. (2010). Enabling stem cell therapies through synthetic stem cell-niche engineering. J Clin Invest *120*, 60-70.

Pestka, S., Krause, C. D. and Walter, M. R. (2004). Interferons, interferon-like cytokines, and their receptors. Immunol Rev *202*, 8-32.

Pestka, S., Langer, J. A., Zoon, K. C. and Samuel, C. E. (1987). Interferons and their actions. Annu Rev Biochem *56*, 727-77.

Pietras, E. M. (2017). Inflammation: a key regulator of hematopoietic stem cell fate in health and disease. Blood *130*, 1693-1698.

Pietras, E. M., Lakshminarasimhan, R., Techner, J. M., Fong, S., Flach, J., Binnewies, M. and Passegue, E. (2014). Re-entry into quiescence protects hematopoietic stem cells from the killing effect of chronic exposure to type I interferons. J Exp Med *211*, 245-62.

Pietras, E. M., Reynaud, D., Kang, Y. A., Carlin, D., Calero-Nieto, F. J., Leavitt, A. D., Stuart, J. M., Göttgens, B. and Passegué, E. (2015). Functionally Distinct Subsets of Lineage-Biased Multipotent Progenitors Control Blood Production in Normal and Regenerative Conditions. Cell Stem Cell *17*, 35-46.

Pina, C., Fugazza, C., Tipping, A. J., Brown, J., Soneji, S., Teles, J., Peterson, C. and Enver, T. (2012). Inferring rules of lineage commitment in haematopoiesis. Nat Cell Biol *14*, 287-94.

Pinho, S., Lacombe, J., Hanoun, M., Mizoguchi, T., Bruns, I., Kunisaki, Y. and Frenette, P. S. (2013). PDGFRα and CD51 mark human nestin+ sphere-forming mesenchymal stem cells capable of hematopoietic progenitor cell expansion. J Exp Med *210*, 1351-67.

Platanias, L. C. (2005). Mechanisms of type-I- and type-II-interferon-mediated signalling. Nat Rev Immunol *5*, 375-86.

Ploemacher, R. E., van der Sluijs, J. P., Voerman, J. S. and Brons, N. H. (1989). An in vitro limiting-dilution assay of long-term repopulating hematopoietic stem cells in the mouse. Blood *74*, 2755-63.

Prendergast Á, M., Kuck, A., van Essen, M., Haas, S., Blaszkiewicz, S. and Essers, M. A. (2017). IFNα-mediated remodeling of endothelial cells in the bone marrow niche. Haematologica *102*, 445-453.

Ragelle, H., Naba, A., Larson, B. L., Zhou, F., Prijić, M., Whittaker, C. A., Del Rosario, A., Langer, R., Hynes, R. O. and Anderson, D. G. (2017). Comprehensive proteomic characterization of stem cell-derived extracellular matrices. Biomaterials *128*, 147-159.

Rand, U., Rinas, M., Schwerk, J., Nohren, G., Linnes, M., Kroger, A., Flossdorf, M., Kaly-Kullai, K., Hauser, H., Hofer, T*., et al.* (2012). Multi-layered stochasticity and paracrine signal propagation shape the type-I interferon response. Mol Syst Biol *8*, 584.

Rando, O. J. (2012). Daddy issues: paternal effects on phenotype. Cell *151*, 702-708.

Rebel, V. I., Miller, C. L., Eaves, C. J. and Lansdorp, P. M. (1996). The repopulation potential of fetal liver hematopoietic stem cells in mice exceeds that of their liver adult bone marrow counterparts. Blood *87*, 3500-7.

Renier, N., Wu, Z., Simon, D. J., Yang, J., Ariel, P. and Tessier-Lavigne, M. (2014). iDISCO: a simple, rapid method to immunolabel large tissue samples for volume imaging. Cell *159*, 896-910.

Rhodes, K. E., Gekas, C., Wang, Y., Lux, C. T., Francis, C. S., Chan, D. N., Conway, S., Orkin, S. H., Yoder, M. C. and Mikkola, H. K. (2008). The emergence of hematopoietic stem cells is initiated in the placental vasculature in the absence of circulation. Cell Stem Cell *2*, 252-63.

Rodriguez-Fraticelli, A. E., Wolock, S. L., Weinreb, C. S., Panero, R., Patel, S. H., Jankovic, M., Sun, J., Calogero, R. A., Klein, A. M. and Camargo, F. D. (2018). Clonal analysis of lineage fate in native haematopoiesis. Nature *553*, 212-216.

Ronnblom, L. (2011). The type I interferon system in the etiopathogenesis of autoimmune diseases. Ups J Med Sci *116*, 227-37.

Roson-Burgo, B., Sanchez-Guijo, F., Del Canizo, C. and De Las Rivas, J. (2014). Transcriptomic portrait of human Mesenchymal Stromal/Stem Cells isolated from bone marrow and placenta. BMC Genomics *15*, 910.

Rossant, J. and Cross, J. C. (2001). Placental development: lessons from mouse mutants. Nat Rev Genet *2*, 538-48.

Rozen, S. and Skaletsky, H. (2000). Primer3 on the WWW for general users and for biologist programmers. Methods Mol Biol *132*, 365-86.

Sadler, A. J. and Williams, B. R. (2008). Interferon-inducible antiviral effectors. Nat Rev Immunol *8*, 559-68.

Sakaguchi, S. and Sakaguchi, N. (2005). Regulatory T cells in immunologic self-tolerance and autoimmune disease. Int Rev Immunol *24*, 211-26.

Sallusto, F., Geginat, J. and Lanzavecchia, A. (2004). Central memory and effector memory T cell subsets: function, generation, and maintenance. Annu Rev Immunol *22*, 745-63.

Samji, T. and Khanna, K. M. (2017). Understanding memory CD8(+) T cells. Immunol Lett *185*, 32-39.

Sanjuan-Pla, A., Macaulay, I. C., Jensen, C. T., Woll, P. S., Luis, T. C., Mead, A., Moore, S., Carella, C., Matsuoka, S., Bouriez Jones, T.*, et al.* (2013). Platelet-biased stem cells reside at the apex of the haematopoietic stem-cell hierarchy. Nature *502*, 232-6.

Sasaki, T., Mizuochi, C., Horio, Y., Nakao, K., Akashi, K. and Sugiyama, D. (2010). Regulation of hematopoietic cell clusters in the placental niche through SCF/Kit signaling in embryonic mouse. Development *137*, 3941-52.

Sato, T. and Clevers, H. (2013). Growing Self-Organizing Mini-Guts from a Single Intestinal Stem Cell: Mechanism and Applications. Science *340*, 1190-1194.

Sato, T., Onai, N., Yoshihara, H., Arai, F., Suda, T. and Ohteki, T. (2009). Interferon regulatory factor-2 protects quiescent hematopoietic stem cells from type I interferon-dependent exhaustion. Nat Med *15*, 696-700.

Sawamiphak, S., Kontarakis, Z. and Stainier, D. Y. (2014). Interferon gamma signaling positively regulates hematopoietic stem cell emergence. Dev Cell *31*, 640-53.

Schindelin, J., Arganda-Carreras, I., Frise, E., Kaynig, V., Longair, M., Pietzsch, T., Preibisch, S., Rueden, C., Saalfeld, S., Schmid, B.*, et al.* (2012). Fiji: an open-source platform for biological-image analysis. Nat Methods *9*, 676-82.

Schneider, W. M., Chevillotte, M. D. and Rice, C. M. (2014). Interferon-stimulated genes: a complex web of host defenses. Annu Rev Immunol *32*, 513-45.

Schofield, R. (1978). The relationship between the spleen colony-forming cell and the haemopoietic stem cell. Blood Cells *4*, 7-25.

Schoggins, J. W., Wilson, S. J., Panis, M., Murphy, M. Y., Jones, C. T., Bieniasz, P. and Rice, C. M. (2011). A diverse range of gene products are effectors of the type I interferon antiviral response. Nature *472*, 481-5.

Schroder, K., Hertzog, P. J., Ravasi, T. and Hume, D. A. (2004). Interferon-gamma: an overview of signals, mechanisms and functions. J Leukoc Biol *75*, 163-89.

Schulz, C., Gomez Perdiguero, E., Chorro, L., Szabo-Rogers, H., Cagnard, N., Kierdorf, K., Prinz, M., Wu, B., Jacobsen, S. E., Pollard, J. W.*, et al.* (2012). A lineage of myeloid cells independent of Myb and hematopoietic stem cells. Science *336*, 86-90.

Shen, F. W., Saga, Y., Litman, G., Freeman, G., Tung, J. S., Cantor, H. and Boyse, E. A. (1985). Cloning of Ly-5 cDNA. Proc Natl Acad Sci U S A *82*, 7360-3.

Shi, Y., Inoue, H., Wu, J. C. and Yamanaka, S. (2017). Induced pluripotent stem cell technology: a decade of progress. Nat Rev Drug Discov *16*, 115-130.

Shortman, K., Egerton, M., Spangrude, G. J. and Scollay, R. (1990). The generation and fate of thymocytes. Semin Immunol *2*, 3-12.

Shultz, L. D., Lyons, B. L., Burzenski, L. M., Gott, B., Chen, X., Chaleff, S., Kotb, M., Gillies, S. D., King, M., Mangada, J.*, et al.* (2005). Human lymphoid and myeloid cell development in NOD/LtSz-scid IL2R gamma null mice engrafted with mobilized human hemopoietic stem cells. J Immunol *174*, 6477-89.

Sieburg, H. B., Cho, R. H., Dykstra, B., Uchida, N., Eaves, C. J. and Muller-Sieburg, C. E. (2006). The hematopoietic stem compartment consists of a limited number of discrete stem cell subsets. Blood *107*, 2311-2316.

Sohawon, D., Lau, K. K., Lau, T. and Bowden, D. K. (2012). Extra-medullary haematopoiesis: a pictorial review of its typical and atypical locations. J Med Imaging Radiat Oncol *56*, 538-44.

Spangrude, G. J. (1992). Characteristics of the hematopoietic stem cell compartment in adult mice. Int J Cell Cloning *10*, 277-85.

Spangrude, G. J., Heimfeld, S. and Weissman, I. L. (1988). Purification and characterization of mouse hematopoietic stem cells. Science *241*, 58-62.

Spivak, J. L., Barosi, G., Tognoni, G., Barbui, T., Finazzi, G., Marchioli, R. and Marchetti, M. (2003). Chronic myeloproliferative disorders. Hematology Am Soc Hematol Educ Program, 200-24.

Sprangers, S., de Vries, T. J. and Everts, V. (2016). Monocyte Heterogeneity: Consequences for Monocyte-Derived Immune Cells. J Immunol Res *2016*, 1475435.

Sprent, J. (1993). Lifespans of naive, memory and effector lymphocytes. Curr Opin Immunol *5*, 433-8.

Sprent, J., Cho, J. H., Boyman, O. and Surh, C. D. (2008). T cell homeostasis. Immunol Cell Biol *86*, 312-9.

Sprent, J. and Tough, D. F. (1994). Lymphocyte life-span and memory. Science *265*, 1395-400.

Steinbusch, M. M. F., Caron, M. M. J., Surtel, D. A. M., van den Akker, G. G. H., van Dijk, P. J., Friedrich, F., Zabel, B., van Rhijn, L. W., Peffers, M. J. and Welting, T. J. M. (2019). The antiviral protein viperin regulates chondrogenic differentiation via CXCL10 protein secretion. J Biol Chem *294*, 5121-5136.

Stepp, W. H., Stamos, J. D., Khurana, S., Warburton, A. and McBride, A. A. (2017). Sp100 colocalizes with HPV replication foci and restricts the productive stage of the infectious cycle. PLoS Pathog *13*, e1006660.

Stewart, T. A., Hultgren, B., Huang, X., Pitts-Meek, S., Hully, J. and MacLachlan, N. J. (1993). Induction of type I diabetes by interferon-alpha in transgenic mice. Science *260*, 1942-6.

Suganuma, T. and Workman, J. L. (2011). Signals and combinatorial functions of histone modifications. Annu Rev Biochem *80*, 473-99.

Sugiyama, T., Kohara, H., Noda, M. and Nagasawa, T. (2006). Maintenance of the hematopoietic stem cell pool by CXCL12-CXCR4 chemokine signaling in bone marrow stromal cell niches. Immunity *25*, 977-88.

Sutherland, H. J., Eaves, C. J., Eaves, A. C., Dragowska, W. and Lansdorp, P. M. (1989). Characterization and partial purification of human marrow cells capable of initiating long-term hematopoiesis in vitro. Blood *74*, 1563-70.

Swann, J. B., Hayakawa, Y., Zerafa, N., Sheehan, K. C., Scott, B., Schreiber, R. D., Hertzog, P. and Smyth, M. J. (2007). Type I IFN contributes to NK cell homeostasis, activation, and antitumor function. J Immunol *178*, 7540-9.

Szilvassy, S. J., Humphries, R. K., Lansdorp, P. M., Eaves, A. C. and Eaves, C. J. (1990). Quantitative assay for totipotent reconstituting hematopoietic stem cells by a competitive repopulation strategy. Proc Natl Acad Sci U S A *87*, 8736-40.

Takahashi, K., Tanabe, K., Ohnuki, M., Narita, M., Ichisaka, T., Tomoda, K. and Yamanaka, S. (2007). Induction of pluripotent stem cells from adult human fibroblasts by defined factors. Cell *131*, 861-72.

Talemi, S. R. and Hofer, T. (2018). Antiviral interferon response at single-cell resolution. Immunol Rev *285*, 72-80.

Tang, J., Yang, Q., Cui, Q., Zhang, D., Kong, D., Liao, X., Ren, J., Gong, Y. and Wu, G. (2020). Weighted gene correlation network analysis identifies RSAD2, HERC5, and CCL8 as prognostic candidates for breast cancer. J Cell Physiol *235*, 394-407.

Taswell, C. (1984). Limiting dilution assays for the determination of immunocompetent cell frequencies. III. Validity tests for the single-hit Poisson model. J Immunol Methods *72*, 29-40.

Teige, I., Treschow, A., Teige, A., Mattsson, R., Navikas, V., Leanderson, T., Holmdahl, R. and Issazadeh-Navikas, S. (2003). IFN-beta gene deletion leads to augmented and chronic demyelinating experimental autoimmune encephalomyelitis. J Immunol *170*, 4776-84.

Throm, A. A., Moncrieffe, H., Orandi, A. B., Pingel, J. T., Geurs, T. L., Miller, H. L., Daugherty, A. L., Malkova, O. N., Lovell, D. J., Thompson, S. D.*, et al.* (2018). Identification of enhanced IFN-γ signaling in polyarticular juvenile idiopathic arthritis with mass cytometry. JCI Insight *3*.

Tie, R., Li, H., Cai, S., Liang, Z., Shan, W., Wang, B., Tan, Y., Zheng, W. and Huang, H. (2019). Interleukin-6 signaling regulates hematopoietic stem cell emergence. Exp Mol Med *51*, 1-12.

Tilg, H. and Peschel, C. (1996). Interferon-alpha and its effects on the cytokine cascade: a pro- and anti-inflammatory cytokine. Leuk Lymphoma *23*, 55-60.

Till, J. E. and McCulloch, E. (1961). A direct measurement of the radiation sensitivity of normal mouse bone marrow cells. Radiat Res *14*, 213-22.

Toles, J. F., Chui, D. H., Belbeck, L. W., Starr, E. and Barker, J. E. (1989). Hemopoietic stem cells in murine embryonic yolk sac and peripheral blood. Proc Natl Acad Sci U S A *86*, 7456-9.

Torisawa, Y. S., Spina, C. S., Mammoto, T., Mammoto, A., Weaver, J. C., Tat, T., Collins, J. J. and Ingber, D. E. (2014). Bone marrow-on-a-chip replicates hematopoietic niche physiology in vitro. Nat Methods *11*, 663-9.

Tovey, M. G., Lallemand, C., Meritet, J. F. and Maury, C. (2006). Adjuvant activity of interferon alpha: mechanism(s) of action. Vaccine *24 Suppl 2*, S2-46-7.

Trinchieri, G. (2010). Type I interferon: friend or foe? J Exp Med *207*, 2053-63.

Tusi, B. K., Wolock, S. L., Weinreb, C., Hwang, Y., Hidalgo, D., Zilionis, R., Waisman, A., Huh, J. R., Klein, A. M. and Socolovsky, M. (2018). Population snapshots predict early haematopoietic and erythroid hierarchies. Nature *555*, 54-60.

Uckelmann, H., Blaszkiewicz, S., Nicolae, C., Haas, S., Schnell, A., Wurzer, S., Wagener, R., Aszodi, A. and Essers, M. A. (2016). Extracellular matrix protein Matrilin-4 regulates stress-induced HSC proliferation via CXCR4. J Exp Med *213*, 1961-71.

van Boxel-Dezaire, A. H., Rani, M. R. and Stark, G. R. (2006). Complex modulation of cell type-specific signaling in response to type I interferons. Immunity *25*, 361-72.

van Os, R., Kamminga, L. M. and de Haan, G. (2004). Stem cell assays: something old, something new, something borrowed. Stem Cells *22*, 1181-90.

Velten, L., Haas, S. F., Raffel, S., Blaszkiewicz, S., Islam, S., Hennig, B. P., Hirche, C., Lutz, C., Buss, E. C., Nowak, D.*, et al.* (2017). Human haematopoietic stem cell lineage commitment is a continuous process. Nat Cell Biol *19*, 271-281.

Verovskaya, E., Broekhuis, M. J. C., Zwart, E., Ritsema, M., van Os, R., de Haan, G. and Bystrykh, L. V. (2013). Heterogeneity of young and aged murine hematopoietic stem cells revealed by quantitative clonal analysis using cellular barcoding. Blood *122*, 523-532.

Vigneau, S., Rohrlich, P. S., Brahic, M. and Bureau, J. F. (2003). Tmevpg1, a candidate gene for the control of Theiler's virus persistence, could be implicated in the regulation of gamma interferon. J Virol *77*, 5632-8.

Walter, D., Lier, A., Geiselhart, A., Thalheimer, F. B., Huntscha, S., Sobotta, M. C., Moehrle, B., Brocks, D., Bayindir, I., Kaschutnig, P.*, et al.* (2015). Exit from dormancy provokes DNA-damage-induced attrition in haematopoietic stem cells. Nature *520*, 549-52.

Wang, Y., Lian, Q., Yang, B., Yan, S., Zhou, H., He, L., Lin, G., Lian, Z., Jiang, Z. and Sun, B. (2015). TRIM30alpha Is a Negative-Feedback Regulator of the Intracellular DNA and DNA Virus-Triggered Response by Targeting STING. PLoS Pathog *11*, e1005012.

Weber, C. M. and Henikoff, S. (2014). Histone variants: dynamic punctuation in transcription. Genes Dev *28*, 672-82.

Weiss, C. M., Trobaugh, D. W., Sun, C., Lucas, T. M., Diamond, M. S., Ryman, K. D. and Klimstra, W. B. (2018). The Interferon-Induced Exonuclease ISG20 Exerts Antiviral Activity through Upregulation of Type I Interferon Response Proteins. mSphere *3*.

Weissman, I. L. and Shizuru, J. A. (2008). The origins of the identification and isolation of hematopoietic stem cells, and their capability to induce donor-specific transplantation tolerance and treat autoimmune diseases. Blood *112*, 3543-53.

Wilkinson, A. C., Ishida, R., Kikuchi, M., Sudo, K., Morita, M., Crisostomo, R. V., Yamamoto, R., Loh, K. M., Nakamura, Y., Watanabe, M.*, et al.* (2019). Long-term ex vivo haematopoietic-stem-cell expansion allows nonconditioned transplantation. Nature *571*, 117-121.

Wilson, A., Laurenti, E., Oser, G., van der Wath, R. C., Blanco-Bose, W., Jaworski, M., Offner, S., Dunant, C. F., Eshkind, L., Bockamp, E.*, et al.* (2008). Hematopoietic stem cells reversibly switch from dormancy to self-renewal during homeostasis and repair. Cell *135*, 1118-29.

Winkler, I. G., Sims, N. A., Pettit, A. R., Barbier, V., Nowlan, B., Helwani, F., Poulton, I. J., van Rooijen, N., Alexander, K. A., Raggatt, L. J.*, et al.* (2010). Bone marrow macrophages maintain hematopoietic stem cell (HSC) niches and their depletion mobilizes HSCs. Blood *116*, 4815-28.

Woehrer, S., Miller, C. L. and Eaves, C. J. (2013). Long-term culture-initiating cell assay for mouse cells. Methods Mol Biol *946*, 257-66.

Woo, S. R., Turnis, M. E., Goldberg, M. V., Bankoti, J., Selby, M., Nirschl, C. J., Bettini, M. L., Gravano, D. M., Vogel, P., Liu, C. L.*, et al.* (2012). Immune inhibitory molecules LAG-3 and PD-1 synergistically regulate T-cell function to promote tumoral immune escape. Cancer Res *72*, 917-27.

Woodworth, A. M. and Holloway, A. F. (2017). The Role of Epigenetic Regulation in Transcriptional Memory in the Immune System. Adv Protein Chem Struct Biol *106*, 43-69.

Woolthuis, C. M. and Park, C. Y. (2016). Hematopoietic stem/progenitor cell commitment to the megakaryocyte lineage. Blood *127*, 1242-8.

Workman, C. J., Cauley, L. S., Kim, I. J., Blackman, M. A., Woodland, D. L. and Vignali, D. A. (2004). Lymphocyte activation gene-3 (CD223) regulates the size of the expanding T cell population following antigen activation in vivo. J Immunol *172*, 5450-5.

Workman, C. J., Rice, D. S., Dugger, K. J., Kurschner, C. and Vignali, D. A. (2002). Phenotypic analysis of the murine CD4-related glycoprotein, CD223 (LAG-3). Eur J Immunol *32*, 2255-63.

Workman, C. J. and Vignali, D. A. (2003). The CD4-related molecule, LAG-3 (CD223), regulates the expansion of activated T cells. Eur J Immunol *33*, 970-9.

Wu, X., Dao Thi, V. L., Huang, Y., Billerbeck, E., Saha, D., Hoffmann, H. H., Wang, Y., Silva, L. A. V., Sarbanes, S., Sun, T.*, et al.* (2018). Intrinsic Immunity Shapes Viral Resistance of Stem Cells. Cell *172*, 423-438.e25.

Wu, X., Gu, Z., Chen, Y., Chen, B., Chen, W., Weng, L. and Liu, X. (2019a). Application of PD-1 Blockade in Cancer Immunotherapy. Comput Struct Biotechnol J *17*, 661-674.

Wu, X., Kwong, A. C. and Rice, C. M. (2019b). Antiviral resistance of stem cells. Curr Opin Immunol *56*, 50-59.

Yamamoto, K., Miwa, Y., Abe-Suzuki, S., Abe, S., Kirimura, S., Onishi, I., Kitagawa, M. and Kurata, M. (2016). Extramedullary hematopoiesis: Elucidating the function of the hematopoietic stem cell niche (Review). Mol Med Rep *13*, 587-91.

Yamamoto, R., Morita, Y., Ooehara, J., Hamanaka, S., Onodera, M., Rudolph, K. L., Ema, H. and Nakauchi, H. (2013). Clonal analysis unveils self-renewing lineage-restricted progenitors generated directly from hematopoietic stem cells. Cell *154*, 1112-1126.

Yamamoto, R., Wilkinson, A. C., Ooehara, J., Lan, X., Lai, C. Y., Nakauchi, Y., Pritchard, J. K. and Nakauchi, H. (2018). Large-Scale Clonal Analysis Resolves Aging of the Mouse Hematopoietic Stem Cell Compartment. Cell Stem Cell *22*, 600-607.e4.

Yamazaki, S., Ema, H., Karlsson, G., Yamaguchi, T., Miyoshi, H., Shioda, S., Taketo, M. M., Karlsson, S., Iwama, A. and Nakauchi, H. (2011). Nonmyelinating Schwann cells maintain hematopoietic stem cell hibernation in the bone marrow niche. Cell *147*, 1146-58.

Yang, C. P. and Bell, E. B. (1992). Functional maturation of recent thymic emigrants in the periphery: development of alloreactivity correlates with the cyclic expression of CD45RC isoforms. Eur J Immunol *22*, 2261-9.

Yoder, M. C. and Hiatt, K. (1997). Engraftment of embryonic hematopoietic cells in conditioned newborn recipients. Blood *89*, 2176-83.

Yoder, M. C., Hiatt, K., Dutt, P., Mukherjee, P., Bodine, D. M. and Orlic, D. (1997). Characterization of definitive lymphohematopoietic stem cells in the day 9 murine yolk sac. Immunity *7*, 335-44.

Yokomizo, T., Yamada-Inagawa, T., Yzaguirre, A. D., Chen, M. J., Speck, N. A. and Dzierzak, E. (2012). Whole-mount three-dimensional imaging of internally localized immunostained cells within mouse embryos. Nat Protoc *7*, 421-31.

Young, H. A. (1996). Regulation of interferon-gamma gene expression. J Interferon Cytokine Res *16*, 563-8.

Yu, V. W. and Scadden, D. T. (2016). Hematopoietic Stem Cell and Its Bone Marrow Niche. Curr Top Dev Biol *118*, 21-44.

Zhang, J., Niu, C., Ye, L., Huang, H., He, X., Tong, W. G., Ross, J., Haug, J., Johnson, T., Feng, J. Q.*, et al.* (2003). Identification of the haematopoietic stem cell niche and control of the niche size. Nature *425*, 836-41.

Zhang, Y., Gao, S., Xia, J. and Liu, F. (2018). Hematopoietic Hierarchy - An Updated Roadmap. Trends Cell Biol *28*, 976-986.

Zhou, F., Li, X., Wang, W., Zhu, P., Zhou, J., He, W., Ding, M., Xiong, F., Zheng, X., Li, Z.*, et al.* (2016). Tracing haematopoietic stem cell formation at single-cell resolution. Nature *533*, 487-92.

Zhou, Y., He, C., Wang, L. and Ge, B. (2017). Post-translational regulation of antiviral innate signaling. Eur J Immunol *47*, 1414-1426.

Zimmermann, H. W., Trautwein, C. and Tacke, F. (2012). Functional role of monocytes and macrophages for the inflammatory response in acute liver injury. Front Physiol *3*, 56.